Pulsed Plant Evolution in Mountain Ecosystems: Identifying Rate Changes of Range Shift and Morphology

Inauguraldissertation

zur
Erlangung der Würde eines Doktors der Philosophie
vorgelegt der
Philosophisch-Naturwissenschaftlichen Fakultät
der Universität Basel

von

Livio Bätscher

2024

Genehmigt von der Philosophisch-Naturwissenschaftlichen Fakultät
auf Antrag von

Erstbetreuer: Prof. Dr. Ansgar Kahmen

Zusätzlicher Erstbetreuer: Dr. Jurriaan de Vos

Zweitbetreuer: Prof. Dr. Walter Salzburger

Externe Expertin: Prof. Dr. Aelys Muriel Humphreys

Basel, den 27. Februar 2024

Prof. Dr. Marcel Mayor

Dekan

Contents

General Introduction

Understanding the origin of plant diversity remains a central and relevant scientific goal. This statement is reflected by a survey conducted by Grierson et al. (2011), where the one hundred most important and urgent questions in plant science were collected. Here, the listed questions were grouped into five sections, and "plant diversity" is prominently represented as one of these sections. Remarkably, these questions - even though some of them might be as old as Darwin's work – are very urgent to be answered, especially in a world where society is confronted with the consequences of climate change. For instance, understanding the rapid and relatively recent diversification of angiosperm species can provide valuable insight into the evolution of genomes and the underlying evolutionary processes (Grierson et al., 2011). Therefore, studying angiosperm plant diversification is crucial, yet addressing such a broad question presents a considerable challenge.

Phylogenetic trees serve as a central tool for studying patterns and processes that underlie angiosperm diversification. Charles Darwin (1809 - 1882) was one of the most famous scientists who promoted this "tree thinking". In "Origin of Species" (Darwin, 1859), he introduced one of the first phylogenetic diagrams. The "Tree of Life", the sole illustration in Darwin's book, represents the relationships among species, both living and extinct, across evolutionary lineages. The diagram's y-axis symbolizes time, where the top represents the present, and below the past with extinct lineages. Identical to family trees the lines (called branches) are used to show the relationship between species and branches below a joint (called internal nodes) represent an ancestral species. These structural representations were coined as phylogenies by Ernst Haeckel in 1866 (McLennan, 2010) and are still used in modern biology. Nowadays specific programs exist to compute phylogenetic trees allowing them to be inferred from morphological, genetic, or both data types (e.g., Höhna et al., 2016). However, thinking of related species as trees is not sufficient to explain the numerous angiosperm species.

Critically, closely related species introduce statistical nonindependence, posing a challenge, and more complex analytical tools are required to study rapid diversification accurately. Felsenstein (1985) addressed this issue using a fictive phylogeny of 40 species, which displays two groups of 20 closely related species. Next, a two-dimensional data set (from these 40 species) is presented, showing a positive correlation between the two characters. Felsenstein then confronts the reader with the same data but reveals what point belongs to which of the closely related groups. The points within each group show no significant correlation, yet the overall significant pattern is illusory and caused by the position of the two "data clouds". Ultimately, Felsenstein suggests overcoming this problem by correcting for the nonindependence caused by the taxa's shared ancestry. Therefore, he uses the structure of the phylogeny and treats evolutionary lineages as replicates. This pioneering work created a new world of powerful and diverse methodological tools called "phylogenetic comparative methods" (Cornwell & Nakagawa, 2017).

These analytical tools enable me to investigate alpine plant diversity and tackle the overarching question: How do rates of evolution vary among lineages and what factors account for potential differences in rates?

MOUNTAIN ECOSYSTEMS

Mountain ecosystems are extraordinarily suitable study systems to address various evolutionary questions. Terrestrial biodiversity is disproportionately distributed relative to the total land area. Mountain systems are habitats for about one-third of the known terrestrial biodiversity but only cover a relatively low fraction of the total landmass (12-16%; Körner, 2021; Spehn et al., 2011). Therefore, mountains are also considered to be evolutionary arenas (Muellner-Riehl, 2019). The unresolved "mystery" of why there are so many species is also called "Humboldt's enigma" (Rahbek et al., 2019) and makes the alpine biome attractive to study diversity, speciation, adaptation, and dispersal. However, even if it may appear trivial, providing a generalizable definition for mountain systems poses significant challenges (Körner et al., 2011).

The lower borders of alpine biomes are well-studied and clearly defined. Modern biome definitions try to summarize similar climatic conditions, similar vegetation structure, and the presence of key species, yet biomes are often a fuzzy concept (Donoghue & Edwards, 2014). Regardless of this issue, alpine biomes have a special lower border: the alpine treeline, which forms the upper niche limit of all tree species (Körner, 2012). This border has been defined by multiple studies, including microclimate data collection on a global scale, development plus evaluation of a climatic model to identify local borders, which is in combination with ruggedness (excluding the non-alpine tundra), accurately capable of predicting the alpine area (Körner et al., 2011; Paulsen & Körner, 2014). Having a well-defined border is very helpful when investigating biome or range shifts. Nevertheless, having a solid biome border definition is not sufficient to address evolutionary questions; the border must also be ecologically relevant.

The upper climatic treeline is associated with significant (micro)climatic change. For example, light availability increases after the treeline ecotone strongly, and the temperature increases by about 6 °C when a plant moves from the upper montane forest into the open alpine habitat (Körner, 2021). Consequently, plants of the alpine biome are small, favor life forms that allow for longevity, and need to adjust to shorter growing seasons (Körner, 2023). Thus, shifts into and out of the alpine biome can be considered major ecological changes, consequently leading to morphological and physiological adaptation.

In conclusion, mountain ecosystems are demonstrated to be highly suitable for disentangling evolutionary processes. Namely, they are species-rich, and have a clearly defined biome border, which is known to cause significant ecological change. Therefore, the number of studies comparing how alpine and non-alpine species evolved grew in the past years (e.g., Ding et al., 2020; Kong et al., 2021; Nürk et al., 2019; Smyčka et al., 2022; Xing & Ree, 2017). Here, the alpine biome strongly propelled the content of this thesis and the question of how and why evolutionary rates vary along lineages.

EVOLUTIONARY RATES

To measure how alpine plant life evolved, metrics are needed that can quantitatively express salient properties of evolution. For this, scientists use evolutionary rates, which facilitate describing evolutionary processes, allow the performance of tests, and simplify comparisons. Frequently used evolutionary rates are for example: diversification, extinction, dispersal, and extirpation rates, or the rate of trait evolution. It is important to note that evolutionary rates have multiple properties, as Simpson famously pointed out (Simpson, 1944). First, there is the "tempo" of evolution, which refers to the speed at which it occurs (e.g., an average increment in the length of a trait per unit of time). Second is the "mode" of evolution, which encompasses the direction and orientation of evolutionary changes. Next, embedded with many fossil examples, Simpson describes three different tempi and modes of evolution. Finally, he concludes that rates of evolution can be described with different tempi and are likely caused by contrasting modes of evolution. However, with the lack of modern phylogenetic methods, Simpson was not capable of testing and comparing different rates of evolution with each other. Nonetheless, his concept was broadly accepted and is still referred to in modern literature.

Only in the current century, models became available that allow us to test if the evolutionary history of a lineage follows a continuous motion (e.g., Brownian motion or Ornstein-Uhlenbeck) or if

Simpson's rapid rate changes are a more realistic scenario. A specific model type that is considered promising are Lévy processes, developed in the last 10 years (e.g., Landis et al. 2013; Duchen et al. 2017; Landis and Schraiber 2017; Bastide and Didier 2023) and are currently still a "niche products". However, these phylogenetic models allow to use of jump-like changes in e.g., trait evolution, also described as 'pulsed evolution'. Therefore, new methods enables me to test if Simpson's old idea of multiple tempi of evolution is true, where and under what circumstances they appear.

THESIS CONTENTS

My thesis aimed to identify how evolutionary rates within mountain systems change between and within different lineages. Specifically, I asked (1) how can automated tip-scoring methods in the alpine context be improved to obtain correct dispersal and extirpation rates, (2) whether the continuous niche proxy (distance to the treeline) evolved under different rates within and between clades, and (3) if we find evidence for different tempo and mode in trait evolution of western New World *Lupinus* clades.

Chapter I: With an increasing number of species in a phylogeny, automated geographical state assignment to tips becomes inevitable. However, such procedures are often known to introduce errors (here called tip-stat-errors) and we are aiming to (1) minimize tip-state-errors and (2) identify the potential impact on downstream analysis i.e., on dispersal and extirpation rates. We use cleaned GIBIF data of the European Alpine Arc to classify species as alpine (above the treeline), non-alpine (below the treeline), or both with two different approaches: a newly developed algorithm ElevDistr and a gridded model of thermal belts. To evaluate the classification performance, we use the highly regarded Flora Alpina (Aeschimann et al., 2004) as a validation dataset. Additionally, we applied DEC models to six focal genera to assess whether the inferred rates are biased. Here, ElevDistr which leverages valuable elevation information, was found to be less error-prone and less sensitive to spatial uncertainty. Further, we found that especially unbalanced false positive to false negative rates biased the estimation of dispersal and extirpation rates on an exponential scale.

Chapter II: Since the algorithm developed in Chapter I provides a continuous horizontal distance to the treeline, we also created a tool for investigating niche shifts. Here, we compare models of gradual evolution with models that consider rapid jump-like and pulsed evolution e.g., Lévy processes. Since we wanted to compare three alpine plant clades with each other, we inferred dated phylogenies from new and existing sequences, collected and cleaned GBIF data, to finally compute with ElevDistr the distance to the treeline and calculate niche proxies. Next, we tested (1) whether our continuous niche proxies are better explained by gradual or pulsed evolution, (2) if the niche proxy evolution has the same tempo in all clades, and (3) if different niche proxies are supported by the same models. The results show that niche centers in *Primula* and *Lupinus* evolved under pulsed evolution, whereas *Ranunculus* follows continuous evolution. Also, the niche proxies seemed to have evolved differently e.g., the upper niche limit seems to always favor continuous evolution, this artifact is potentially caused by the microclimate because the remaining parameters show pulsed niche shift (at least in one genera). This leads to the conclusion that pulsed niche shifts are existent but not omnipresent.

Chapter III: After discovering pulsed niche evolution with a strong signal in *Lupinus*, I decided that looking into *Lupinus* trait evolution would be the next logical step to further investigate changes in evolutionary rates. We asked if also morphological characters in *Lupinus* evolved with pulses and whether potential pulses are caused by the interaction with the environment, or rather the life form. To answer this question, different traits are tested if they evolved under continuous or pulsed evolution (with the dated phylogeny inferred in the previous chapter). Further climatic niche parameters were extracted from a global database by using GIBIF occurrence records, and climatic niche parameters were summarized by life forma and continent. Finally, we also computed with a phylomorphospace the covered trait space. The results showed that some but not all traits followed a pulsed evolution. Results show that life forms and climatic variables are correlated with pulses and/or increased trait space. This phenomenon only occurs in perennial Andean species. Therefore, we conclude that the life form is only the cause of pulsed evolution in combination with a suitable environment. Further, we argue that this pattern reminds us of Simpson’s quantum evolution.

In the last part, the *general discussion* can be found. Here, I synthesize the findings of my chapters to provide overarching conclusions and an outlook for potential future research.

REFERENCES

Aeschimann, D., Lauber, K., Moser, D. M., & Theurillat, J.-P. (2004). *Flora alpina: atlas des 4500 plantes vasculaires des Alpes*. Haupt Publisher. https://doi.org/10.2307/25065454

Cornwell, W., & Nakagawa, S. (2017). Phylogenetic comparative methods. *Current Biology*, *27*(9), R333–R336. https://doi.org/10.1016/j.cub.2017.03.049

Darwin, C. (1859). *On the origin of species*. John Murray.

Donoghue, M. J., & Edwards, E. J. (2014). Biome Shifts and Niche Evolution in Plants. *Annual Review of Ecology, Evolution, and Systematics*, *45*(1), 1–26. https://doi.org/10.1146/annurev-ecolsys-120213-091905

Felsenstein, J. (1985). Phylogenies and the Comparative Method. *The American Naturalist*, *125*(1), 1–15. https://doi.org/10.1086/284325

Grierson, C. S., Barnes, S. R., Chase, M. W., Clarke, M., Grierson, D., Edwards, K. J., Jellis, G. J., Jones, J. D., Knapp, S., Oldroyd, G., Poppy, G., Temple, P., Williams, R., & Bastow, R. (2011). One hundred important questions facing plant science research. *New Phytologist*, *192*(1), 6–12. https://doi.org/10.1111/j.1469-8137.2011.03859.x

Höhna, S., Landis, M. J., Heath, T. A., Boussau, B., Lartillot, N., Moore, B. R., Huelsenbeck, J. P., & Ronquist, F. (2016). RevBayes: Bayesian Phylogenetic Inference Using Graphical Models and an Interactive Model-Specification Language. *Systematic Biology*, *65*(4), 726–736. https://doi.org/10.1093/sysbio/syw021

Körner, C. (2012). *Alpine Treelines, Functional Ecology of the Global High Elevation Tree Limits*. https://doi.org/10.1007/978-3-0348-0396-0

Körner, C. (2021). *Alpine Plant Life, Functional Plant Ecology of High Mountain Ecosystems*. https://doi.org/10.1007/978-3-030-59538-8

Körner, C. (2023). Concepts in Alpine Plant Ecology. *Plants*, *12*(14), 2666. https://doi.org/10.3390/plants12142666

Körner, C., Paulsen, J., & Spehn, E. M. (2011). A definition of mountains and their bioclimatic belts for global comparisons of biodiversity data. *Alpine Botany*, *121*(2), 73. https://doi.org/10.1007/s00035-011-0094-4

McLennan, D. A. (2010). How to Read a Phylogenetic Tree. *Evolution: Education and Outreach*, *3*(4), 506–519. https://doi.org/10.1007/s12052-010-0273-6

Muellner-Riehl, A. N. (2019). Mountains as Evolutionary Arenas: Patterns, Emerging Approaches, Paradigm Shifts, and Their Implications for Plant Phylogeographic Research in the Tibeto-Himalayan Region. *Frontiers in Plant Science*, *10*, 195. https://doi.org/10.3389/fpls.2019.00195

Paulsen, J., & Körner, C. (2014). A climate-based model to predict potential treeline position around the globe. *Alpine Botany*, *124*(1), 1–12. https://doi.org/10.1007/s00035-014-0124-0

Rahbek, C., Borregaard, M. K., Colwell, R. K., Dalsgaard, B., Holt, B. G., Morueta-Holme, N., Nogues-Bravo, D., Whittaker, R. J., & Fjeldså, J. (2019). Humboldt's enigma: What causes global patterns of mountain biodiversity? *Science*, *365*(6458), 1108–1113. https://doi.org/10.1126/science.aax0149

Simpson, G. G. (1944). *Tempo and Mode in Evolution*. Columbia University Press. https://doi.org/10.7312/simp93040

Spehn, E. M., Rudmann-Maurer, K., & Körner, C. (2011). Mountain biodiversity. *Plant Ecology & Diversity*, *4*(4), 301–302. https://doi.org/10.1080/17550874.2012.698660

Chapter I: Avoiding Impacts of Phylogenetic Tip-state-errors on Dispersal and Extirpation Rates in Alpine Plant Biogeography

Livio Bätscher, Jurriaan M. de Vos

Accepted in *Journal of Biogeography*

SUMMARY

Aim: Many biogeographic analyses require some form of automated state assignment to tips of phylogenetic trees, reflecting a species presence or absence in a particular area, e.g., a biome. As datasets get exponentially larger, such procedures may increasingly induce errors (here called tip-state-error), but the specific algorithmic cause and consequence on downstream estimation of dispersal and extinction rates remains poorly known. We aim to improve automated tip-scoring methods in the context of the alpine biome by leveraging elevation information. We document the profound effect of tip-state-errors on Dispersal-Extirpation-Cladogenesis (DEC) models.

Location: The European Alpine Arc.

Taxon: 3,317 vascular plant species, emphasizing six focal genera: *Campanula*, *Carex*, *Festuca*, *Ranunculus*, *Saxifraga,* and *Viola*.

Methods: We use GBIF data to classify whether species occur above the upper climatic treeline using a newly developed algorithm ElevDistr or a gridded landscape model of thermal belts, under various filtering thresholds. We compared classification performance using the Flora Alpina as validation data. To determine if tip-state-error biases the dispersal and extirpation rate estimation, we fit DEC models for selected clades using tip-states from different classification models.

Results: ElevDistr is less error prone than other approaches. Filtering thresholds lower the false positive rate but increase the false negative rate. Inflated false positive rates bias the dispersal rate estimation upward, while inflated false negative rates lead to upward bias in extirpation rate estimation.

Main conclusions: Even moderate tip-state-error may lead to profound systematic bias in dispersal and extinction rate estimation if an unbalanced ratio between false positive and false negative rates occurs. Therefore, careful validation is imperative, though ElevDistr alleviates this problem in the context of the alpine environment. Overall, our results suggest contrasting rates of alpine biome shifts across the studied genera and have major implications for studies addressing the likelihood of niche evolution versus geographic dispersal.

INTRODUCTION

The long-term interest in understanding the drivers of the geographic distribution of life on Earth has recently become a highly computational endeavor. Since its onset in the early 19th century, biogeography mostly entailed describing plant communities in the context of their environment (Humboldt, 1805; Wallace, 1876). These careful descriptions fueled Darwin's ideas on natural selection (Darwin, 1859), motivating Alfred Russel Wallace to infer that species respond dynamically to biotic and abiotic factors, eventually leading to sharp transition lines (e.g., Wallace Line; Browne, 1984; Shermer, 2002). This "discrete" quality of the distribution of life was further emphasized when Alfred Wegner concluded in the early 20th century based on fossil distributions that landmasses are drifting away from Pangea (Wegener, 1922). Since island theory showed that species richness can be explained by area size, dispersal, and extirpation rates (MacArthur & Wilson, 1967), understanding the drivers of dispersal and extirpation rates has become a central goal in biogeography (Hackel & Sanmartín, 2021).

To document species distributions and their drivers across discrete areas, a diverse array of methodological approaches has been developed: first in terms of area cladograms (Humphries & Parenti, 1999) and later in terms of the processes that underlie them (Avise et al., 1987), such as dispersal and vicariance (Ronquist, 1997), or dispersal, extinction, and speciation (Ree et al., 2005). Acknowledging the statistical non-independence of species (Felsenstein, 1985), parametric statistical approaches combine spatial, environmental, and phylogenetic data to model the mode and tempo of changes in lineage distribution (Hackel & Sanmartín, 2021). These models differ in their assumptions, for instance, whether dispersal barriers or areas are modeled (Landscape Evolution Models; Albert et al., 2017), whether states or regions affect lineage's speciation and extinction rates (GeoSSE; Goldberg et al., 2011; Maddison et al., 2007), or whether biomes are static through time (Landis et al., 2021). Among these, dispersal-extirpation-cladogenesis (DEC) models are the most widely adopted

(Andersen et al., 2018; Asadi et al., 2019; Pelser et al., 2019; Rowe et al., 2019). Using presence or absence in discrete areas (e.g., continents, islands, or biomes), DEC models infer anagenetic range evolution (dispersal and extirpation rates) and a fixed cladogenetic range evolution, in a maximum likelihood (Ree et al., 2008) or Bayesian framework (Höhna et al., 2016; Landis et al., 2018), enabling to model macroevolutionary processes (e.g., lineage dispersal, local extirpation) and ancestral range reconstruction within increasingly realistic and flexible frameworks (Hackel & Sanmartín, 2021). Thus, DEC models allow us to not just reconstruct the history of biogeographic patterns but also provide a means to quantify the biogeographic processes that underlie them. Understanding their performance is thus of central importance in biogeography.

Simultaneously with these methodological developments, data availability to address biogeographic questions has exploded, presenting formidable opportunities and daunting challenges. On the one hand, computational advances now allow reconstructing very large phylogenies with thousands of tips (e.g., Ding et al., 2020; Figueroa et al., 2022; Kerkhoff et al., 2014; Ringelberg et al., 2023; Zanne et al., 2014), that hold the promise of uncovering general trends. However, they preclude manually assigning a state (discrete or continuous) to each phylogenetic tip, instead requiring at least partially automated approaches (e.g., Figueroa et al., 2022; Gori et al., 2022; Vasconcelos et al., 2020; Zanne et al., 2014). Moreover, the availability of spatial occurrence data is exponentially increasing. For instance, the Global Biodiversity Information Facility (GBIF) currently contains 2.3 billion database entries (April 2023) and an annual growth of 1.5% (Heberling et al., 2021). GBIF data is a valuable source for (additional) data (Beck et al., 2013) but is also incomplete and contains well-known biases, which can affect downstream analyses (Beck et al., 2014; Qian et al., 2018). Methods for automated GBIF data collection or cleaning (e.g., Chamberlain et al., 2022; Zizka et al., 2019), are widely adopted and thought to mitigate issues arising from biased and/or incomplete data.

Nevertheless, tip-scoring is unlikely to be perfect, and imperfect phylogenetic data may be generally expected to bias results. For instance, taxonomically "complete" phylogenies generated with birth–death polytomy resolvers (Jetz et al., 2012) were shown to result in a bias toward faster rates of trait evolution (Rabosky, 2015). Similarly, minor subjective decisions in data cleaning procedures led to dramatically different reconstructions of trait evolution (Edwards et al., 2015 in response to Zanne et al., 2014), and imperfect molecular clock dating was suggested to result in bias (Lu et al. 2018; critique: Qian 2019; rebuttal: Lu et al. 2020). Particularly important for biogeography is that tip-state-errors may be of two kinds, with potentially diametrically different effects: Type I errors or false positives: wrongly assuming a species occurs somewhere while it does not; and Type II errors or false negatives: wrongly assuming a species is absent somewhere while it is present. Although the advantages of high data availability are obvious, it remains largely undocumented whether tip-scoring-error (which is likely to arise in large data sets) may introduce a systematic bias in biogeographic inference.

Beyond noisy spatial data, tip-state-error should also be particularly likely when discretizing continuous environmental gradients without considering their spatial heterogeneity. A particularly illustrative and important example can be found along mountain slopes. Here many environmental parameters change with increasing elevation, such as increased solar radiation under a clear sky (Barry, 1978), decreased atmospheric pressure, air temperature, air humidity (Körner, 2021), and land area (Körner, 2007). Mountains are more species-rich than their area suggests: one-third of terrestrial biodiversity is found in mountains (Spehn et al., 2011) and they provide, therefore, "natural laboratories" of evolution and biogeography (López-Angulo et al., 2018; Mittelbach et al., 2007). Importantly, thermal belts, within which vegetation is rather homogeneous, stratify diversity both spatially and ecologically such that the continuous climatic gradients become discrete vegetation units. The boundaries between these discrete belts have a long history of investigation (Humboldt, 1805; Schröter et al., 1926) and their climatic thresholds are well-defined (Körner et al., 2011). Strikingly, boundaries between thermal belts are only locally correlated with absolute elevation, e.g., due to the "Massenerhebungs"-effect (mountain mass elevation effect that explains that central versus front ranges of a mountain system differ in their treeline elevation), and latitude-associated global effects (Körner, 2021; Schröter et al., 1926). Automated classification of any single coordinate of occurrence as a presence/absence in a particular thermal belt thus poses formidable challenges because associated elevation, climatic layers, and their interpretation in terms of thermal belts, plus species identification, are prone to error. Moreover, mountains are the epitome of topographic heterogeneity, resulting in the associated problem that the spatial resolution of actual climate types is much more finely grained than available global weather and climate data (Körner & Hiltbrunner, 2021; Scherrer & Körner, 2010). Given the broad interest in understanding the evolution of plants in mountainous areas (Antonelli et al., 2018; Parisod et al., 2022; Perrigo et al., 2020; Rahbek et al., 2019), classifying species occurrences as being above ('alpine') or below ('non-alpine') the climatic treeline offers a valuable opportunity to test the accuracy of automated tip-scoring and infer the effects of tip-scoring-errors on reconstructing the evolution of species biome occupancy.

In this study, we investigate how false positive and false negative tip-state-errors impact dispersal and extirpation rate inference. We focus on clades with alpine plants because their state assignment may be particularly challenging. Because investigating error rates requires knowing the actual thermal belt occupancy of each species, we study the European Alpine Arc, one of the world's best-known floras, including many clades with species occurring above, below, or above and below the treeline (Aeschimann et al., 2004). First, across hundreds of thousands of occurrence records, we compare the performance of multiple automated tip-scoring methods, classifying the species as 'alpine' or 'non-alpine'. This includes one approach that we newly developed, ElevDistr, which leverages that vertical precision (elevation) may usually exceed coordinate precision (latitude, longitude), making it in principle suitable for all vertically structured biome boundaries, thermal belts, or vertical species ranges in aquatic (depth) and terrestrial (elevation) contexts. To ask whether false positive and false negative error biases model parameterization, specifically of dispersal and extirpation rates, we use DEC-models in six of the most speciose Alpine genera based on the tip-state scoring from different classification methods. Specifically, after evaluating performance of different classification methods, we infer which of the three possible outcomes arises when an increasing fraction of tips are scored incorrectly: (1) no effect, (2) an increase in estimation uncertainty, or (3) a systematically biased estimate as a function of the tip classification error rate. We reveal that Type I and Type II classification errors bias DEC model inference differently but systematically, reinforcing the importance of accurate classification algorithms and their careful validation in any biogeographic context.

MATERIAL AND METHODS

Experimental design

The lower border of the alpine area is given by the treeline, which has been defined in various ways (Körner, 2021). We use the definition 'upper climatic treeline' (i.e., the upper range limit of all trees >3 m) because it is well-defined in the TREELIM model (Paulsen & Körner, 2014). We classify species from the European Alpine Arc as occurring above ('alpine') or below ('non-alpine') the climatic treeline, or above and below ('both'), comparing automated approaches with a "true" validation dataset to evaluate algorithm performance. We base classifications on cleaned spatial occurrences from GBIF because they are largest in number and most widely used. Validation data comes from the highly regarded Flora Alpina of Aeschimann et al. (2004), to which numerous experts contributed. The Flora is an authoritative synthesis of different national floras, presenting all 4,491 vascular plant taxa of the European Alpine Arc, one of the floristically best-known areas in the world. Importantly, it includes ecological characterizations including thermal belt occupancy. We consider two classification methods combined with various filtering settings: (1) coordinates are assigned to raster cells of broadly adopted thermal belt data (Körner et al., 2011), which is incorporated in the Global Mountain Biodiversity Assessment and the Mountain Portal (https://www.gmba.unibe.ch/), and (2) using ElevDistr, a newly developed algorithm that evaluates the elevation of the local treeline and compares it to the coordinate elevation.

To investigate the effects of the obtained tip-state-errors, we select the six most species-rich clades from the European Alps that have sufficient phylogenetic data and use Bayesian inference to parameterize a DEC model for each clade and classification. If classification error is unimportant, DEC model parameterization under all classification models should be identical or very similar to the parameterization under the Flora Alpina classification. If more extreme error rates lead to less precisely inferred rates, we expect broader intervals of highest posterior density, but no significant trend in posterior mean estimate. However, if classification error biases DEC model results, we expect a positive or negative slope of posterior means of model parameters with increasing error rates.

Data acquisition and cleaning

We extracted all 8,146,192 occurrence records of vascular plant species in a large polygon spanning the Alpine Arc (42° - 49° N, 4°- 18° E) from GBIF (https://www.gbif.org/occurrence/download/0262521-210914110416597, accessed March 2022). Of these, we retained the 7,351,509 records of 3,317 species with the following characteristics: species identification matching a species name in Aeschimann et al. (2004); elevation between 0 and 5,000 m a.s.l.; stated uncertainty ≤10 km; no close proximity to country capitals, province centroids, the GBIF headquarter, biodiversity institutions, or within the sea; no presence within indicated country borders, using custom R scripts based on Zizka et al., 2019. Thus, we excluded species where taxon harmonization may have been required, given that the names backbone of Aeschimann et al. (2004) deviates from the NCBI taxonomic backbone employed in the GBIF and GenBank databases consulted below. We then randomly selected a maximum of 100 records per taxon (329,992 remaining records).

To obtain validation data, we transcribed the Flora Alpina (Aeschimann et al., 2004). This flora states for all species of the European Alpine Arc whether they are ‘regularly present’, ‘weakly present’, ‘absent’, or rarely ‘uncertainly present’ in each of five thermal belts (colline, montane, subalpine, alpine, and nival). We assume these statements to be true and converted ‘regular’ and ‘weak’ presences to 'present'. Additionally, we changed 'absences' and 'uncertain presences' to 'absent' and lumped infraspecific taxa. We converted nival and alpine to 'alpine' (because they are above the upper climatic treeline) and the other climatic belts to 'non-alpine' (including the subalpine, which is the poorly defined transition zone where trees still occasionally occur, i.e., below the upper climatic treeline: Körner, 2021). Thus, we score each species as 'alpine', 'non-alpine', or 'both', allowing for comparison across classification algorithms.

Polygon classification algorithm

The first classification approach is based on a gridded data product (here called polygon), with each cell assigned to one of seven thermal belts at a resolution of 2' 30'' (Körner et al., 2011), where the thermal belts above the treeline (i.e., 'nival', 'upper alpine', and 'lower alpine') were considered to be 'alpine', and the remaining thermal belts 'non-alpine'. For each coordinate, we determined with an R script whether it fell into an 'alpine' polygon or a 'non-alpine' polygon. In the rare case of not available, it remained unclassified ('none'). We classified species as 'alpine', 'non-alpine', or 'both', based on all their coordinate classifications employing three filtering thresholds: unfiltered, 5%, or 20%. These thresholds represent the minimal percentage of coordinates required for a classification to be accepted (e.g., threshold 5% means: $\geq$ 5% of the observations need an alpine classification for the species to be categorized as present in the alpine). Although the grid cells are rather coarse, this product remains widely used as one of the only off-the-shelf alpine biome layers (e.g., Carbutt, 2019; Figueroa et al., 2022; Zwaan et al., 2022).

ElevDistr classification algorithm

For the second classification approach, we developed a new algorithm 'ElevDistr', that computes presence in the alpine biome based on coordinates' vertical distance to the local, upper climatic treeline. The upper climatic treeline, i.e., the upper fundamental niche limit of all tree species, represents the spatial boundary of the alpine biome according to the TREELIM model (Paulsen & Körner, 2014). TREELIM specifies the lower alpine boundary based on a minimum number of consecutive growing season days (i.e., growing season length: when daily mean temperature exceeds 0.9°C) of >94 days and a mean temperature of all growing season days (i.e., growing season temperature) of >6.4°C, because these values were empirically shown to preclude tree growth. Growing season length and growing season temperature are publicly available for the world's land surface based on high-resolution 30'' climatic data (CHELSA V2.1; Karger et al., 2017).

The algorithm of ElevDistr (Fig. 1) leverages that elevation is frequently available for spatial points and often more accurate and precise than latitude and longitude. To determine whether a focal coordinate is above the treeline, ElevDistr first determines which of a pre-loaded set of coordinates representing points close to a treeline is nearest to the focal coordinate (using a k-d tree and the nearest neighbor search, Arya et al., 2019). ElevDistr by default considers the corners of all grid cells above the treeline (from the Global Mountain Biodiversity Assessment V1.2; Körner et al., 2011). That spatial point then becomes the center of a grid (default size of the sampled area: 10 x 10 km), within which many spatial points are drawn (with a default resolution of 0.0025' or ~5 m). For each spatial point, it determines whether it meets the TREELIM climatic criteria (Paulsen & Körner, 2014) to be

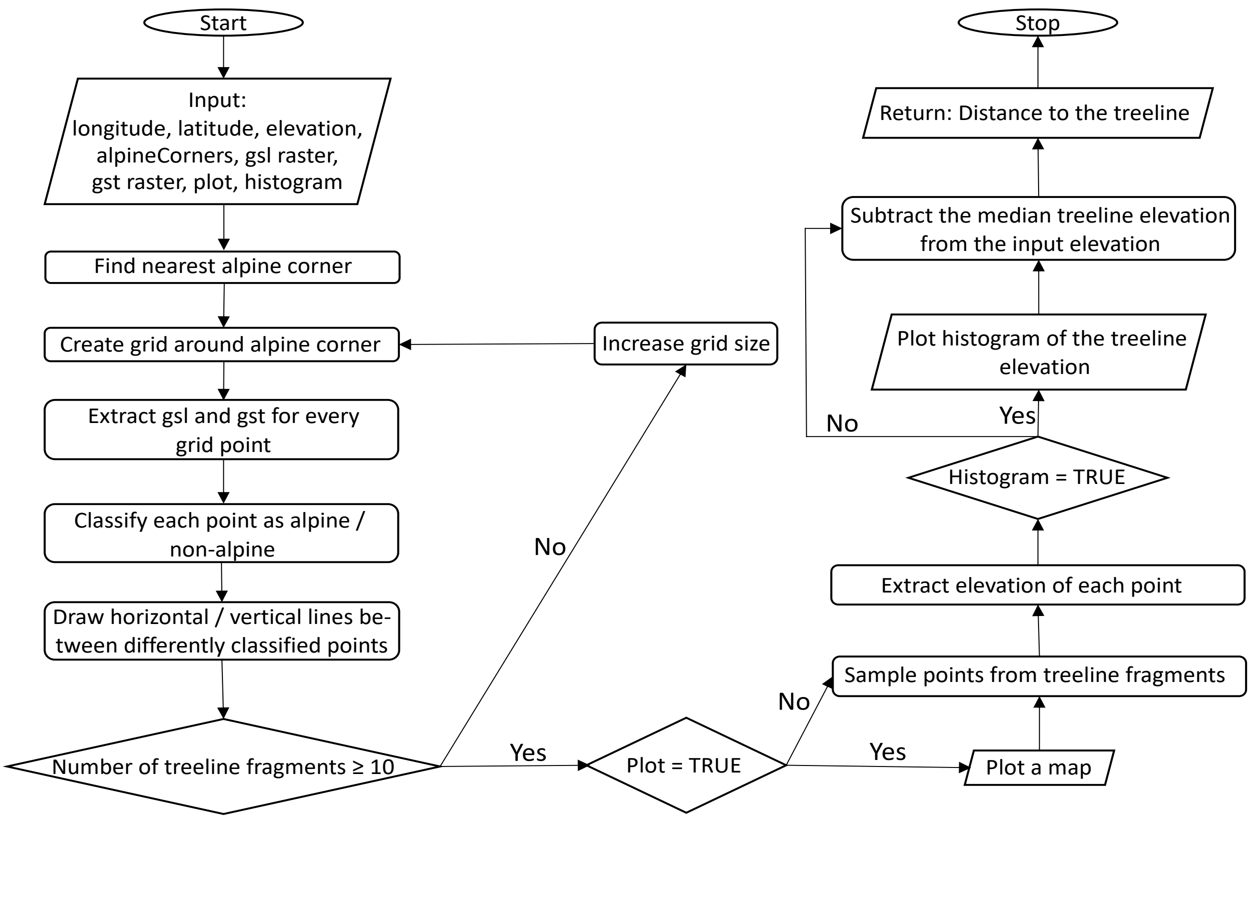

FIGURE 1: Process flowchart of the R-package ElevDistr, developed here. Arrows show the order of operations, ovals indicate the start or stop, rectangles represent operations, and diamonds depict decisions or conditional operations. Gsl: growing season length; gst for growing season temperature. Negative distance-to-treeline values represent a 'non-alpine' classification.

above the treeline, here based on CHELSA V2.1 (Karger et al., 2017). Vertical and horizontal lines are then drawn between adjacent points that were classified differently; these lines represent the local treeline. Then the median elevation of points drawn along the lines is extracted from a digital elevation model (Miliaresis & Argialas, 1999) to represent the elevation of the local treeline. Finally, the elevation of the input coordinate is subtracted from the local treeline elevation to classify it as above ('alpine') or below ('non-alpine') the local treeline, and to calculate the absolute vertical distance to the treeline. Thus, the algorithm is relatively insensitive to spatial uncertainty in latitude and longitude, due to its leveraging of coordinate elevation (sensitivity analysis in supplementary text S1). Finally, we used ElevDistr and the same filtering thresholds as for the polygon method (i.e., unfiltered, 5% and 20%) to classify species as 'alpine', 'non-alpine' or 'both'.

The ElevDistr algorithm is implemented as a computationally efficient R-package that requires ca. 0.45 seconds per spatial point on a laptop computer (MacBook Pro 2019 with a 2.4 GHz Quad-Core Intel Core i5 processor). A more detailed description is provided online (GitHub Wiki page "How the wrapper works"; https://github.com/LivioBaetscher/ElevDistr/wiki/ElevDistr#how-the-wrapper-works).

Classification Performance

For each of the three classes (i.e., 'alpine', 'non-alpine', or 'both'), we measured the performance of the six classifications (i.e., polygon method and ElevDistr, each with three filtering thresholds) across the 3,317 species using the following metrics: fraction of species correctly assigned to a class (i.e., precision), fraction of species retrieved from the "true" class (i.e., recall), fraction of species classified as present but truly absent (i.e., false positive rate or Type I error rate) and fraction of species classified as absent but truly present (i.e., false negative rate or Type II error rate). Finally, for the six focal clades selected below, we computed the fraction of false positive errors (FFP) under each classification model.

$$FFP = \frac{false\ positive\ rate}{(false\ positive\ rate + false\ negative\ rate)}$$

Modeling Dispersal and Extirpation

To determine how tip-state-error affects dispersal and extirpation rate estimation, we used DEC models parameterized for six clades of one genus each (plus outgroups). These genera span the phylogenetic diversity of alpine lineages, have sufficient species to reliably parameterize DEC models, and contain ample lineages that radiated in the Alps: *Campanula* (including *Phyteuma, Physoplexis,* and *Adenophora)*, *Carex* (including *Cobresia*), *Festuca* (including allied genera), *Ranunculus* (including *Ficaria*), *Saxifraga* (excluding *Micranthes*)*,* and *Viola*, all among the 10 most speciose genera in Aeschimann et al., 2004 (detailed justification of circumscription and taxon sampling in supplementary text S1). For each genus, we inferred a time-calibrated phylogeny using the OneTwoTree pipeline (Drori et al., 2018), which takes a list of taxa as input. First it performs name resolution (accounting for synonyms relative to the NCBI names backbone, misspellings, etc.), and downloads all relevant sequence data from GenBank's nucleotide archive. Next, OneTwoTree joins ITS1 and ITS2, and uses a modified OrthoMCL (Li et al., 2003) to cluster "non-ITS" sequences into orthologous groups that are treated as phylogenetic loci (circumventing issues of inconsistent locus naming in GenBank). Then, it aligns phylogenetic loci using MAFFT (Katoh & Standley, 2013), and performs a concatenated phylogenetic analysis using RAxML (Stamatakis, 2015). Accession matrices are provided in Supplementary Table S1. We confirmed high topological congruence with published phylogenies and transformed each tree into a chronogram using a correlated molecular clock model (Paradis, 2013) implemented in the R-package ape (Paradis & Schliep, 2019). We considered ten lambda values (from 0.1 to 1 with an increment of 0.1), retaining the one resulting in the highest log-likelihood. Absolute time-calibration was derived from published studies (Cai et al., 2019; Emadzade & Hörandl, 2011; Inda et al., 2008; Jones et al., 2017; Villaverde et al., 2020; Zhang et al., 2020). Next, we implemented Bayesian DEC models (in RevBayes; Höhna et al., 2016) to compute posterior distributions of the dispersal and extirpation rates using the inferred phylogenies plus presence-absence data of the ranges 'alpine', 'non-alpine' (from different classification approaches). Priors for both rates were log-uniform distributions; cladogenetic range evolution considered the event types: allopatry, subset sympatry, and full sympatry. We ran the Markov chain Monte Carlos (MCMC) analysis for 10^5 iterations (or 10^7 if required to reach an effective sample size of more than 200), removed 10% of the chain length as burn-in, and computed the posterior mean and 95% highest posterior density (HPD) interval of the dispersal and extirpation rates, and thinned them to 100 samples. Finally, to test the hypothesis that tip-state-error biases DEC model parameterization, we ran two Bayesian phylogenetic regression analyses (one for dispersal rate and one for extirpation rate), using the R-package brms (Bürkner, 2019), thus fully accounting for DEC-model parameterization uncertainty. Specifically, we set the dispersal or extirpation rate MCMC samples as the response variable, included the fraction of false positive tip-state-assignment (FFP) as predictor, and the genus as a covariate. To account for the phylogenetic relations among genera, we computed the phylogenetic variance-covariance matrix from a maximum likelihood chronogram for the 6 genera obtained using the OneTwoTree pipeline and Paradis (2013) as described above. Each brms model used 4 chains, with 50,000 iterations after 50,000 generations warm-up. If the 95% HPD interval for the effect of FFP does not include 0, we conclude that FFP biases the model parameterization, while taking full account of parameter uncertainty within each genus, as well as possible confounding effects due to phylogenetic relations among genera.

RESULTS

Classification Performance Metrics

The distribution of plant species over the classes 'non-alpine', 'both', and 'alpine' were skewed towards the 'non-alpine' (Table 1), with 75.7%, 23.7% and 0.6% species assigned to them in the validation data, respectively (Table 1 for detailed results). Overall, ElevDistr outperformed the polygon method (Table 1). Under its optimal filtering threshold of ≥5%, ElevDistr classifies more species correctly (89.72%) than the polygon method under its optimal setting (20% filtering, 85.95% correct). Importantly, filtering strongly impacted all performance indicators (Table 1, S2, Fig 2). Specifically, increased filtering lowered the number of species that are (correctly or incorrectly) classified as 'both' for both algorithms: from 1,734 (52.28%) to 569 (17.15%) for the polygon method; from 965 (29.09%) to 328 (9.89%) species for ElevDistr (Table 1). For the classes 'alpine' and 'non-alpine' under both approaches, increased filtering caused a decline in precision and an increase in recall (Fig. 2A and C), while the inverse trend occurred for the class 'both' (Fig 2B). Moreover, increased filtering decreased the false positive rate (Fig. 2D) and increased the false negative rate (Fig. 2E), leading to a decrease of the fraction of false positive (Fig. 2F). The most balanced FFP of 0.5 (i.e., when the proportion of false positives to false negatives is equal) was best approached when using ElevDistr and no filtering (FFP = 0.71). The polygon method achieved a less balanced error rate: without filtering, the rate is strongly skewed toward false positives (FFP=0.92), but decreases to 0.27 with 20% filtering, which was otherwise optimal. Thus, while the polygon method required strong filtering to achieve most correct class assignments, this came at the cost of a relatively high false negative rate. ElevDistr did not require strong filtering and was therefore less susceptible to skewed error rates.

TABLE 1: Classification results of the 3,317 species of the European Alps, under two methods combined with three filtering thresholds. The "true class" represents expert opinion (Flora Alpina) and "classified as" represents the class assigned to a species using the approach declared in the top row. Shaded rows highlight the correct classifications. The sum of correct classified species is indicated. The number in parentheses represents the overall percentage rounded to two digits.

True class	**Classified as**	**Polygon unfiltered**	**Polygon (≥5%)**	**Polygon (≥20%)**	**ElevDistr unfiltered**	**ElevDistr (≥5%)**	**ElevDistr (≥20%)**
Alpine (n=20; 0.6%)	Alpine	3 (0.09%)	4 (0.12%)	7 (0.21%)	4 (0.12%)	5 (0.15%)	9 (0.27%)
	Both	16 (0.48%)	15 (0.45%)	11 (0.33%)	16 (0.48%)	15 (0.45%)	10 (0.3%)
	Non-alpine	1 (0.03%)	1 (0.03%)	2 (0.06%)	0 (0%)	0 (0%)	1 (0.03%)
Both (n=786; 23.7%)	Alpine	6 (0.18%)	10 (0.3%)	61 (1.84%)	10 (0.3%)	19 (0.57%)	81 (2.44%)
	Both	706 (21.28%)	659 (19.87%)	449 (13.54%)	658 (19.84%)	527 (15.89%)	307 (9.26%)
	Non-alpine	74 (2.23%)	117 (3.53%)	276 (8.32%)	118 (3.56%)	240 (7.24%)	398 (12%)
Non-alpine (n=2,511; 75.7%)	Alpine	2 (0.06%)	3 (0.09%)	5 (0.15%)	0 (0%)	0 (0%)	1 (0.03%)
	Both	1,012 (30.51%)	453 (13.66%)	109 (3.29%)	291 (8.77%)	67 (2.02%)	11 (0.33%)
	Non-alpine	1,495 (45.07%)	2,053 (61.89%)	2,395 (72.2%)	2,220 (66.93%)	2,444 (73.68%)	2,499 (75.34%)
	None*	2 (0.06%)	2 (0.06%)	2 (0.06%)	0 (0%)	0 (0%)	0 (0%)
Total correctly classified		2,204 (66.45%)	2,716 (81.88%)	2,851 (85.95%)	2,882 (86.89%)	2,976 (89.72%)	2,815 (84.87%)

*: undefined climatic belt in (Körner et al., 2011)

DEC Model Bias

Across the six clades, tip-state-error strongly affected dispersal and extirpation rate estimation (Fig. 3, Table S3), ElevDistr overall greatly outperforming the polygon method, in congruence with its better classification results. Specifically, ElevDistr (unfiltered) underestimated the extirpation rate by 8.98%, while the Polygon method underestimated it 27.03% (unfiltered) or overestimated it 55.09% (20% filtering). The dispersal rate responded even more extreme to tip-state-error: using ElevDistr (unfiltered) led to an underestimation by 0.74%, while the polygon method overestimated it by 145.88% (unfiltered) or underestimated it by 61.95% (20% filtering; Table S3).

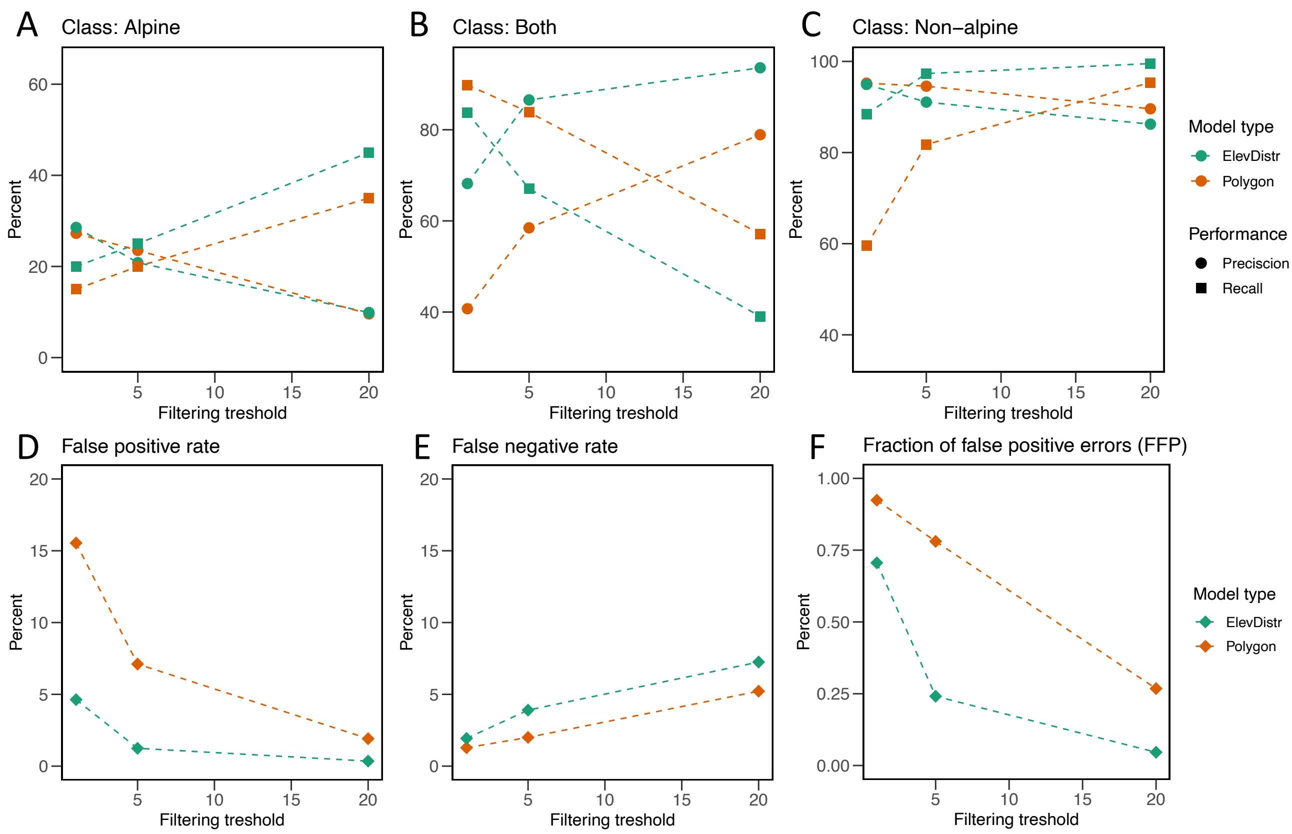

FIGURE 2: Performance metrics as a function of filtering thresholds across the different classification methods. Colors represent the different classification approaches: green, ElevDistr; orange, polygon approach. Note that across panels a-c, the absolute range of the y-axis differs but the scale is identical. a) to c) contain precision (circle) and recall (squares) of the different classes: a) alpine, b) both and c) non-alpine. d) contains the false positive rates, e) shows the false negative rates and f) the fraction of false positive errors (FFP).

Because tip-scoring methods resulted in different fractions of false positive errors (FFP; Fig. 2), we can interpret DEC model parameterization as a function of FFP. Indeed, our phylogenetic regression models that account for parameterization uncertainty revealed that FFP drives biased rate estimation (Fig. 3, Table S3). Specifically, FFP was overall significantly positively related to the dispersal rate (posterior mean slope 1.32, 95% HPD interval 1.26 - 1.38) and significantly negatively related to the extirpation rate (posterior mean slope -0.43, 95% HPD interval -0.45 - -0.41). This demonstrates that tip-scoring-error strongly affected DEC model parameterization, therefore we reject the null hypothesis of no effect. Nevertheless, the posterior mean DEC model rates under the Flora Alpina scoring differed across genera (Table S3): dispersal (i.e., the ability of gaining alpine biome occupancy) ranged three orders of magnitudes, from 0.0079 to 9.2 shifts per lineage per million years in *Viola*

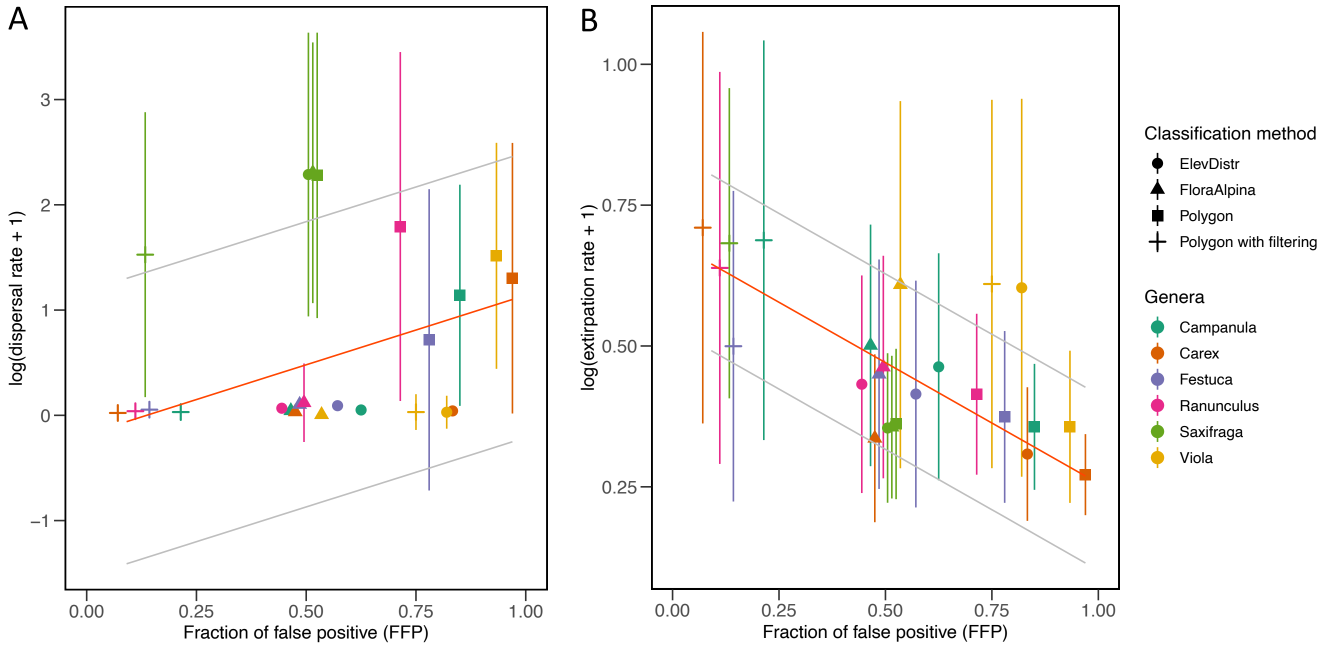

FIGURE 3: The fraction of false positive tip-scoring-error drives dispersal rate (panel a) and extirpation rate (panel b) estimation. Red lines show the estimated posterior mean regression line of the phylogenetic regression, gray lines represent the upper and lower 95% confidence interval of the model. The point color represents the different genera, and the point shape illustrates the classification model (see legend on the right). Vertical bars extend one standard deviation in either direction.

and *Saxifraga*, respectively. The extirpation rate (i.e., the loss of alpine biome occupancy) varied considerably less, from 0.39 to 0.87 shifts per lineage per million years in *Carex* and *Viola*, respectively. Indeed, genera varied significantly in dispersal and extirpation rates, with genus explaining 86% (95% HPD interval 68 - 98%) and 50% (95% HPD interval 22 - 86%) of the total rate variation, respectively.

DISCUSSION

As phylogenetic trees (e.g., Figueroa et al., 2022; Kerkhoff et al., 2014; Zanne et al., 2014) and relevant spatial data sources (Heberling et al., 2021) are becoming increasingly large, some form of automated tip-scoring has become inevitable, underscoring the importance of understanding possible effects of tip-state-errors on biogeographic inference. Curiously, the causes and consequences of such misclassifications have rarely been explicitly evaluated (but see: Edwards et al., 2015 in response to Zanne et al., 2014), possibly because of the usual implicit assumption that phylogenetic noise does not necessarily equate bias (L. Lu et al., 2020). Nevertheless, our results reveal that various approaches to tip-scoring greatly matter (Table 1, Fig 2), because they ultimately result in significantly differently parameterized DEC models (Fig 3, Table S3), with false positive and false negative rates having distinct effects (Fig 3, Table S2). Here we discuss how to mitigate tip-state-errors when classifying species as ‘alpine’ or ‘non-alpine’ and interpret our results more broadly in the context of alpine plant evolution.

Avoiding tip-state-errors

Phylogenetic biogeographic inference usually involves classifying whether taxa are present or absent across a range of predefined geographic areas. Often this is unproblematic, for instance when the areas of interest are well-defined, such as continents or islands (Caujapé-Castells et al., 2022; Emadzade & Hörandl, 2011; Matzke, 2014). However, classifying tips becomes a greatly more challenging when areas of interest have irregular or spatially complex borders, such as biomes (Donoghue & Edwards, 2014; Ringelberg et al., 2020; Thomas et al., 2023). This is particularly true for the alpine biome. Accordingly, the polygon classification using the global thermal belt layers (Körner et al., 2011), resulted in every third species being wrongly classified (2,204 of 3,317 species classifications were correct, Table 1). Therefore, more than a thousand ‘non-alpine’ species were wrongly assigned to also occur above the treeline using a naive polygon classification approach. Here, requiring >20% of the observations to be above the treeline for it to be classified as present improves this, but at the cost of strongly negatively affecting precision of species classified as ‘alpine’ (Fig. 2A) and the recall of ‘both’ (Fig. 2B), also leading to most errors being false negatives (Fig. 2E), causing important downstream effects (see below).

The reason for this poor performance must lie in the nature of the climatic treeline: although its climatic boundary is very well-defined (based on the combination of temperature and duration thresholds; Paulsen & Körner, 2014), the resulting topographic boundary is much more fine-grained than the thermal belt layers can capture. The upper climatic treeline is locally affected by slope exposure and topography, the mountain mass elevation effect, as well as the latitude (Körner, 2012). Therefore, the climatic treeline only locally coincides with a particular elevation, varying about five vertical kilometers globally, and hundreds of meters within the European Alpine Arc (Körner, 2021). Due to the steep nature of the Alps, a grid-cell containing a slope with ≥30° inclination likely spans multiple thermal belts, while only one value can be assigned.

ElevDistr circumvents the issue of high topographic heterogeneity and greatly improves classification results, even without filtering (Table 1), by leveraging that vertical precision very frequently exceeds horizontal coordinate precision. Often, elevation is known independently of and more precisely than latitude and longitude, for instance because an altimeter reading was provided on an otherwise crudely georeferenced herbarium label (pers. obs.), or national data centers provide GBIF with gridded rather than individual point localities but retain original coordinate elevation (pers. obs.). Comparing the stated elevation to a locally computed treeline elevation resulted in low error rates, plus adequate precision, and recall (Fig. 2), as well as low noise sensitivity, outperforming the polygon method (supplementary text S1 and Fig. S1). Strict exclusion settings for spatial uncertainty can thus be avoided, optimizing the amount of information extracted from noisy spatial data.

Though default behavior of ElevDistr currently is tailored towards the climatic treeline, it can be easily adjusted to capture a range of vertically structured biome boundaries, such as other thermal belts or depth-stratified occurrences of aquatic organisms, as it is programmed to rapidly process any kind of noisy GBIF data (e.g., gsl and gst thresholds can easily be adjusted). Furthermore, gsl and gst can be replaced by any numerical climatic product, making it potentially useful for many thresholds in any continuous climatic cline (speculative examples include the number of frost days to model mangrove distributions, or fire frequency to model savannah boundaries). Finally, the modularity of the package facilitates advanced users to use certain functions in a horizontal context (e.g., finding the nearest point of a biome, gridded sampling, or plotting / data visualization).

We also reveal the effect of different filtering thresholds on classification performance more generally, which to our knowledge has not been generally discussed. We show that many species are initially (without filtering) classified as 'both', but under an increasingly stringent filtering threshold these species are reassigned to the class 'non-alpine' (Table 1). This can be explained because filtering reallocates species with <5% or <20% observations above or below the treeline away from the class 'both', into the classes 'non-alpine' or 'alpine'. Because the number of species strictly occurring in the lowland greatly exceeds the number of the remaining categories (Aeschimann et al., 2004; Schröter et al., 1926), the effect of filtering seems to be beneficial to classification performance specifically in an alpine context, where too many species are assigned to the class 'both'. However, filtering leads to an increase in the false negative and a decrease in the false positive rate irrespective of classification method (Fig. 2), which we will now reveal is a major cause of DEC model bias.

DEC model bias

Typically, tip scoring occurs based on incomplete knowledge of species distribution and biology, making it very critical to know if potentially unavoidable tip-state-errors affect the estimated rates: is it noise or bias? We used a DEC model to infer dispersal and extirpation rate for six clades native to and species-rich in the Alpine Arc (Table S3). This area is particularly well known, allowing us to detect tip-scoring-error and compare “true” rates with those based on different automated approaches. Strikingly, posterior mean rates differ generally 1-2 orders of magnitude across classification approaches (Table S3): in general, stringent filtering leads to increased extirpation rates and decreased dispersal rates (Table S3). This is because filtering penalizes occurrence in the alpine (see above), meaning that the DEC model infers a high probability of lineages to lose the ability to occur in the alpine (high extirpation), and a low probability of lineages to gain the ability to occur there (low dispersal).

That the DEC model bias is driven by the relative frequency of false positive compared to false negative error, is underlined by the phylogenetic regressions of the fraction of false positives (FFP, Fig. 3), that document significant biases: a positive effect of FFP on dispersal rates, and a negative effect on extirpation rates. To exemplify, the polygon filtering approach on *Ranunculus* (Fig.3, Table S3) led to a low false positive rate (0.0114) and a much higher false negative rate (0.1136), because many species that belong to the class ‘both’ were classified as ‘non-alpine’ (i.e., FFP of 0.09). The DEC model compensates in two ways: with a low dispersal rate into the Alps (0.0386; validation rate: 0.1465) and a high extirpation rate (0.8980; validation rate: 0.6020). The same is true with the inverse scenario: high FFP caused by a high false positive and a low false negative rate. Here the DEC model needs to compensate for many wrong presences (i.e., to many species are wrongly assigned to the class ‘both’), leading to an overestimated dispersal and an underestimated extirpation rate. These results likely transfer well to other study systems using DEC models and automated tip-scoring and warrant a careful validation of tip scoring. Strikingly, both the dispersal and the extirpation rate react so strongly to the FFP, that we were required to natural-log-transform the rates to find a linear correlation, revealing that the overall magnitude of the estimation error changes exponentially with the fraction of false positive classifications. We suggest that the FFP is a good measure to assess the risk of DEC model bias, which careful validation of a subset of automated phylogenetic tip classifications would reveal.

Biome shifts into the alpine environment

Phylogenetic studies of plant evolution within or into particular biomes are broadly relevant, because they shed light on the fundamental nature of niche evolution (Donoghue & Edwards, 2014; Ringelberg et al., 2020; Smyčka et al., 2022). Although several phylogenetic studies have documented the timing of biome shifts into the alpine (e.g., Ding et al., 2020; Ebersbach et al., 2017) and shifted diversification rates in relation to such niche shifts (e.g., Kong et al., 2021), it is poorly known what drives the rate of evolution of biome occupancy per se. By comparing the rates of biome shifts across the 6 genera (based on the "true" classification of species) we can tentatively suggest that this rate differs greatly across genera. Particularly, our phylogenetic regressions that accounts for the phylogenetic relations among genera showed a very high phylogenetic variance component (86 and 50%), indicating genus-specific differences in dispersal and extirpation rate, respectively (Table S3). However, it is important to note that rate comparisons across genera are tentative, because we geographically subsampled the focal clades (namely by those taxa that occur in the European Alpine Arc), resulting in low and differing sampling fractions for each clade (i.e., the fraction of alpine species among the non-sampled species may differ for each genus). Nevertheless, our results are similar to those of Smyčka et al. (2022), who found clade-specific speciation rates, and that clades differed in whether cold episodes promoted or hindered speciation, tentatively suggesting that clade-specific rates of biome shifts may not represent methodological artifact but biological reality. If so, it would reflect that biome shifts may be easily accessible in genera that are already pre-adapted (Donoghue & Edwards, 2014; Edwards & Donoghue, 2013), for instance in species in low-elevation rocky outcrops or in subalpine avalanche gullies where they are already adapted to open habitat. Overall, these results are in line with the framework of Donoghue & Edwards (2014) who suggest that the probability of biome shifting depends on the geographical opportunity (i.e., distance to the biome border), preexisting adaptations (i.e., “enabler” traits), and ecological interactions with other species. Because the six genera differ in their distributions (Aeschimann et al., 2004), have different traits, and may have different species interactions (positive or negative), our results agree with the general expectation that rates of niche evolution may be lineage specific.

Moreover, that non-alpine-only species so greatly outnumber alpine-only species (Table 1) implies that biome shifts are likely asymmetric, mostly entailing non-alpine species dispersing into the alpine biome (i.e., becoming frost tolerant and adjusting to a short growing season), rather than alpine species dispersing below the treeline (i.e., becoming shade tolerant and more competitive). Disentangling the underlying drivers of differential biome shift rates and directional asymmetries would require more fine-grained analyses including critical dimensions such as geographical and microclimatic distance. Further, it would require near complete taxonomic sampling of large monophyletic clades of which species limits are clear, and occurrence relative to the climatic treeline is well-known across their entire range. We tentatively suggest as a promising avenue analyzing biome shifts as a series of continuous climatic determinants, rather than simplifying biomes to a simple discrete state where species occurring one meter above sea-level are not differentiated from species one meter below the treeline. Indeed, ElevDistr potentially offers the formidable opportunity to use the vertical distance to the treeline as a proxy for the climatic distance to the biome border in form of a continuous variable to reconstruct biome shifts. This would also allow to leverage a broader suit of phylogenetic comparative methods to more accurately model the evolution of biome shifts (Hackel & Sanmartín, 2021; Höhna et al., 2016).

CONCLUSION

Exponentially increasing phylogenetic and geographic data availability in recent years may inevitably dictate automated assignment of states to phylogenetic tips. We show in an Alpine context that suitable algorithms may minimize tip-state-errors, exemplified by our approach ElevDistr, because it appropriately handles spatial heterogeneity and is less sensitive to spatial uncertainty. Importantly, tip-state-errors bias parameterization of DEC models, where the relative prevalence of false positive errors leads to upward bias of dispersal rates and downward bias of extirpation rates. Thus, the fraction of false positive errors (FFP) provides an illuminating summary statistic to gauge whether DEC model bias is to be expected, necessitating careful validation in any biogeographic context. These results suggest that studies combining automated tip-scoring and DEC models are susceptible to these biases. Finally, our results tentatively suggest differences in dispersal and extirpation rates across the six examined genera, which may indicate that the probability of alpine biome shifts may be strongly dependent on genus-specific trait evolvability (Edwards & Donoghue, 2013) and geographic opportunity through time (Landis et al., 2021).

ACKNOWLEDGEMENT

We thank our colleagues from the Physiological Plant Ecology Group in Basel for discussing the content of this paper and for providing useful advice and comments. This work was supported by the Swiss National Science Foundation (grant 310030_185251 to JMdV). In this study, no permits were required.

REFERENCES

Aeschimann, D., Lauber, K., Moser, D. M., & Theurillat, J.-P. (2004). *Flora alpina: atlas des 4500 plantes vasculaires des Alpes*. Haupt Publisher. https://doi.org/10.2307/25065454

Albert, J. S., Schoolmaster, D. R., Tagliacollo, V., & Duke-Sylvester, S. M. (2017). Barrier Displacement on a Neutral Landscape: Toward a Theory of Continental Biogeography. *Systematic Biology*, *66*(2), syw080. https://doi.org/10.1093/sysbio/syw080

Andersen, M. J., McCullough, J. M., Mauck, W. M., Smith, B. T., & Moyle, R. G. (2018). A phylogeny of kingfishers reveals an Indomalayan origin and elevated rates of diversification on oceanic islands. *Journal of Biogeography*, *45*(2), 269–281. https://doi.org/10.1111/jbi.13139

Antonelli, A., Kissling, W. D., Flantua, S. G. A., Bermúdez, M. A., Mulch, A., Muellner-Riehl, A. N., Kreft, H., Linder, H. P., Badgley, C., Fjeldså, J., Fritz, S. A., Rahbek, C., Herman, F., Hooghiemstra, H., & Hoorn, C. (2018). Geological and climatic influences on mountain biodiversity. *Nature Geoscience*, *11*(10), 718–725. https://doi.org/10.1038/s41561-018-0236-z

Arya, S., Mount, D., Kemp, S. E., & Jefferis, G. (2019). *RANN: fast nearest neighbour search (wraps ANN library) using L2 metric* (2.1).

Asadi, A., Montgelard, C., Nazarizadeh, M., Moghaddasi, A., Fatemizadeh, F., Simonov, E., Kami, H. G., & Kaboli, M. (2019). Evolutionary history and postglacial colonization of an Asian pit viper (Gloydius halys caucasicus) into Transcaucasia revealed by phylogenetic and phylogeographic analyses. *Scientific Reports*, *9*(1), 1224. https://doi.org/10.1038/s41598-018-37558-8

Avise, J. C., Arnold, J., Ball, R. M., Bermingham, E., Lamb, T., Neigel, J. E., Reeb, C. A., & Saunders, N. C. (1987). Intraspecific Phylogeography: The Mitochondrial DNA Bridge Between Population Genetics and Systematics. *Annual Review of Ecology and Systematics*, *18*(1), 489–522. https://doi.org/10.1146/annurev.es.18.110187.002421

Barry, R. G. (1978). H.-B. de Saussure: The First Mountain Meteorologist. *Bulletin of the American Meteorological Society*, *59*(6), 702–705. https://doi.org/10.1175/1520-0477(1978)059<0702:HBDSTF>2.0.CO;2

Beck, J., Ballesteros-Mejia, L., Nagel, P., & Kitching, I. J. (2013). Online solutions and the 'Wallacean shortfall': what does GBIF contribute to our knowledge of species' ranges? *Diversity and Distributions*, *19*(8), 1043–1050. https://doi.org/10.1111/ddi.12083

Beck, J., Böller, M., Erhardt, A., & Schwanghart, W. (2014). Spatial bias in the GBIF database and its effect on modeling species' geographic distributions. *Ecological Informatics*, *19*, 10–15. https://doi.org/10.1016/j.ecoinf.2013.11.002

Browne, J. (1984). The secular ark: studies in the history of biogeography. *Journal of the History of Biology*, *17*.

Bürkner, P.-C. (2019). Bayesian Item Response Modeling in R with brms and Stan. *ArXiv*. https://doi.org/10.48550/arxiv.1905.09501

Cai, L., Xi, Z., Amorim, A. M., Sugumaran, M., Rest, J. S., Liu, L., & Davis, C. C. (2019). Widespread ancient whole-genome duplications in Malpighiales coincide with Eocene global climatic upheaval. *New Phytologist*, *221*(1), 565–576. https://doi.org/10.1111/nph.15357

Carbutt, C. (2019). The Drakensberg Mountain Centre: A necessary revision of southern Africa's high-elevation centre of plant endemism. *South African Journal of Botany*, *124*, 508–529. https://doi.org/10.1016/j.sajb.2019.05.032

Caujapé-Castells, J., García-Verdugo, C., Sanmartín, I., Fuertes-Aguilar, J., Romeiras, M. M., Zurita-Pérez, N., & Nebot, R. (2022). The late Pleistocene endemicity increase hypothesis and the origins of diversity in the Canary Islands Flora. *Journal of Biogeography*, *49*(8), 1469–1480. https://doi.org/10.1111/jbi.14394

Chamberlain, S., Oldoni, D., & Waller, J. (2022). *rgbif: Interface to the Global Biodiversity Information Facility API.*

Darwin, C. (1859). *On the origin of species*. John Murray.

Ding, W.-N., Ree, R. H., Spicer, R. A., & Xing, Y.-W. (2020). Ancient orogenic and monsoon-driven assembly of the world's richest temperate alpine flora. *Science*, *369*(6503), 578–581. https://doi.org/10.1126/science.abb4484

Donoghue, M. J., & Edwards, E. J. (2014). Biome Shifts and Niche Evolution in Plants. *Annual Review of Ecology, Evolution, and Systematics*, *45*(1), 1–26. https://doi.org/10.1146/annurev-ecolsys-120213-091905

Drori, M., Rice, A., Einhorn, M., Chay, O., Glick, L., & Mayrose, I. (2018). OneTwoTree: An online tool for phylogeny reconstruction. *Molecular Ecology Resources*, *18*(6), 1492–1499. https://doi.org/10.1111/1755-0998.12927

Ebersbach, J., Muellner-Riehl, A. N., Michalak, I., Tkach, N., Hoffmann, M. H., Röser, M., Sun, H., & Favre, A. (2017). In and out of the Qinghai-Tibet Plateau: divergence time estimation and historical biogeography of the large arctic-alpine genus Saxifraga L. *Journal of Biogeography*, *44*(4), 900–910. https://doi.org/10.1111/jbi.12899

Edwards, E. J., & Donoghue, M. J. (2013). Is it easy to move and easy to evolve? Evolutionary accessibility and adaptation. *Journal of Experimental Botany*, *64*(13), 4047–4052. https://doi.org/10.1093/jxb/ert220

Edwards, E. J., Vos, J. M. de, & Donoghue, M. J. (2015). Doubtful pathways to cold tolerance in plants. *Nature*, *521*(7552), E5–E6. https://doi.org/10.1038/nature14393

Emadzade, K., & Hörandl, E. (2011). Northern Hemisphere origin, transoceanic dispersal, and diversification of Ranunculeae DC. (Ranunculaceae) in the Cenozoic. *Journal of Biogeography*, *38*(3), 517–530. https://doi.org/10.1111/j.1365-2699.2010.02404.x

Felsenstein, J. (1985). Phylogenies and the Comparative Method. *The American Naturalist*, *125*(1), 1–15. https://doi.org/10.1086/284325

Figueroa, H. F., Marx, H. E., Cortez, M. B. de S., Grady, C. J., Engle-Wrye, N. J., Beach, J., Stewart, A., Folk, R. A., Soltis, D. E., Soltis, P. S., & Smith, S. A. (2022). Contrasting patterns of phylogenetic diversity and alpine specialization across the alpine flora of the American mountain range system. *Alpine Botany*, *132*(1), 107–122. https://doi.org/10.1007/s00035-021-00261-y

Goldberg, E. E., Lancaster, L. T., & Ree, R. H. (2011). Phylogenetic Inference of Reciprocal Effects between Geographic Range Evolution and Diversification. *Systematic Biology*, *60*(4), 451–465. https://doi.org/10.1093/sysbio/syr046

Gori, B., Ulian, T., Bernal, H. Y., & Diazgranados, M. (2022). Understanding the diversity and biogeography of Colombian edible plants. *Scientific Reports*, *12*(1), 7835. https://doi.org/10.1038/s41598-022-11600-2

Hackel, J., & Sanmartín, I. (2021). Modelling the tempo and mode of lineage dispersal. *Trends in Ecology & Evolution*, *36*(12), 1102–1112. https://doi.org/10.1016/j.tree.2021.07.007

Heberling, J. M., Miller, J. T., Noesgaard, D., Weingart, S. B., & Schigel, D. (2021). Data integration enables global biodiversity synthesis. *Proceedings of the National Academy of Sciences*, *118*(6), e2018093118. https://doi.org/10.1073/pnas.2018093118

Höhna, S., Landis, M. J., Heath, T. A., Boussau, B., Lartillot, N., Moore, B. R., Huelsenbeck, J. P., & Ronquist, F. (2016). RevBayes: Bayesian Phylogenetic Inference Using Graphical Models and an Interactive Model-Specification Language. *Systematic Biology*, *65*(4), 726–736. https://doi.org/10.1093/sysbio/syw021

Humboldt, A. von. (1805). *Essai sur la géographie des plantes: accompagne d'un tableau physique des régions équinoxiales, fondé sur des mesures exécutées, depuis le dixième degré la latitude boréale juasqu'au dixième degré de latitude australe, pendant les années 1799, 1800, 1801, 1802 et 1803 par AI.*

Humphries, C. J., & Parenti, L. R. (1999). *Cladistic biogeography*. OUP Oxford.

Inda, L. A., Segarra-Moragues, J. G., Müller, J., Peterson, P. M., & Catalán, P. (2008). Dated historical biogeography of the temperate Loliinae (Poaceae, Pooideae) grasses in the northern and southern hemispheres. *Molecular Phylogenetics and Evolution*, *46*(3), 932–957. https://doi.org/10.1016/j.ympev.2007.11.022

Jetz, W., Thomas, G. H., Joy, J. B., Hartmann, K., & Mooers, A. O. (2012). The global diversity of birds in space and time. *Nature*, *491*(7424), 444–448. https://doi.org/10.1038/nature11631

Jones, K. E., Korotkova, N., Petersen, J., Henning, T., Borsch, T., & Kilian, N. (2017). Dynamic diversification history with rate upshifts in Holarctic bell-flowers (Campanula and allies). *Cladistics*, *33*(6), 637–666. https://doi.org/10.1111/cla.12187

Karger, D. N., Conrad, O., Böhner, J., Kawohl, T., Kreft, H., Soria-Auza, R. W., Zimmermann, N. E., Linder, H. P., & Kessler, M. (2017). Climatologies at high resolution for the earth's land surface areas. *Scientific Data*, *4*(1), 170122. https://doi.org/10.1038/sdata.2017.122

Katoh, K., & Standley, D. M. (2013). MAFFT Multiple Sequence Alignment Software Version 7: Improvements in Performance and Usability. *Molecular Biology and Evolution*, *30*(4), 772–780. https://doi.org/10.1093/molbev/mst010

Kerkhoff, A. J., Moriarty, P. E., & Weiser, M. D. (2014). The latitudinal species richness gradient in New World woody angiosperms is consistent with the tropical conservatism hypothesis. *Proceedings of the National Academy of Sciences*, *111*(22), 8125–8130. https://doi.org/10.1073/pnas.1308932111

Kong, H., Condamine, F. L., Yang, L., Harris, A. J., Feng, C., Wen, F., & Kang, M. (2021). Phylogenomic and Macroevolutionary Evidence for an Explosive Radiation of a Plant Genus in the Miocene. *Systematic Biology*, *71*(3), syab068. https://doi.org/10.1093/sysbio/syab068

Körner, C. (2007). The use of 'altitude' in ecological research. *Trends in Ecology & Evolution*, *22*(11), 569–574. https://doi.org/10.1016/j.tree.2007.09.006

Körner, C. (2012). *Alpine Treelines, Functional Ecology of the Global High Elevation Tree Limits*. https://doi.org/10.1007/978-3-0348-0396-0

Körner, C. (2021). *Alpine Plant Life, Functional Plant Ecology of High Mountain Ecosystems*. https://doi.org/10.1007/978-3-030-59538-8

Körner, C., & Hiltbrunner, E. (2021). Why Is the Alpine Flora Comparatively Robust against Climatic Warming? *Diversity*, *13*(8), 383. https://doi.org/10.3390/d13080383

Körner, C., Paulsen, J., & Spehn, E. M. (2011). A definition of mountains and their bioclimatic belts for global comparisons of biodiversity data. *Alpine Botany*, *121*(2), 73. https://doi.org/10.1007/s00035-011-0094-4

Landis, M. J., Edwards, E. J., & Donoghue, M. J. (2021). Modeling Phylogenetic Biome Shifts on a Planet with a Past. *Systematic Biology*, *70*(1), 86–107. https://doi.org/10.1093/sysbio/syaa045

Landis, M. J., Freyman, W. A., & Baldwin, B. G. (2018). Retracing the Hawaiian silversword radiation despite phylogenetic, biogeographic, and paleogeographic uncertainty. *Evolution*, *72*(11), 2343–2359. https://doi.org/10.1111/evo.13594

Li, L., Stoeckert, C. J., & Roos, D. S. (2003). OrthoMCL: Identification of Ortholog Groups for Eukaryotic Genomes. *Genome Research*, *13*(9), 2178–2189. https://doi.org/10.1101/gr.1224503

López-Angulo, J., Pescador, D. S., Sánchez, A. M., Mihoč, M. A. K., Cavieres, L. A., & Escudero, A. (2018). Determinants of high mountain plant diversity in the Chilean Andes: From regional to local spatial scales. *PLoS ONE*, *13*(7), e0200216. https://doi.org/10.1371/journal.pone.0200216

Lu, L., Hu, H., Peng, D., Liu, B., Ye, J., Yang, T., Li, H., Sun, M., Smith, S. A., Soltis, P. S., Soltis, D. E., & Chen, Z. (2020). Noise does not equal bias in assessing the evolutionary history of the angiosperm flora of China: A response to Qian (2019). *Journal of Biogeography*, *47*(10), 2286–2291. https://doi.org/10.1111/jbi.13947

Lu, L.-M., Mao, L.-F., Yang, T., Ye, J.-F., Liu, B., Li, H.-L., Sun, M., Miller, J. T., Mathews, S., Hu, H.-H., Niu, Y.-T., Peng, D.-X., Chen, Y.-H., Smith, S. A., Chen, M., Xiang, K.-L., Le, C.-T., Dang, V.-C., Lu, A.-M., … Chen, Z.-D. (2018). Evolutionary history of the angiosperm flora of China. *Nature*, *554*(7691), 234–238. https://doi.org/10.1038/nature25485

MacArthur, R., & Wilson, E. O. (1967). *The Theory of Island Biogeography*. Princeton University Press.

Maddison, W. P., Midford, P. E., & Otto, S. P. (2007). Estimating a Binary Character's Effect on Speciation and Extinction. *Systematic Biology*, *56*(5), 701–710. https://doi.org/10.1080/10635150701607033

Matzke, N. J. (2014). Model Selection in Historical Biogeography Reveals that Founder-Event Speciation Is a Crucial Process in Island Clades. *Systematic Biology*, *63*(6), 951–970. https://doi.org/10.1093/sysbio/syu056

Miliaresis, G. C., & Argialas, D. P. (1999). Segmentation of physiographic features from the global digital elevation model/GTOPO30. *Computers & Geosciences*, *25*(7), 715–728. https://doi.org/10.1016/s0098-3004(99)00025-4

Mittelbach, G. G., Schemske, D. W., Cornell, H. V., Allen, A. P., Brown, J. M., Bush, M. B., Harrison, S. P., Hurlbert, A. H., Knowlton, N., Lessios, H. A., McCain, C. M., McCune, A. R., McDade, L. A., McPeek, M. A., Near, T. J., Price, T. D., Ricklefs, R. E., Roy, K., Sax, D. F., … Turelli, M. (2007). Evolution and the latitudinal diversity gradient: speciation, extinction and biogeography. *Ecology Letters*, *10*(4), 315–331. https://doi.org/10.1111/j.1461-0248.2007.01020.x

Paradis, E. (2013). Molecular dating of phylogenies by likelihood methods: A comparison of models and a new information criterion. *Molecular Phylogenetics and Evolution*, *67*(2), 436–444. https://doi.org/10.1016/j.ympev.2013.02.008

Paradis, E., & Schliep, K. (2019). ape 5.0: an environment for modern phylogenetics and evolutionary analyses in R. *Bioinformatics*, *35*(3), 526–528. https://doi.org/10.1093/bioinformatics/bty633

Parisod, C., Lavergne, S., Sun, H., & Kadereit, J. W. (2022). Plant evolutionary ecology in mountain regions in space and time. *Alpine Botany*, *132*(1), 1–4. https://doi.org/10.1007/s00035-022-00279-w

Paulsen, J., & Körner, C. (2014). A climate-based model to predict potential treeline position around the globe. *Alpine Botany*, *124*(1), 1–12. https://doi.org/10.1007/s00035-014-0124-0

Pelser, P. B., Nickrent, D. L., Ee, B. W. van, & Barcelona, J. F. (2019). A phylogenetic and biogeographic study of Rafflesia (Rafflesiaceae) in the Philippines: Limited dispersal and high island endemism. *Molecular Phylogenetics and Evolution*, *139*, 106555. https://doi.org/10.1016/j.ympev.2019.106555

Perrigo, A., Hoorn, C., & Antonelli, A. (2020). Why mountains matter for biodiversity. *Journal of Biogeography*, *47*(2), 315–325. https://doi.org/10.1111/jbi.13731

Qian, H. (2019). Biases in assessing the evolutionary history of the angiosperm flora of China. *Journal of Biogeography*, *46*(5), 1096–1099. https://doi.org/10.1111/jbi.13530

Qian, H., Deng, T., Beck, J., Sun, H., Xiao, C., Jin, Y., & Ma, K. (2018). Incomplete species lists derived from global and regional specimen-record databases affect macroecological analyses: A case study on the vascular plants of China. *Journal of Biogeography*, *45*(12), 2718–2729. https://doi.org/10.1111/jbi.13462

Rabosky, D. L. (2015). No substitute for real data: A cautionary note on the use of phylogenies from birth–death polytomy resolvers for downstream comparative analyses. *Evolution*, *69*(12), 3207–3216. https://doi.org/10.1111/evo.12817

Rahbek, C., Borregaard, M. K., Antonelli, A., Colwell, R. K., Holt, B. G., Nogues-Bravo, D., Rasmussen, C. M. Ø., Richardson, K., Rosing, M. T., Whittaker, R. J., & Fjeldså, J. (2019). Building mountain biodiversity: Geological and evolutionary processes. *Science*, *365*(6458), 1114–1119. https://doi.org/10.1126/science.aax0151

Ree, R. H., Moore, B. R., Webb, C. O., & Donoghue, M. J. (2005). A LIKELIHOOD FRAMEWORK FOR INFERRING THE EVOLUTION OF GEOGRAPHIC RANGE ON PHYLOGENETIC TREES. *Evolution*, *59*(11), 2299–2311. https://doi.org/10.1111/j.0014-3820.2005.tb00940.x

Ree, R. H., Smith, S. A., & Baker, A. (2008). Maximum Likelihood Inference of Geographic Range Evolution by Dispersal, Local Extinction, and Cladogenesis. *Systematic Biology*, *57*(1), 4–14. https://doi.org/10.1080/10635150701883881

Ringelberg, J. J., Koenen, E. J. M., Sauter, B., Aebli, A., Rando, J. G., Iganci, J. R., Queiroz, L. P. de, Murphy, D. J., Gaudeul, M., Bruneau, A., Luckow, M., Lewis, G. P., Miller, J. T., Simon, M. F., Jordão, L. S. B., Morales, M., Bailey, C. D., Nageswara-Rao, M., Nicholls, J. A., … Hughes, C. E. (2023). Precipitation is the main axis of tropical plant phylogenetic turnover across space and time. *Science Advances*, *9*(7), eade4954. https://doi.org/10.1126/sciadv.ade4954

Ringelberg, J. J., Zimmermann, N. E., Weeks, A., Lavin, M., & Hughes, C. E. (2020). Biomes as evolutionary arenas: Convergence and conservatism in the trans-continental succulent biome. *Global Ecology and Biogeography*, *29*(7), 1100–1113. https://doi.org/10.1111/geb.13089

Ronquist, F. (1997). Dispersal-Vicariance Analysis: A New Approach to the Quantification of Historical Biogeography. *Systematic Biology*, *46*(1), 195–203. https://doi.org/10.1093/sysbio/46.1.195

Rowe, K. C., Achmadi, A. S., Fabre, P., Schenk, J. J., Steppan, S. J., & Esselstyn, J. A. (2019). Oceanic islands of Wallacea as a source for dispersal and diversification of murine rodents. *Journal of Biogeography*, *46*(12), 2752–2768. https://doi.org/10.1111/jbi.13720

Scherrer, D., & Körner, C. (2010). Infra-red thermometry of alpine landscapes challenges climatic warming projections. *Global Change Biology*, *16*(9), 2602–2613. https://doi.org/10.1111/j.1365-2486.2009.02122.x

Schröter, C., Brockmann-Jerosch, H., Brockmann-Jerosch, M. C., Günthart, A., & Huber-Pestalozzi, G. (1926). *Das Pflanzenleben der Alpen: Eine Schilderung der Hochgebirgsflora*. A. Raustein.

Shermer, M. (2002). *In Darwin's Shadow: The Life and Science of Alfred Russel Wallace : a ... - Michael Shermer - Google Books*. Oxford University Press.

Smyčka, J., Roquet, C., Boleda, M., Alberti, A., Boyer, F., Douzet, R., Perrier, C., Rome, M., Valay, J.-G., Denoeud, F., Šemberová, K., Zimmermann, N. E., Thuiller, W., Wincker, P., Alsos, I. G., Coissac, E., Roquet, C., Boleda, M., Alberti, A., … Lavergne, S. (2022). Tempo and drivers of plant diversification in the European mountain system. *Nature Communications*, *13*(1), 2750. https://doi.org/10.1038/s41467-022-30394-5

Spehn, E. M., Rudmann-Maurer, K., & Körner, C. (2011). Mountain biodiversity. *Plant Ecology & Diversity*, *4*(4), 301–302. https://doi.org/10.1080/17550874.2012.698660

Stamatakis, A. (2015). Using RAxML to Infer Phylogenies. *Current Protocols in Bioinformatics*, *51*(1), 6.14.1-6.14.14. https://doi.org/10.1002/0471250953.bi0614s51

Thomas, A., Meudt, H. M., Larcombe, M. J., Igea, J., Lee, W. G., Antonelli, A., & Tanentzap, A. J. (2023). Multiple origins of mountain biodiversity in New Zealand's largest plant radiation. *Journal of Biogeography*, *50*(5), 947–960. https://doi.org/10.1111/jbi.14589

Vasconcelos, T. N. C., Alcantara, S., Andrino, C. O., Forest, F., Reginato, M., Simon, M. F., & Pirani, J. R. (2020). Fast diversification through a mosaic of evolutionary histories characterizes the endemic flora of ancient Neotropical mountains. *Proceedings of the Royal Society B*, *287*(1923), 20192933. https://doi.org/10.1098/rspb.2019.2933

Villaverde, T., Jiménez-Mejías, P., Luceño, M., Waterway, M. J., Kim, S., Lee, B., Rincón-Barrado, M., Hahn, M., Maguilla, E., Roalson, E. H., Hipp, A. L., GROUP, T. G. C., Wilson, K. L., Larridon, I., Gebauer, S., Hoffmann, M. H., Simpson, D. A., Naczi, R. F. C., Reznicek, A. A., … Martín-Bravo, S. (2020). A new classification of Carex (Cyperaceae) subgenera supported by a HybSeq backbone phylogenetic tree. *Botanical Journal of the Linnean Society*, *194*(2), 141–163. https://doi.org/10.1093/botlinnean/boaa042

Wallace, A. R. (1876). *The geographical distribution of animals: with a study of the relations of living and extinct faunas as elucidating the past changes of the earth's surface*. https://doi.org/10.5962/bhl.title.100631

Wegener, A. (1922). *Die entstehung der kontinente und ozeane* (Vol. 66). F. Vieweg & Söhne AG.

Zanne, A. E., Tank, D. C., Cornwell, W. K., Eastman, J. M., Smith, S. A., FitzJohn, R. G., McGlinn, D. J., O'Meara, B. C., Moles, A. T., Reich, P. B., Royer, D. L., Soltis, D. E., Stevens, P. F., Westoby, M., Wright, I. J., Aarssen, L., Bertin, R. I., Calaminus, A., Govaerts, R., … Beaulieu, J. M. (2014). Three keys to the radiation of angiosperms into freezing environments. *Nature*, *506*(7486), 89–92. https://doi.org/10.1038/nature12872

Zhang, M., Wang, C., Zhang, C., Zhang, D., Li, K., Nie, Z., & Meng, Y. (2020). Phylogenetic relationships and biogeographic history of the unique Saxifraga sect. Irregulares (Saxifragaceae) from eastern Asia. *Journal of Systematics and Evolution*, *58*(6), 958–971. https://doi.org/10.1111/jse.12547

Zizka, A., Silvestro, D., Andermann, T., Azevedo, J., Ritter, C. D., Edler, D., Farooq, H., Herdean, A., Ariza, M., Scharn, R., Svantesson, S., Wengström, N., Zizka, V., & Antonelli, A. (2019). CoordinateCleaner: Standardized cleaning of occurrence records from biological collection databases. *Methods in Ecology and Evolution*, *10*(5), 744–751. https://doi.org/10.1111/2041-210x.13152

Zwaan, D. R. de, Scridel, D., Altamirano, T. A., Gokhale, P., Kumar, R. S., Sevillano-Ríos, S., Barras, A. G., Arredondo-Amezcua, L., Asefa, A., Carrillo, R. A., Green, K., Gutiérrez-Chávez, C. A., Lehikoinen, A., Li, S., Lin, R.-S., Norment, C. J., Oswald, K. N., Romanov, A. A., Salvador, J., … Martin, K. (2022). GABB: A global dataset of alpine breeding birds and their ecological traits. Scientific Data, 9(1), 627. https://doi.org/10.1038/s41597-022-01723-6

SUPPLEMENTARY MATERIAL

Taxon Sampling

To avoid paraphyletic taxon sampling in our study we sampled the six genera based on the latest phylogenies and included all the nested genera or species. The Campanulaceae (*sensu stricto*) phylogeny showed, that *Campanula* L. is only monophyletic if the genera: *Adenophora* Fisch., *Jasione* L., *Legousia* Durande, *Physoplexis* Schur and *Phyteuma* L. are included (Xu & Hong, 2021). *Carex* L. is since the efforts of the Global *Carex* Group a monophyletic genus, this includes the nested former genus *Kobresia* Willd. (The Global Carex Group, 2015; The Global Carex Group et al., 2016). *Festuca* Tourn. ex L. is only monophyletic if the nested genera: *Lolium* L., *Micropyrum* (Gaudin) Link, *Psilurus* Trin., and *Vulpia* C.C.Gmel. are included, therefore we use the *sensu lato* description of *Festuca* (Cheng et al., 2016; Torrecilla et al., 2004). All species described as "core *Ranunculus*" (i.e., *Ranunculus* L. *sensu stricto*) this excludes the genus *Ficaria* Guett. and *Myosurus* L. (Emadzade et al., 2010; Lehnebach et al., 2007). *Saxifraga* Tourn. ex L. excluding *Micranthes stellaris* (syn. *Saxifraga stellaris*) is a monophyletic genus (Ebersbach et al., 2017; Prieto et al., 2013). *Viola* L. is according to latest phylogenetic knowledge a monophyletic genus (Wahlert et al., 2014). Additionally, we checked all the Heterotypic Synonym names from Plants of the World Online (https://powo.science.kew.org/) to avoid excluding any nested genera or species.

Sensitivity Analysis

To demonstrate the robustness of ElevDistr against spatial uncertainty, we compare the effect of noise on the two different classification methods. Here, a point in the central Swiss Alps is selected, that lays in steep and heterogeneous terrain (46.76895° N, 8.67172° E), but with an elevation of 522 meters clearly is below the treeline. Around this center point, noise is generated using a grid sampling with a continuous step size of 0.0025° (9'') and different lateral grid lengths: 1, 2, 3, 5, and 10km. The lateral length represents the "amount" of uncertainty we simulate. Each of the sampled points is classified by ElevDistr and the polygon method (i.e., using a thermal belt grid). Finally, the classification success (in percent) is calculated for both methods under different "amounts" of uncertainty, as well as the percentage of the different results: thermal belts under the polygon method and meters below the treeline for ElevDistr.

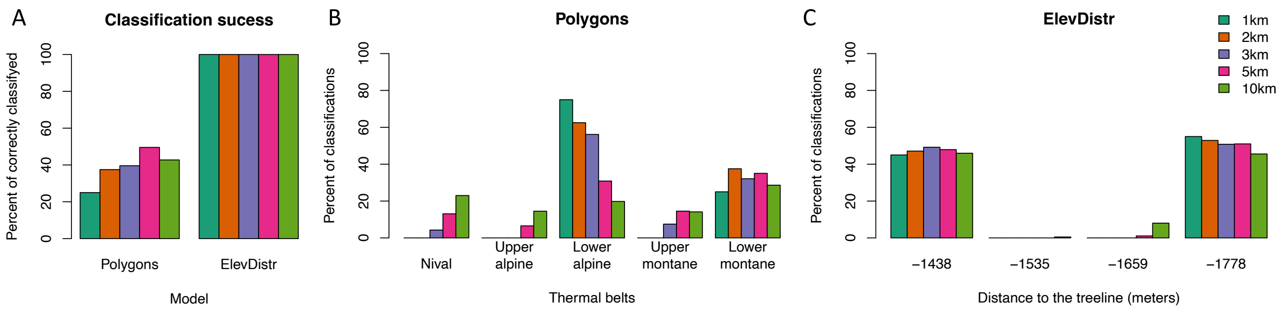

FIGURE S1: Results of the sensitivity analysis. The y-axis shows the percentage share, and colors represent the different "amounts" of simulated noise reaching from 1 to 10km. A represents the percent of correctly classified points: for the polygon approach in the left panel and for ElevDistr in the right panel. B contains the percentage of different outcomes for the polygon and C shows the outcome using ElevDistr.

Effect of Spatial Noise

The two model systems and their output variables are highly different. On one hand, the polygon method returns a classification into any of the seven bioclimatic belts from: nival, upper alpine, lower alpine, upper mountain, lower mountain, remaining area with or without freezing (defined in Körner et al., 2011). On the other hand, ElevDistr returns a value in meters, describing the distance to the local treeline. Despite the different output variables, we can compare how the two models behave, if noise is introduced and how this affects classification success (i.e., how many percent are correctly classified as 'non-alpine').

The selected point is representing a "best case" scenario for ElevDistr, even under 10km of simulated uncertainty ElevDistr makes no wrong classification (Fig. S1A). The polygon approach performs much worse, fewest correct classifications (25%) are achieved under 1km uncertainty and slightly improves with more added noise (37.5, 39.6, 49.5 and 42.7% under 2, 3, 5 or 10km uncertainty, respectively).

When using the polygon method, the selected point is classified as lower alpine (Fig. S1B), but with bigger uncertainty, it becomes more and more unlikely that the model comes to this conclusion. Under 1km uncertainty, 75% of all simulated points are assigned to the class lower alpine, with 2km it drops to 62.5% and with 3km we get 56.1%. Increasing the uncertainty further to 5km the class lower alpine is no longer most frequently found (30.9%) and points are assigned to all possible classes except: remaining area with or without freezing. In case of introducing 10km uncertainty, the model assigns the points to all classes with rather equal proportions: 23% nival, 14.5% upper alpine, 19.8% lower alpine, 14.1% upper mountain, and 28.6% in the lower mountain zone.

ElevDistr computes independent of the introduced uncertainty two distances to the treeline: -1438 and -1778m, which make up at least 91.5% of all results (Fig. S1C). Only under 5km uncertainty 1% of all results return -1659m and 8% under 10km. Also, with10km uncertainty the model returns in 0.5% of the cases -1535. Different distances to the treeline are caused by different "amounts" of uncertainty, however under ElevDistr the only thing affected by spatial uncertainty is the selection of the nearest alpine corner (main text, Fig. 1). The evaluation of the grid around this point and the computed distance to the treeline are always identical (if the function parameters are unchanged). Assuming that the treeline in this area is 2100-2200 meters above sea level, we have (given the used input data and the default parameters) an uncertainty of roughly +/- 150m regardless of the introduced "amount" of spatial noise.

Next page; **TABLE S1:** Accession matrix for Campanula, Carex, Festuca, Ranunculus, Saxifraga and Viola resulting from oneTwoTree. Left column shows the species name and the taxonomy ID according to the NCBI taxonomy database, top row contains the cluster description assigned by oneTwoTree and the remaining cells contain the GenBank accession number if applicable.

Note: To avoid an even smaller font size, the table is split by genus, the order above is maintained.

Specie\Loci	1-Campanula cervicaria chloroplast petB gene (partial) petB-petD intergenic spacer and petD gene (partial) isolate CAM037	13-ITS	2-Campanula latifolia voucher Antonelli 252(GB) ribulose-15-bisphosphate carboxylase/oxygenase large subunit (rbcL) gene partial cds; chloroplast	3-Campanula bononiensis chloroplast matK gene for maturase K and partial trnK gene intron isolate CAM038	4-Campanula cochleariifolia tRNA-Leu (trnL-UAA) gene partial sequence; trnL-trnF intergenic spacer complete sequence; and tRNA-Phe (trnF-GAA) gene partial sequence; plastid	5-Campanula rotundifolia voucher Steele 1318 ATP synthase CF1 beta subunit (atpB) gene complete cds; plastid	6-Campanula cenisia pentatricopeptide repeat-containing protein 70 gene partial cds	7-Campanula macrorhiza pentatricopeptide repeat-containing protein 11 gene partial cds	8-Campanula rapunculoides chloroplast partial rpl16 gene intron isolate CAM036	9-Campanula erinus voucher AZB:CE-MDCF-001 PsbA (psbA) gene partial cds; psbA-trnH intergenic spacer complete sequence; and tRNA-His (trnH) gene partial sequence; chloroplast	10-Campanula sibirica voucher no voucher atpB and atpB-rbcL intergenic spacer partial sequence; chloroplast	11-Campanula medium isolate LL213 rpl32-trnL intergenic spacer partial sequence; chloroplast	12-Campanula glomerata haplotype h38 pop variant Prenj trnG-trnS intergenic spacer region partial sequence; chloroplast
1475209-Campanula fritschii	-	KF918794.1	-	-	-	-	-	-	-	-	-	-	-
1399317-Phyteuma sieberi	-	KC455647.1	-	KC455877.1	KC455762.1	-	-	-	-	-	-	-	-
1533168-Legousia scabra	-	-	-	-	-	-	-	-	-	-	-	-	-
1399303-Phyteuma charmelii	-	KC455584	-	KC455812	KC455697	-	-	-	-	-	-	-	-
703219-Phyteuma cordatum	-	KC455586	-	KC455814	KC455692	-	-	-	-	-	-	-	-
361411-Phyteuma globulariifolium	-	DQ304583	-	KC455846	KC455733	-	-	-	-	-	-	-	-
1399308-Phyteuma hedraianthifolium	-	KC455627	-	KC455856	KC455741	-	-	-	-	-	-	-	-
1399309-Phyteuma michelii	-	KC455578	-	KC455816	KC455701	-	-	-	-	-	-	-	-
239399-Campanula barbata	FN396989.1	AY322011.1	KJ512614.1	LT706582.1	KJ512658.1	KJ512514.1	-	KJ512185.1	LT673921.1	HG800505.1	-	-	-
361377-Campanula caespitosa	FN396994.1	DQ304621.1	KJ512624.1	KJ512567.1	KJ512655.1	KJ512518.1	KJ512339.1	-	-	-	-	-	-
649652-Campanula cervicaria	FN396997.1	MK651999.1	-	LT706575.1	-	KJ512522.1	KJ512350.1	-	LT673929.1	KY785162.1	-	-	KY785126.1
428162-Campanula cochleariifolia	FN397002.1	KY009278.1	KJ512628.1	LT706626.1	JX445917.1	JN571926.1	KJ512359.1	KJ512206.1	LT673968.1	HG800506.1	-	KY034487.1	-
361381-Campanula elatinoides	FN397008.1	DQ304625.1	KJ512630.1	LT706584.1	FJ426578.1	KJ512525.1	KJ512373.1	KJ512214.1	LT673924.1	-	-	-	-
82281-Campanula glomerata	FN397012.1	AH006455.2	KM360690.1	LT706563.1	HM590251.1	KJ512530.1	KJ512393.1	KJ512311.1	LT673900.1	KY785142.1	-	-	KY785113.1
239410-Campanula latifolia	FN397022.1	KX165651.1	EF141027.1	LT706585.1	DQ356169.1	EU437606.1	KJ512407.1	-	LT673925.1	-	-	-	-
56154-Campanula medium	FN397024.1	KY624384.1	FJ587261.1	LT706573.1	EF088738.1	EU437607.1	KJ512415.1	-	LT673911.1	-	-	KP014048.1	-
440359-Campanula patula	FN397025.1	KX167142.1	KJ512640.1	LT706739.1	EF213148.1	KJ512540.1	KJ512420.1	KJ512246.1	LT674103.1	-	EF213350.1	-	-
239416-Campanula persicifolia	FN397027.1	DQ304590.1	FJ587264.1	KC455763.1	EF213149.1	EU437657.1	KJ512426.1	KJ512250.1	LT674075.1	-	EF213351.1	-	-
239419-Campanula pyramidalis	FN397031.1	KC181012.1	EU713429.1	EU713322.1	GQ254919.1	KJ512543.1	KJ512430.1	KJ512255.1	-	KC181003.1	-	-	KC180863.1
209536-Campanula rapunculoides	FN397032.1	EF090545.1	FJ587271.1	LT706574.1	EF213152.1	EU437620.1	KJ512434.1	KJ512257.1	LT673912.1	HQ596619.1	EF213354.1	-	-
649663-Campanula rhomboidalis	FN397033.1	KF918821.1	KJ512644.1	LT706738.1	KJ512689.1	KJ512545.1	KJ512439.1	KJ512260.1	LT674102.1	-	-	-	-
239422-Campanula rotundifolia	FN397034.1	KY009262.1	KT178143.1	-	EF213153.1	KT176271.1	KJ512441.1	KJ512262.1	LT674078.1	-	EF213355.1	KY034519.1	-
361399-Campanula scheuchzeri	FN397039.1	KY009283.1	KF602098.1	JN571962.1	KF957749.1	KJ512547.1	KJ512447.1	KJ512267.1	-	HG800510.1	-	KY034482.1	-
361401-Campanula spicata	FN397044.1	DQ304574.1	FJ587281.1	LT706583.1	EF088769.1	KJ512550.1	KJ512459.1	KJ512274.1	LT673922.1	-	-	-	-
239427-Campanula thyrsoides	FN397046.1	AY331455.1	EU643723.1	LT706769.1	KJ512699.1	KJ512552.1	KJ512462.1	-	LT673938.1	-	-	-	-
85178-Campanula trachelium	FN397049.1	KY009338.1	FJ587285.1	LT706592.1	DQ356171.1	AJ235423.2	KJ512465.1	KJ512277.1	LT673898.1	-	-	KY034532.1	-
239452-Jasione montana	FN397070	DQ304566	EU713354	EU713247	JX445918	EU437582	KJ512480	KJ512288	MK556766	-	EU437582	-	-
239456-Legousia speculum-veneris	FN397071	OL415916	EU713365	EU713258	KY697411	EU437593	KJ512485	KJ512293	-	-	EU437593	-	-
239466-Physoplexis comosa	FN397082	DQ304585	EU713362	KC455832	KC455717	EU437590	KJ512488	KJ512297	LT673893	HG800551	EU437590	-	-
649683-Phyteuma betonicifolium	FN397084	KC455572	HG417022	KC455800	KC455685	-	-	-	MK556660	HG800552	-	-	-
649684-Phyteuma hemisphaericum	FN397085	KC455608	MK555596	KC455835	KC455723	-	-	-	-	-	-	-	-
649685-Phyteuma scheuchzeri	FN397086	KC455634	HG417024	KC455865	KC455758	-	-	-	LT673923	HG800554	MK556107	-	-
361413-Campanula sibirica	JX914681.1	KU892002.1	FJ587279.1	LT706607.1	EF213157.1	KJ512548.1	KJ512451.1	KJ512269.1	LT673949.1	-	EF213359.1	KC792359.1	KC792455.1
361397-Campanula raineri	JX914694.1	DQ304604.1	HG416979.1	-	-	-	-	-	-	HG800509.1	-	-	-
361375-Campanula cenisia	JX914726.1	DQ304622.1	KJ512627.1	KJ512570.1	KJ512673.1	KJ512521.1	KJ512348.1	KJ512202.1	-	-	-	-	-
361374-Campanula bononiensis	JX914730.1	DQ304571.1	EU713381.1	LT706576.1	KJ512663.1	EU437609.1	KJ512330.1	KJ512190.1	LT673914.1	-	-	-	-
239455-Legousia falcata	JX914808	DQ304589	AY655152	LT706753	-	EU437645	KJ512481	KJ512289	LT674079	-	EU437645	-	-
440356-Campanula alpestris	JX914817.1	-	KJ512612.1	KJ512557.1	EF213141.1	KJ512512.1	KJ512314.1	-	-	-	EF213343.1	-	-
361372-Campanula alpina	JX914819.1	DQ304573.1	KJ414432.1	LT706588.1	-	-	-	-	LT673928.1	-	-	-	-
1241126-Campanula macrorhiza	JX914952.1	KF918800.1	KJ512636.1	KJ512578.1	KJ512683.1	KJ512532.1	KJ512411.1	KJ512238.1	-	-	-	-	-
361396-Campanula pulla	JX914977.1	DQ304605.1	-	-	-	-	-	-	-	-	-	-	-
361393-Campanula morettiana	JX915102.1	DQ304602.1	-	-	-	-	-	-	-	-	-	-	-
1241047-Campanula carnica	JX915166.1	MK652015.1	KJ512625.1	LT706651.1	KJ512670.1	KJ512519.1	KJ512342.1	-	LT673994.1	-	-	-	-
440364-Campanula witasekiana	JX915168.1	MK652083.1	KJ512653.1	KJ512595.1	EF213164.1	KJ512554.1	KJ512472.1	KJ512281.1	-	-	EF213366.1	-	-
1241076-Campanula excisa	JX915169.1	-	KJ512631.1	KJ512573.1	KJ512675.1	KJ512527.1	KJ512382.1	KJ512220.1	-	-	-	-	-
239417-Campanula petraea	JX915207.1	AY322031.1	KJ512641.1	KJ512583.1	KJ512688.1	KJ512541.1	KJ512427.1	KJ512252.1	-	-	-	-	-
1241227-Phyteuma ovatum	JX915213	KC455569	HG417023	KC455797	KC455682	-	KJ512490	KJ512299	-	-	-	-	-
1241226-Phyteuma humile	JX915214	KC455615	-	KC455844	KC455729	-	KJ512489	KJ512298	-	-	-	-	-
361368-Adenophora liliifolia	JX915239	DQ304581	KC146540	KC146500	KU984070	KU983887	KT970227	OR161446	HQ704590	-	HQ704473	-	MN530083
1241035-Campanula bertolae	KJ512598.1	KF918790.1	KJ512617.1	KJ512561.1	KJ512660.1	KJ512517.1	KJ512327.1	KJ512187.1	-	-	-	-	-
361402-Campanula stenocodon	KJ512604.1	DQ304620.1	KJ512650.1	KJ512592.1	KJ512697.1	KJ512551.1	KJ512460.1	KJ512275.1	-	-	-	-	-
239469-Phyteuma spicatum	KJ512606	DQ304584	EU643712	KC455792	KC455709	EU437589	KJ512492	-	MK556757	-	EU437589	-	-
239403-Campanula erinus	KY091452.1	KY091353.1	EU713398.1	LT706677.1	EF088720.1	EU437626.1	KJ512379.1	KT753107.1	LT674021.1	KY091497.1	KT753238.1	KC792362.1	KC792458.1
428196-Campanula rapunculus	LT674580.1	KY009328.1	KJ512643.1	LT706744.1	EF088758.1	KJ512544.1	KJ512435.1	KJ512258.1	LT674109.1	HE966531.1	-	-	-
368679-Legousia hybrida	MK556223	-	EU643706	EU713327	DQ356234	EU437660	-	-	MK556658	-	EU437660	-	-
239468-Phyteuma orbiculare	MK556228	KC455549	KF997454	KC455783	KC455667	-	-	-	MK556754	-	-	-	-
1288169-Phyteuma scorzonerifolium	MK556230	KC455577	MK555465	HF586688	HF586689	-	-	-	MK556756	-	MK556108	-	-
1399304-Phyteuma confusum	MK556370	KC455624	MK555595	KC455854	KC455739	-	-	-	-	-	-	-	-

Specie\Loci	22-ITS	1-Carex vulpinoidea tRNA-Thr partial sequence; trnT-trnL intergenic spacer tRNA-Leu and trnL-trnF intergenic spacer complete sequence; and tRNA-Phe partial sequence; chloroplast genes for chloroplast products	2-Carex bigelowii chloroplast matK gene for maturase K and partial trnK gene intron specimen voucher Gillespie Consaul & Bull 7799 (ALA)	3-Carex atrofusca isolate MICH 1362501 external transcribed spacer 1 partial sequence	4-Carex punctata ribulose-15-bisphosphate carboxylase/oxygenase large subunit (rbcL) gene partial cds; chloroplast	5-Carex remota isolate YUG rps16 gene intron; chloroplast	6-Carex nigra ribulose-bisphosphate carboxylase large subunit (RBCL) gene partial cds; plastid	7-Carex hostiana isolate Hos_2 tRNA-Lys (trnK) gene intron; chloroplast	8-Carex sylvatica isolate SWI rpl32-trnL(UAG) intergenic spacer partial sequence; chloroplast	9-Carex bicolor voucher CAN-583982 AtpF (atpF) gene partial cds; atpF-atpH intergenic spacer complete sequence; and AtpH (atpH) gene partial sequence; plastid	10-Carex buekii cytochrome b6/f complex subunit VIII (petN) and photosystem II M protein genes partial cds; chloroplast	11-Carex brunnescens isolate 4E8EMS13 photosystem II protein D1 (psbA) gene partial cds; and psbA-trnH intergenic spacer partial sequence; plastid	12-Carex halleriana chloroplast partial ndhF gene for NADH dehydrogenase subunit F specimen voucher G.G. Besnard 12-2007	13-Carex bicolor voucher CAN-583982 RNA polymerase beta (rpoC1) gene partial cds; plastid	14-Carex brunnescens ATPase cadmium transporter (CATP) gene partial cds	15-Carex chordorrhiza trnC-ycf6 intergenic spacer partial sequence; and cytochrome b6/f complex subunit VIII (petN) gene partial cds; chloroplast	16-Carex chordorrhiza ATP synthase CF0 subunit IV (atpI) gene partial cds; and atpI-atpH intergenic spacer partial sequence; chloroplast	17-Carex maritima trnE-trnY intergenic spacer partial sequence; tRNA-Tyr (trnY) gene and trnY-trnD intergenic spacer complete sequence; and tRNA-Asp (trnD) gene partial sequence; chloroplast	18-Carex remota glyceraldehyde-3-phosphate dehydrogenase (G3PDH) gene partial cds	19-Carex fuliginosa voucher CAN-586559 RNA polymerase subunit (rpoB) gene partial cds; plastid	20-Carex paniculata GATA transcription factor (GZF) gene partial cds	21-Carex paniculata NADH-plastoquinone oxidoreductase subunit J (ndhJ) gene partial cds; ndhJ-trnF intergenic spacer and tRNA-Phe (trnF) gene complete sequence; and trnF-trnL intergenic spacer partial sequence; chloroplast
140792-Carex bohemica	AY779073.1	JQ653160.1	-	JN903108.1	-	-	-	-	-	-	-	-	-	-	-	-	-	-	-	-	-	-
140797-Carex capitata	DQ115118.1	GQ244704.1	KJ513585.1	DQ115119.1	JN965352.1	MF669280.	-	-	-	KP996291.1	-	-	KJ513493.1	-	-	-	-	-	-	-	-	-
291103-Trichophorum alpinum	MF669180.1	AY757496.1	KJ513656.1	AY757400.1	-	MF669242.	AB369973.1	-	-	-	-	-	AM999971.1	-	-	-	-	AY757464.1	-	-	-	-
240691-Carex brunnescens	KF977435.1	AY757481.1	HQ593204.1	DQ115115.1	KF977470.1	EU541837.	-	KY055325.1	KY055177.1	HQ594601.1	KY055289.1	KU998112.1	-	-	KY055028.1	KY055251.1	KU997978.1	AY757449.1	KP979823.1	-	KY055075.1	KY055118.1
140796-Carex canescens	KX166685.1	AY757480.1	KX676955.1	MH208850.1	-	KY189238.	GQ469845.1	KY189194.1	KY055178.1	-	KY055290.1	KU998111.1	-	-	KY055029.1	KY055252.1	KU997977.1	AY757448.1	KP979855.1	-	KY055076.1	KY055119.1
241203-Carex capillaris	KT960127.1	DQ998958.1	KU496569.1	DQ998852.1	KX677885.1	-	-	-	-	FJ548397.1	-	-	-	FJ548176.1	-	-	-	-	-	FJ548306.1	-	-
240692-Carex chordorrhiza	KX167494.1	AY757485.1	MK519769.1	KY055057.1	MG227761.1	-	-	-	KY055172.1	FJ548400.1	KY055284.1	KY055151.1	-	FJ548180.1	KY055023.1	KY055246.1	KY055358.1	AY757453.1	KY055064.1	FJ548310.1	-	-
140803-Carex diandra	DQ115144.1	AY757473.1	KU496570.1	MH208853.1	KX678841.1	-	-	-	-	-	-	-	-	-	-	-	-	AY757441.1	-	-	-	-
240685-Carex elongata	DQ115166.1	-	JN895742.1	DQ115167.1	JN893126.1	KY055208.	-	KY055320.1	KY055171.1	-	KY055283.1	KY055150.1	-	-	KY055022.1	KY055245.1	KY055357.1	-	KP979815.1	-	KY055071.1	KY055113.1
140816-Carex flava	AY278310.1	AY757523.1	KU939681.1	JX409821.1	KX677808.1	JN627776.	-	MF804350.1	KU939760.1	-	-	-	-	-	-	-	-	-	-	-	-	-
240690-Carex heleonastes	MG215890.1	AY757484.1	KP980037.1	AY757388.1	MG226226.1	KY055219.	-	KY055331.1	KY055183.1	-	KY055295.1	KU998105.1	-	-	KY055034.1	KY055257.1	KU997971.1	AY757452.1	KP979866.1	-	KY055081.1	KY055124.1
240688-Carex lachenalii	KX167263.1	KU496618.1	KP979990.1	KP980175.1	KC482300.1	EU541840.	-	KY055334.1	KY055186.1	FJ548415.1	KY055298.1	KU998113.1	-	FJ548193.1	KY055037.1	KY055260.1	KU997979.1	-	KP979812.1	FJ548322.1	KY055084.1	KY055127.1
240683-Carex paniculata	KX166515.1	EU288446.1	JN894850.1	DQ115235.1	JN891912.1	KR827140.	-	KY055317.1	KY055168.1	-	KY055280.1	KY055147.1	-	-	KY055019.1	KY055242.1	KY055354.1	-	KP979863.1	-	KY055068.1	KY055110.1
234465-Carex remota	DQ998944.1	DQ998997.1	JN894576.1	JN903123.1	KJ204312.1	KR827141.	-	KY055319.1	KY055170.1	-	KY055282.1	KY055149.1	-	-	KY055021.1	KY055244.1	KY055356.1	-	KP979846.1	-	KY055070.1	KY055112.1
240682-Carex spicata	DQ115284.1	-	JN894304.1	DQ115285.1	MG227071.1	KY055206.	-	KY055318.1	KY055169.1	-	KY055281.1	KY055148.1	-	-	KY055020.1	KY055243.1	KY055355.1	-	KP979904.1	-	KY055069.1	KY055111.1
140793-Carex brevicollis	AF285011.1	AF284909.1	KF811445.1	-	-	-	-	-	-	-	-	-	-	-	-	-	-	-	-	-	-	-
140814-Carex flacca	DQ998915.1	DQ998968.1	KY562656.1	DQ998862.1	MG226669.1	-	KF602138.1	-	-	-	-	-	-	-	-	-	-	-	-	-	-	-
100286-Carex rupestris	AY244521.1	GQ244745.1	KJ513591.1	AY244522.1	KT960683.1	MF669233.	-	-	-	FJ548446.1	-	-	KJ513498.1	FJ548225.1	-	-	-	-	-	FJ548352.1	-	-
241232-Carex sempervirens	AY278278.1	EU288449.1	KF811446.1	-	-	-	KF602164.1	-	-	-	-	-	-	-	-	-	-	-	-	-	-	-
241234-Carex sylvatica	AY278306.1	AY344175.1	JN896090.1	AY757660.1	KJ204313.1	AY344152.	KF602132.1	KC122386.1	KU939761.1	FJ395286.1	-	-	-	FJ395776.1	-	-	-	-	-	-	-	-
240678-Carex vulpina	AY280547.1	-	-	JN903127.1	-	-	KF997370.1	-	-	-	-	-	-	-	-	-	-	-	-	-	-	-
241197-Carex atrofusca	KT960353.1	AM085580.1	KT021439.1	KT021031.1	MF572167.1	AM085610.	-	-	-	FJ548384.1	-	-	-	FJ548164.1	-	-	-	-	-	FJ548293.1	-	-
241200-Carex bigelowii	AY278303.1	GQ244699.1	LK021890.1	GQ223499.1	KT960434.1	LK021828.	-	-	-	-	-	-	-	-	-	-	-	-	-	-	-	-
241202-Carex buxbaumii	AY278262.1	KU496615.1	LK021891.1	KT021041.1	MG226272.1	LK021829.	-	-	-	-	-	-	-	-	-	-	-	-	-	-	-	-
234467-Carex echinata	AH012951.2	AY757477.1	KU496571.1	DQ461063.1	HM849852.1	-	-	-	-	-	-	-	-	-	-	-	-	AY757445.1	-	-	-	-
241210-Carex fuliginosa	AY278254.1	GQ244706.1	FJ548089.1	-	KT960519.1	-	-	-	-	FJ548403.1	-	-	-	FJ548185.1	-	-	-	-	-	FJ548313.1	-	-
140829-Carex limosa	AY278298.1	GQ244715.1	KT021406.1	KT021067.1	MG225560.1	-	JX644630.1	-	-	-	-	-	-	-	-	-	-	-	-	-	-	-
240694-Carex maritima	AY280570.1	AY757493.1	KC474346.1	AY757397.1	-	KR827159.	GQ469840.1	GQ469856.1	-	FJ548425.1	-	-	-	FJ548203.1	-	-	-	AY757461.1	-	FJ548331.1	-	-
241220-Carex norvegica	AY278264.1	GQ244733.1	KT021386.1	KT021087.1	KT960692.1	-	-	-	-	FJ548439.1	-	-	-	FJ548221.1	-	-	-	-	-	FJ548347.1	-	-
140843-Carex pauciflora	AH012968.2	LC487525.1	JN896248.1	-	-	LC486357.	GQ469850.1	-	-	-	-	-	-	-	-	-	-	-	-	-	-	-
241230-Carex rostrata	AY278294.1	KU496621.1	HG915876.1	KR902931.1	-	HG915785.	GQ469851.1	EU812681.1	-	JN314477.1	-	-	-	-	-	-	-	-	-	-	-	-
140858-Carex supina	KT960263.1	GQ244753.1	-	-	KT960622.1	-	-	-	-	-	-	-	-	-	-	-	-	-	-	-	-	-
241235-Carex vaginata	AY278285.1	AY757557.1	KU496591.1	KT021119.1	MG225817.1	-	-	-	-	-	-	-	-	-	-	-	-	-	-	-	-	-
241236-Carex vesicaria	AY278289.1	KR902945.1	HG915885.1	KR902934.1	KJ841218.1	HG915794.	-	-	-	JN314442.1	-	-	-	-	-	-	-	-	-	-	-	-
111420-Carex dioica	AH012948.2	AF191816.1	JN895942.1	EU001132.1	JN893399.1	-	-	-	-	-	-	-	AF191808.1	-	-	-	-	-	-	-	-	-
502425-Carex pairae	FJ694689.1	EU288445.1	HM850846.1	-	HE963383.1	-	HM849859.1	-	-	-	-	HE966540.1	-	-	-	-	-	-	-	-	-	-
240677-Carex brizoides	DQ115108.1	-	-	DQ115109.1	-	-	-	-	-	-	-	-	-	-	-	-	-	-	-	-	-	-
241213-Carex lasiocarpa	AY278297.1	DQ998978.1	HG915858.1	DQ998872.1	MG226024.1	HG915767.	-	-	-	-	-	-	-	-	-	-	-	-	-	-	-	-
234464-Carex nigra	AH012945.2	GQ244732.1	JN895336.1	-	-	-	GQ469838.1	-	MH094143.1	-	JN627583.1	-	-	-	-	-	-	-	-	-	-	-
241224-Carex panicea	AY278284.1	DQ998990.1	LK021925.1	LK021738.1	-	LK021863.	KF602160.1	-	-	-	-	-	-	-	-	-	-	-	-	-	-	-
240662-Carex repens	AY280528.1	-	-	-	-	-	-	-	-	-	-	-	-	-	-	-	-	-	-	-	-	-
140866-Carex vulpinoidea	MG216551.1	AF284866.1	KP273710.1	AY757372.1	HQ590018.1	KP273822.	-	-	-	HQ594623.1	-	HQ596632.1	KP273764.1	-	-	-	-	AY757436.1	-	-	-	-
234476-Carex curvula	AH012963.2	AY757564.1	-	-	-	EU541828.	-	-	-	-	-	-	-	-	-	-	-	-	-	-	-	-
234461-Carex depauperata	AH012943.2	AY757549.1	JN895024.1	-	JN893398.1	-	-	-	-	-	-	-	-	-	-	-	-	-	-	-	-	-
240679-Carex appropinquata	DQ115096.1	-	-	DQ115097.1	-	-	-	-	-	-	-	-	-	-	-	-	-	-	-	-	-	-
241204-Carex demissa	AY278307.1	-	KU939680.1	JX409833.1	-	JN627757.	-	JN627702.1	KU939759.1	-	-	-	-	-	-	-	-	-	-	-	-	-
241205-Carex distans	DQ384121.1	-	JN895486.1	KU939522.1	-	JN627821.	GQ469848.1	JN627754.1	KU939757.1	-	-	-	-	-	-	-	-	-	-	-	-	-
240695-Carex disticha	KX165858.1	EU288433.1	JN895943.1	DQ115153.1	MG226434.1	-	-	-	-	-	-	-	-	-	-	-	-	-	-	-	-	-
140806-Carex divisa	DQ115154.1	AF284889.1	-	DQ115155.1	JN893131.1	-	-	-	-	-	-	-	-	-	-	-	-	-	-	-	-	-
241214-Carex lepidocarpa	AY278293.1	-	-	-	-	MF804347.	-	MF804352.1	-	-	-	-	-	-	-	-	-	-	-	-	-	-
372273-Carex leporina	DQ384113.1	-	-	-	-	-	-	-	-	-	-	-	-	-	-	-	-	-	-	-	-	-
241218-Carex mairei	DQ384168.1	-	-	-	-	EF198171.	-	EU812600.1	-	-	-	-	-	-	-	-	-	-	-	-	-	-
140839-Carex otrubae	KX166331.1	AF284894.1	MF543492.1	DQ115227.1	MF572169.1	-	HM849857.1	-	-	-	-	-	-	-	-	-	-	-	-	-	-	-
240661-Carex praecox	DQ115248.1	-	-	DQ115249.1	-	-	-	-	-	-	-	-	-	-	-	-	-	-	-	-	-	-
312762-Carex punctata	DQ384178.1	AY757525.1	JN896087.1	AY757659.1	HM849864.1	EF198172.	-	EU812618.1	KU939758.1	-	-	-	-	-	-	-	-	-	-	-	-	-
140783-Carex acutiformis	AY278300.1	AF284891.1	KY562635.1	AY757644.1	MG225812.1	HG915751.	-	-	MF945763.1	-	MF966957.1	-	-	-	-	-	-	-	-	-	-	-
241195-Carex alba	AY278259.1	-	-	KR857282.1	-	-	-	-	-	-	-	-	-	-	-	-	-	-	-	-	-	-
241196-Carex atrata	AY278263.1	JX644766.1	LK021882.1	KT021027.1	JN892343.1	LK021819.	KF602127.1	-	-	-	-	-	-	-	-	-	-	-	-	-	-	-
241199-Carex bicolor	LK021765.1	EU288427.1	LK021889.1	KT021040.1	MG225990.1	LK021827.	-	-	-	FJ548387.1	-	-	-	FJ548167.1	-	-	-	-	-	FJ548295.1	-	-
241201-Carex brachystachys	AY278277.1	-	-	-	-	-	-	-	-	-	-	-	-	-	-	-	-	-	-	-	-	-
240674-Carex davalliana	KX167496.1	EU288432.1	-	-	-	GU176247.	-	-	-	-	-	-	-	-	-	-	-	-	-	-	-	-
140805-Carex digitata	AY278267.1	AY757552.1	-	AY757684.1	JN892144.1	-	-	-	-	-	-	-	-	-	-	-	-	-	-	-	-	-
240680-Carex divulsa	KX167254.1	-	HM850840.1	JN903112.1	JN893132.1	-	HM849851.1	-	-	-	-	-	-	-	-	-	-	-	-	-	-	-
241206-Carex elata	AY278255.1	HM590257.1	JN895554.1	AY770440.1	JN893129.1	-	-	-	-	-	-	-	-	-	-	-	-	-	-	-	-	-
140809-Carex ericetorum	AY278281.1	HM590259.1	-	AY325437.1	-	-	-	-	-	-	-	-	-	-	-	-	-	-	-	-	-	-
241208-Carex ferruginea	AY278275.1	EU288434.1	-	-	-	-	KF602166.1	-	-	-	-	-	-	-	-	-	-	-	-	-	-	-
140813-Carex firma	AY278279.1	AF284893.1	-	-	-	-	KF602145.1	-	-	-	-	-	-	-	-	-	-	-	-	-	-	-
240675-Carex foetida	AY280544.1	-	-	-	-	-	-	-	-	-	-	-	-	-	-	-	-	-	-	-	-	-
241209-Carex frigida	AY278291.1	-	-	-	-	-	-	-	-	-	-	-	-	-	-	-	-	-	-	-	-	-
15193-Carex hirta	AY278296.1	HM590261.1	HG915853.1	-	MG226633.1	HG915762.	-	-	-	-	-	-	-	-	-	-	-	-	-	-	-	-
241211-Carex hispida	AY278272.1	EU288438.1	-	-	-	-	-	-	-	-	-	-	-	-	-	-	-	-	-	-	-	-
13399-Carex hostiana	AY278309.1	EU288439.1	JN895279.1	JX409829.1	-	JN627781.	GQ469841.1	JN627713.1	-	-	-	-	-	-	-	-	-	-	-	-	-	-
140822-Carex humilis	AY278260.1	AF284906.1	FR865043.1	-	KJ746313.1	-	-	-	-	-	-	-	-	-	-	-	-	-	-	-	-	-
241215-Carex liparocarpos	AY278261.1	-	-	-	-	-	-	-	-	-	-	-	-	-	-	-	-	-	-	-	-	-
234725-Carex microglochin	AY244519.1	GU176113.1	KP273698.1	AY244520.1	-	KP273808.	GQ469844.1	GQ469859.1	-	-	-	-	KP273752.1	-	-	-	-	-	-	-	-	-
140837-Carex montana	AY278271.1	AF284877.1	JN895152.1	-	JN892319.1	-	-	-	-	-	-	-	-	-	-	-	-	-	-	-	-	-
241219-Carex mucronata	AY278257.1	-	-	-	-	-	-	-	-	-	-	-	-	-	-	-	-	-	-	-	-	-
241222-Carex ornithopoda	AY278269.1	-	-	KR857280.1	-	-	-	-	-	-	-	-	-	-	-	-	-	-	-	-	-	-
140842-Carex pallescens	AY278299.1	AY757539.1	KY562669.1	AY757673.1	KJ841191.1	-	KF602149.1	-	-	-	-	-	-	-	-	-	-	-	-	-	-	-
241225-Carex parviflora	AY278265.1	EU288447.1	LK021927.1	KT021016.1	-	LK021864.	-	-	-	-	-	-	-	-	-	-	-	-	-	-	-	-
241226-Carex pilosa	AY278286.1	-	-	-	-	-	-	-	-	-	-	-	-	-	-	-	-	-	-	-	-	-
140848-Carex pilulifera	AY278280.1	AF284873.1	JN893867.1	AY325438.1	JN891691.1	-	HM849863.1	-	-	-	-	-	-	-	-	-	-	-	-	-	-	-
241227-Carex pseudocyperus	AY278295.1	-	HG915871.1	-	KJ841201.1	HG915780.	-	-	-	JN314482.1	-	-	-	-	-	-	-	-	-	-	-	-
240667-Carex stenophylla	AY280535.1	-	-	EU001224.1	-	KR827143.	JX848455.1	KR827194.1	-	-	-	-	-	-	-	-	-	-	-	-	-	-
140859-Carex tomentosa	AY278287.1	AF284945.1	-	-	-	-	-	-	-	-	-	-	-	-	-	-	-	-	-	-	-	-
140863-Carex umbrosa	AY278270.1	-	-	-	-	-	-	-	-	-	-	-	-	-	-	-	-	-	-	-	-	-
140782-Carex acuta	KX166914.1	HM590254.1	JN895251.1	AY770434.1	JN892450.1	-	-	-	JN222813.1	-	JN222839.1	-	-	-	-	-	-	-	-	-	-	-
502401-Carex caryophyllea	KX166686.1	EU288430.1	JN895022.1	-	JN893402.1	-	-	-	-	-	-	-	-	-	-	-	-	-	-	-	-	-
312760-Carex pendula	KU939626.1	AY757527.1	JN896249.1	AY757661.1	JN893828.1	-	HM849861.1	KC122384.1	KU939785.1	-	-	-	FM160522.1	-	-	-	-	-	-	-	-	-
502415-Carex hartmanii	LK021774.1	EU288436.1	LK021898.1	LK021711.1	-	LK021836.	-	-	-	-	-	-	-	-	-	-	-	-	-	-	-	-
2043217-Carex buekii	MF945751.1	-	-	MF945736.1	-	-	-	-	MF945766.1	-	MH094145.1	-	-	-	-	-	-	-	-	-	-	-
910631-Carex cespitosa	MF945752.1	HM590256.1	-	MF945737.1	-	-	-	-	MF945767.1	-	MF966961.1	-	-	-	-	-	-	-	-	-	-	-
312765-Carex riparia	HG915829.1	AY757498.1	HG915875.1	AY757633.1	JN893598.1	HG915784.	-	-	-	-	-	-	-	-	-	-	-	-	-	-	-	-
912472-Carex melanostachya	JN634644.1	-	HG915862.1	-	-	JN627823.	-	JN627756.1	-	-	-	-	-	-	-	-	-	-	-	-	-	-
442460-Carex baldensis	GU176152.1	GU176107.1	KP273671.1	EF363121.1	-	KP273780.	-	-	-	-	-	-	KP273725.1	-	-	-	-	-	-	-	-	-
502412-Carex fimbriata	EU288551.1	EU288435.1	-	-	-	-	-	-	-	-	-	-	-	-	-	-	-	-	-	-	-	-
234471-Carex pulicaris	-	AY757563.1	KJ513590.1	-	-	KP273813.	GQ469843.1	GQ469858.1	-	-	-	-	KJ513576.1	-	-	-	-	-	-	-	-	-
529425-Carex halleriana	-	KY697560.1	-	-	-	-	AM999795.1	-	-	-	-	-	FM160521.1	-	-	-	-	-	-	-	-	-
1155257-Carex strigosa	-	-	JN896041.1	-	JN893601.1	-	-	-	-	-	-	-	-	-	-	-	-	-	-	-	-	-
46331-Carex simpliciuscula	MH348240.1	EU288541.1	JX065088.1	AH012937.2	MG227629.1	KP273828.	U49232.1	-	-	FJ548467.1	-	-	AF163462.1	FJ548243.1	-	-	-	-	-	FJ548372.1	-	EU288541.1

Specie\Loci	10-ITS	1-Festuca altissima tRNA-Leu (trnL) gene and trnL-trnF intergenic spacer partial sequence; chloroplast gene for chloroplast product	2-Festuca norica trnT-trnL intergenic spacer partial sequence; chloroplast	3-Festuca valesiaca maturase K gene complete cds; plastid	4-Festuca quadriflora ribulose-15-bisphosphate carboxylase/oxygenase large subunit gene partial cds; chloroplast	5-Festuca rubra tRNA-Leu (trnL) gene intron	6-Festuca rubra voucher PI 595056 trnQ-rps16 intergenic spacer region partial sequence; chloroplast	7-Festuca ovina CEN (CEN) gene partial cds	8-Festuca circummediterranea plastid acetyl-CoA carboxylase (Acc1) gene partial cds; nuclear gene for plastid product	9-Festuca ovina voucher YDK2008440 NADH dehydrogenase subunit F (ndhF) gene partial cds; chloroplast
98750-Festuca ovina	AF532959.1	KX372426.1	DQ367406.1	HM453067	KP711235.1	GQ244980.1	KT439047.1	HM453146.1	HM453100.1	KM538748.1
145848-Festuca paniculata	KP296037.1	JQ972972.1	EF585101.1	MF999124.	MF998457.1	-	-	-	-	-
145834-Festuca alpina	KF917222.1	AF478522.1	EF585001.1	-	-	-	-	-	-	KJ529515.1
52153-Festuca rubra	KF917291.1	KX372428.1	EF585011.1	EF137498.	AJ746261.1	DQ860562.1	KT439052.1	-	-	U71015.1
208425-Festuca rupicola	AJ508379.1	KU600325.1	-	KJ746197.1	KJ746319.1	AY583731.1	-	-	-	-
745661-Festuca vivipara	KX166180.1	-	-	JN894537.	KT960433.1	LT160676.1	-	-	-	-
145835-Festuca altissima	HM453182.1	AF478505.1	EF585003.1	AM234585.	JN891928.1	HE993613.1	-	HM453157.1	HM453082.1	JX438147.1
89682-Festuca heterophylla	AJ240159.1	-	EF585049.1	HE966927.	KT438955.1	-	KT439039.1	-	-	-
199741-Festuca dimorpha	AF519982.1	AF519987.1	EF585032.1	-	-	-	-	-	-	-
89683-Festuca filiformis	AJ240160.1	-	-	JN894715.	MG226816.1	-	-	-	-	-
145851-Festuca quadriflora	AF519983.1	AF519988.1	EF585089.1	-	KF602176.1	-	-	-	-	-
98753-Festuca valesiaca	HM453198.1	EF593011.1	EF585112.1	HM453069	KT438971.1	AY583734.1	KT439055.1	HM453171.1	HM453122.1	-
98749-Festuca lemanii	KX166434.1	-	-	JN896072.1	KT438959.1	DQ376060.1	KT439043.1	-	-	-
225185-Festuca pallens	AY254373.1	EF592990.1	-	HM453066	-	AY583728.1	-	HM453144.1	HM453123.1	-
225186-Festuca pseudodalmatica	AY254374.1	-	-	-	-	AY583729.1	-	-	-	-
225187-Festuca stricta	AY254377.1	-	-	-	-	AY583732.1	-	-	-	-
1532827-Festuca laxa	KY368816.1	KY368867.1	KY368917.1	-	-	-	-	-	-	-
1532828-Festuca nitida	KY368826.1	KY368878.1	KY368924.1	-	-	-	-	-	-	-
2056065-Festuca picturata	KY368827.1	KY368879.1	KY368925.1	-	-	-	-	-	-	-
906890-Festuca circummediterranea	HM453195.1	-	-	HM453068	-	-	-	HM453145.1	HM453089.1	-
464085-Festuca violacea	EF584979.1	EF593012.1	EF585113.1	-	KF602187.1	-	-	-	-	-
464034-Festuca amethystina	EF584919.1	EF592950.1	EF585004.1	-	-	-	-	-	-	-
464054-Festuca halleri	EF584942.1	EF592975.1	EF585047.1	-	-	-	-	-	-	-
464058-Festuca intercedens	EF584948.1	EF592979.1	EF585055.1	-	-	-	-	-	-	-
464060-Festuca laevigata	EF584950.1	EF592981.1	EF585059.1	-	-	-	-	-	-	-
464066-Festuca norica	EF584955.1	EF592987.1	EF585072.1	-	-	-	-	-	-	-
464079-Festuca scabriculmis	EF584970.1	EF593003.1	EF585099.1	-	-	-	-	-	-	-
116553-Festuca rupicaprina	AF171145.1	-	-	-	-	-	-	-	-	-
470288-Trisetum distichophyllum	-	KX872870.1	-	KX873531.	-	-	-	-	-	-
199742-Festuca pulchella	-	-	EF585085.1	KJ529399.1	KT438966.1	-	KT439050.1	-	-	KJ529510.1
370715-Festuca gracilior	-	-	-	-	-	DQ376064.1	-	-	-	-
4521-Lolium multiflorum	AF532946	KX372443.1	EF379022.1	FN908061.	LT576830.1	EU119375.1	KT439058.1	HM453159.1	HM453078.1	KM538757.1
4522-Lolium perenne	KJ598999	JN187653	EF379024.1	DQ786925.	KP711237.1	EU119376.1	KT439060.1	HM453158.1	HM453079.1	ON759378.1
89675-Lolium remotum	AF171159	EF378978	EF379031	-	-	EF378979	-	-	-	KJ529481
89674-Lolium rigidum	ON243862	EF378980	KF797243	DQ786926	LT576831	DQ376043	KT439064	XR_006987897	AF343457	DQ786854
34176-Lolium temulentum	AJ240145	EF378986	EF379040	HM453063	MF998456	EF378988	KT439066	HM453148	HM453077	KM538758
200271-Micropyrum tenellum	KF917334	AF478534	EF585116	KJ529387	-	AF478534	-	-	-	KJ529488
200275-Psilurus incurvus	KF917299	LR606692	JQ973013	HE646587	EF125155	LR606692	-	-	-	JX438159
200278-Festuca bromoides	KJ598933	AF487616	KJ529296	LN906796	LN908031	AF487616	-	-	-	KJ529497
200279-Festuca ambigua	MT145309	AF478527	EF585120	KJ529386	EF125157	AY118105	-	-	-	KJ529487
200524-Festuca muralis	KF917262	AY118102	EF585126	KJ529391	HM850471	AY118102	-	-	-	KJ529496
89686-Festuca myuros	AY118095	LR606694	DQ631489	LR606896	KF713070	MZ965293	KT439068	-	-	KM538776
200282-Festuca unilateralis	AY118095	AY118107	EF585130	HE646590	KF997332	AY118107	-	-	-	KJ529491

Specie\Loci	17-ITS	1-Ranunculus glacialis voucher J.T. Johansson s.n. trnK gene intron; and maturase K (matK) gene complete cds; chloroplast	2-Ranunculus alpestris ribulose-15-bisphosphate carboxylase/oxygenase large subunit gene partial cds; chloroplast	3-Ranunculus gramineus trnL gene intron; chloroplast	4-Ranunculus crenatus voucher Hoerandl 2818 PsbJ (psbJ) gene partial cds; and psbJ-petA intergenic spacer partial sequence; chloroplast	5-Ranunculus aquatilis isolate NMW3988 maturase K (matK) gene partial cds; chloroplast	6-Ranunculus fluitans isolate 21Batr_fluit_Vilnia_2 trnH-psbA intergenic spacer partial sequence; and photosystem II protein D1 (psbA) gene partial cds; chloroplast	7-Ranunculus lingua tRNA-Leu (trnL) gene partial sequence; trnL-trnF intergenic spacer complete sequence; and tRNA-Phe (trnF) gene partial sequence; chloroplast	8-Ranunculus circinatus isolate 1117 trnL-rpl32 intergenic spacer partial sequence; chloroplast	9-Ranunculus rionii isolate 502 psbE-petL intergenic spacer partial sequence; chloroplast	10-Ranunculus aconitifolius isolate ACON1 ribosomal protein L32 (rpl32) gene partial cds; rpl32-trnL intergenic spacer complete sequence; and tRNA-Leu (trnL) gene partial sequence; chloroplast	11-Ranunculus kuepferi isolate CSTA21 rpl20-rps12 intergenic spacer partial sequence; chloroplast	12-Ranunculus acris voucher BM000954718 RNA polymerase C (rpoC1) gene partial cds; chloroplast	13-Ranunculus bulbosus voucher BM000954794 atpF-atpH intergenic spacer partial sequence; chloroplast	14-Ranunculus trichophyllus chloroplast DNA psbB-psbF intergenic spacer	15-Ranunculus trichophyllus chloroplast rps16 gene intron	16-Ranunculus penicillatus chloroplast trnK gene intron 5 region
286847-Ranunculus aconitifolius	KU974069.1	AY954217.1	KF602169.1	EU792596.1	HQ338172.1	-	-	-	-	-	JX025321.1	EU792719.1	-	-	-	-	-
235900-Ranunculus glacialis	JX105174.1	AY954219.1	KF602157.1	GQ244636.1	GU258027.1	-	-	-	-	-	JX118539.1	JX118349.1	-	-	-	-	-
286907-Ranunculus gramineus	JX025232.1	AY954227.1	-	KY697505.1	-	-	-	-	-	-	JX025325.1	-	-	-	-	-	-
105186-Ranunculus lingua	KX167029.1	AY954206.1	JN892595.1	-	HQ338236.1	-	-	JX280910.1	-	-	-	-	-	-	-	-	-
137665-Ranunculus repens	JQ439869.1	HM565166.1	KF602173.1	JQ041850.1	HQ338287.1	JN114770.1	-	-	-	-	-	-	FJ395757.1	FJ395270.1	-	-	-
3447-Ranunculus acris	KX165735.1	AY954199.1	KF602170.1	KX667979.1	-	-	-	-	-	-	-	-	FJ395840.1	HQ594827.1	-	-	-
278071-Ranunculus flammula	KX166222.1	AY954204.1	HM850295.1	KX668071.1	GU258025.1	-	-	-	-	-	-	-	-	-	-	-	-
286924-Ranunculus lanuginosus	AY680163.1	AY954194.1	-	KX668006.1	HQ338231.1	-	-	-	-	-	-	-	-	-	-	-	-
286898-Ranunculus fluitans	AY680069.1	AY954129.1	JN891886.1	-	FJ619880.1	HQ894446.1	MF167629.1	AB296150.1	MG162724.1	MG162821.1	-	-	-	-	AB296153.1	AB296152.1	AB296151.1
286964-Ranunculus peltatus	KX166651.1	-	JN892102.1	-	-	JN894996.1	HQ894438.1	-	MG162763.1	MG162860.1	-	-	-	-	AB296156.1	AB296155.1	AB296154.1
286966-Ranunculus penicillatus	MG098966.1	-	JN892100.1	-	-	KF871230.1	MF167611.1	AB296157.1	MG162771.1	MG162868.1	-	-	-	-	AB296160.1	AB296159.1	AB296158.1
147635-Ranunculus sceleratus	KX277667.1	GU257993.1	AB517148.1	DQ410746.1	-	-	HQ596811.1	-	KC842129.1	-	-	-	HQ594101.1	HQ594829.1	-	-	-
286984-Ranunculus pygmaeus	MG237006.1	AY954122.1	KT960698.1	DQ860599.1	HQ338232.1	-	-	-	-	-	KC842126.1	-	-	-	-	-	-
74828-Ranunculus bulbosus	KX166669.1	-	HM850293.1	KY697496.1	-	HM851057.1	FJ493303.1	FJ490812.1	-	-	-	-	FJ395770.1	FJ395281.1	-	-	-
286858-Ranunculus arvensis	KX166591.1	AY954193.1	JN892029.1	-	-	-	-	AB617672.1	-	-	KC842099.1	-	-	-	-	-	-
147622-Ranunculus circinatus	KX165828.1	-	GU344677.1	-	-	HQ894448.1	HQ894442.1	AB296146.1	MG162710.1	MG162807.1	-	-	-	-	AB296149.1	AB296148.1	AB296147.1
286974-Ranunculus polyanthemos	MN151385.1	AY954185.1	-	HM590338.1	GU258040.1	-	-	AB617679.1	-	-	-	-	-	-	-	-	-
22903-Ranunculus trichophyllus	DQ311658.1	AY954133.1	L08766.1	-	-	HQ894447.1	HQ894441.1	AB296165.1	MG162780.1	MG162877.1	-	-	-	-	AB296168.1	AB296167.1	AB296166.1
286945-Ranunculus muricatus	DQ410718.1	AY954191.1	HM850296.1	DQ410740.1	-	-	-	-	-	-	-	-	-	-	-	-	-
568533-Ranunculus auricomus	KX165825.1	FM242739.1	HE574635.1	-	-	-	-	-	-	-	-	-	FJ395782.1	FJ395292.1	-	-	-
568530-Ranunculus aquatilis	KX166597.1	-	MG247653.1	-	-	JN893994.1	KC620498.1	-	MG162700.1	MG162797.1	-	-	-	-	-	-	-
568561-Ranunculus polyanthemoides	FM242865.1	FM242801.1	-	KU974025.1	-	-	-	-	-	-	-	-	-	-	-	-	-
35930-Ranunculus sardous	KX166649.1	AY954186.1	MG249692.1	-	-	-	-	-	-	-	-	-	-	-	-	-	-
286986-Ranunculus reptans	AY680186.1	AY954205.1	-	GQ245381.1	HQ338288.1	-	-	-	-	-	-	-	-	-	-	-	-
286962-Ranunculus parviflorus	MG237667.1	AY954202.1	HM850297.1	-	HQ338270.1	-	-	-	-	-	-	-	-	-	-	-	-
568570-Ranunculus rionii	MG098973.1	FM242791.1	-	-	-	-	-	-	MG162778.1	MG162875.1	-	-	-	-	-	-	-
286849-Ranunculus aduncus	AY680088.1	AY954143.1	-	-	HQ338206.1	-	-	-	-	-	-	-	-	-	-	-	-
286851-Ranunculus alpestris	AY680078.1	AY954221.1	KF602171.1	-	HQ338239.1	-	-	-	-	-	-	-	-	-	-	-	-
286861-Ranunculus bilobus	AY680077.1	AY954220.1	-	-	HQ338169.1	-	-	-	-	-	-	-	-	-	-	-	-
286878-Ranunculus carinthiacus	AY680093.1	AY954145.1	-	-	-	-	-	-	-	-	-	-	-	-	-	-	-
286892-Ranunculus crenatus	AY680086.1	AY954228.1	-	-	HQ338191.1	-	-	-	-	-	-	-	-	-	-	-	-
286914-Ranunculus hybridus	AY680189.1	AY954211.1	-	-	HQ338222.1	-	-	-	-	-	-	-	-	-	-	-	-
286941-Ranunculus montanus	AY680094.1	AY954149.1	KF602172.1	-	-	-	-	-	-	-	-	-	-	-	-	-	-
286971-Ranunculus platanifolius	EU792846.1	AY954216.1	-	EU792600.1	HQ338276.1	-	-	-	-	-	-	EU792723.1	-	-	-	-	-
320426-Ranunculus traunfellneri	AY954245.1	AY954222.1	-	-	-	-	-	-	-	-	-	-	-	-	-	-	-
287004-Ranunculus velutinus	AY680173.1	AY954198.1	-	-	-	-	-	-	-	-	-	-	-	-	-	-	-
287005-Ranunculus venetus	AY680087.1	AY954144.1	-	-	-	-	-	-	-	-	-	-	-	-	-	-	-
287006-Ranunculus villarsii	AY680099.1	AY954153.1	-	-	-	-	-	-	-	-	-	-	-	-	-	-	-
286868-Ranunculus breyninus	AY680115.1	AY954172.1	-	-	-	-	-	-	-	-	-	-	-	-	-	-	-
286992-Ranunculus seguieri	EU792856.1	AY954215.1	-	EU792610.1	-	-	-	-	-	-	KF528845.1	EU792733.1	-	-	-	-	-
287000-Ranunculus thora	AY680188.1	AY954210.1	-	-	-	-	-	-	-	-	-	-	-	-	-	-	-
168007-Anemone sylvestris	AM267276.1	-	MK551082.1	KJ746402.1	-	-	-	-	-	-	-	-	-	-	-	-	-
286921-Ranunculus kuepferi	EU792758.1	-	-	EU792561.1	-	-	-	-	-	-	-	EU792673.1	-	-	-	-	-
1000426-Ranunculus tuberosus	-	-	KF602158.1	-	-	-	-	-	-	-	-	-	-	-	-	-	-

Specie\Loci	9-ITS	1-Saxifraga diapensioides chloroplast DNA containing trnL(UAA) gene (5 exon intron and 3 exon) trnL-F IGS trnF(GAA) gene specimen voucher N. Tkach 231 & M. Roeser (HAL)	2-Saxifraga rotundifolia plastid:chloroplast DNA containing partial rpl32 gene rpl32-trnL(UAG) IGS and partial trnL(UAG) gene specimen voucher N. Tkach 68 (HAL)	3-Saxifraga presolanensis voucher C. Mermod s.n. (NEU) maturase K (matK) gene partial cds; chloroplast	4-Saxifraga paniculata voucher Aiken_04-053_CAN ribulose-15-bisphosphate carboxylase/oxygenase large subunit (rbcL) gene partial cds; chloroplast	5-Saxifraga hostii genomic DNA containing psbA-trnH IGS specimen voucher MIB:ZPL:04256	6-Saxifraga oppositifolia chloroplast ribulose-15-bisphosphate carboxylase/oxygenase large subunit (rbcL) gene partial cds	7-Saxifraga bryoides chloroplast DNA containing trnL(UAA) gene (3 exon) trnL-F IGS trnF(GAA) gene specimen voucher M. Roeser 9602 (HAL)	8-Saxifraga oppositifolia 26S ribosomal RNA gene partial sequence
29771-Saxifraga oppositifolia	AY354300.1	LM654503.1	LT971175.1	L34143.1	-	AF374739.1	U06217.1	KF196418.1	AF374834.1
192742-Saxifraga biflora	KU645958.1	LN812595.1	-	-	-	-	-	-	-
102716-Saxifraga caesia	LN812373.1	LN812607.1	LT971064.1	AF133136.1	HG417042.1	HG800572.1	-	-	-
29769-Saxifraga cernua	KX166956.1	AF374779.1	-	L34140.1	-	AF374736.1	U06215.1	-	AF374831.1
102722-Saxifraga cuneifolia	LN812404.1	LN812639.1	LT971091.1	KU524236.1	-	-	KC749992.1	-	-
134778-Saxifraga depressa	KU524113.1	-	-	KU524239.1	-	-	-	-	-
102725-Saxifraga florulenta	AF087591.1	-	-	AF133137.1	-	-	-	KU524372.1	-
83409-Saxifraga granulata	AJ233860.1	LN812676.1	LT971128.1	KU524260.1	JN892372.1	-	-	-	-
159962-Saxifraga hirculus	KX166339.1	DQ860620.1	LT971133.1	KC475848.1	KT960736.1	AF374738.2	-	-	AF374833.1
1534585-Saxifraga presolanensis	LN812507.1	LN812743.1	-	KU524289.1	-	-	-	-	-
85263-Saxifraga retusa	KU645981.1	-	-	-	-	-	-	-	-
134793-Saxifraga sedoides	KU524182.1	-	-	KU524300.1	-	-	-	-	-
102737-Saxifraga squarrosa	AF087587.1	KU524435.1	-	AF133135.1	-	-	-	-	-
406025-Saxifraga adscendens	EF028688.1	LN812575.1	LT971038.1	-	MG245942.1	-	-	-	-
406026-Saxifraga tridactylites	EF028687.1	LN812790.1	LT971234.1	JN894658.1	MG247985.1	-	-	-	-
102714-Saxifraga aizoides	KX166010.1	AF374787.1	LT971039.1	KC475819.1	-	HG800571.1	KM360971.1	-	AF374839.1
83410-Saxifraga exarata	AJ233861.1	LN812652.1	LT971104.1	-	-	-	-	-	-
84738-Saxifraga fragosoi	AJ233867.1	LN812665.1	LT971118.1	-	-	-	-	-	-
102728-Saxifraga hostii	LN812452.1	LN812687.1	LT971136.1	AF133132.1	HG417043.1	HG800573.1	-	-	-
23265-Saxifraga rotundifolia	LN812519.1	LN812754.1	LT971198.1	-	HG417044.1	AF374740.1	-	X71989.1	AF374835.1
102734-Saxifraga paniculata	MG236575.1	LN812731.1	LT971176.1	KC475859.1	KC484073.1	-	KF602178.1	-	-
134767-Saxifraga androsacea	LT970993.1	LN812584.1	LT971044.1	-	-	-	-	-	-
134768-Saxifraga aphylla	LT970994.1	LT970893.1	LT971047.1	-	-	-	-	-	-
1385495-Saxifraga aspera	KF196319.1	LN812590.1	LT971051.1	-	-	-	-	KF196371.1	-
1385497-Saxifraga bryoides	KF196318.1	-	LT971062.1	-	-	-	-	LN812605.1	-
134772-Saxifraga bulbifera	LN812372.1	LN812606.1	LT971063.1	-	-	-	-	-	-
102719-Saxifraga cochlearis	LN812391.1	LN812625.1	LT971079.1	AF133133.1	-	-	-	-	-
102720-Saxifraga cotyledon	LN812401.1	LN812636.1	LT971088.1	-	-	-	-	-	-
102721-Saxifraga crustata	LN812402.1	LN812637.1	LT971089.1	-	-	-	-	-	-
1534576-Saxifraga diapensioides	LN812408.1	LN812643.1	LT971095.1	-	-	-	-	-	-
134794-Saxifraga facchinii	LT970995.1	LT970894.1	LT971105.1	-	-	-	-	-	-
102732-Saxifraga mutata	LN812486.1	LN812720.1	LT971170.1	AF133138.1	-	-	-	-	-
1534583-Saxifraga paradoxa	LN812495.1	LN812732.1	LT971177.1	-	-	-	-	-	-
1534584-Saxifraga petraea	LN812501.1	LN812738.1	LT971183.1	-	-	-	-	-	-
1534586-Saxifraga seguieri	LN812528.1	LN812762.1	LT971206.1	-	-	-	-	-	-
1534587-Saxifraga tenella	LN812547.1	LN812783.1	LT971227.1	-	-	-	-	-	-
102717-Saxifraga callosa	LN812374.1	LN812608.1	-	-	-	-	-	-	-
102735-Saxifraga pedemontana	AF087606.1	-	-	-	-	-	-	-	-
182070-Saxifraga stolonifera	-	LN812775.1	LT971220.1	KC737243.1	-	-	KC737395.1	-	-
78511-Ribes nigrum	-	KX667935.1	-	HE967476.1	MG247103.1	-	-	-	-

Specie\Loci	13-ITS	1-Viola mirabilis voucher KWNU 65496 maturase K (matK) gene complete cds; chloroplast	2-Viola canina clone canCHS2A chalcone synthase gene exon 1 intron 1 exon 2 and partial cds	3-Viola collina voucher Yoo814 tRNA-Leu (trnL) gene partial sequence; trnL-trnF intergenic spacer complete sequence; and tRNA-Phe (trnF) gene partial sequence; chloroplast	4-Viola canina tRNA-Ser (trnS) gene partial sequence; trnS-trnG intergenic spacer complete sequence; and tRNA-Gly (trnG) gene partial sequence	5-Viola jordanii clone jorCHS1 chalcone synthase gene exon 1 intron 1 exon 2 and partial cds	6-Viola cucullata voucher AP011 ribulose-15-bisphosphate carboxylase/oxygenase large subunit (rbcL) gene partial cds; chloroplast	7-Viola odorata ribulose-15-bisphosphate carboxylase/oxygenase large subunit gene partial cds; chloroplast	8-Viola mirabilis voucher TM675 clone C glucose-6-phosphate isomerase (GPI) gene partial sequence	9-Viola collina voucher KWNU Yoo814 RNA polymerase beta subunit-1 (rpoC1) gene exon 2 and partial cds; chloroplast	10-Viola biflora clone A NRPD2/NRPE2-like protein gene partial sequence	11-Viola hirta clone M shikimate dehydrogenase-like protein gene partial sequence	12-Viola arvensis voucher AP460 AtpF (atpF) gene partial cds; atpH-atpF intergenic spacer complete sequence; and AtpH (atpH) gene partial cds; chloroplast
97443-Viola pinnata	JQ950572.1	JQ950598.1	-	JQ950645.1	-	-	-	JQ950625.1	JQ950672.1	-	-	-	-
214053-Viola tricolor	AY148243.1	JN894507.1	-	KC699708.1	-	-	-	KC699617.1	-	-	-	-	-
97441-Viola odorata	KX166897.1	JN895231.1	EU311458.1	-	EU311519.1	EU311432.1	-	MG946877.1	-	-	-	-	-
97450-Viola reichenbachiana	DQ055384.1	JN895230.1	EU311488.1	KY697465.1	EU311526.1	EU311435.1	JN893278.1	-	-	FJ395774.1	-	-	-
214052-Viola riviniana	AY148242.1	KJ747842.1	EU311470.1	-	EU311525.1	EU311449.1	JN892436.1	-	-	-	-	-	-
75704-Salix alba	KU724219.1	EU790677.1	-	AJ849556.1	-	-	FN689366.1	AB012780.1	-	FN689647.1	-	-	-
97415-Viola arvensis	DQ055340.1	KJ204559.1	-	-	-	-	-	KM361034.1	-	HQ594185.1	-	-	HQ594926.1
214529-Viola biflora	DQ055348.1	DQ842607.1	EU311455.1	DQ085922.1	EU311528.1	-	-	KF602183.1	JF767023.1	GQ262491.1	GU289574.1	KJ138098.1	GQ262549.1
97420-Viola calcarata	AY148229.1	-	-	KJ138157.1	-	-	-	KF602163.1	KJ137997.1	-	GU289614.1	KJ138099.1	-
97427-Viola elatior	MG879276.1	-	EU311476.1	-	EU311516.1	EU311441.1	-	KF997501.1	-	-	-	-	-
369421-Viola hirta	DQ358856.1	JN895879.1	-	JF767170.1	-	-	FR865127.1	-	JF767065.1	-	GU289582.1	KJ138118.1	-
369422-Viola mirabilis	DQ358835.1	GQ262544.1	EU311469.1	GQ262534.1	EU311529.1	-	-	-	JF767085.1	GQ262501.1	GU289584.1	KJ138121.1	GQ262559.1
502511-Viola canina	KU974083.1	JN894337.1	EU311472.1	-	EU311515.1	EU311439.1	JN893570.1	-	-	-	-	-	-
333555-Viola collina	FJ002880.1	DQ842571.1	-	DQ085887.1	-	-	-	-	JF767044.1	GQ262494.1	KU949395.1	KU949406.1	GQ262552.1
214047-Viola lutea	DQ055377.1	JN894505.1	-	-	-	-	JN892428.1	-	-	-	-	-	-
369424-Viola suavis	FN400816.1	-	EU311457.1	-	EU311518.1	EU311434.1	-	-	-	-	-	-	-
214043-Viola comollia	AY148232.1	-	-	-	-	-	-	-	-	-	-	-	-
97424-Viola cucullata	MG237103.1	HQ593502.1	-	-	-	-	HQ590335.1	-	-	HQ594189.1	-	-	HQ594930.1
214046-Viola kitaibeliana	AY148235.1	-	-	-	-	-	MG247797.1	-	-	-	-	-	-
214054-Viola valderia	AY148244.1	-	-	-	-	-	-	-	-	-	-	-	-
502524-Viola stagnina	KX166475.1	-	EU311481.1	-	EU311510.1	EU311442.1	-	-	JF767134.1	-	KU949392.1	KU949403.1	-
462882-Viola palustris	KX166144.1	JN894506.1	-	JF767187.1	-	-	MG249728.1	HM850468.1	JF767100.1	-	-	-	-
502521-Viola rupestris	KX166965.1	-	EU311483.1	HM483566.1	EU311517.1	EU311437.1	-	-	-	-	-	-	-
369417-Viola alba	HM851449.1	-	EU311460.1	KR150205.1	EU311522.1	EU311433.1	-	-	-	-	-	-	-
1042420-Viola pyrenaica	JF683821.1	-	-	-	-	-	-	-	-	-	-	-	-
1042419-Viola thomasiana	JF683842.1	-	-	-	-	-	-	-	-	-	-	-	-
501336-Viola ambigua	EU413936.1	-	-	-	-	-	-	-	-	-	-	-	-
502514-Viola jordanii	-	-	EU311462.1	-	EU311512.1	EU311436.1	-	-	-	-	-	-	-
502519-Viola pumila	-	-	EU311474.1	-	EU311514.1	EU311444.1	-	-	-	-	-	-	-
1534726-Viola argenteria	-	-	-	KU558448.1	-	-	-	-	-	KU558208.1	-	-	KU558128.1

TABLE S2: Performance metrics of the different models and classes. The columns show two different classification methods combined without and with two filtering thresholds. The first six rows contain the performance metrics of the different classes. The remaining rows show weighted means, false positive, false negative rates, and the fraction of false positive errors (computed for the whole model).

Performance metrics	Polygon unfiltered	Polygon (≥ 5%)	Polygon (≥ 20%)	ElevDistr unfiltered	ElevDistr (≥ 5%)	ElevDistr (≥ 20%)
Precision alpine	27.27%	23.53%	9.59%	28.57%	20.83%	9.89%
Recall alpine	15.00%	20.00%	35.00%	20.00%	25.00%	45.00%
Precision both	40.72%	58.47%	78.91%	68.19%	86.54%	93.60%
Recall both	89.82%	83.84%	57.13%	83.72%	67.05%	39.06%
Precision non-alpine	95.22%	94.56%	89.60%	94.95%	91.06%	86.23%
Recall non-alpine	59.54%	81.76%	95.38%	88.41%	97.33%	99.52%
Weighted mean precision	81.90%	85.58%	86.58%	88.21%	89.57%	87.52%
Weighted mean recall	66.45%	81.88%	85.95%	86.89%	89.72%	84.86%
False positive rate	15.54%	7.11%	1.91%	4.63%	1.24%	0.35%
False negative rate	1.28%	2.00%	5.22%	1.93%	3.90%	7.25%
Fraction of false positive rate	0.92	0.78	0.27	0.71	0.24	0.05

TABLE S3: Results of the 24 DEC models and the mean over all models. Every row represents a different DEC model that is a combination of the six modeled clades and four different classification models. The dispersal and extirpation rate are shown together with the 95% highest probability density (HPD), the number of states in the MCMC, the false positive and false negative rate, as well as the FFP and the deviation from inferred expert (i.e., rate inferred from the Flora Alpina) dispersal and extirpation rate.

Genus	Classification models	Posterior mean of the dispersal rate	95% HPD dispersal rate	Posterior mean of the extirpation rate	95% HPD extirpation rate	States	False positive rate	False negative rate	Fraction of false positive errors	Deviation from inferred expert dispersal rate	Deviation from inferred expert extirpation rate
Campanula	ElevDistr	0.0522	0.0233 - 0.0899	0.5730	0.1986 - 1.0007	100,000	0.0439	0.0263	0.63	28.57	-13.13
Campanula	Flora Alpina	0.0406	0.0152 - 0.0711	0.6596	0.2095 - 1.1753	100,000	0	0	0.50	0.00	0.00
Campanula	Polygon plus filtering	0.0308	0.0118 - 0.0542	1.0191	0.3015 - 1.8685	100,000	0.0263	0.0965	0.21	-24.14	54.50
Campanula	Polygon	2.0900	0.0876 - 5.7460	0.4386	0.2259 - 0.6780	10,000,000	0.1491	0.0263	0.85	5047.78	-33.51
Carex	ElevDistr	0.0431	0.0283 - 0.0583	0.3535	0.1375 - 0.6079	100,000	0.0500	0.0100	0.83	31.40	-10.60
Carex	Flora Alpina	0.0328	0.0205 - 0.0447	0.3954	0.1322 - 0.6843	100,000	0	0	0.50	0.00	0.00
Carex	Polygon plus filtering	0.0229	0.0133 - 0.0333	1.0570	0.3510 - 1.8951	100,000	0.0100	0.1000	0.09	-30.18	167.32
Carex	Polygon	2.8569	0.0578 - 8.5982	0.3045	0.1726 - 0.4509	10,000,000	0.1600	0.0050	0.97	8610.06	-22.99
Festuca	ElevDistr	0.0949	0.0134 - 0.1506	0.5050	0.1649 - 0.9206	10,000,000	0.0465	0.0349	0.57	-11.97	-11.08
Festuca	Flora Alpina	0.1078	0.0513 - 0.1716	0.5679	0.1936 - 1.0211	10,000,000	0	0	0.50	0.00	0.00
Festuca	Polygon plus filtering	0.0550	0.0226 - 0.0926	0.6418	0.1877 - 1.2090	1,000,000	0.0116	0.0698	0.14	-48.98	13.01
Festuca	Polygon	0.8561	0.0452 - 4.2927	0.4610	0.1576 - 0.8085	10,000,000	0.0930	0.0233	0.80	694.16	-18.82
Ranunculus	ElevDistr	0.0708	0.0284 - 0.1217	0.5449	0.1815 - 0.9842	100,000	0.0455	0.0568	0.44	-51.67	-9.49
Ranunculus	Flora Alpina	0.1465	0.0280 - 0.1912	0.6020	0.2144 - 1.0646	10,000,000	0	0	0.50	0.00	0.00
Ranunculus	Polygon plus filtering	0.0386	0.0147 - 0.0666	0.8980	0.2778 - 1.6853	100,000	0.0114	0.1136	0.09	-73.65	49.17
Ranunculus	Polygon	5.0399	0.0625 - 12.1327	0.5201	0.2382 - 0.8535	10,000,000	0.1136	0.0455	0.71	3340.20	-13.60
Saxifraga	ElevDistr	9.1526	2.5827 - 14.3140	0.4180	0.1889 - 0.6860	10,000,000	0.025	0.025	0.50	-0.46	0.19
Saxifraga	Flora Alpina	9.1953	3.1167 - 14.4656	0.4172	0.1838 - 0.6819	10,000,000	0	0	0.50	0.00	0.00
Saxifraga	Polygon plus filtering	3.4410	0.0293 - 7.6397	1.0036	0.4224 - 1.6897	10,000,000	0.0250	0.1625	0.13	-62.58	140.56
Saxifraga	Polygon	9.1127	1.5749 - 13.9368	0.4171	0.1885 - 0.6849	10,000,000	0.0375	0.0375	0.50	-0.90	-0.02
Viola	ElevDistr	0.0469	0.0046 - 0.0291	0.8046	0.2244 - 1.4982	100,000	0.0667	0.0167	0.80	493.67	-7.79
Viola	Flora Alpina	0.0079	0.0002 - 0.0134	0.8726	0.2408 - 1.713	100,000	0	0	0.50	0.00	0.00
Viola	Polygon plus filtering	0.0385	0.0030 - 0.0255	0.8314	0.2324 - 1.5975	10,000,000	0.0500	0.0167	0.75	387.34	-4.72
Viola	Polygon	3.4790	0.0321 - 6.3231	0.4234	0.1769 - 0.7147	10,000,000	0.2333	0.0167	0.93	43937.97	-51.48
Overall mean	ElevDistr	1.5768	NA	0.5332	NA	3,400,000	0.0463	0.0283	0.63	-0.74	-8.98
Overall mean	Flora Alpina	1.5885	NA	0.5858	NA	5,050,000	0.0000	0.0000	0.50	0.00	0.00
Overall mean	Polygon plus filtering	0.6045	NA	0.9085	NA	3,550,000	0.0224	0.0932	0.24	-61.95	55.09
Overall mean	Polygon	3.9058	NA	0.4275	NA	10,000,000	0.1311	0.0257	0.79	145.88	-27.03

References

Cheng, Y., Zhou, K., Humphreys, M. W., Harper, J. A., Ma, X., Zhang, X., Yan, H., & Huang, L. (2016). Phylogenetic Relationships in the Festuca-Lolium Complex (Loliinae; Poaceae): New Insights from Chloroplast Sequences. *Frontiers in Ecology and Evolution*, *4*, 89. https://doi.org/10.3389/fevo.2016.00089

Ebersbach, J., Muellner-Riehl, A. N., Michalak, I., Tkach, N., Hoffmann, M. H., Röser, M., Sun, H., & Favre, A. (2017). In and out of the Qinghai-Tibet Plateau: divergence time estimation and historical biogeography of the large arctic-alpine genus Saxifraga L. *Journal of Biogeography*, *44*(4), 900–910. https://doi.org/10.1111/jbi.12899

Emadzade, K., Lehnebach, C., Lockhart, P., & Hörandl, E. (2010). A molecular phylogeny, morphology and classification of genera of Ranunculeae (Ranunculaceae). *TAXON*, *59*(3), 809–828. https://doi.org/10.1002/tax.593011

Körner, C., Paulsen, J., & Spehn, E. M. (2011). A definition of mountains and their bioclimatic belts for global comparisons of biodiversity data. *Alpine Botany*, *121*(2), 73. https://doi.org/10.1007/s00035-011-0094-4

Lehnebach, C. A., Cano, A., Monsalve, C., McLenachan, P., Hörandl, E., & Lockhart, P. (2007). Phylogenetic relationships of the monotypic Peruvian genus Laccopetalum (Ranunculaceae). *Plant Systematics and Evolution*, *264*(1–2), 109–116. https://doi.org/10.1007/s00606-006-0488-8

Prieto, J. A. F., Arjona, J. M., Sanna, M., Pérez, R., & Cires, E. (2013). Phylogeny and systematics of Micranthes (Saxifragaceae): an appraisal in European territories. *Journal of Plant Research*, *126*(5), 605–611. https://doi.org/10.1007/s10265-013-0566-2

Torrecilla, P., López-Rodríguez, J.-A., & Catalán, P. (2004). Phylogenetic Relationships of Vulpia and Related Genera (Poeae, Poaceae) Based on Analysis of ITS and trnL-F Sequences on JSTOR. *Annals of the Missouri Botanical Garden*, *Vol. 91*, 124–158. https://www.jstor.org/stable/3298573?seq=13

The Global Carex Group. (2015). Making Carex Monophyletic. *Botanical Journal of the Linnean Society*, *179*(1), 1–42. https://doi.org/10.1111/boj.12298

The Global Carex Group, Jiménez-Mejías, P., Hahn, M., Lueders, K., Starr, J. R., Brown, B. H., Chouinard, B. N., Chung, K.-S., Escudero, M., Ford, B. A., Ford, K. A., Gebauer, S., Gehrke, B., Hoffmann, M. H., Jin, X.-F., Jung, J., Kim, S., Luceño, M., Maguilla, E., … Roalson, E. H. (2016). Megaphylogenetic Specimen-Level Approaches to the Carex (Cyperaceae) Phylogeny Using ITS, ETS, and matK Sequences: Implications for ClassificationThe Global Carex Group. *Systematic Botany*, *41*(3), 500–518. https://doi.org/10.1600/036364416x692497

Xu, C., & Hong, D. (2021). Phylogenetic analyses confirm polyphyly of the genus Campanula (Campanulaceae s. str.), leading to a proposal for generic reappraisal. Journal of Systematics and Evolution, 59(3), 475–489. https://doi.org/10.1111/jse.12586

Chapter II: Phylogenetic Evidence for Pulsed Niche Evolution in Three Alpine Plant Clades (Primula, Lupinus, Ranunculus)

Livio Bätscher, Giacomo Potente, Elena Conti, Bruno Nevado, Colin E. Hughes, Jurriaan M. de Vos

Manuscript in preparation for submission to *Evolution*.

SUMMARY

Phylogenetic approaches have much improved our understanding of whether lineages can successfully transition into new biomes, but the mode of underlying continuous niche evolution remains poorly examined. One reason is that most studies considered only gradual evolution, without considering episodes of rapid jump-like, pulsed evolution (i.e., Lévy processes). Clades of species that diversified across mountain ranges are particularly suited to investigate the mode of niche evolution, because of great niche diversity in close geographic proximity. Here we test whether: (1) evolution of a continuous proxy for niche distance to the alpine biome boundary is best explained by pulsed or gradual evolution; (2) the mode of its evolution varies across three clades of mountain plants; (3) different niche proxies (niche center, lower and upper niche limit) find support in the same model. We find evidence for pulsed evolution in *Primula* and *Lupinus*, but not in *Ranunculus*, which may relate to clade-specific trait evolvability. Niche borders behave differently from niche centers, probably because upper niche limits are microclimate-dominated, while lower niche limits might be more affected by competition. Overall, our results suggest that pulsed niche evolution may be common but not ubiquitous, underlining the importance of considering appropriate models of trait evolution.

INTRODUCTION

Angiosperms dominate approximately all terrestrial biomes, providing profound opportunity to study how major ecological transitions occur, such as the ability of a phylogenetic lineage to colonize new biomes (Crepet and Niklas 2009). Even though "biome" is a fuzzy concept, it captures how key climatic conditions are associated with characteristic biotic assemblages, and therefore biome shifts are important systems for understanding evolution, biogeography, and ecosystem composition (Donoghue and Edwards 2014). Whether a particular lineage can occur in a biome may be impacted by three main processes: a geographic opportunity for movement into a new environment, ecological interaction with species already occupying the new environment, and possibly most importantly the lineage's potential to evolutionarily adapt to the new climatic conditions (Donoghue and Edwards 2014). In consequence, the tempo and mode with which a linage can adapt its climatic "envelope" (i.e., niche evolvability) or not (i.e., niche conservatism) might be a major determinants for biome shift frequencies within clades.

Many phylogenetic studies have attempted to quantify the rate of niche evolution within lineages (e.g., Wiens et al. 2010; Crisp and Cook 2012; Pyron et al. 2015). One general result frequently found is that there are intrinsic limits to niche evolvability, for instance, because biome occupancy tends to be phylogenetically clustered (e.g., Fine et al. 2014; Kerkhoff et al. 2014). This poses the question how climatic niche diversity evolves, and whether this might differ across clades. Answering these questions requires an adequate measure of species niches and appropriate models for its evolution, which inevitably includes phylogenetic relationships of lineages (Kelchner and Thomas 2007; Shepherd and Klaere 2018). Niche evolution is usually modeled as a continuous trait, typically based on Brownian motion (BM) or a derivate thereof. Under BM, a character evolves randomly with a mean displacement of zero and a variance termed the rate of BM (σ^2; Felsenstein (1985). The Ornstein–Uhlenbeck process (OU; Martins 1994) expands upon BM by adding a selective pull (also known as the "rubber band" parameter) to prevent a character from drifting far into either direction. Both models are frequently used to model phylogenetic niche evolution: a preference for an OU process over BM is frequently seen as evidence of niche conservatism (e.g., Boucher et al. 2014; Morinière et al. 2016). Although several other derivates of BM are commonly employed (e.g., Harmon et al. 2010; Beaulieu et al. 2012), they all consider evolution to be exclusively gradual, even if the rate of gradual evolution may itself evolve over the tree (but see Hansen and Martins 1996; Bokma 2008; Uyeda et al. 2011).

However, evolutionary theory predicts that pulses or evolutionary jumps that break continuity may often better characterize niche evolution (e.g., Simpson's 1944 "new adaptive zones" or Gould and Eldredge's 1972 "punctuated equilibrium"). For instance, the rapid evolution of broad ecological and morphological variation during adaptive radiation is generally expected to be poorly described by models of gradual evolution (Schluter 2000), instead requiring occasional pulses. Such pulsed evolution can be described by Lévy processes which are defined as processes with an independent and stationary increment (Landis et al. 2013). Therefore, this class of models can combine a BM and a pure-jump process that infers jumps from the Lévy measure (the exact drawing of jumps varies from model to model; Landis et al. 2013). In a phylogenetic context, Lévy models allow us to test if continuous-character evolution is interrupted by abrupt changes i.e., if there is evidence for pulsed or jump-like evolution. Even though only a few algorithms exist for phylogenetic Lévy processes (i.e., Landis et al. 2013; Duchen et al. 2017; Landis and Schraiber 2017; Bastide and Didier 2023), they are considered promising models with a general appeal (Sauquet and Magallón 2018; Martin and Richards 2019; Hackel and Sanmartín 2021). However, only a few studies explicitly compared support for Lévy processes versus other models (Brennan and Keogh 2018; Rowsey et al. 2019; Barua and Mikheyev 2020; García-Navas et al. 2021; Smith et al. 2023); to our knowledge, the only study focusing on plant niches found no support for pulsed evolution (Ogburn and Edwards 2015).

Plant clades in mountain regions with species occurring within and below the alpine biome provide formidable opportunities to study the mode of niche evolution. Mountains (defined by ruggedness; Körner et al. 2011) are considered evolutionary arenas (Muellner-Riehl 2019), as they make up only a small fraction of total land surface (12-16%), but they contain about one-third of known terrestrial biodiversity (Spehn et al. 2011; Körner 2021). Importantly, the alpine biome has clearly defined and accurately predictable boundaries (i.e., the upper climatic treeline), corresponding to precise thresholds in continuous elevation-associated temperature clines (Paulsen and Körner 2014), and is present on all continents (Körner et al. 2011; Körner 2021). Moreover, physiological, and morphological adaptations in "typical" high-elevation life forms are well-known, illustrating that biome shifts into the alpine are profound. In general, alpine plants become smaller and belong usually to a characteristic life form (i.e., cushion plants, dwarf shrubs, tussock- or rosette-forming). Likely caused by exacting environmental conditions, requiring small stature to decouple from the air temperature, longevity, rapid seasonal development, and the ability to endure snow cover or freezing tolerance (Körner 2023). These "requirements" are set by multiple environmental variables that change with increasing elevation: foremost, decreasing air temperature and air pressure (Körner 2021) or increase in solar radiation under clear sky (Barry 1978). Nevertheless, several clades display evidence of repeated alpine biome shifts, (e.g., Xing & Ree 2017; Ding et al. 2020; Smyčka et al. 2022), but whether the mode of niche evolution underpinning these biome shifts is purely gradual or rather pulsed remains unknown.

Here, we use a recently developed continuous climatic proxy to test whether three mountain plant clades show phylogenetic evidence for pulsed evolution of different climatic niche parameters, ElevDistr (Bätscher and de Vos, accepted). The climatic proxy describes an occurrence's position relative to the theoretical, climatic, local treeline (implemented in R package ElevDistr), allowing to compare occurrences across mountain ranges and making it a good proxy for environmental gradients because it contains elevation, which correlates with many environmental factors (Schröter et al. 1926; Körner 2021). This proxy was developed, because the absolute elevation of the theoretical treeline varies greatly across the globe (Körner 2012, 2021; Paulsen and Körner 2014), making alpine biome classifications from occurrence data challenging and potentially greatly biasing biome shift inference (Bätscher and de Vos, accepted). While helpful for modeling biome shifts as discrete characters (i.e., "alpine" and "non-alpine"), this proxy also enables describing species niches as a continuous character (i.e., elevation distance to theoretical treeline) with the benefit of avoiding masking potentially relevant information (Hackel and Sanmartín 2021). Finally, this approach allows to define not only the central niche of a species, but also niche limits, which may differ in their evolutionary dynamics (e.g., Patsiou et al. 2021).

In this study, we first generate new species-level phylogenetic hypotheses for three large plant clades that are predominantly distributed in mountain systems and include alpine and non-alpine species (i.e., *Primula* L., *Lupinus* L., and *Ranunculus* L., incl. nested genera) based on hundreds of newly sequenced loci and published data. From spatial observations we then compute the vertical distance to the theoretical local climatic treeline, defining the abundance median center as a proxy for species central niche. Additionally, we selected for the lower and upper niche limits the 2.5% quantile respectively 97.5% to exclude potential outliers. Finally, we phylogenetically test the mode of evolution of the climatic niche proxy in each clade considering a set of gradual and pulsed evolution models (Lévy processes). Overall, we find evidence for pulsed evolution of the species niche proxy, which is either overwhelming or absent, revealing that the mode of evolution may differ across components of a particular flora, with profound implications for the nature of niche evolution.

MATERIAL AND METHODS

Taxon sampling

We selected three clades of predominantly herbaceous plants that met the following criteria: large species numbers for adequate statistical power (>200 species), representing diverse phylogenetic affinities, prior phylogenetic studies available, and distribution mainly in mountain regions across all thermal belts. We, therefore, chose the clades *Primula* (s.l., Primulaceae, Ericales, basal Asterids, including the phylogenetically nested *Cortusa*, *Dionysia, and Dodecatheon,* ca. 550 spp. De Vos et al. 2014), *Lupinus* (Fabaceae, Fabales, Rosids, ca. 267 ssp. Drummond et al. 2012) and *Ranunculus* (s.l., Ranunculaceae, basal Eudicots, including early-branching genera such as *Ficaria*, but excluding apomictic "micro"-species complexes, ca. 600 spp.; (Baltisberger and Hörandl 2016). To obtain well-supported and densely sampled phylogenic hypotheses from each clade, we combined de-novo generated sequences of species representing all main phylogenetic lineages using a custom phylogenomic bait set with publicly available sequences of many additional species. Thereto, we obtained silica-dried and herbarium leaf tissue for 194 taxa that were prior mostly unsequenced (*Primula*: 68, *Lupinus*: 67 and *Ranunculus*: 59; Table S1). The final phylogenies contain 296, 178, 342 of *Primula*, *Lupinus*, and *Ranunculus* and after cross-referencing the availability of geographic information (see below), we could include 293, 150, 340 species representing ca. 53%, 56%, and 57%, percent of taxa, representatively, in the final analyses.

Molecular and bioinformatic methods

Computational intense analyses were performed on the sciCORE high-performance cluster from the University of Basel.

<u>Custom bait design</u>

For de novo sequencing, we developed a novel bait set aimed at expanding taxon sampling of existing phylogenetic loci, supplemented with the Angiosperms353 gene set (Johnson et al. 2018), and 69 other loci of interest. Specifically, for genomic data from which data baits could be designed, we first downloaded and assembled 5 genomes and 38 transcriptomes of species within or close to the target clades (detailed description: supplementary text). To expand the set of loci used for phylogeny reconstruction beyond the Angiosperm353 kit, which does not always yield sufficient resolution (Lee et al. 2021), we included additional loci of genes of potential functional interest in future studies. Specifically, we downloaded sequences for all genes of the pathway "circadian rhythm" and genes involved in flowering response (Andrés and Coupland 2012) from the KEGG database (https://www.genome.jp/kegg/genome/plant.html) for the species *Arabidopsis thaliana* and *Solanum lycopersicum,* and we included loci of the S-locus exons controlling heterostyly in *Primula* (Potente et al. 2022).

Additionally, four genes frequently sequenced for *Lupinus* were extracted from GenBank (http://www.ncbi.nlm.nih.gov; Table S2).

Because existing bait design pipelines could not process the amount of input data in a reasonable time (e.g., Kadlec et al. 2017), we implemented a new pipeline using bash and Perl scripts (available from https://github.com/LivioBaetscher/marker_selection). Specifically, results of a BLAST search (Camacho et al. 2009) using genomes and transcriptomes as query and the genes of interest as database was filtered using a custom Perl script removing hits not fulfilling these criteria: E-value ≤ 0.01 and result length ≥ 100 bases plus present in ≥ 2 transcriptomes or genomes. We manually checked the remaining result summary and for orthologs present in multiple genomes, we retained the longer sequences. In addition, when for a locus Old and New World *Lupinus* sequences were available, we retained the New World sequence; similarly, we preferred *Ranunculus* over other Ranunculaceae sequences. Next, the selected sequences were aligned for each gene and clade separately using MAFFT v7.3.0 (Katoh and Standley 2013). Final alignments of target loci plus a reference genome or transcriptome for each genus were sent to Daicel Arbor Biosciences (MI, USA), where a sliding window was used to split the sequences into 80 nucleotide baits with 3x tiling. Loci smaller than the bait length or with few baits per sequence were excluded and a bait screening was performed to exclude baits that bind unspecific to the reference genomes. After adding baits from the Angiosperms353 kit (Daicel Arbor Biosciences (MI, USA), catalog number: 308108.v5), we selectively amplified 422 loci.

Library preparation and sequencing

DNA extraction was performed with the PTB protocol from Kistler (2011), followed by three quality control procedures. First, DNA amounts were measured by using the Qubit dsDNA HS assay kit (Invitrogen) with a Qubit 3 Fluorometer (Invitrogen). In case of low yield (<1µg DNA) the extraction was repeated, pooled, and the volume reduced to >200µl with a CentriVap benchtop vacuum concentrator (LABCONCO). Secondly, we analyzed A260/A280 and A260/A230 ratios using a NanoDrop One^{C} (Thermo Scientific) and thirdly, we evaluated DNA degradation using gel electrophoresis. For adequate isolates, library preparation and target enrichment (see above) were outsourced to Daicel Arbor Biosciences (MI, USA). After enrichment, we added 15% unenriched library to ensure good coverage of ribosomal and chloroplast loci. Sequencing was performed on a NovaSeq 6000 platform (Illumina) using NovaSeq S4 Flow Cells (Ilumina), creating 2x 150 bp long reads.

Read assembly and paralog removal

Quality control of raw reads involved FastQC v0.11.8 (https://www.bioinformatics.babraham.ac.uk/projects/fastqc/), MultiQC v1.11 (Ewels et al. 2016), and read trimming and clipping with Trimmomatic v0.39 (Bolger et al. 2014) using the recommended settings for paired-end sequences. We used HybPiper v1.3.1 (Johnson et al. 2016) to assemble the cleaned reads into contigs and a customized target file following McLay et al. (2021): filtering the Angiosperm353 loci for the orders Ericales, Fabales, and Ranunculales, and adding relevant sequences from all transcriptomes from the bait design for the remaining loci derived from the bait design procedure. Finally, cpDNA and rDNA assembly was performed with “get_organelle_from_reads.py” from the GetOrganelle pipeline (Jin et al. 2020) and in the case of multiple assembled graphs, the longest contig was kept for rDNA or version 1.1 for cpDNA. To remove loci with poor sequence recovery and putative paralog genes, we excluded loci with a high proportion of SNPs across all samples and in each sample individually, executing the first three HybPhaser v2.0 scripts (Nauheimer et al. 2021) with default settings and separate runs for each clade. We then aligned loci using MAFFT and trimmed alignment gaps using trimAl with the setting ‘-gt 0.51’ (Capella-Gutiérrez et al. 2009) followed by manual control.

Adding publicly available sequence data

Alignments of de-novo sequences for each locus were supplemented with GenBank data. Specifically, we used the oneTwoTree pipeline (Drori et al. 2018) such that it downloaded sequences for all species of *Primula*, *Ranunculus*, and *Lupinus* (incl. nested genera, as above) from the GenBank nucleotide archive, clustered these into orthologous sets per clade using a modified version of OrthoMCL (Li et al. 2003), and aligned these using MAFFT with default settings (Table S3-S5 for accession information). Next, we blasted the organelle scaffolds against the corresponding organelle clusters, extracted the best match (for every cluster and scaffold) with a Perl script and pasted it into the cluster. To add the four frequently sequenced *Lupinus* genes to their GenBank clusters, we performed the same operation manually. Finally, the clusters were aligned with MAFFT, trimmed with trimAl, and inspected by hand to avoid irregularities and species names were harmonized based on plants of the world online (POWO; https://powo.science.kew.org/), with some deviations based on expert opinion (pers. obs. CEH; Andean *Lupinus*).

Phylogenetic analysis

The following analyses were performed independently for each clade. First, we computed a maximum likelihood gene tree for each locus using RAxML-NG (Kozlov et al. 2019) using a GTR+G substitution model. To resolve conflict among gene trees and infer the species tree with the highest local posterior probability topology, we used ASTRAL v5.7.7 (Zhang et al. 2018), an approach congruent with the coalescent which assumes conflict results from incomplete lineage sorting. To account for statistical uncertainty in the phylogenetic data, we computed a posterior distribution of branch lengths in proportion to time using a Bayesian approach in RevBayes V1.2.1 (Höhna et al. 2016), with a birth-death tree model that contains a GTR+G+I substitution model partitioned by locus, a tree prior with fixed topology corresponding to the best ASTRAL tree, and a UCLN clock model (Drummond et al. 2006). To make the dating analyses computationally tractable, we selected a subset of 12 loci based on the following criteria: the seven Angiosperms353 loci available for all newly sequenced species with the lowest normalized Robinson-Foulds distance to the ASTRAL topology (R-package phangorn; Schliep 2011), plus the five loci available for the most taxa. Calibration of species divergence times used the same prior distributions as employed by previous studies (Emadzade and Hörandl 2011; Drummond et al. 2012; Vos et al. 2014; supplementary text S1). We computed four independent MCMC runs each with 105,000 iterations, of which 5'000 generations were burn-in. After confirming adequate mixing, convergence and burnin using Tracer v1.7.1 (Rambaut et al. 2018), we thinned the posterior distribution to 100 samples, for downstream analyses. This set of trees jointly accounts for uncertainty in branch length estimation but is conditioned on the best species tree topology. To ensure that results are not biased by topological uncertainty, nodes that remained unresolved in the ASTRAL tree were collapsed and 100 times randomly resolved and converted into a chronogram using the correlated rate model chronos from the R-package ape (Paradis and Schliep 2019), using the root ages as calibration (supplementary text). Branch lengths in this set of trees are likely less accurate than in the result of the RevBayes analysis, hence, if hypothesis testing is congruent across both sets of trees, this provides strong support for their generality. Finally, we also inferred for each clade a maximum a posteriori (MAP) tree from all posterior trees of the four chains using the RevBayes "mapTree" function computing the median node age.

Geographic and climatic data

We downloaded occurrence records from GBIF (https://doi.org/10.15468/dl.xkw2rg, accessed Mai 2023, 5’158’910 records) for all species of the three clades and from iDigBio (accessed Mai 2023, 165’335 records). Additionally, we used for the eastern South American *Lupins* a manually checked and expert validated set of georeferenced herbarium specimens containing 996 records. We then filtered GBIF data using CoordinateCleaner (Zizka et al. 2019) with the following criteria: plain zero coordinates; locations within oceans; coordinates outside the indicated country; records near capitals, country or region centroids, biodiversity institutions, the GBIF headquarters; indicated uncertainty >50km; species or data sets containing rasterized or strongly rounded coordinates. For the remaining 3’182’986 GIBIF records, taxon names were harmonized as described for the GenBank data. Next, we randomly selected 200 spatial points per species, prioritizing records with indicated elevation and if not available for a high coordinate precision; for species with <200 records we added observations from herbarium vouchers and iDigBio. Missing elevation was inferred from a high-resolution digital elevation model (GTOPO30; Miliaresis and Argialas 1999). We then computed for all remaining 57’009 records the vertical distance to the local climatic treeline with ElevDistr (Bätscher and de Vos, accepted) using the default settings, the recommended climate layers from CHELSA V2.1 (Karger et al. 2017) and GTOPO30 (Miliaresis and Argialas 1999) as elevation model. In case the algorithm returned no value for a spatial point, the analysis was repeated with a grid size of 50 and then 100km, or in rare cases where there was still no return value the data point was removed. This distance can be interpreted as vertical distance to the local climatic treeline. Hence, it is a continuous climatic proxy that allows classifying an occurrence point as within (distance >0m) or below (distance <0m) the alpine biome, allowing an adequate comparison of species niches across mountain ranges where absolute elevations of the climatic treeline will dramatically differ (Körner 2021). In the current study, we extract its continuous value, rather than discretizing it, thus interpreting it as the primary climatic axis along which evolution is required for species to move into and out of the alpine biome. Specifically, for each species, we computed the median vertical distance to the local climatic treeline as a proxy for the abundance center and central niche, and the 2.5%-quantile (i.e., minimum) and the 97.5%-quantile (i.e., maximum) as proxies for lower and upper range limits, respectively.

Testing for pulsed evolution

We testes whether the three climatic niche proxies (niche center, lower and upper distribution limits) evolve in a gradual (continuous) or pulsed (non-linear, discontinuous, jump-like) fashion in each clade. Therefore, we compared the fit of three climatic proxies to nine phylogenetic models of continuous character evolution, for every clade separately. Specifically, we considered three models of gradual evolution: Brownian Motion (BM; Felsenstein 1985) which includes only random drift, Ohrnstein-Uhlenbeck (OU; Martins 1994) which considers drift plus a "pull" toward a selective optimum, and Early Burst (EB; Harmon et al. 2010) that reflects drift of which the rate increases or decreases exponentially through time. In addition, we considered three pure-jump processes consisting of a Lévy measure (characterizing the size and frequency of the evolutionary jumps): jump normal (JN), variance gamma (VG), normal inverse Gaussian (NIG; mathematical characterization in Landis and Schraiber 2017). These three models differ in how jumps are drawn from an underlying distribution over time. Here, JN captures stasis followed by rapid adaptation and consists of exponentially distributed waiting times until a usually rather large jump is drawn from a Gaussian distribution. In contrast, VG and NIG are infinitely active processes, meaning they entail a continuous series of jumps of which most are rather small. Both processes represent the situation that rapid evolution may occur rather frequently but differ in how jumps are modeled. Furthermore, we also considered the full Lévy process: a Brownian motion in combination with one of the three pure-jump processes (sometimes referred to as jump-diffusion processes) i.e., BM+JN, BM+NIG, BM+VG. We used the maximum likelihood method of the R-package pulsR (Landis and Schraiber 2017) to fit each niche parameter to each of the nine models, using the two sets of phylogeny distributions: 100 trees from the posterior of the RevBayes analysis, and 100 trees from the random polytomy resolution approach.

For each combination of phylogeny set, clade, and niche parameter, we selected the Lévy process with the best AICc, plus the three continuous models, and computed Akaike weights using the R-package geiger v2.0.11 (Pennell et al. 2014). We consider support for pulsed character evolution over gradual character evolution for a combination of clade and niche parameter as significant, if the median AICc weight across the 100 phylogenies in both phylogeny sets is twice as large for the best Lévy process compared to any other models (Landis and Schraiber 2017). In case of significant support for pulsed evolution, we identified branches with evidence for pulses, by computing the branch-normalized signal-to-noise ratios using the software creepy-jerk (Landis et al. 2013), using the best corresponding model type and each clade's maximum a posteriori (MAP) tree. These ratios are defined as the mean divided by the standard deviation of the posterior distribution of the sampled jumps, multiplied by the inversed square root of the branch length. This measure identifies branches where the amount of implied trait change is sufficiently explained by BM (values close to zero) or better explained by a Lévy process (non-zero values). We then qualitatively evaluated the phylogenetic pattern of the thus identified branches. Creepy-jerk does not implement the NIG model, and therefore these models were approximated by an alpha-stable process, which is also infinitely active and has similar properties (Landis et al. 2013; Landis & Schraiber 2017).

RESULTS

The inferred phylogenies of the three genera were overall congruent with previously inferred phylogenetic hypotheses of these clades. The trees including posterior probabilities of the nodes, the 95% HPDs of the inferred node ages, are presented in Fig. S1-S6. The results of the total 16,200 fitted models reveal significantly pulsed niche evolution in *Primula* and *Lupinus*, but not in *Ranunculus*, with different patterns for the lower, central, and upper niche parameters (Fig. 1, S7 and Table 1, S6). Here and in Table 1 we present the results on the phylogeny set from RevBayes analyses, which was fully congruent with the results based on the randomly resolved polytomies (Table S6). Specifically,

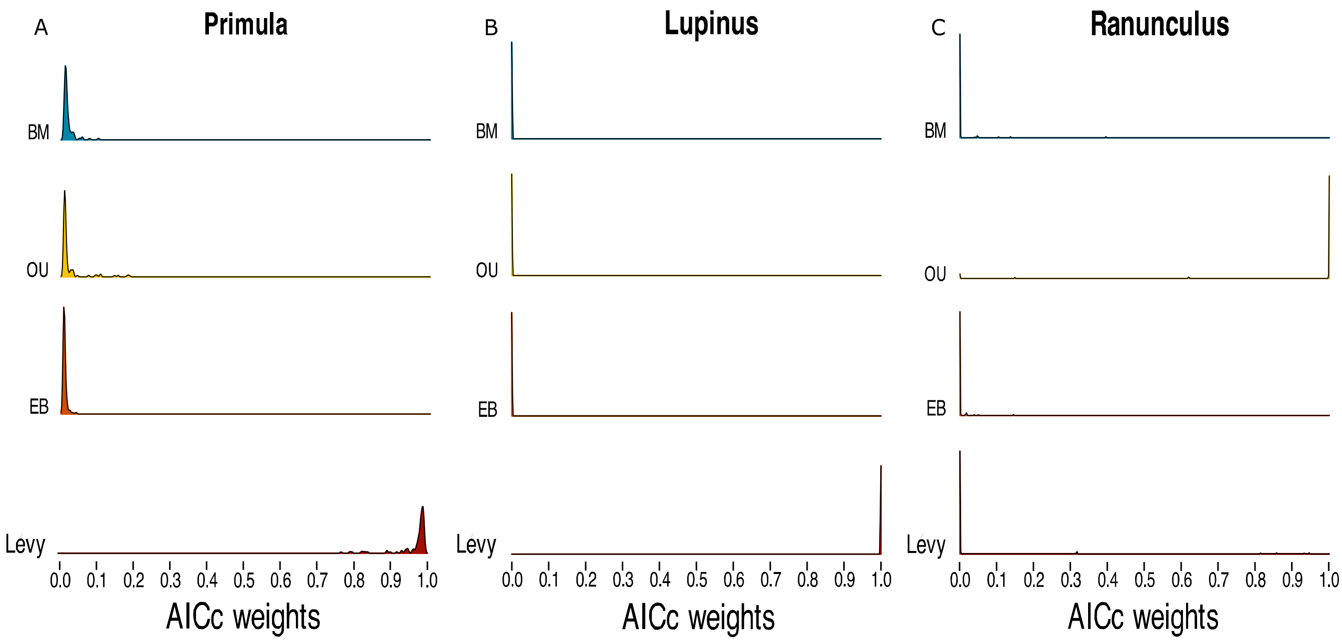

FIGURE 1: Density distribution of AICc weights of the best-supported Lévy process (see Table 1) for the evolution of the central niche versus two models of gradual evolution and early burst (rows) across the posterior of phylogenies (RevBayes analysis) for the three clades: A) *Primula*, B) *Lupinus*, and C) *Ranunculus*

for *Primula*, a model of pulsed evolution best describes evolution of the niche center (NIG, in 85% of the trees of the posterior, with the remainder of support for other Lévy processes), but BM better describes evolution of the lower niche limit (100% across the posterior), while the support for BM and Lévy processes was similar for the upper niche limit (50% and 45%, respectively). In *Lupinus*, the central and lower niche limit evolved in a pulsed fashion (nearly all support across four Lévy processes), while BM better described the upper niche limit (100%). In stark contrast, we find no evidence for pulsed evolution in *Ranunculus* in any of the three niche parameters (Table 1). These results were qualitatively identical and quantitatively similar to the results obtained across the phylogeny set with randomly resolved polytomies. This indicates that the model fitting results were not confounded by phylogenetic uncertainty (Table S6).

TABLE 1: Model support for each of the nine candidate models of evolution (three gradual and six jump processes) for all genera and all niche parameters, expressed as the fraction trees from the posterior for which the model provided the best fit based on AICc. Candidate models: Brownian motion (BM), Ornstein-Uhlenbeck (OU), early burst (EB), jump normal (JN), variance Gamma (VG), normal inverse Gaussian (NIG) and combinations of Brownian motion and jump processes (BM+JN, BM+NIG, BM+VG). Grey marked are the models that performed best across the phylogeny set based on the RevBayes analysis. Results based on the randomly resolved polytomies are presented in Table S6.

Clade	**Niche parameter**				**Lévy Processes**					
		BM	**OU**	**EB**	**JN**	**VG**	**NIG**	**BM+JN**	**BM+VG**	**BM+NIG**
Primula	Lower limit	1.00	0	0	0	0	0	0	0	0
	Niche center	0	0	0	0.01	0.13	0.85	0.01	0	0
	Upper limit	0.50	0.05	0	0.29	0.16	0	0	0	0
Lupinus	Lower limit	0	0.01	0	0.70	0	0.01	0.29	0	0
	Niche center	0	0	0	0.81	0.07	0.01	0.11	0	0
	Upper limit	1.00	0	0	0	0	0	0	0	0
Ranunculus	Lower limit	0	1.00	0	0	0	0	0	0	0
	Niche center	0.01	0.95	0	0.04	0	0	0	0	0
	Upper limit	0.44	0.54	0	0	0.01	0.01	0	0	0

Where Lévy processes were preferred across the posterior distribution of trees, their stronger support (based on AICc weights) was very pronounced, as illustrated for the central niche (Fig. 1and S7). Specifically, shown by the density distribution of the AICc weights for BM, OU, EB, and the best fitting Lévy process across the trees in either the RevBayes (Fig 1) or random polytomy resolution phylogenetic set (Fig S7). Here, in *Primula* and *Lupinus* the Lévy process receives almost all AICc weight (median of 0.983 and 0.999, in the RevBayes phylogenies; and 0.796, respectively 0.819 in the randomly resolved polytomy set), whereas in *Ranunculus* approximately all AICc weight favor the OU model (Fig. 1 and S7). Furthermore, in *Lupinus*, the lower niche shows also significant support for Lévy processes: median AICc weights are 1.0000 for Lévy models and for the gradual models: BM: 0.0000, OU: 0.0000, and EB: 0.0000 (posterior distributions) and with the randomly resolved phylogenies 0.5730 for Lévy models, and BM: 0.1656, OU: 0.1623, EB: 0.0609.

Reconstructing niche evolution under a Lévy process

Creepy-jerk parameterization and reconstructions of the evolution of the niche center (using BM, JN, VG, or α-stable [AS] as proxy for a NIG process, as appropriate), allowed us to compare absolute rates of niche evolution (Table 2). Further we compute the branch-normalized signal-to-noise ratios, which indicate evidence that Brownian motion cannot adequately describe the implied episodic pulses of niche evolution (Fig. 2). Interpreting the parameterization allows to roughly gauge the absolute properties of pulsed evolution, even though given the highly stochastic nature of Lévy processes, precise reconstructions of ancestral states are challenging. The overall rate of niche evolution, approximated by the BM component of each model, differs strongly between the three genera, as the rate in *Ranunculus* was about twice as large (posterior mean σ 0.67, 95% HPD interval 0.61 – 0.72) as *Primula* (posterior mean σ 0.23, 95% HPD interval 0.01 – 0.53) and *Lupinus* (posterior mean σ 0.34, 95% HPD interval 0.28 – 0.41; Table 2). *Primulas* Lévy measure parameters that express the intensity of jumps have a stability parameter of moderate magnitude (posterior mean α 1.59, 95% HPD interval 1.32 – 1.94; $0 \leq \alpha \leq 2$, where $\alpha=2$ is the mathematical equivalent of BM) and a large scaling parameter (posterior mean β 0.37, 95% HPD interval 0.19 – 0.49), controlling the jump magnitude, that the low amount of drift-like evolution is punctuated by pulsed episodes, of which roughly every third jump is of the magnitude of a million years of BM. The jump normal model preferred for *Lupinus* allows for the more straightforward interpretation that every ~7.0 Myr a jump occurs (posterior mean λ 0.14, 95% HPD interval 0.03 – 0.29), and the jump size (posterior mean δ 1.21, 95% HPD interval 0.65 – 1.83) has the equivalent of ~3.6 Myr of BM, revealing fewer but more

TABLE 2: Model parameterization under the best-support model for the niche parameter inferred from the creepy-jerk analysis, indicating means and 95%highest posterior density (HPD) interval.

Clade	**Niche parameter**	**Model**	**Model parameter**	**Mean**	**95% HPD interval**
Primula	Lower limit	Brownian motion	Rate of BM (σ)	1.093	1.0007 – 1.1885
	Niche center	α-stable	Rate of BM (σ)	0.234	0.0045 – 0.5249
			Relative rate of small jumps (α)	1.592	1.3160 – 1.9418
			Size of jumps (β)	0.366	0.1938 – 0.4854
	Upper limit	Brownian motion	Rate of BM (σ)	1.008	0.9213 – 1.0954
Lupinus	Lower limit	Jump normal	Rate of BM (σ)	0.234	0.1283 – 0.3567
			Rate of jumps (λ)	0.258	0.0638 – 0.5199
			Standard deviation of jump size (δ)	1.111	0.6075 – 1.617
	Niche center	Jump normal	Rate of BM (σ)	0.336	0.2670 – 0.4076
			Rate of jumps (λ)	0.142	0.0316 – 0.2921
			Standard deviation of jump size (δ)	1.210	0.6484 – 1.8335
	Upper limit	Brownian motion	Rate of BM (σ)	0.860	0.7629 – 0.9593
Ranunculus	Lower limit	Brownian motion	Rate of BM (σ)	0.699	0.6423 – 0.8316
	Niche center	Brownian motion	Rate of BM (σ)	0.666	0.6119 – 0.7194
	Upper limit	Brownian motion	Rate of BM (σ)	0.859	0.7919 – 0.9312

intense episodes of pulsed evolution in *Lupinus* compared to *Primula,* while niche evolution in *Ranunculus* can be fully explained by a rather high rate of drift-like evolution.

Congruently, *Primula* and *Lupinus* display multiple branches with clearly non-zero branch-normalized signal-to-noise ratios. Fewer jumps are present in *Lupinus* than *Primula*, in line with the fewer more intense episodes of pulsed evolution in *Lupinus* (evidenced from the interpretation of parameterization above), indicating that niche centers evolve faster on the respective branch than what can

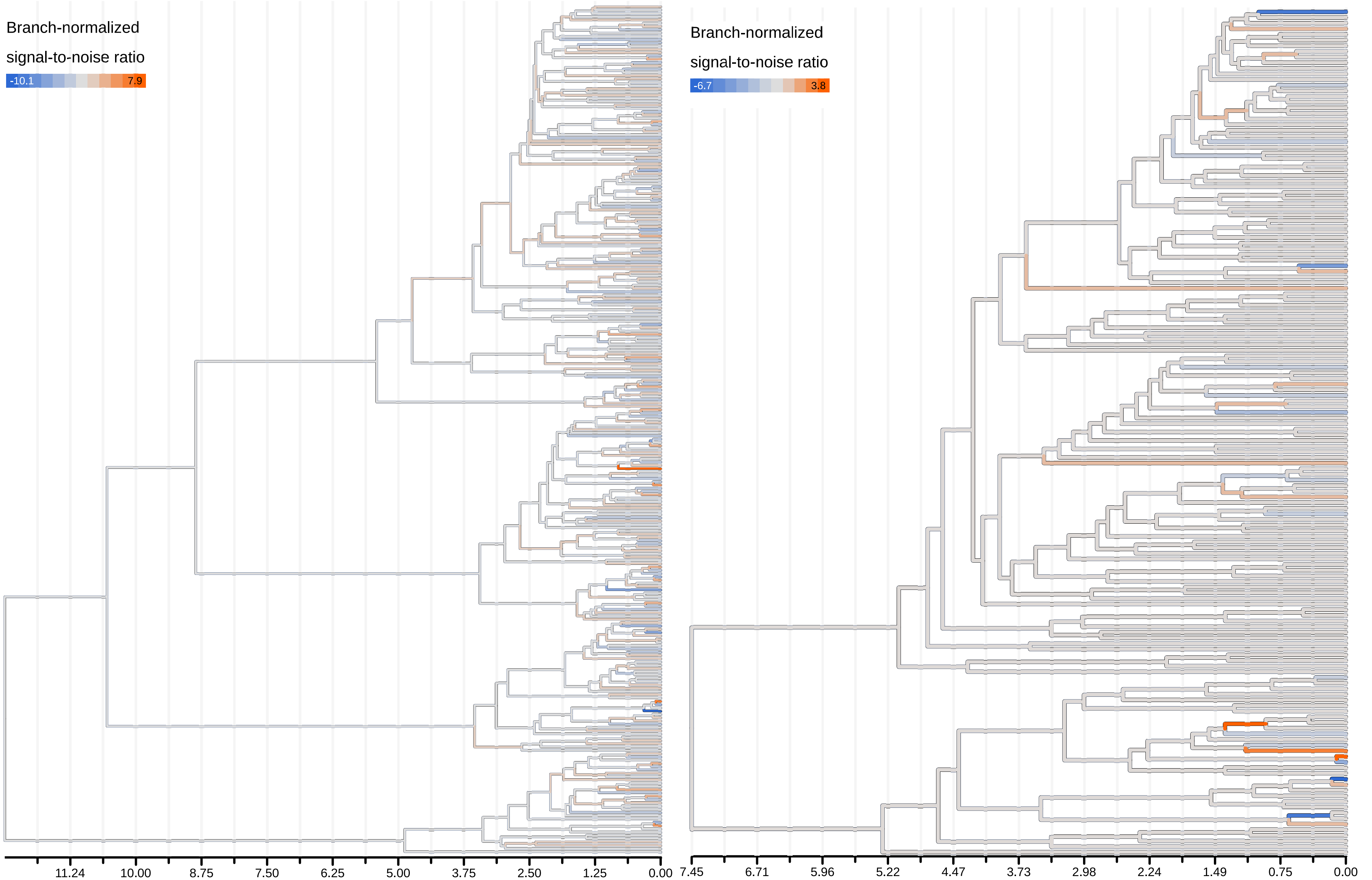

FIGURE 2: Branch-normalized signal-to-noise ratios of posterior jump distributions of the central niche parameter on maximum clade credibility phylogenies of clades with significant evidence for pulsed evolution (*Primula*, left panel; *Lupinus*, right panel). The pulses are indicated by a color scale from low (blue, indicating downward jump) to high values (red, indicating upward jump) and evolution along grey branches is congruent with Brownian motion. The x-axis represents divergence times in million years. Note that color scales differ between clades.

be explained with the BM. Additionally in both clades, most of the large ratios (positive or negative) are found on short branches or terminal phylogenetic branches.

DISCUSSION

One of the major hurdles since the New Synthesis remains to reconcile (a) population processes resulting in gradual, microevolutionary change within species with (b) macroevolutionary patterns that often display an additional "discrete" quality as evolutionary change may happen episodically exceptionally rapidly or slowly (e.g., Simpson 1944). In current phylogenetic biology, nevertheless, continuous-character evolution is usually described with either diffusion-like processes like simple BM, OU, or variations that include multiple such processes for different parts of the phylogeny (OUwie, Beaulieu et al. 2012), or gradual changes in rates (EB, Harmon et al. 2010). However, these approaches assume linear time-homogeneity and cannot reveal pulsed evolution (Landis et al. 2013; Landis and Schraiber 2017). In line with classic evolutionary theory, we found strong support for a class of models of continuous character evolution (i.e., Lévy processes) that include stochastic jumps or approximately instantaneous pulses of rapid evolutionary change (Fig. 1, 2, S7 and Table 1, S6). Though developed a decade ago and widely employed in other fields (e.g. Barndorff-Nielsen et al. 2001), Lévy models are not frequently used yet in phylogenetic biology. Previous work revealed pulsed evolution of body mass and endocranial volume in primates (Landis et al. 2013), female body-size evolution in *Anolis*, and digestive system morphology in a clade of parrots (Duchen et al. 2017), and in body size in 21 out of 66 tested vertebrate clades (Landis and Schraiber 2017). Our study appears to be the first to find evidence for Lévy processes in plants, as the only study focusing on plants Ogburn and Edwards (2015), found no evidence for jumps in mean annual temperature occupancy. Intriguingly, however, we find support for Lévy processes of episodically rapid evolutionary change especially in the central niche, rather than niche limits, and in two out of three clades, suggesting that episodes of pulsed evolution in niche space may be common but not ubiquitous throughout plant diversification. This shifts the question from whether niche evolution may be pulsed to what factors determine whether pulses occur. Here, we first discuss methodological aspects before moving to their biological implications.

Identifiability of Lévy processes

Intriguingly, we mostly found either strong support for Lévy processes (*Primula*: central niche; *Lupinus*, central and lower niche limit; Table 1) or not at all, with only the upper niche of *Primula* having equivocal support for either model class. Given that phylogenetic uncertainty did not impede model selection (i.e., no qualitative difference between the results based on either phylogeny set; Table 1 and S6), this could mean that our niche proxy, based on ElevDistr (Bätscher and de Vos, accepted) is unreliable, or that Lévy models cannot be reliably fitted, or indeed that macroevolution of niches is only in some cases jump-like. Methodological considerations support the latter.

ElevDistr is likely a good, one-dimensional representation of a major niche axis in these clades (Bätscher and de Vos, accepted) because many niche components are tightly correlated with relative elevation (Körner 2021) and ElevDistr accounts for absolute differences in the treeline across mountain ranges (e.g. due to latitude-associated effects and the mountain-mass elevation effects; Schröter et al. 1926; Körner 2021) enabling global comparisons. However, this approach assumes that range limits are essentially niche limits, discarding dispersal limitation as an explanation for distribution differences (Willi and Buskirk 2022). This assumption is unproblematic for the niche cent, which represents the median of the relative abundance per species. However, tails of the abundance relative to the local treeline serve as lower and upper niche limits, which represent the marginal occurrence of few individuals and are thus inherently "noisier". Therefore, the niche center comparison might most accurately catch the fundamental environmental attributes of a species (Körner 2021). Nevertheless, beyond dispersal limitation, the biological processes governing niche center, upper, and lower limits of species likely differ (Willi and Buskirk 2022), hence differences in dynamics between niche centers and niche limits are generally expected (Patsiou et al. 2021).

Statistically detecting support for pulsed evolution is more difficult for the lower niche end compared to the central and upper niche limits, because the maximum distance to the treeline is limited by the elevation of the local treeline, which is much higher around the equator (Körner 2021) e.g., ranging from >4,000m to <1,000m from the Andes to Alaska (Körner 2012). Thus, pulsed evolution of the lower niche may be more difficult to identify in *Ranunculus* (where we did not find it; Table 1, S6), which has much fewer species at low latitudes compared to *Primula* and especially *Lupinus*. The upper niche end is probably less affected by this bias because most mountain systems have a nival zone, where there is geographic space to occur, but the climate is too severe to survive (Körner 2007). In contrast, however, the precision of the upper niche limit might be most strongly impeded due to stronger effects of the microclimate that is particularly heterogeneous above the treeline. For instance, a 2K change in soil temperature difference can be found within a 10m horizontal distance (e.g. due to substrate type and exposition), equivalent to a temperature decrease of 350m along elevational gradients (Körner 2021)

Nevertheless, it is unlikely that noise in our data leads to false support of a Lévy process when evolution would not be pulsed (Landis and Schraiber 2017). In general, noisy data may lead to support for OU models, where the phylogenetic information decays exponentially through time, rather than BM, where it decays linearly. Instead, we found strong support for BM over OU for *Primula* and *Lupinus* (Table 1 and S6). Moreover, Lévy processes are unlikely to be falsely detected in datasets that evolve under diffusion-like models (Landis and Schraiber 2017). Jointly, we are therefore confident that Lévy models are indeed the best descriptors of niche evolution in *Primula* and *Lupinus*, but not in *Ranunculus*, especially regarding niche centers.

Despite the strong evidence for models of pulsed evolution, identifying the exact branches that experienced pulses remains inherently challenging (Fig. 2; Landis et al. 2013). Jump processes lead to heavy-tailed trait distributions, characterized by excess kurtosis, which significantly differs from a pure diffusion process (Landis et al. 2013; Landis and Schraiber 2017). However, the excess kurtosis erodes over time, this implies that pulsed evolution is very hard to detect on long internal branches compared to short terminal branches (Landis and Schraiber 2017). However, we nevertheless detected multiple branches in *Primula* and *Lupinus* with a very clear signal-to-noise ratio, including internal and/or long branches (Fig. 2), is taken to be strong evidence for the presence of evolutionary jumps in the particular branches. Jointly, these methodological considerations allow us to biologically interpret the parameterizations of our best-supported models (Table 2), because they are very unlikely to be driven by methodological artifact.

Factors driving pulsed evolution

The model support for pulsed evolution was particularly pronounced for niche centers (Table 1, Table S6, Fig. 1, and Fig. S7). All AICc weights of niche center models in *Primula* or *Lupinus* 7favor Lévy processes, with weights more than twice as large as any other model, some even twice as large as the summed AICc weight of the three continuous models. Parameterizing these models using creepy-jerk (Table 2) and mapping posterior jump distributions (Fig. 2) reveal that in both cases, detectable jumps are scattered throughout the phylogeny, concentrated mostly around recent branches. *Lupinus* (Fig. 2; right panel), of which continental-scale biogeographic patterns are well-known (Drummond et al.

2012), Central and South America were colonized from the central-west North American mountains. Interestingly, in the South American clade (upper half in Fig. 2; right panel), we infer stronger downward pulses in niche evolution than upward pulses (more extreme negative compared to positive values, see scale bar), suggesting that there is more opportunity for downwards movement along the enormous elevation of Andean slopes. In contrast, in the North American clade (bottom half of Fig. 2; right panel), we detect multiple very pronounced upward pulses, all occurring within the Pleistocene. Similarly, *Primula*, which has its centers of diversity in Eurasian Mountains, but for which detailed biogeographic reconstructions are absent (de Vos et al. 2014), we find upward and downward pulses of evolution across the phylogeny (Fig. 2; left panel) in a similar timescale. Even though jumps may be more easily detectable in recent times, this general timeframe fits very well with the global Cenozoic cooling plus Pleistocene ice cycles, which are broadly thought to have driven alpine plant evolution on continental scales (e.g., Nevado et al. 2018; Ding et al. 2020; Smyčka et al. 2022).

Nevertheless, it remains unclear whether the continuous niche jumps indeed constitute biome shifts, not least because a broadly accepted definition of alpine species is lacking (Körner 2021). However, Körner (2021) agrees with Gjaerevoll (1990), who suggests only species with a niche center above the climatic treeline should be considered as "true" alpine species. Indeed, most plant species occurring above the climatic treeline in the European Alps also occur below it (Aeschimann et al. 2004, Bätscher and de Vos, accepted).

Despite strong evidence for pulsed changes in *Primula* and *Lupinus* niche centers, no evidence for evolutionary jumps in *Ranunculus* was found. Nonetheless, niche center changes in *Ranunculus* can be explained with an Ornstein-Uhlenbeck process it is the best model based on AICc weights (Table 1, Table S6, Fig. 1, and Fig. S7). This does not mean, that in *Ranunculus* evolutionary changes of the niche, center are absent, but compared to *Primula* and *Lupinus* the niche center does not evolve in jumps (i.e., no episodes of relatively rapid or slow niche evolution). This is supported by the inferred model parameters of creepy-jerk (Table 2): *Ranunculus* has a twice as large variance parameter (σ). However, in *Primula* and *Lupinus,* a substantial part is explained by the Lévy measure, which infers in *Primula* with a high probability (~30%) that a jump drawn from the α-stable distribution is larger than the BM and in *Lupinus* jumps occurring all ~4.5 Myr with a jump size of ~3 Myr of BM.

Even though the absence of evolutionary jumps in Ranunculus seems to be a conundrum there are some biological explanations why this might be the case. First, it is since Charles Darwin well-known and widely accepted, that different taxa can have different evolutionary histories. Furthermore, Simpson suggested in his highly cited book "Tempo and Mode in Evolution" (1944), that multiple tempos can be found in fossil records. In an alpine context, it was shown twice that different plant lineages have different diversification rates in the Hengduan Mountains (Xing and Ree 2017) and the European Alps (Smyčka et al. 2022). Furthermore, Bätscher and de Vos (accepted) showed in a recent study that six plant clades in the Alpine Arch have contrasting rates of alpine biome shifts. We also speculate that a different bauplan or different ancestral adaptation (e.g., key innovations) might cause this evolutionary different pattern. Therefore, more homogenous Ranunculus growth forms might be an indicator, that this clade has fewer chances to evolve pulsed. On the other hand, the Lupinus radiation in the Andes with its diverse growth forms (annuals, small herbaceous plants with taproots, (dwarf) shrubs, or trees) appearing all over the young radiation. This implies a less strict bauplan and an episode of rapid change (Drummond et al. 2012; Nevado et al. 2018; Nürk et al. 2019). Additionally, it is very likely, that the most recent common ancestor of *Ranunculus* was a Northern hemisphere species (Emadzade and Hörandl 2011) and was probably already "pre-adapted" to alpine-arctic conditions. Potentially most of the species from this taxon have maintained these physiological and morphological adaptions.

Additionally, to finding strong evidence for pulsed evolution in *Primula* and *Lupinus* niche center, results from the branch-normalized signal-to-noise ratio (Fig. 2) support these findings: many branches sow a non-zero ratio, implying that the Lévy process explains the data better than a pure BM. Furthermore, both creepy-jerk reconstructions imply that pulsed evolution (i.e., periods of faster and slower change) can be detected from the Pliocene to the present, where the backbone shows no evidence for jumps in the niche center for *Primula* and *Lupinus*. However, (as discussed above) we cannot be sure, that the absence of pulsed evolution on long phylogenetic branches is not only caused by over time decreasing excess kurtosis.

Nonetheless, multiple phylogenetic studies of plants in mountain systems confirm, that the period from the Pliocene to the present indicates increased change. For example, *Saxifraga* shows an increased upward biome shift in the most recent 5 Myr (Carruthers et al., in press), in the Qinghai-Tibet Plateau (QTP) rates of *in situ* diversification moderately increased 5 Myr ago (Ding et al. 2020), and dispersal rates between the Hengduan Mountains and Himalayas-QTP gradually increase over the last 4-5 Myr (Xing and Ree 2017), plus in European *Gentiana* the majority of bedrock shifts and expansions happened during the Pliocene (Favre et al. 2022).

All these findings highlight the importance of the drastic climatic changes over the last 5 Myr where multiple glacier expansions and retractions largely affected the mountain systems. For example, it is well-known, that within the last 800,000 years, the air temperature changed up to 12K within ~20,000 years. Therefore, it is a fair assumption, that the upper climatic treeline (i.e., the border of the alpine biome) moved strongly: downwards in cooler and upwards in warmer periods. Because our niche thresholds are computed relatively to the treeline, a species that does not change its niche threshold oscillates with the treeline (i.e., absolute niche conservation; Donoghue and Edwards 2014). Otherwise, a species that adapts *in situ* and does not move with the treeline needs to perform niche evolution (Donoghue and Edwards 2014). Consequently, this means that pulsed evolution indicates a rapid movement of the treeline or that a lineage moved even in the opposite direction than the treeline.

In conclusion, our results suggest that the driver of pulsed niche center shifts in *Primula* and *Lupinus* is likely connected to the glacial cycles in the Pleistocene. This hypothesis is directly in line with findings of the Andean *Lupinus* clade, where gene flow between species is likely connected to changes in habitat connectivity during Pleistocene glacial cycles (Nevado et al. 2018). Also, our results are supported by a study in the European Alps with six plant clades, which stimulated migration during Pleistocene glaciation (Smyčka et al. 2022).

CONCLUSION

The idea, that evolutionary rates may differ through time and across lineages has long been recognized (Simpson 1944). Although the phylogenetic toolkit has contained an opportunity to address this explicitly for continuous characters for roughly 10 years using Lévy processes (Landis et al. 2013), they have remained poorly adopted, with only a single previous application in plants (Ogburn and Edwards 2015). The differences that we document in jump-like processes across lineages using three niche proxies reveal significantly pulsed evolution in *Primula* and *Lupinus*, but not *Ranunculus*. Relevant differences across these taxa that may shed light on the when and why of pulsed niche evolution include past biogeographical opportunity, key innovations, and the genera's overall flexibility of bauplan (e.g., with stark contrasts from annual herbs to trees and diversification in aseasonal tropical mountains in *Lupinus*, to *Ranunculus* displaying rather homogenous growth forms). The pulses that we identify in *Primula* and *Lupinus* start around the Pleistocene, in line with global cooling and glacial cycles. This study thus opens the opportunity to start investigating what morphological or physiological changes underpin individual pulses of niches, to shed more light on the evolution in the face of major ecological constraints.

ACKNOWLEDGEMENT

We thank James Mickley and Aaron Liston from the Oregon State University Herbarium for donating *Lupinus* tissue for sequencing, and our colleagues from the Physiological Plant Ecology Group in Basel for discussing the content of this paper and for providing useful advice and comments. This work was supported by the Swiss National Science Foundation (grant 310030_185251 to JMdV).

REFERENCES

Aeschimann, D., K. Lauber, D. M. Moser, and J.-P. Theurillat. 2004. Flora alpina: atlas des 4500 plantes vasculaires des Alpes. Haupt Publisher.

Andrés, F., and G. Coupland. 2012. The genetic basis of flowering responses to seasonal cues. Nat. Rev. Genet. 13:627–639.

Baltisberger, M., and E. Hörandl. 2016. Karyotype evolution supports the molecular phylogeny in the genus Ranunculus (Ranunculaceae). Perspect. Plant Ecol., Evol. Syst. 18:1–14.

Barndorff-Nielsen, O. E., T. Mikosch, and S. I. Resnick. 2001. Lévy Processes: theory and applications. Springer Science & Business Media.

Barry, R. G. 1978. H.-B. de Saussure: The First Mountain Meteorologist. B Am Meteorol Soc 59:702–705.

Barua, A., and A. S. Mikheyev. 2020. Toxin expression in snake venom evolves rapidly with constant shifts in evolutionary rates. Proc. R. Soc. B 287:20200613.

Bastide, P., and G. Didier. 2023. The Cauchy Process on Phylogenies: a Tractable Model for Pulsed Evolution. Syst. Biol., doi: 10.1093/sysbio/syad053.

Beaulieu, J. M., D. Jhwueng, C. Boettiger, and B. C. O'Meara. 2012. Modeling stabilizing selection: expanding the Ornstein–Uhlenbeck model of adabtive evolution. Evolution 66:2369–2383.

Bokma, F. 2008. Detection of "Punctuated Equilibrium" by Bayesian Estimation of Speciation and Extinction Rates, Ancestral Character States, and Rates of Anagenetic and Cladogenetic Evolution on a Molecular Phylogeny. Evolution 62:2718–2726.

Bolger, A. M., M. Lohse, and B. Usadel. 2014. Trimmomatic: a flexible trimmer for Illumina sequence data. Bioinformatics 30:2114–2120.

Boucher, F. C., W. Thuiller, T. J. Davies, and S. Lavergne. 2014. Neutral Biogeography and the Evolution of Climatic Niches. Am. Nat. 183:573–584.

Brennan, I. G., and J. S. Keogh. 2018. Miocene biome turnover drove conservative body size evolution across Australian vertebrates. Proc. R. Soc. B 285:20181474.

Camacho, C., G. Coulouris, V. Avagyan, N. Ma, J. Papadopoulos, K. Bealer, and T. L. Madden. 2009. BLAST+: architecture and applications. BMC Bioinform. 10:421.

Capella-Gutiérrez, S., J. M. Silla-Martínez, and T. Gabaldón. 2009. trimAl: a tool for automated alignment trimming in large-scale phylogenetic analyses. Bioinformatics 25:1972–1973.

Crepet, W. L., and K. J. Niklas. 2009. Darwin's second "abominable mystery": Why are there so many angiosperm species? Am. J. Bot. 96:366–381.

Crisp, M. D., and L. G. Cook. 2012. Phylogenetic niche conservatism: what are the underlying evolutionary and ecological causes? N. Phytol. 196:681–694.

Ding, W.-N., R. H. Ree, R. A. Spicer, and Y.-W. Xing. 2020. Ancient orogenic and monsoon-driven assembly of the world's richest temperate alpine flora. Science 369:578–581.

Donoghue, M. J., and E. J. Edwards. 2014. Biome Shifts and Niche Evolution in Plants. Annu Rev Ecol Evol Syst 45:1–26.

Drori, M., A. Rice, M. Einhorn, O. Chay, L. Glick, and I. Mayrose. 2018. OneTwoTree: An online tool for phylogeny reconstruction. Mol Ecol Resour 18:1492–1499.

Drummond, A. J., S. Y. W. Ho, M. J. Phillips, and A. Rambaut. 2006. Relaxed Phylogenetics and Dating with Confidence. PLoS Biol. 4:e88.

Drummond, C. S., R. J. Eastwood, S. T. S. Miotto, and C. E. Hughes. 2012. Multiple Continental Radiations and Correlates of Diversification in Lupinus (Leguminosae): Testing for Key Innovation with Incomplete Taxon Sampling. Syst. Biol. 61:443–460.

Duchen, P., C. Leuenberger, S. M. Szilágyi, L. Harmon, J. Eastman, M. Schweizer, and D. Wegmann. 2017. Inference of Evolutionary Jumps in Large Phylogenies using Lévy Processes. Syst. Biol. 66:syx028.

Emadzade, K., and E. Hörandl. 2011. Northern Hemisphere origin, transoceanic dispersal, and diversification of Ranunculeae DC. (Ranunculaceae) in the Cenozoic. J Biogeogr 38:517–530.

Ewels, P., M. Magnusson, S. Lundin, and M. Käller. 2016. MultiQC: summarize analysis results for multiple tools and samples in a single report. Bioinformatics 32:3047–3048.

Favre, A., J. Paule, and J. Ebersbach. 2022. Incongruences between nuclear and plastid phylogenies challenge the identification of correlates of diversification in Gentiana in the European Alpine System. Alp. Bot. 132:29–50.

Felsenstein, J. 1985. Phylogenies and the Comparative Method. Am. Nat. 125:1–15.

Fine, P. V. A., F. Zapata, and D. C. Daly. 2014. Investigating Processes of Neotropical Rain Forest Tree Diversification by Examining the Evolution and Historical Biogeography of the Protieae (Burseraceae). Evolution 68:1988–2004.

García-Navas, V., J. A. Tobias, M. Schweizer, D. Wegmann, R. Schodde, J. A. Norman, and L. Christidis. 2021. Trophic niche shifts and phenotypic trait evolution are largely decoupled in Australasian parrots. BMC Ecol. Evol. 21:212.

Gjaerevoll, O. 1990. Alpine plants. The Royal Norwegian Society of Science and Tapir Publisher, Trondheim.

Gould, S. J., and N. Eldredge. 1972. Punctuated equilibria: An alternative to phyletic gradualism. Models in paleobiology 82–115.

Hackel, J., and I. Sanmartín. 2021. Modelling the tempo and mode of lineage dispersal. Trends Ecol Evol 36:1102–1112.

Hansen, T. F., and E. P. Martins. 1996. Translating between microevolutionary process and macroevolutionary patterns: the correlation structure of interspecific data. Evolution 50:1404–1417.

Harmon, L. J., J. B. Losos, T. J. Davies, R. G. Gillespie, J. L. Gittleman, W. B. Jennings, K. H. Kozak, M. A. McPeek, F. Moreno-Roark, T. J. Near, A. Purvis, R. E. Ricklefs, D. Schluter, J. A. S. II, O. Seehausen, B. L. Sidlauskas, O. Torres-Carvajal, J. T. Weir, and A. Ø. Mooers. 2010. Early bursts of body size and shape evolution are rare in comparative data. Evolution 64:2385–2396.

Höhna, S., M. J. Landis, T. A. Heath, B. Boussau, N. Lartillot, B. R. Moore, J. P. Huelsenbeck, and F. Ronquist. 2016. RevBayes: Bayesian Phylogenetic Inference Using Graphical Models and an Interactive Model-Specification Language. Systematic Biol 65:726–736.

Jin, J.-J., W.-B. Yu, J.-B. Yang, Y. Song, C. W. dePamphilis, T.-S. Yi, and D.-Z. Li. 2020. GetOrganelle: a fast and versatile toolkit for accurate de novo assembly of organelle genomes. Genome Biol. 21:241.

Johnson, M. G., E. M. Gardner, Y. Liu, R. Medina, B. Goffinet, A. J. Shaw, N. J. C. Zerega, and N. J. Wickett. 2016. HybPiper: Extracting Coding Sequence and Introns for Phylogenetics from High-Throughput Sequencing Reads Using Target Enrichment. Appl. Plant Sci. 4:1600016.

Johnson, M. G., L. Pokorny, S. Dodsworth, L. R. Botigué, R. S. Cowan, A. Devault, W. L. Eiserhardt, N. Epitawalage, F. Forest, J. T. Kim, J. H. Leebens-Mack, I. J. Leitch, O. Maurin, D. E. Soltis, P. S. Soltis, G. K. Wong, W. J. Baker, and N. J. Wickett. 2018. A Universal Probe Set for Targeted Sequencing of 353 Nuclear Genes from Any Flowering Plant Designed Using k-Medoids Clustering. Syst. Biol. 68:594–606.

Kadlec, M., D. U. Bellstedt, N. C. L. Maitre, and M. D. Pirie. 2017. Targeted NGS for species level phylogenomics: “made to measure” or “one size fits all”? PeerJ 5:e3569.

Karger, D. N., O. Conrad, J. Böhner, T. Kawohl, H. Kreft, R. W. Soria-Auza, N. E. Zimmermann, H. P. Linder, and M. Kessler. 2017. Climatologies at high resolution for the earth’s land surface areas. Sci Data 4:170122.

Katoh, K., and D. M. Standley. 2013. MAFFT Multiple Sequence Alignment Software Version 7: Improvements in Performance and Usability. Mol. Biol. Evol. 30:772–780.

Kelchner, S. A., and M. A. Thomas. 2007. Model use in phylogenetics: nine key questions. Trends Ecol. Evol. 22:87–94.

Kerkhoff, A. J., P. E. Moriarty, and M. D. Weiser. 2014. The latitudinal species richness gradient in New World woody angiosperms is consistent with the tropical conservatism hypothesis. Proc National Acad Sci 111:8125–8130.

Kistler, L. 2011. Ancient DNA, Methods and Protocols. Methods Mol. Biol. 840:71–79.

Körner, C. 2021. Alpine Plant Life, Functional Plant Ecology of High Mountain Ecosystems.

Körner, C. 2012. Alpine Treelines, Functional Ecology of the Global High Elevation Tree Limits.

Körner, C. 2007. Climatic Treelines: Conventions, Global Patterns, Causes (Klimatische Baumgrenzen: Konventionen, globale Muster, Ursachen).

Körner, C. 2023. Concepts in Alpine Plant Ecology. Plants 12:2666.

Körner, C., J. Paulsen, and E. M. Spehn. 2011. A definition of mountains and their bioclimatic belts for global comparisons of biodiversity data. Alpine Bot 121:73.

Kozlov, A. M., D. Darriba, T. Flouri, B. Morel, and A. Stamatakis. 2019. RAxML-NG: A fast, scalable, and user-friendly tool for maximum likelihood phylogenetic inference. Bioinformatics 35:4453–4455.

Landis, M. J., and J. G. Schraiber. 2017. Pulsed evolution shaped modern vertebrate body sizes. Proc National Acad Sci 114:13224–13229.

Landis, M. J., J. G. Schraiber, and M. Liang. 2013. Phylogenetic Analysis Using Lévy Processes: Finding Jumps in the Evolution of Continuous Traits. Systematic Biol 62:193–204.

Lee, A. K., I. S. Gilman, M. Srivastav, A. D. Lerner, M. J. Donoghue, and W. L. Clement. 2021. Reconstructing Dipsacales phylogeny using Angiosperms353: issues and insights. Am. J. Bot. 108:1122–1142.

Li, L., C. J. Stoeckert, and D. S. Roos. 2003. OrthoMCL: Identification of Ortholog Groups for Eukaryotic Genomes. Genome Res. 13:2178–2189.

Martin, C. H., and E. J. Richards. 2019. The Paradox Behind the Pattern of Rapid Adaptive Radiation: How Can the Speciation Process Sustain Itself Through an Early Burst? Annu. Rev. Ecol., Evol., Syst. 50:1–25.

Martins, E. P. 1994. Estimating the Rate of Phenotypic Evolution from Comparative Data. Am. Nat. 144:193–209.

McLay, T. G. B., J. L. Birch, B. F. Gunn, W. Ning, J. A. Tate, L. Nauheimer, E. M. Joyce, L. Simpson, A. N. Schmidt-Lebuhn, W. J. Baker, F. Forest, and C. J. Jackson. 2021. New targets acquired: Improving locus recovery from the Angiosperms353 probe set. Appl. Plant Sci. 9:10.1002/aps3.11420.

Miliaresis, G. C., and D. P. Argialas. 1999. Segmentation of physiographic features from the global digital elevation model/GTOPO30. Comput Geosci 25:715–728.

Morinière, J., M. H. V. Dam, O. Hawlitschek, J. Bergsten, M. C. Michat, L. Hendrich, I. Ribera, E. F. A. Toussaint, and M. Balke. 2016. Phylogenetic niche conservatism explains an inverse latitudinal diversity gradient in freshwater arthropods. Sci. Rep. 6:26340.

Muellner-Riehl, A. N. 2019. Mountains as Evolutionary Arenas: Patterns, Emerging Approaches, Paradigm Shifts, and Their Implications for Plant Phylogeographic Research in the Tibeto-Himalayan Region. Front. Plant Sci. 10:195.

Nauheimer, L., N. Weigner, E. Joyce, D. Crayn, C. Clarke, and K. Nargar. 2021. HybPhaser: A workflow for the detection and phasing of hybrids in target capture data sets. Appl. Plant Sci. 9:10.1002/aps3.11441.

Nevado, B., N. Contreras-Ortiz, C. Hughes, and D. A. Filatov. 2018. Pleistocene glacial cycles drive isolation, gene flow and speciation in the high-elevation Andes. N. Phytol. 219:779–793.

Nürk, N. M., G. W. Atchison, and C. E. Hughes. 2019. Island woodiness underpins accelerated disparification in plant radiations. N. Phytol. 224:518–531.

Ogburn, R. M., and E. J. Edwards. 2015. Life history lability underlies rapid climate niche evolution in the angiosperm clade Montiaceae. Mol. Phylogenetics Evol. 92:181–192.

Paradis, E., and K. Schliep. 2019. ape 5.0: an environment for modern phylogenetics and evolutionary analyses in R. Bioinformatics 35:526–528.

Patsiou, T., N. Walden, and Y. Willi. 2021. What drives species' distributions along elevational gradients? Macroecological and -evolutionary insights from Brassicaceae of the central Alps. Glob. Ecol. Biogeogr. 30:1030–1042.

Paulsen, J., and C. Körner. 2014. A climate-based model to predict potential treeline position around the globe. Alpine Bot 124:1–12.

Pennell, M. W., J. M. Eastman, G. J. Slater, J. W. Brown, J. C. Uyeda, R. G. FitzJohn, M. E. Alfaro, and L. J. Harmon. 2014. geiger v2.0: an expanded suite of methods for fitting macroevolutionary models to phylogenetic trees. Bioinformatics 30:2216–2218.

Potente, G., É. Léveillé-Bourret, N. Yousefi, R. R. Choudhury, B. Keller, S. I. Diop, D. Duijsings, W. Pirovano, M. Lenhard, P. Szövényi, and E. Conti. 2022. Comparative genomics elucidates the origin of a supergene controlling floral heteromorphism. Mol. Biol. Evol. 39:msac035-.

Pyron, R. A., G. C. Costa, M. A. Patten, and F. T. Burbrink. 2015. Phylogenetic niche conservatism and the evolutionary basis of ecological speciation. Biol. Rev. 90:1248–1262.

Rambaut, A., A. J. Drummond, D. Xie, G. Baele, and M. A. Suchard. 2018. Posterior Summarization in Bayesian Phylogenetics Using Tracer 1.7. Systematic Biol 67:901–904.

Rowsey, D. M., L. R. Heaney, and S. A. Jansa. 2019. Tempo and mode of mandibular shape and size evolution reveal mixed support for incumbency effects in two clades of island-endemic rodents (Muridae: Murinae)*. Evolution 73:1411–1427.

Sauquet, H., and S. Magallón. 2018. Key questions and challenges in angiosperm macroevolution. N. Phytol. 219:1170–1187.

Schliep, K. P. 2011. phangorn: phylogenetic analysis in R. Bioinformatics 27:592–593.

Schluter, D. 2000. The Ecology of Adaptive Radiation. OUP Oxford.

Schröter, C., H. Brockmann-Jerosch, M. C. Brockmann-Jerosch, A. Günthart, and G. Huber-Pestalozzi. 1926. Das Pflanzenleben der Alpen: Eine Schilderung der Hochgebirgsflora. A. Raustein.

Shepherd, D. A., and S. Klaere. 2018. How Well Does Your Phylogenetic Model Fit Your Data? Syst. Biol. 68:157–167.

Simpson, G. G. 1944. Tempo and Mode in Evolution. Columbia University Press.

Smith, E. G., J. M. Surm, J. Macrander, A. Simhi, G. Amir, M. Y. Sachkova, M. Lewandowska, A. M. Reitzel, and Y. Moran. 2023. Micro and macroevolution of sea anemone venom phenotype. Nat. Commun. 14:249.

Smyčka, J., C. Roquet, M. Boleda, A. Alberti, F. Boyer, R. Douzet, C. Perrier, M. Rome, J.-G. Valay, F. Denoeud, K. Šemberová, N. E. Zimmermann, W. Thuiller, P. Wincker, I. G. Alsos, E. Coissac, C. Roquet, M. Boleda, A. Alberti, F. Boyer, R. Douzet, C. Perrier, M. Rome, J.-G. Valay, F. Denoeud, N. E. Zimmermann, W. Thuiller, P. Wincker, I. G. Alsos, E. Coissac, S. Lavergne, and S. Lavergne. 2022. Tempo and drivers of plant diversification in the European mountain system. Nat Commun 13:2750.

Spehn, E. M., K. Rudmann-Maurer, and C. Körner. 2011. Mountain biodiversity. Plant Ecol Divers 4:301–302.

Uyeda, J. C., T. F. Hansen, S. J. Arnold, and J. Pienaar. 2011. The million-year wait for macroevolutionary bursts. Proc. Natl. Acad. Sci. 108:15908–15913.

Vos, J. M. de, C. E. Hughes, G. M. Schneeweiss, B. R. Moore, and E. Conti. 2014. Heterostyly accelerates diversification via reduced extinction in primroses. Proc Royal Soc B Biological Sci 281:20140075.

Wiens, J. J., D. D. Ackerly, A. P. Allen, B. L. Anacker, L. B. Buckley, H. V. Cornell, E. I. Damschen, T. J. Davies, J. Grytnes, S. P. Harrison, B. A. Hawkins, R. D. Holt, C. M. McCain, and P. R. Stephens. 2010. Niche conservatism as an emerging principle in ecology and conservation biology. Ecol. Lett. 13:1310–1324.

Willi, Y., and J. V. Buskirk. 2022. A review on trade-offs at the warm and cold ends of geographical distributions. Philos. Trans. R. Soc. B 377:20210022.

Xing, Y., and R. H. Ree. 2017. Uplift-driven diversification in the Hengduan Mountains, a temperate biodiversity hotspot. Proc. Natl. Acad. Sci. 114:E3444–E3451.

Zhang, C., M. Rabiee, E. Sayyari, and S. Mirarab. 2018. ASTRAL-III: polynomial time species tree reconstruction from partially resolved gene trees. BMC Bioinform. 19:153.

Zizka, A., D. Silvestro, T. Andermann, J. Azevedo, C. D. Ritter, D. Edler, H. Farooq, A. Herdean, M. Ariza, R. Scharn, S. Svantesson, N. Wengström, V. Zizka, and A. Antonelli. 2019. CoordinateCleaner: Standardized cleaning of occurrence records from biological collection databases. Methods Ecol Evol 10:744–751.

SUPPLEMENTARY MATERIAL

Omics data collection for bait design

We downloaded genome assemblies, transcriptome shotgun assemblies and sequence read archives for *Primula, Lupinus*, and *Ranunculus* from GenBank (detailed list: Table S7). Next, we conducted quality control with FastQC v0.11.8 (https://www.bioinformatics.babraham.ac.uk/projects/fastqc/) and identified eight sequence read archives that need light trimming and adapter removal, performed with Trimmomatic v0.39 (Bolger et al. 2014) detailed parameters are stated in Table S7. Afterwards, quality control was repeated to ensure suffitient read quality. Next, *Primula* and *Lupinus* reads are back-mapped using the Burrows-Wheeler alignment tool v0.7.15 (Li & Durbin 2009) and the reference genome of *L. angustifolius* (accession number: PRJNA299755), respectively a *P. veris* genome (PRJEB44353; assembled as described in Potente et al. 2022). We then used a combination of SAMtools v 1.9 (Li et al. 2009), BEDtools v 2.27.1 (Quinlan & Hall 2010) and BCFtools v 1.10.2 (Danecek & McCarthy 2017), to convert the contigs into FASTA format. Due to a missing reference genome, we assembled *Ranunculus* sequences de novo with SPAdes v 3.13.0 (Bankevich et al. 2012), controlled assembly quality with QUAST v 5.0.0 (Gurevich et al. 2013) and excluded *L. luteus* (SRR2075858) because of assembly issues. Inorderto, further increasing the amount of data we downloaded seven transcriptomes from the 1000 Plant Transcriptomes Initiative (https://db.cngb.org/onekp/search/; sample code: CMFF, CYVA, GBVZ, TTRG, UPOG, VGHH and ZUHO). Additionally, 11 transcriptomes were downloaded (assembled as described in Nevado et al. 2016; detailed list: Table S8) and we included an unpublished *L. mutabilis* draft genome from Bruno Nevado.

Parameter selection for the dating of the phylogenies

To inferre meaningful priors, we consulted the literature of previous phylogenetic studies, for *Primula* (de Vos et al. 2014), *Lupinus* (Drummond et al. 2012) and *Ranunculus* (Emadzade & Hörandl 2011). For calibrating the *Primula* root age, we selected a normal (gaussian) distribution with a mean of 20.7, a standard deviation (sd) of 5.025, and the 95% probability density interval (12.1 – 32.2) is used to define the maximum and the minimum of the distribution. In *Lupinus* a normal distribution with a mean of 11.8, sd of 2.6, and the 95% probability interval (6.8 - 17.2) using as distribution maximum and minimum, were selected for the calibration. For inferring the root age of *Ranunculus* a normal distribution, with a mean of 38.36, a sd of 4.6 and a 95% probability density interval, (28.7 - 47.1) defining the upper and lower limit of the distribution. We used additional three calibration points in *Ranunculus*: 1.) for the most recent common ancestor (MRCA) of *Myrosurus minimus* (according to POWO synonym of: *Ranunculus minimus*), *Ceratocephala falcata* (syn. *Ranunculus falcatus*) and *Ceratocephala Orthoceras* (syn. *Ranunculus testiculatus*) a log-normal distribution with a mean of 1, a sd of 1 and an offset of 22.518 was used; 2.) for the MRCA of *Ranunculus carpaticola* (synonym of: *Ranunculus cassubicifolius*), and *Ranunculus notabilis* a normal distribution was implemented, with a mean of 0.914 and a sd of 0.34; 3.), and for the MRCA of *Ranunculus caprarum* and *Ranunculus peduncularis* we choose a uniform distribution from 0–2.

FIGURE S1: ASTRAL species tree of the genera *Primula*. Branch labels show posterior probability and branch lengths are based on ASTRAL coalescent units.

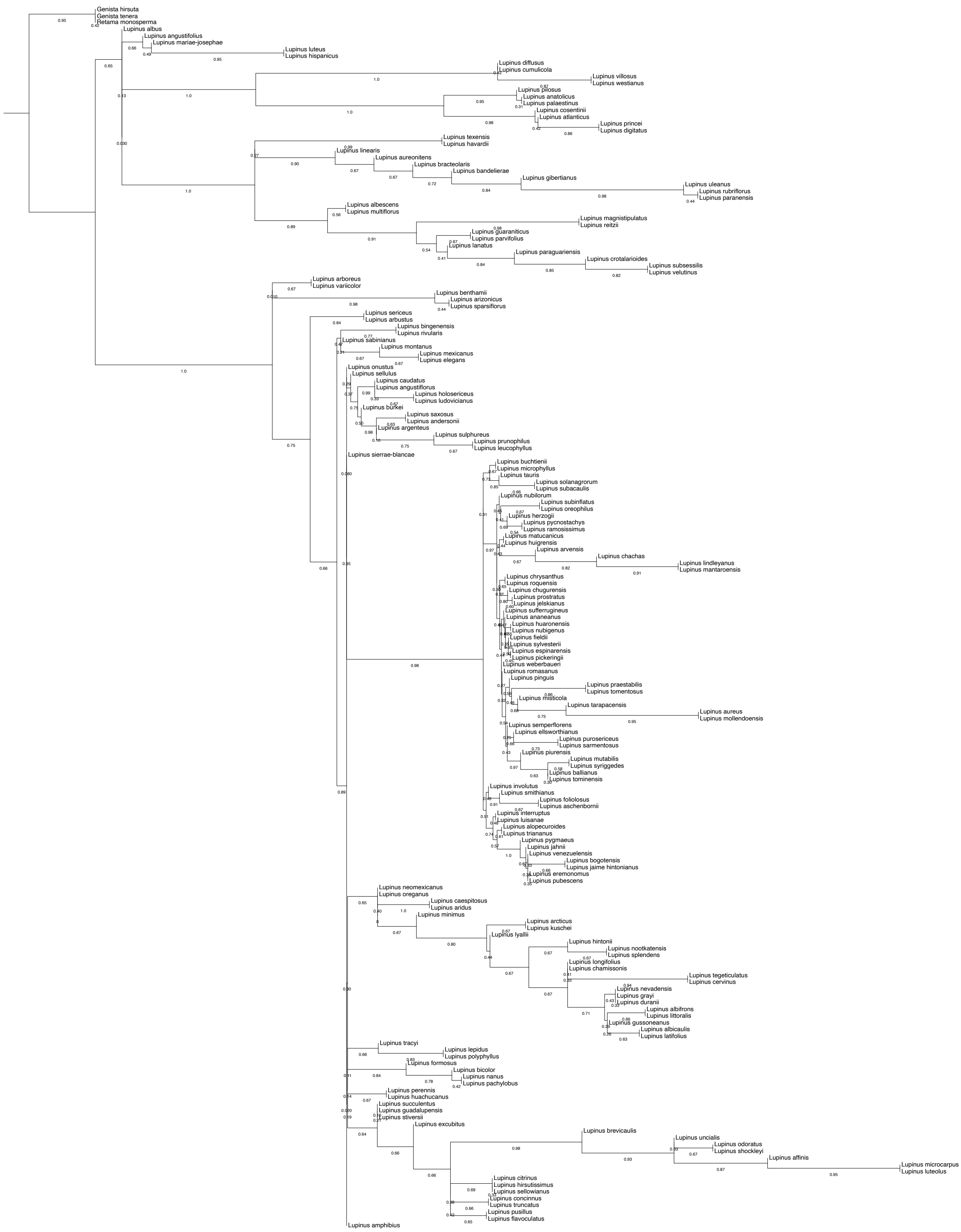

FIGURE S2: ASTRAL species tree of the genera *Lupinus*. Branch labels show posterior probability and branch lengths are based on ASTRAL coalescent units.

FIGURE S3: ASTRAL species tree of the genera *Ranunculus*. Branch labels show posterior probability and branch lengths are based on ASTRAL coalescent units.

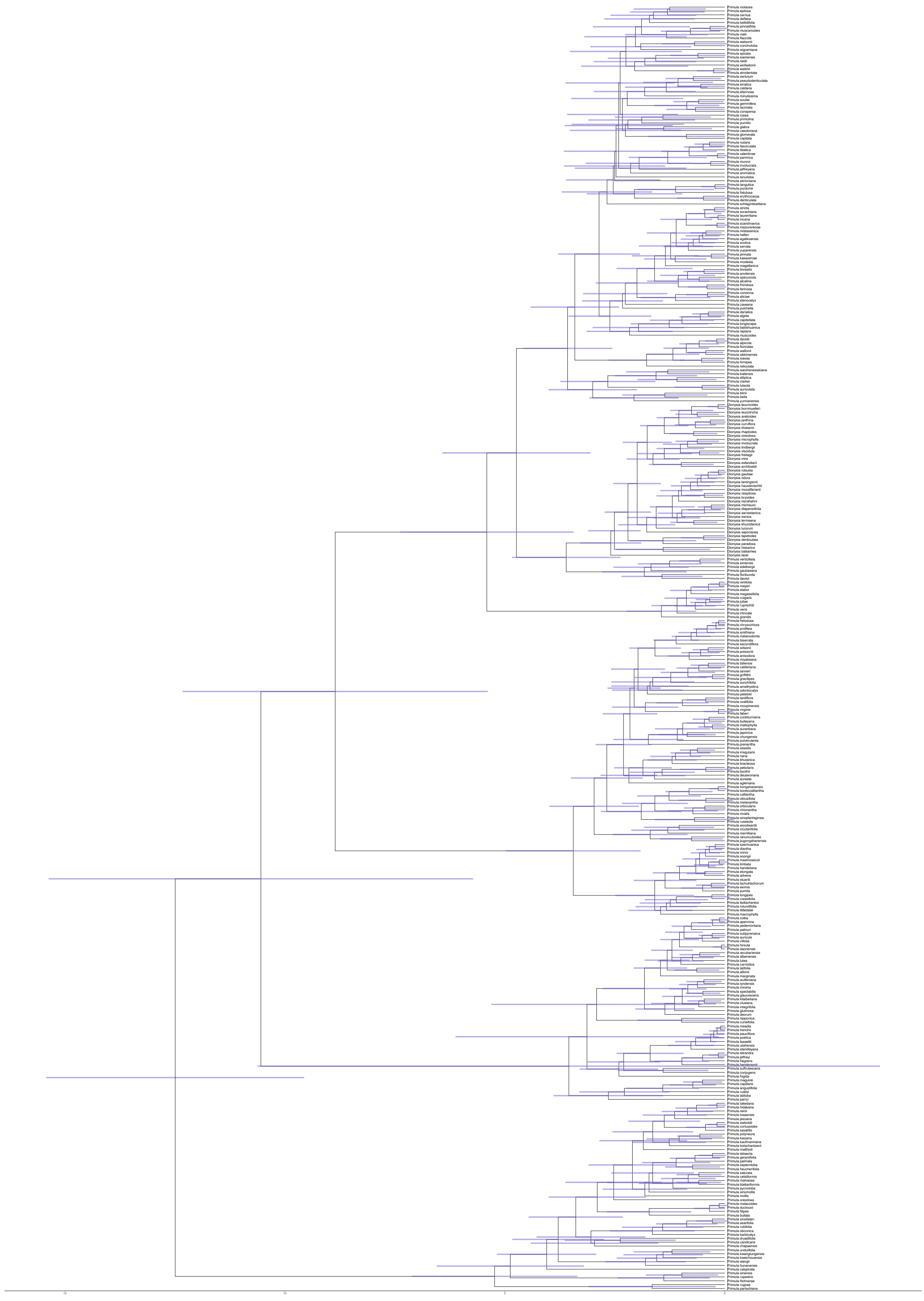

FIGURE S4: RevBayes time-calibrated *Primula* phylogeny. Horizontal bars show the 95% highest posterior density, and the x-axis is time in millions of years.

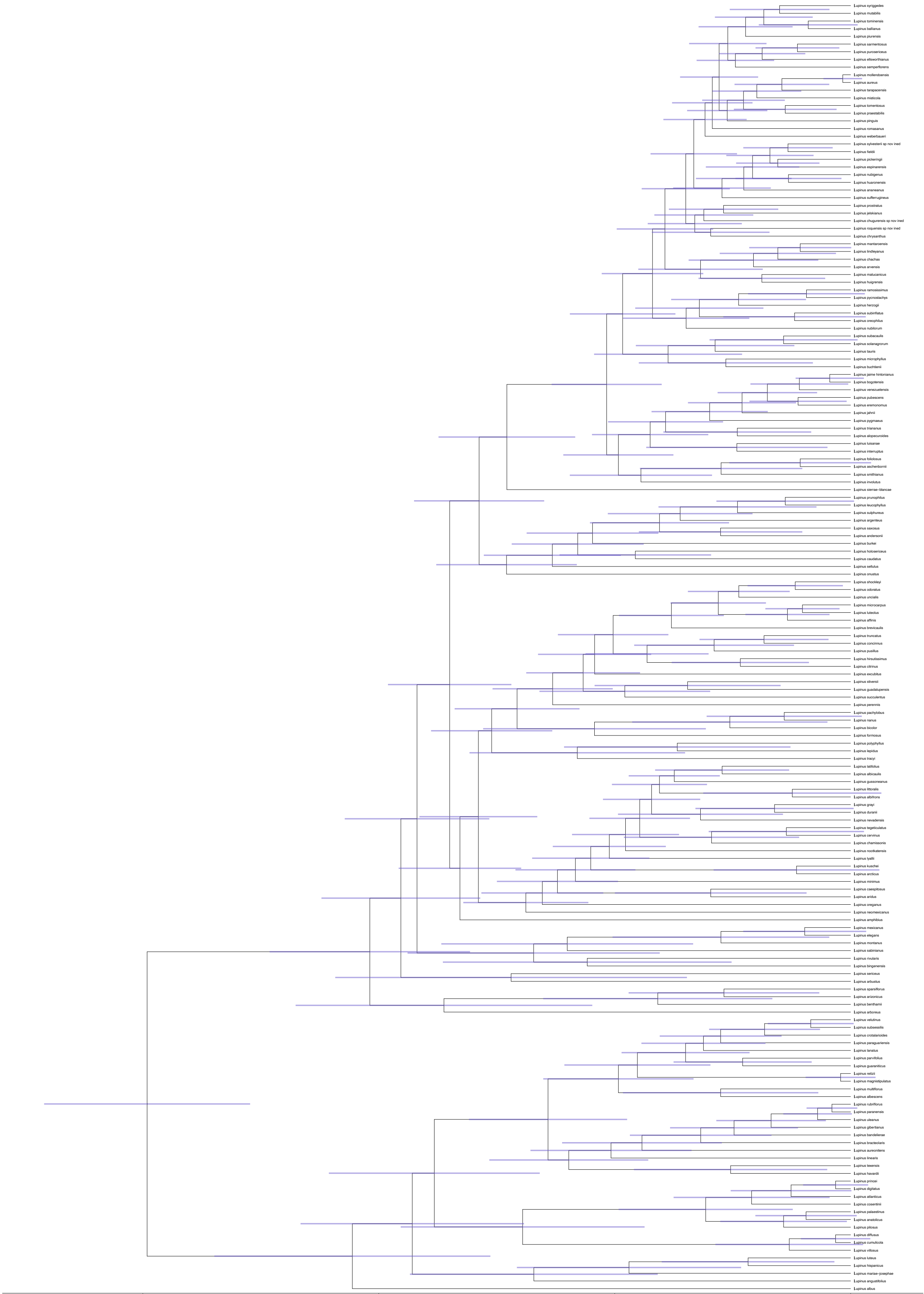

FIGURE S5: RevBayes time-calibrated *Lupinus* phylogeny. Horizontal bars show the 95% highest posterior density, and the x-axis is time in millions of years.

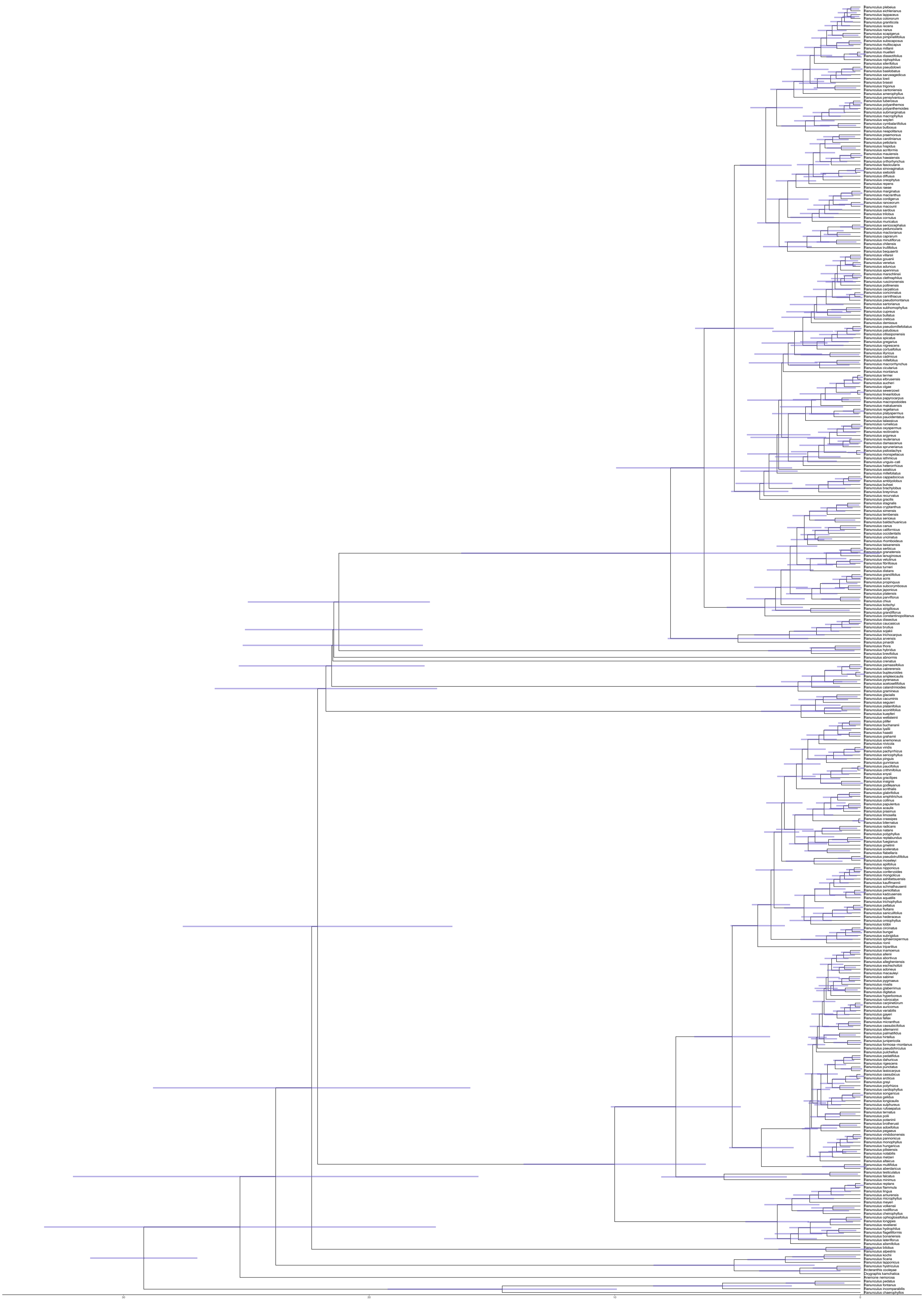

FIGURE S6: RevBayes time-calibrated *Ranunculus* phylogeny. Horizontal bars show the 95% highest posterior density, and the x-axis is time in millions of years.

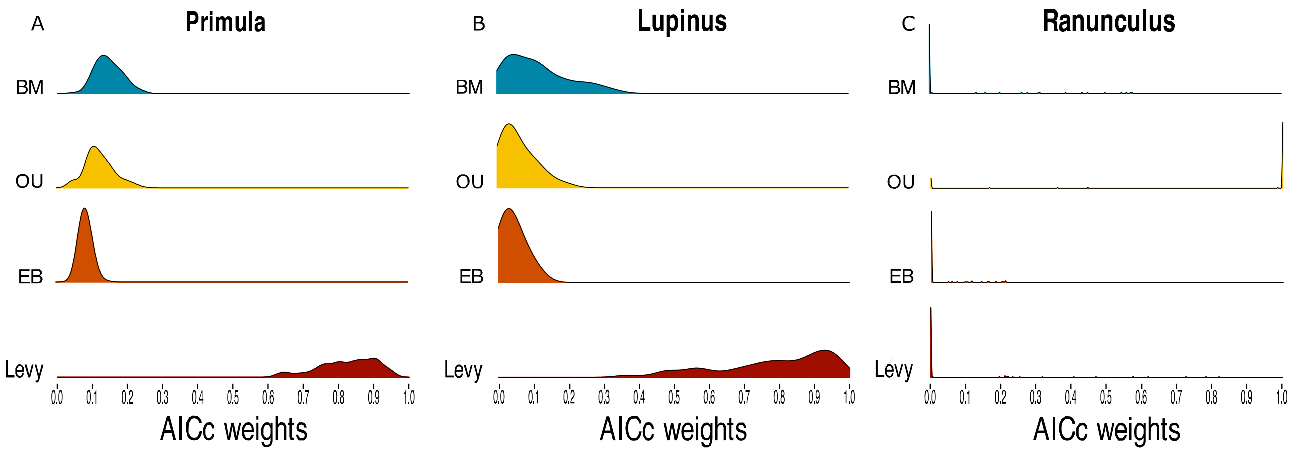

FIGURE S7: Density distribution of Akaike weights (under 100 randomly resolved polytomies), of the different genera: A) Primula, B) Lupinus, and C) Ranunculus. The different rows represent the different models: Brownian motion (BM), Ornstein-Uhlenbeck (OU), early burst (EB), and Lévy processes (Lévy).

TABLE S1: List of all samples used for DNA extraction, including voucher accession numbers and the source of the sample.

Lable	Voucher accession number	Genus	Epithet	Intraspecific epthet	Source
13P	BASBG-00184944	Ranunculus	parviflorus		Herbarium Basel
14P	BASBG-00184988	Ranunculus	platanifolius		Herbarium Basel
20P	LB-NU01	Ranunculus	bulbosus		Field collection
22	AE2546(2)	Ranunculus	californicus		Herbarium Basel
23	AE2546	Ranunculus	eschscholtzii		Herbarium Basel
24	BASBG-00182865	Ranunculus	abnormis		Herbarium Basel
25	BASBG-00183358	Ranunculus	brevifolius		Herbarium Basel
26	BASBG-00183496	Ranunculus	bupleuroides		Herbarium Basel
27	BASBG-00183499	Ranunculus	cadmicus		Herbarium Basel
28	BASBG-00183537	Ranunculus	chaerophyllos		Herbarium Basel
29	BASBG-00183553	Ranunculus	clethraphilus		Herbarium Basel
30	BASBG-00183603	Ranunculus	concinnatus		Herbarium Basel
31	BASBG-00183566	Ranunculus	cordiger		Herbarium Basel
32	BASBG-00183608	Ranunculus	cymbalariifolius		Herbarium Basel
33	BASBG-00183615	Ranunculus	demissus	var. major	Herbarium Basel
34	BASBG-00183642	Ranunculus	falcatus	ssp. incurvus	Herbarium Basel
35	BASBG-00183660	Ranunculus	ficaria		Herbarium Basel
36	BASBG-00183849	Ranunculus	fontanus		Herbarium Basel
37	BASBG-00184068	Ranunculus	incomparabilis		Herbarium Basel
38	BASBG-00184071	Ranunculus	isthmicus		Herbarium Basel
39	BASBG-00184302	Ranunculus	lobbii		Herbarium Basel
40	BASBG-00183619	Ranunculus	longipes		Herbarium Basel
41	BASBG-00184304	Ranunculus	macrophyllus		Herbarium Basel
42	BASBG-00184377	Ranunculus	monspeliacus		Herbarium Basel
43	BASBG-00184720	Ranunculus	nigrescens		Herbarium Basel
44	BASBG-00184728	Ranunculus	nodiflorus		Herbarium Basel
45	BASBG-00184963	Ranunculus	pedatus		Herbarium Basel
46	BASBG-00185025	Ranunculus	platensis		Herbarium Basel
47	BASBG-00185027	Ranunculus	platyspermus		Herbarium Basel
48	BASBG-00181952	Ranunculus	peltatus		Herbarium Basel
49	BASBG-00185328	Ranunculus	rectirostris		Herbarium Basel
50	BASBG-00185185	Ranunculus	reuterianus		Herbarium Basel
51	BASBG-00185193	Ranunculus	revelierei		Herbarium Basel
52	BASBG-00185240	Ranunculus	ruscinonensis		Herbarium Basel
53	BASBG-00185434	Ranunculus	serpens	ssp. nemorosus	Herbarium Basel
54	BASBG-00185448	Ranunculus	subhomophyllus		Herbarium Basel
55	BASBG-00185457	Ranunculus	thora		Herbarium Basel
56	BASBG-00185504	Ranunculus	trichocarpus		Herbarium Basel
57	BASBG-00185524	Ranunculus	unguis-cati		Herbarium Basel
58	LB-GR03	Ranunculus	alpestris		Field collection
59	LB-GR03(2)	Ranunculus	montanus		Field collection
60	ORE51975	Lupinus	amphibius		Herbarium Oregon
61	OSC-V-024832	Lupinus	albicaulis	var. shastensis	Herbarium Oregon
62	OSC-V-024853	Lupinus	argenteus	var. heteranthus	Herbarium Oregon
63	OSC-V-024944	Lupinus	argenteus	var. holosericeus	Herbarium Oregon
64	OSC-V-025003	Lupinus	lepidus	var. aridus	Herbarium Oregon
65	OSC-V-025044	Lupinus	latifolius x sericeus		Herbarium Oregon
66	OSC-V-025062	Lupinus	onustus		Herbarium Oregon
67	OSC-V-025084	Lupinus	polyphyllus	var. prunophilus	Herbarium Oregon
68	OSC-V-025128	Lupinus	polyphyllus	var. saxosus	Herbarium Oregon
69	OSC-V-025174	Lupinus	sericeus		Herbarium Oregon
70	OSC-V-025444	Lupinus	arbustus		Herbarium Oregon
71	OSC-V-025946	Lupinus	polyphyllus	var. prunophilus	Herbarium Oregon
72	OSC-V-026218	Lupinus	lepidus	var. lepidus	Herbarium Oregon
73	OSC-V-026245	Lupinus	lepidus	var. lobbii	Herbarium Oregon
74	OSC-V-026500	Lupinus	lepidus	var. utahensis	Herbarium Oregon
75	OSC-V-026980	Lupinus	polyphyllus	var. burkei	Herbarium Oregon
76	OSC-V-027198	Lupinus	sabinianus		Herbarium Oregon
77	OSC-V-027213	Lupinus	oreganus		Herbarium Oregon
78	OSC-V-027233	Lupinus	sulphureus	ssp. subsaccatus	Herbarium Oregon
79	OSC-V-027262	Lupinus	tracyi		Herbarium Oregon
80	CEH2005	Lupinus	roquensis sp nov ined.		Collection / Loan Collin Hughes
81	CEH2012	Lupinus	semperflorens		Collection / Loan Collin Hughes
82	CEH2042	Lupinus	prostratus		Collection / Loan Collin Hughes
83	CEH2229	Lupinus	romasanus		Collection / Loan Collin Hughes

84	CEH2239	Lupinus	nubigenus		Collection / Loan Collin Hughes
85	CEH2241	Lupinus	huaronensis		Collection / Loan Collin Hughes
86	CEH2248	Lupinus	purosericeus		Collection / Loan Collin Hughes
87	CEH2252	Lupinus	herzogii		Collection / Loan Collin Hughes
88	CEH2266	Lupinus	ananeanus		Collection / Loan Collin Hughes
89	CEH2267	Lupinus	pickeringii		Collection / Loan Collin Hughes
90	CEH2302	Lupinus	mutabilis		Collection / Loan Collin Hughes
91	CEH2319	Lupinus	subinflatus		Collection / Loan Collin Hughes
92	CEH2322	Lupinus	sufferugineus		Collection / Loan Collin Hughes
93	CEH2328	Lupinus	tarijensis		Collection / Loan Collin Hughes
94	CEH2353	Lupinus	praestabilis		Collection / Loan Collin Hughes
95	CEH2354	Lupinus	misticola		Collection / Loan Collin Hughes
96	CEH2390	Lupinus	chrysanthus		Collection / Loan Collin Hughes
97	CEH2392	Lupinus	espinarensis		Collection / Loan Collin Hughes
98	CEH2421	Lupinus	nubilorum		Collection / Loan Collin Hughes
99	CEH2444	Lupinus	bangii		Collection / Loan Collin Hughes
100	CEH2665	Lupinus	huigrensis		Collection / Loan Collin Hughes
101	CEH3067	Lupinus	syriggedes		Collection / Loan Collin Hughes
102	CEH3079	Lupinus	chugurensis sp nov ined.		Collection / Loan Collin Hughes
103	GWA50	Lupinus	interruptus		Collection / Loan Collin Hughes
104	GWA60	Lupinus	triananus		Collection / Loan Collin Hughes
105	GWA79	Lupinus	alopecuroides		Collection / Loan Collin Hughes
106	NCO50	Lupinus	luisanae		Collection / Loan Collin Hughes
107	RJE105	Lupinus	jelskianus		Collection / Loan Collin Hughes
108	RJE113	Lupinus	piurensis		Collection / Loan Collin Hughes
109	RJE141	Lupinus	matucanicus		Collection / Loan Collin Hughes
110	RJE157	Lupinus	fieldii		Collection / Loan Collin Hughes
111	RJE158	Lupinus	ellsworthianus		Collection / Loan Collin Hughes
112	RJE160	Lupinus	pinguis		Collection / Loan Collin Hughes
113	RJE169	Lupinus	involutus		Collection / Loan Collin Hughes
114	RJE171	Lupinus	tauris	var. lespedezioides	Collection / Loan Collin Hughes
115	RJE184	Lupinus	foliolosus		Collection / Loan Collin Hughes
116	RJE185	Lupinus	microphyllus		Collection / Loan Collin Hughes
117	RJE201	Lupinus	smithianus		Collection / Loan Collin Hughes
118	RJE210	Lupinus	solanagrorum		Collection / Loan Collin Hughes
119	RJE52	Lupinus	weberbaueri		Collection / Loan Collin Hughes
120	SPS1153	Lupinus	sylvesterii sp nov ined.		Collection / Loan Collin Hughes
121	VC141	Lupinus	pygmaeus		Collection / Loan Collin Hughes
122	VC158	Lupinus	humilis		Collection / Loan Collin Hughes
123	VC184	Lupinus	venezuelensis		Collection / Loan Collin Hughes
124	VC199	Lupinus	eremonomus		Collection / Loan Collin Hughes
125	VC65	Lupinus	jahnii		Collection / Loan Collin Hughes
126	Weigend 97/703	Lupinus	aureus		Collection / Loan Collin Hughes
127	1455	Primula	stenocalyx		Tissue collection Elena Conti
128	1461	Primula	atrodentata		Tissue collection Elena Conti
129	1463	Primula	candicans		Tissue collection Elena Conti
130	1464	Primula	cawdoriana		Tissue collection Elena Conti
131	1478	Primula	bellidifolia		Tissue collection Elena Conti
132	1486	Primula	souliei		Tissue collection Elena Conti
133	1565	Primula	cortusoides		Tissue collection Elena Conti
134	1566	Primula	filipes		Tissue collection Elena Conti
135	1570	Primula	malacoides		Tissue collection Elena Conti
136	1573	Primula	rusbyi		Tissue collection Elena Conti
137	1576	Primula	capitata		Tissue collection Elena Conti
138	1578	Primula	sieboldii		Tissue collection Elena Conti
139	1581	Primula	frondosa		Tissue collection Elena Conti
140	1582	Primula	specuicola		Tissue collection Elena Conti
141	1586	Primula	polyneura		Tissue collection Elena Conti
142	1588	Primula	vialii		Tissue collection Elena Conti
143	1589	Primula	farinosa		Tissue collection Elena Conti
144	1590	Primula	bullata	var. forrestii	Tissue collection Elena Conti
145	1591	Primula	poissonii		Tissue collection Elena Conti
148	1596	Primula	kisoana		Tissue collection Elena Conti
149	1617	Primula	firmipes		Tissue collection Elena Conti
150	1618	Primula	wilsonii		Tissue collection Elena Conti
151	1636	Primula	grandis		Tissue collection Elena Conti
152	1649	Primula	juliae		Tissue collection Elena Conti

153	1658	Primula	vulgaris		Tissue collection Elena Conti
154	1659	Primula	sinolisteri		Tissue collection Elena Conti
155	1663	Primula	chionantha		Tissue collection Elena Conti
156	1664	Primula	sonchifolia		Tissue collection Elena Conti
157	1665	Primula	amethystina	var. brevifolia	Tissue collection Elena Conti
158	1667	Primula	deflexa		Tissue collection Elena Conti
159	1670	Primula	pulchella		Tissue collection Elena Conti
160	1702	Primula	lutea		Tissue collection Elena Conti
161	1673 (I)	Primula	scotica		Tissue collection Elena Conti
162	1780	Primula	marginata		Tissue collection Elena Conti
163	171	Primula	mollis		Tissue collection Elena Conti
164II	181	Primula	septemloba		Tissue collection Elena Conti
165	187	Primula	crassifolia		Tissue collection Elena Conti
166	238	Primula	cuneifolia		Tissue collection Elena Conti
167	240	Primula	suffrutescens		Tissue collection Elena Conti
168	244	Primula	davidii		Tissue collection Elena Conti
169	252	Primula	erythrocarpa		Tissue collection Elena Conti
170	258	Primula	dryadifolia		Tissue collection Elena Conti
171	264	Primula	fedtschenkoi		Tissue collection Elena Conti
172	278	Primula	concholoba		Tissue collection Elena Conti
173	310	Primula	japonica		Tissue collection Elena Conti
174II	314	Primula	prenantha		Tissue collection Elena Conti
175II	331	Primula	jaffreyana		Tissue collection Elena Conti
176	341	Primula	tosaensis		Tissue collection Elena Conti
178II	377	Primula	wollastonii		Tissue collection Elena Conti
179	393	Primula	verticillata		Tissue collection Elena Conti
180	398	Primula	edelbergii		Tissue collection Elena Conti
181	510	Dionysia	bornmuelleri		Tissue collection Elena Conti
182	512	Dionysia	lacei		Tissue collection Elena Conti
183	551	Primula	rosea		Tissue collection Elena Conti
184	587	Primula	bhutanica		Tissue collection Elena Conti
185	588	Primula	gracilipes		Tissue collection Elena Conti
186	593	Primula	griffithii		Tissue collection Elena Conti
187	596	Primula	nana		Tissue collection Elena Conti
188	601	Primula	pulchra		Tissue collection Elena Conti
189	603	Primula	sessilis		Tissue collection Elena Conti
190	608	Primula	irregularis		Tissue collection Elena Conti
191	BASBG-00091730	Primula	intricata		Herbarium Basel
192	BASBG-00092075	Primula	meyeri		Herbarium Basel
193	BASBG-00181754	Ranunculus	aquatilis		Herbarium Basel
194	BASBG-00183351	Ranunculus	brachylobus		Herbarium Basel
195	BASBG-00183367	Ranunculus	brutius		Herbarium Basel
196	BASBG-00183626	Ranunculus	dissectus		Herbarium Basel
197	BASBG-00183646	Ranunculus	fibrillosus		Herbarium Basel
198	BASBG-00184366	Ranunculus	millefolius	ssp. millefolius	Herbarium Basel
199	BASBG-00184800	Ranunculus	orthorhynchus		Herbarium Basel
200	BASBG-00184801	Ranunculus	oxyspermus		Herbarium Basel
201	BASBG-00185329	Ranunculus	pedatifidus	ssp. affinis	Herbarium Basel
202	BASBG-00185430	Ranunculus	serieus		Herbarium Basel
203	BASBG-00185450	Ranunculus	sulphureus		Herbarium Basel
204	BASBG-00183283	Ranunculus	arvensis		Herbarium Basel
205	BASBG-00184073	Ranunculus	insignis		Herbarium Basel
206	BASBG-00184733	Ranunculus	occidentalis		Herbarium Basel
207	BASGB-00185341	Ranunculus	scleratus		Herbarium Basel
208	BASBG-00185505	Ranunculus	trilobus		Herbarium Basel
209	BASBG-00183339	Ranunculus	asiaticus		Herbarium Basel
210	BASBG-00183775	Ranunculus	flammula		Herbarium Basel
211	BASBG-00090931	Dionysia	tapetodes		Herbarium Basel
212	JdV515	Primula	halleri		Field collection
213	BASBG-00092095	Primula	nutans		Herbarium Basel
214	BASBG-00092064	Primula	laurentiana		Herbarium Basel
DRW	DRW	Primula	pauciflora		DNA extract Ellena Conti

TABLE S2: GenBank accession numbers from the genes used for the bait design.

Accession number	Database
AT2G18790	KEGG
AT1G09570	KEGG
AT4G08920	KEGG
AT1G04400	KEGG
AT2G32950	KEGG
AT5G23730	KEGG
AT5G52250	KEGG
AT2G46340	KEGG
AT4G11110	KEGG
AT3G17609	KEGG
AT5G11260	KEGG
AT2G25930	KEGG
AT1G22770	KEGG
AT1G09530	KEGG
AT1G68050	KEGG
AT5G60100	KEGG
AT5G62430	KEGG
AT2G23070	KEGG
AT2G23080	KEGG
AT3G50000	KEGG
AT5G67380	KEGG
AT2G44680	KEGG
AT3G60250	KEGG
AT4G17640	KEGG
AT5G47080	KEGG
AT5G15840	KEGG
AT1G56650	KEGG
AT5G13930	KEGG
AT1G65480	KEGG
AT4G20370	KEGG
AT5G57360	KEGG
AT5G61380	KEGG
AT5G08330	KEGG
AT5G23280	KEGG
AT2G46830	KEGG
AT1G01060	KEGG
AT5G24470	KEGG
AT5G02810	KEGG
AT2G46790	KEGG
101262847	KEGG
544176	KEGG
101245619	KEGG
101265040	KEGG
101267430	KEGG
101268174	KEGG
101267355	KEGG
543596	KEGG
543688	KEGG
544219	KEGG
101249698	KEGG
101259391	KEGG
543547	KEGG
101249027	KEGG
101263834	KEGG
543733	KEGG
101255788	KEGG
101258346	KEGG
101256908	KEGG
101246029	KEGG
101245061	KEGG
101263032	KEGG
101266107	KEGG
778294	KEGG
778295	KEGG
101244750	KEGG
101246108	KEGG
101256338	KEGG
101245655	KEGG
101246833	KEGG
101249856	KEGG
101257119	KEGG
101262932	KEGG
101249224	KEGG
101254785	KEGG
101250283	KEGG
101262866	KEGG
101261662	KEGG
100736457	KEGG
100736520	KEGG
101259163	KEGG
101259425	KEGG
JQ966690.1	GenBank
AY338920.1	GenBank
AY338918.1	GenBank
DQ529935.1	GenBank
AY338923.1	GenBank
AH015549.2	GenBank
DQ529962.1	GenBank
AY338922.1	GenBank
DQ529944.1	GenBank
DQ529942.1	GenBank
DQ529782.1	GenBank
GU045299.1	GenBank

DQ529813.1	GenBank
DQ529778.1	GenBank
AY338904.1	GenBank
AY338909.1	GenBank
DQ529749.1	GenBank
DQ529755.1	GenBank
DQ529974.1	GenBank
AY338905.1	GenBank
DQ529968.1	GenBank
DQ529877.1	GenBank
DQ529914.1	GenBank
DQ529820.1	GenBank
DQ529826.1	GenBank
DQ529816.1	GenBank
DQ529763.1	GenBank
DQ529895.1	GenBank
DQ529793.1	GenBank
DQ529960.1	GenBank
AY338921.1	GenBank
DQ529855.1	GenBank
DQ529745.1	GenBank
DQ529885.1	GenBank
DQ529851.1	GenBank
DQ529954.1	GenBank
DQ529950.1	GenBank
DQ529780.1	GenBank
DQ529770.1	GenBank
DQ529871.1	GenBank
DQ529849.1	GenBank
DQ529940.1	GenBank
DQ529889.1	GenBank
DQ529846.1	GenBank
DQ529937.1	GenBank
DQ529759.1	GenBank
DQ529774.1	GenBank
DQ529887.1	GenBank
DQ529933.1	GenBank
DQ529809.1	GenBank
DQ529844.1	GenBank
DQ529931.1	GenBank
DQ529875.1	GenBank
DQ529930.1	GenBank
DQ529926.1	GenBank
DQ529924.1	GenBank
DQ529836.1	GenBank
DQ529814.1	GenBank
DQ529822.1	GenBank
DQ529791.1	GenBank
DQ529879.1	GenBank
DQ529776.1	GenBank
DQ529772.1	GenBank
DQ529761.1	GenBank
DQ529832.1	GenBank
DQ529842.1	GenBank
DQ529805.1	GenBank
DQ529801.1	GenBank
DQ529920.1	GenBank
DQ529803.1	GenBank
DQ529907.1	GenBank
DQ529840.1	GenBank
DQ529899.1	GenBank
DQ529905.1	GenBank
DQ529824.1	GenBank
DQ529916.1	GenBank
DQ529838.1	GenBank
DQ529818.1	GenBank
DQ529811.1	GenBank
AY338913.1	GenBank
AY338908.1	GenBank
AY338911.1	GenBank
JN628016.1	GenBank
JN628017.1	GenBank
JN628018.1	GenBank
JQ966695.1	GenBank
DQ852367.1	GenBank
DQ852382.1	GenBank
DQ852405.1	GenBank
DQ852411.1	GenBank
DQ852368.1	GenBank
DQ852388.1	GenBank
DQ852400.1	GenBank
DQ852402.1	GenBank
DQ852371.1	GenBank
DQ852429.1	GenBank
DQ852375.1	GenBank
DQ852364.1	GenBank
DQ852503.1	GenBank
DQ852378.1	GenBank
DQ852385.1	GenBank
DQ852490.1	GenBank
DQ852455.1	GenBank
DQ852500.1	GenBank
DQ852476.1	GenBank
DQ852505.1	GenBank
DQ852452.1	GenBank
DQ852392.1	GenBank

DQ852464.1	GenBank
DQ852389.1	GenBank
DQ852372.1	GenBank
DQ852510.1	GenBank
DQ852374.1	GenBank
DQ852484.1	GenBank
DQ852512.1	GenBank
DQ852514.1	GenBank
DQ852395.1	GenBank
DQ852369.1	GenBank
DQ852460.1	GenBank
DQ852517.1	GenBank
DQ852401.1	GenBank
DQ852480.1	GenBank
DQ852518.1	GenBank
DQ852520.1	GenBank
DQ852444.1	GenBank
DQ852465.1	GenBank
DQ852482.1	GenBank
DQ852496.1	GenBank
DQ852427.1	GenBank
DQ852522.1	GenBank
DQ852406.1	GenBank
DQ852492.1	GenBank
DQ852403.1	GenBank
DQ852525.1	GenBank
DQ852523.1	GenBank
DQ852529.1	GenBank
DQ852434.1	GenBank
DQ852471.1	GenBank
DQ852459.1	GenBank
DQ852489.1	GenBank
DQ852466.1	GenBank
DQ852461.1	GenBank
DQ852530.1	GenBank
DQ852531.1	GenBank
DQ852487.1	GenBank
DQ852443.1	GenBank
DQ852408.1	GenBank
DQ852468.1	GenBank
DQ852532.1	GenBank
DQ852498.1	GenBank
DQ852470.1	GenBank
DQ852473.1	GenBank
DQ852414.1	GenBank
DQ852533.1	GenBank
DQ852535.1	GenBank
DQ852457.1	GenBank
AY338871.1	GenBank
HM562700.1	GenBank
AY338874.1	GenBank
AH015550.2	GenBank
AY338873.1	GenBank
HM562704.1	GenBank
HM562696.1	GenBank
AY382155.1	GenBank
AY338855.1	GenBank
AY338860.1	GenBank
AY338854.1	GenBank
HM562693.1	GenBank
HM562699.1	GenBank
HM562686.1	GenBank
AY338872.1	GenBank
HM562701.1	GenBank
HM562679.1	GenBank
HM562694.1	GenBank
HM562677.1	GenBank
HM562676.1	GenBank
HM562683.1	GenBank
HM562685.1	GenBank
HM562688.1	GenBank
HM562692.1	GenBank
HM562689.1	GenBank
HM562678.1	GenBank
HM562691.1	GenBank
HM562698.1	GenBank
HM562681.1	GenBank
AY338864.1	GenBank
AY338859.1	GenBank
AY338862.1	GenBank
DQ852548.1	GenBank
DQ852541.1	GenBank
DQ852552.1	GenBank
DQ852553.1	GenBank
DQ852564.1	GenBank
DQ852555.1	GenBank
DQ852542.1	GenBank
DQ852551.1	GenBank
DQ852545.1	GenBank
DQ852561.1	GenBank
DQ852571.1	GenBank
DQ852550.1	GenBank
DQ852543.1	GenBank

TABLE S3: Accession matrix for Primula resulting from oneTwoTree. The left column shows the species name and the taxonomy ID according to the NCBI taxonomy database. The top row contains the cluster description assigned by oneTwoTree and the remaining cells contain the GenBank accession number if applicable.

Specie \ Loci	1-Primula capitata isolate P.capiH367 tRNA-Leu (trnL) gene and trnL(UAA)-trnF(GAA) intergenic spacer partial sequence chloroplast	14-ITS	2-Primula cachemiriana maturase K (matK) gene complete cds chloroplast	3-Primula farinosa isolate PRIM70 ribosomal protein L16 (rpl16) gene intron chloroplast	4-Dionysia freitagii isolate 195 ribosomal protein S16 (rps16) gene intron chloroplast	5-Primula capitata ribulose-15-bisphosphate carboxylase/oxygenase large subunit (rbcL) gene partial cds chloroplast gene for chloroplast product	6-Primula reptans trnL-trnF intergenic spacer partial sequence chloroplast	7-Primula frondosa isolate PRIM15 trnT-trnL intergenic spacer partial sequence chloroplast	8-Primula deorum isolate 2 trnD-trnT intergenic spacer complete sequence chloroplast	9-Primula tardiflora voucher GXJ204 psbA-trnH intergenic spacer region partial sequence chloroplast	10-Primula rusbyi trnS-trnG intergenic spacer partial sequence chloroplast	11-Primula vulgaris photosystem II protein D1 (psbA) gene partial cds psbA-trnH intergenic spacer complete sequence and tRNA-His (trnH) gene partial sequence chloroplast
110760-Primula edelbergii	AY647673.1	-	AY647528.1	AF402452.1	AY647603.1	AF213797.1	AY647743.1	AY647880.1	-	-	AY647813.1	-
175034-Dionysia tapetodes	AF402338.1	-	DQ378300.1	DQ378436.1	-	AF394992.1	DQ378705.1	-	-	-	-	-
175106-Primula yunnanensis	FJ794200.1	KM198359.	DQ378301.1	AF402457.1	FJ786569.1	JF943728.1	DQ378706.1	-	-	-	-	JN046600.1
175082-Primula membranifolia	AF402340.1	JF978007.1	DQ378304.1	AF402458.1	-	JF943663.1	DQ378709.1	-	-	-	-	JN046536.1
175060-Primula elliptica	AF402341.1	-	DQ378306.1	AF402459.1	-	-	DQ378711.1	-	-	-	-	-
175051-Primula clarkei	AF402342.1	-	DQ378307.1	AF402460.1	-	-	DQ378712.1	-	-	-	-	-
175078-Primula luteola	AF402343.1	-	DQ378309.1	AF402461.1	-	-	DQ378714.1	-	-	-	-	-
175043-Primula auriculata	AF402344.1	HM629105	DQ378310.1	AF402462.1	-	-	DQ378715.1	-	-	-	-	-
175085-Primula muscarioides	AF402345.1	-	DQ378311.1	DQ378441.1	-	AF394970.1	DQ378716.1	-	-	-	-	-
175044-Primula bellidifolia	FJ794221.1	JF977948.1	DQ378312.1	AF402464.1	FJ786590.1	JF943602.1	-	-	-	-	-	JN046476.1
175065-Primula flaccida	DQ378536.1	-	DQ378318.1	AF402465.1	-	-	DQ378723.1	-	-	-	-	-
175103-Primula vialii	AF402348.1	-	DQ378313.1	AF402466.1	-	-	DQ378718.1	-	-	-	-	-
175092-Primula reidii	AF402349.1	-	DQ378320.1	AF402467.1	-	-	DQ378725.1	-	-	-	-	-
175062-Primula erratica	AF402353.1	-	DQ378322.1	AF402471.1	-	-	DQ378727.1	-	-	-	-	-
175055-Primula denticulata	AF402354.1	JF977979.1	JF955695.1	AF402472.1	-	JF943633.1	-	-	-	-	-	JN046505.1
175083-Primula minutissima	AF402355.1	-	-	AF402473.1	-	-	-	-	-	-	-	-
159006-Primula frondosa	EF218536.1	EF218200.1	-	EF218264.1	EF218353.1	-	-	EF218082.1	EF218450.1	-	-	-
159009-Primula laurentiana	DQ379746.1	DQ993877.	DQ378348.1	EF218285.1	DQ379919.1	AF394967.1	-	DQ379802.1	DQ994089.1	-	-	-
175107-Primula yuparensis	AF402362.1	-	-	AF402480.1	-	-	-	-	-	-	-	-
175090-Primula pulchella	DQ378552.1	JF978034.1	DQ378339.1	AF402492.1	-	JF943692.1	DQ378744.1	-	-	-	-	JN046568.1
175091-Primula pumilio	KT259840.1	-	DQ378327.1	AF402493.1	KT259654.1	-	DQ378732.1	-	-	-	-	KT259777.1
175069-Primula gemmifera	KT259818.1	AY545759.	DQ378332.1	DQ378458.1	KT259630.1	AF394999.1	-	-	-	-	-	KT259754.1
175093-Primula reptans	AF402376.1	-	DQ378336.1	AF402496.1	-	-	DQ378741.1	-	-	-	-	-
175071-Primula glomerata	AF402377.1	-	DQ378324.1	DQ378451.1	-	-	DQ378729.1	-	-	-	-	-
166116-Primula florindae	AF402379.1	AF396691.1	-	AF402499.1	-	-	-	-	-	-	-	-
175105-Primula waltonii	AF402380.1	-	DQ378359.1	AF402500.1	-	-	DQ378764.1	-	-	-	-	-
175064-Primula firmipes	AF402382.1	-	DQ378360.1	AF402502.1	-	-	DQ378765.1	-	-	-	-	-
175059-Primula elatior	AF402384.1	JX231015.1	DQ378361.1	JX231055.1	-	KF602222.1	DQ378766.1	-	-	-	HM628983.1	-
175081-Primula megaseifolia	AF402387.1	HM629145	DQ378363.1	AF402507.1	-	AF394997.1	DQ378768.1	-	-	-	HM629010.1	-
175101-Primula taliensis	AF402390.1	-	-	AF402510.1	-	-	-	-	-	-	-	-
175045-Primula boothii	AF402391.1	-	-	DQ378475.1	-	-	-	-	-	-	-	-
175086-Primula petiolaris	AF402392.1	AJ491431.1	-	AF402512.1	-	-	-	-	-	-	-	-
175097-Primula sonchifolia	AF402393.1	JF978059.1	DQ378373.1	AF402513.1	-	JF943715.1	DQ378778.1	-	-	JN046585.1	-	-
175047-Primula calderiana	AF402394.1	JF977961.1	DQ378374.1	AF402514.1	-	JF943615.1	DQ378779.1	-	-	JN046489.1	-	-
175052-Primula cockburniana	AF402395.1	KP638581.	DQ378380.1	DQ378483.1	-	HM018321.1	DQ378785.1	-	-	HM018468.1	-	-
175050-Primula chungensis	AF402396.1	KY400255.	DQ378381.1	DQ378484.1	-	AF394984.1	DQ378786.1	-	-	KP638699.1	-	-
65565-Primula wilsonii	AF402398.1	KP638602.	KP638642.1	AF402518.1	-	KP638682.1	-	-	-	-	-	-
175088-Primula prenantha	KY400254.1	KY400266.	DQ378383.1	AF402519.1	-	KP638672.1	DQ378788.1	-	-	KP638713.1	-	-
175089-Primula prolifera	AF402401.1	-	DQ378384.1	DQ378485.1	-	-	DQ378789.1	-	-	-	-	-
159005-Primula eximia	AF402402.1	MG218061	AY647525.1	AF402522.1	AY647600.1	MG221975.1	AY647740.1	AY647877.1	-	-	AY647810.1	-
159017-Primula tschuktschorum	AF402403.1	AM920495.	DQ378395.1	AF402523.1	-	-	DQ378800.1	-	-	-	-	-
175061-Primula elongata	AF402404.1	-	-	AF402524.1	-	-	-	-	-	-	-	-
175040-Primula advena	AF402405.1	-	DQ378396.1	AF402525.1	-	-	DQ378801.1	-	-	-	-	-
175063-Primula fedtschenkoi	AF402406.1	-	DQ378399.1	AF402526.1	-	-	DQ378804.1	-	-	-	-	-
175094-Primula rotundifolia	AF402407.1	-	DQ378402.1	DQ378500.1	-	-	DQ378807.1	-	-	-	-	-
159004-Primula clusiana	AF402408.1	AJ427770.1	AY647490.1	AY528534.1	AY647565.1	-	AY647705.1	AY647842.1	JQ755539.1	-	AY647775.1	-
175074-Primula integrifolia	AF402409.1	AJ427780.1	AY647500.1	AJ427896.1	AY647575.1	-	AY647715.1	AY647852.1	-	-	AY647785.1	-
175080-Primula marginata	AF402410.1	JQ755666.1	AY647492.1	AF402530.1	AY647567.1	-	AY647707.1	AY647844.1	JQ755552.1	-	AY647777.1	-
175056-Primula deorum	AF402411.1	AJ427773.1	AY647497.1	AY528539.1	AY647572.1	AF394989.1	AY647712.1	AY647849.1	JQ755526.1	-	AY647782.1	-
110762-Primula palinuri	AF402412.1	AJ427790.1	AY647489.1	AF402532.1	AY647564.1	AF213801.1	AY647704.1	AY647841.1	JQ755544.1	-	AY647774.1	-
159007-Primula glutinosa	AF402413.1	AJ427775.1	AY647495.1	AY528538.1	AY647570.1	-	AY647710.1	AY647847.1	JQ755538.1	-	AY647780.1	-
49648-Primula cuneifolia	AF402414.1	AB011623.	-	AF402534.1	-	AF394962.1	D85737.1	AB003567.1	JQ755528.1	-	-	-
49650-Primula nipponica	AF402415.1	AB011626.	AY647507.1	AY528546.1	AY647582.1	-	AY647722.1	AY647859.1	-	-	AY647793.1	-
159002-Primula angustifolia	AF402416.1	EU886997.	AY647514.1	AF402536.1	AY647589.1	-	AY647729.1	AY647866.1	-	-	AY647799.1	-
152140-Primula parryi	AF402417.1	AJ306364.1	AY647511.1	AY528548.1	AY647586.1	-	AY647727.1	AY647863.1	JQ755524.1	-	AY647796.1	-
175099-Primula suffrutescens	AF402418.1	EU887000.	AY647509.1	AY528547.1	AY647584.1	-	AY647725.1	AY647862.1	-	-	AY647794.1	-
175035-Primula pauciflora	AF402419.1	MG219510	KX677415.1	AF402539.1	-	KX678844.1	-	-	-	-	-	-
175067-Primula forbesii	AF402420.1	-	AY647520.1	AF402540.1	AY647595.1	-	AY647735.1	AY647872.1	-	-	AY647805.1	-
170924-Primula obconica	JX258207.1	JX258292.1	DQ378403.1	AF402542.1	JX258175.1	JF943676.1	DQ378808.1	-	-	JN046549.1	-	-
175084-Primula mollis	AF402427.1	KM198428	DQ378418.1	DQ378510.1	-	-	DQ378823.1	-	-	-	-	-
175057-Primula dryadifolia	AF402431.1	-	DQ378406.1	DQ378503.1	AY647596.1	AF394994.1	DQ378811.1	AY647873.1	-	-	AY647806.1	-
125047-Pentaphylax euryoides	AJ430881.1	-	AJ429291.1	-	AJ431003.1	AF320785.1	-	-	-	-	-	-
87536-Primula conjugens	AJ237009.1	-	-	-	-	-	-	-	-	-	-	-
175104-Primula vulgaris	AJ237010.1	JQ927168.	DQ378362.1	JX231044.1	JQ927075.1	HQ619773.1	FJ490810.1	-	-	-	HM629035.1	FJ493301.1
170927-Primula veris	AJ430883.1	JX231022.1	AJ429293.1	JX231064.1	AJ431005.1	AF394981.1	JQ927130.1	AY647882.1	-	-	AY647815.1	-
3772-Roridula gorgonias	AJ430884.1	KR819523.	KR819680.1	-	AJ431006.1	KR819580.1	KR819730.1	-	-	-	-	-
3625-Actinidia chinensis	AJ549030.1	AB253776.	KR819665.1	-	-	KR819565.1	KC408175.1	-	-	-	-	-
59976-Primula meadia	AM990515.1	AJ491436.1	AY647482.1	AY528527.1	AY647557.1	U96658.1	-	AY647834.1	-	GU066768.1	AY647767.1	-
229528-Dionysia curviflora	AY680826.1	AY680739.	-	-	AY680782.1	-	-	-	-	-	-	-
175076-Primula juliae	AY274938.1	HM629108	DQ378364.1	AF402508.1	-	-	-	-	-	-	HM629009.1	-
159013-Primula scandinavica	AY274941.1	DQ994022	DQ378351.1	EF218279.1	DQ379906.1	-	-	DQ379805.1	DQ994090.1	-	-	-
184184-Primula kitaibeliana	AY274942.1	AJ427782.1	-	-	-	-	-	-	-	-	-	-
175111-Androsace vitaliana	AY274965.1	AJ491443.1	KF907841.1	KF907957.1	-	AF395006.1	-	-	-	-	-	-
272084-Primula hendersonii	AY647609.1	MG218361	AY647464.1	AY528507.1	AY647537.1	KX678942.1	AY647677.1	AY647817.1	-	-	AY647747.1	-
272085-Primula jeffreyi	AY647618.1	MG217408	AY647473.1	AY528518.1	AY647548.1	MG221176.1	AY647688.1	AY647827.1	-	-	AY647758.1	-
272078-Primula tetrandra	AY647620.1	-	AY647475.1	AY528521.1	AY647550.1	-	AY647690.1	AY647829.1	-	-	AY647760.1	-
272087-Primula fragrans	AY647622.1	EU887001.	AY647477.1	AY528522.1	AY647552.1	-	AY647692.1	-	-	-	AY647762.1	-
272079-Primula fassettii	AY647626.1	-	AY647481.1	AY528526.1	AY647556.1	MK525717.1	AY647696.1	AY647833.1	-	HM778145.1	AY647766.1	-
933358-Primula frenchii	AY647628.1	-	AY647483.1	AY528528.1	AY647558.1	-	AY647698.1	AY647835.1	-	HM778149.1	AY647768.1	-
272098-Primula standleyana	AY647631.1	-	AY647486.1	AY528531.1	AY647561.1	-	AY647701.1	AY647838.1	-	-	AY647771.1	-
272099-Primula utahensis	AY647632.1	-	AY647487.1	AY528532.1	AY647562.1	-	AY647702.1	AY647839.1	-	-	AY647772.1	-
272086-Primula poetica	AY647633.1	-	AY647488.1	AY528533.1	AY647563.1	-	AY647703.1	AY647840.1	-	-	AY647773.1	-
159010-Primula minima	AY647638.1	AJ427787.1	AY647493.1	AJ427899.1	AY647568.1	-	AY647708.1	AY647845.1	JQ755540.1	-	AY647778.1	-
184183-Primula hirsuta	AY647644.1	AJ427777.1	AY647499.1	AJ427895.1	AY647574.1	-	AY647714.1	AY647851.1	JQ755543.1	-	AY647784.1	-
272091-Primula rusbyi	AY647658.1	EU886998.	AY647513.1	AY528549.1	AY647588.1	-	AY647728.1	AY647865.1	-	-	AY647798.1	-
272089-Primula capillaris	AY647664.1	EU886996.	AY647519.1	AY528554.1	AY647594.1	-	AY647734.1	AY647871.1	-	-	AY647804.1	-
272088-Primula amethystina	AY647668.1	KM198439	AY647523.1	AY528556.1	AY647598.1	JF943592.1	AY647738.1	AY647875.1	-	JN046467.1	AY647808.1	-
272090-Primula faberi	FJ794202.1	KM198433	AY647524.1	AY528557.1	AY647599.1	JF943643.1	-	AY647876.1	-	JN046517.1	AY647809.1	-
184987-Dionysia involucrata	AY680793.1	AY680705.	-	-	AY680750.1	AF394991.1	-	-	-	-	-	-
184989-Dionysia microphylla	AY680794.1	AY680706.	-	-	AY680751.1	AF394993.1	-	-	-	-	-	-
175066-Primula floribunda	AY680795.1	AY680707.	DQ378296.1	AF402454.1	AY680752.1	AF394996.1	-	-	-	-	-	-
303259-Dionysia balsamea	AY680796.1	AY680709.	-	-	-	-	-	-	-	-	-	-
303260-Primula davisii	AY680797.1	AY680710.	-	-	-	-	-	-	-	-	-	-
184988-Dionysia janthina	AY680798.1	AY680711.	-	-	AY680754.1	AF395007.1	-	-	-	-	-	-
303261-Dionysia esfandiarii	AY680799.1	AY680712.	-	-	AY680755.1	AY753634.1	-	-	-	-	-	-
303262-Dionysia diapensiifolia	AY680800.1	AY680713.	-	-	AY680756.1	AY753635.1	-	-	-	-	-	-
303263-Dionysia michauxii	AY680801.1	AY680714.	-	-	AY680757.1	-	-	-	-	-	-	-
303264-Dionysia sarvestanica	AY680802.1	AY680715.	-	-	AY680758.1	-	-	-	-	-	-	-
303265-Dionysia mozaffarianii	AY680803.1	AY680716.	-	-	AY680759.1	-	-	-	-	-	-	-
303266-Dionysia leucotricha	AY680804.1	AY680717.	-	-	AY680760.1	AY753636.1	-	-	-	-	-	-
303267-Dionysia lurorum	AY680805.1	AY680718.	KF907869.1	KF907963.1	AY680761.1	AY753637.1	-	-	-	-	-	-
303268-Dionysia odora	AY680806.1	AY680719.	-	-	AY680762.1	-	-	-	-	-	-	-
303270-Dionysia denticulata	AY680808.1	AY680721.	-	-	AY680764.1	-	-	-	-	-	-	-
303271-Dionysia viscidula	AY680809.1	AY680722.	-	-	AY680765.1	-	-	-	-	-	-	-
175033-Dionysia aretioides	AY680810.1	AY680723.	DQ378298.1	AF402455.1	AY647604.1	-	DQ378703.1	AY647881.1	-	-	AY647814.1	-
303258-Dionysia paradoxa	AY680811.1	AY680708.	-	-	AY680753.1	AY753633.1	-	-	-	-	-	-
303272-Dionysia hissarica	AY680812.1	AY680725.	DQ378299.1	DQ378435.1	AY680768.1	-	-	-	-	-	-	-
303273-Dionysia khuzistanica	AY680813.1	AY680727.	-	-	AY680770.1	-	-	-	-	-	-	-
303274-Dionysia bryoides	KF907997.1	AY680728.	KF907868.1	KF907959.1	AY680771.1	-	-	-	-	-	-	-
303275-Dionysia freitagii	AY680815.1	AY680729.	-	-	AY680772.1	-	-	-	-	-	-	-
175102-Primula verticillata	AY680818.1	HM629103	DQ378294.1	AF402453.1	AY680775.1	AF394968.1	-	-	-	-	HM629016.1	-
303279-Dionysia mira	AY680819.1	AY680733.	-	-	AY680776.1	AY753638.1	-	-	-	-	-	-
303280-Dionysia teucrioides	AY680820.1	AY680734.	-	-	AY680777.1	-	-	-	-	-	-	-
303294-Dionysia saponacea	AY680821.1	-	-	-	AY680778.1	-	-	-	-	-	-	-
303281-Dionysia iranshahrii	AY680822.1	AY680735.	-	-	-	-	-	-	-	-	-	-
303284-Dionysia archibaldii	AY680824.1	AY680737.	-	-	AY680780.1	-	-	-	-	-	-	-
303285-Dionysia caespitosa	AY680825.1	AY680738.	-	-	AY680781.1	-	-	-	-	-	-	-
303287-Dionysia iranica	AY680828.1	AY680741.	-	-	AY680784.1	-	-	-	-	-	-	-
303288-Dionysia khatamii	AY680829.1	AY680742.	-	-	AY680785.1	-	-	-	-	-	-	-
303289-Dionysia lamingtonii	AY680830.1	AY680743.	-	-	AY680786.1	-	-	-	-	-	-	-
303290-Dionysia oreodoxa	AY680831.1	AY680744.	-	-	AY680787.1	-	-	-	-	-	-	-
303291-Dionysia rhaptodes	AY680832.1	AY680745.	-	-	AY680788.1	-	-	-	-	-	-	-
303292-Dionysia termeana	AY680834.1	AY680747.	-	-	AY680790.1	-	-	-	-	-	-	-
303293-Dionysia lindbergii	AY680835.1	AY680748.	KF907882.1	KF907962.1	AY680791.1	-	-	-	-	-	-	-
184997-Primula maguirei	AY786535.1	EU886994.	AY647516.1	AY528551.1	AY647591.1	AF394995.1	AY786534.1	AY647868.1	-	-	AY647801.1	-
199711-Primula simensis	DQ378521.1	AJ491432.1	DQ378295.1	DQ378432.1	-	-	DQ378700.1	-	-	-	-	-
110761-Primula gaubaeana	DQ378522.1	KU697387	DQ378297.1	DQ378433.1	-	AF213798.1	DQ378702.1	-	-	-	-	-
370661-Primula florida	DQ378526.1	-	DQ378302.1	DQ378437.1	-	-	DQ378707.1	-	-	-	-	-
370645-Primula aliciae	DQ378527.1	-	DQ378303.1	DQ378438.1	-	-	DQ378708.1	-	-	-	-	-
370681-Primula souliei	DQ378528.1	HM629060	DQ378305.1	DQ378439.1	-	-	DQ378710.1	-	-	-	-	-
370688-Primula warshenewskiana	DQ378529.1	AM920477	DQ378308.1	DQ378440.1	-	-	DQ378713.1	-	-	-	-	-
370689-Primula watsonii	FJ794215.1	MF785632	DQ378314.1	DQ378443.1	FJ786584.1	MF786670.1	DQ378719.1	-	-	-	-	MF785938.1
370657-Primula deflexa	FJ794226.1	KM198376	DQ378315.1	DQ378444.1	FJ786595.1	JF943627.1	-	-	-	-	-	JN046501.1
370675-Primula pinnatifida	FJ794201.1	KM198360	FJ828603.1	DQ378445.1	KT259607.1	-	-	-	-	-	-	KT259731.1
370655-Primula cernua	DQ378535.1	-	DQ378317.1	DQ378446.1	-	-	DQ378722.1	-	-	-	-	-
370678-Primula siamensis	DQ378537.1	HM629062	DQ378319.1	DQ378448.1	-	-	DQ378724.1	-	-	-	-	-
370690-Primula wigramiana	DQ378538.1	-	DQ378321.1	DQ378449.1	-	-	DQ378726.1	-	-	-	-	-
370652-Primula cachemiriana	DQ378541.1	-	DQ378325.1	DQ378452.1	-	-	DQ378730.1	-	-	-	-	-
175048-Primula capitata	FJ794246.1	KM198429	DQ378326.1	DQ378453.1	FJ786614.1	AF394971.1	-	-	-	-	-	-
184993-Primula involucrata	DQ379777.1	DQ993772	DQ378328.1	EF218337.1	KT259635.1	AF394974.1	-	EF218157.1	EF218519.1	-	-	KT259759.1

370660-Primula fasciculata	DQ379776.1	DQ993773	DQ378329.1	EF218335.1	KT259613.1	JF943646.1	-	DQ379839.1	DQ994137.1	-	-	KT259737.1
370687-Primula valentinae	DQ378545.1	AM920475.	DQ378330.1	DQ378456.1	-	-	DQ378735.1	-	-	-	-	-
370662-Primula glabra	DQ378546.1	-	DQ378331.1	DQ378457.1	-	-	DQ378736.1	-	-	-	-	-
370682-Primula stirtoniana	DQ378548.1	-	DQ378334.1	DQ378459.1	-	-	DQ378739.1	-	-	-	-	-
370676-Primula primulina	FJ794245.1	-	DQ378335.1	DQ378460.1	FJ786613.1	-	DQ378740.1	-	-	-	-	-
370669-Primula muscoides	DQ378550.1	-	DQ378337.1	DQ378461.1	-	-	DQ378742.1	-	-	-	-	-
370685-Primula tenuiloba	DQ378551.1	-	DQ378338.1	DQ378462.1	-	-	DQ378743.1	-	-	-	-	-
370650-Primula baldshuanica	DQ378553.1	-	DQ378342.1	DQ378464.1	-	-	DQ378747.1	-	-	-	-	-
370677-Primula serrata	DQ378554.1	AM920469	DQ378343.1	DQ378465.1	-	-	DQ378748.1	-	-	-	-	-
370674-Primula pinnata	EF218532.1	EF218174.	DQ378344.1	DQ378466.1	EF218350.1	-	-	EF218079.1	EF218441.1	-	-	-
175049-Primula capitellata	EF218531.1	EF218166.	DQ378353.1	EF218260.1	EF218349.1	-	-	EF218078.1	EF218440.1	-	-	-
166119-Primula reticulata	KT259795.1	AF396694.	DQ378358.1	DQ378470.1	KT259608.1	-	DQ378763.1	-	-	-	-	KT259732.1
170920-Primula cicutariifolia	FJ794195.1	HQ199848	DQ378365.1	DQ378471.1	FJ786564.1	-	-	-	-	-	-	-
370659-Primula exscapa	DQ378561.1	-	DQ378367.1	DQ378472.1	-	-	DQ378772.1	-	-	-	-	-
370671-Primula odontocalyx	DQ378562.1	-	DQ378368.1	DQ378473.1	-	-	DQ378773.1	-	-	-	-	-
370673-Primula petelotii	DQ378563.1	-	DQ378369.1	DQ378474.1	-	-	DQ378774.1	-	-	-	-	-
370651-Primula bracteosa	DQ378565.1	-	DQ378371.1	DQ378476.1	-	-	DQ378776.1	-	-	-	-	-
370658-Primula deuteronana	DQ378566.1	-	DQ378372.1	DQ378477.1	-	-	DQ378777.1	-	-	-	-	-
370649-Primula aureata	DQ378567.1	-	DQ378375.1	DQ378478.1	-	-	DQ378780.1	-	-	-	-	-
370648-Primula aurantiaca	DQ378570.1	KP638570.	DQ378378.1	DQ378481.1	-	HM018322.1	DQ378783.1	-	-	KP638690.1	-	-
184994-Primula japonica	DQ378571.1	AM920496	DQ378379.1	DQ378482.1	LC198618.1	AF394979.1	DQ378784.1	-	-	-	-	-
166118-Primula pulverulenta	DQ378575.1	HM018170	DQ378385.1	DQ378486.1	-	HM018317.1	DQ378790.1	-	-	KP638715.1	-	-
370672-Primula orbicularis	DQ378578.1	-	DQ378388.1	DQ378489.1	-	-	DQ378793.1	-	-	-	-	-
370670-Primula nivalis	DQ378579.1	AM920493	DQ378389.1	DQ378490.1	-	-	DQ378794.1	-	-	-	-	-
370664-Primula hongshanensis	DQ378581.1	-	DQ378391.1	DQ378492.1	-	-	DQ378796.1	-	-	-	-	-
370683-Primula stuartii	DQ378582.1	-	DQ378392.1	DQ378493.1	-	-	DQ378797.1	-	-	-	-	-
370680-Primula soongii	DQ378583.1	-	DQ378393.1	DQ378494.1	-	-	DQ378798.1	-	-	-	-	-
370668-Primula minor	DQ378584.1	-	DQ378394.1	DQ378495.1	-	-	DQ378799.1	-	-	-	-	-
370653-Primula calliantha	FJ794218.1	KM198441	FJ828618.1	JQ737152.1	FJ786587.1	JF943618.1	-	-	-	JN046490.1	-	-
370667-Primula maximowiczii	DQ378586.1	AM920497	DQ378398.1	DQ378497.1	-	-	DQ378803.1	-	-	-	-	-
370654-Primula caveana	FJ794244.1	KM198397	FJ828640.1	DQ378498.1	FJ786612.1	-	DQ378805.1	-	-	-	-	-
370666-Primula littledalei	DQ378588.1	-	DQ378401.1	DQ378499.1	-	-	DQ378806.1	-	-	-	-	-
229530-Primula sinolisteri	FJ794238.1	-	DQ378404.1	DQ378501.1	FJ786606.1	-	-	-	-	-	-	-
370647-Primula asarifolia	DQ378591.1	-	DQ378405.1	DQ378502.1	-	-	DQ378810.1	-	-	-	-	-
110759-Primula cortusoides	DQ378594.1	AM920488	DQ378412.1	DQ378505.1	-	AF213800.1	DQ378817.1	-	-	-	-	-
370663-Primula heucherifolia	DQ378597.1	KM198443	DQ378415.1	DQ378508.1	-	JF943652.1	DQ378820.1	-	MF590694.1	JN046527.1	-	-
370665-Primula latisecta	FJ794207.1	KM198366	DQ378416.1	DQ378509.1	FJ786576.1	-	-	-	-	-	-	-
133892-Primula farinosa	DQ379724.1	KX166110.	DQ378345.1	EF218265.1	KT259605.1	KF602223.1	-	DQ379787.1	DQ994103.1	-	-	KT259729.1
175041-Primula alcalina	DQ379731.1	DQ993803	DQ378356.1	AF402489.1	DQ379908.1	-	-	DQ379792.1	DQ994079.1	-	-	-
175098-Primula specuicola	DQ379732.1	DQ993751	DQ378354.1	AF402487.1	DQ379909.1	-	-	DQ379793.1	DQ994078.1	-	-	-
370646-Primula anvilensis	DQ379733.1	DQ993731	DQ378355.1	EF218273.1	DQ379911.1	-	-	DQ379794.1	DQ994080.1	-	-	-
49649-Primula modesta	EF218544.1	DQ993730	DQ378357.1	EF218272.1	EF218362.1	AF394978.1	-	EF218090.1	DQ994077.1	-	-	-
159003-Primula borealis	DQ379736.1	DQ993843	AY647527.1	EF218274.1	AY647602.1	MG222091.1	-	AY647879.1	EF218455.1	-	AY647812.1	-
175079-Primula magellanica	DQ379737.1	DQ993825.	-	EF218306.1	EF218396.1	-	-	DQ379811.1	DQ994083.1	-	-	-
159008-Primula incana	DQ379740.1	DQ993868	DQ378347.1	EF218283.1	EF218372.1	MG222760.1	-	DQ379799.1	DQ994093.1	-	-	-
159016-Primula stricta	DQ379745.1	DQ993918	KC475524.1	EF218296.1	DQ379924.1	AF394975.1	-	DQ379808.1	EF218481.1	-	-	-
159011-Primula mistassinica	DQ379751.1	DQ993834	DQ378352.1	EF218314.1	KT259606.1	MG223918.1	-	DQ379822.1	DQ994119.1	-	-	KT259730.1
159012-Primula nutans	DQ379767.1	DQ993775	AY647526.1	EF218327.1	KT259642.1	MG221598.1	-	AY647878.1	DQ994132.1	-	AY647811.1	KT259767.1
175075-Primula ioessa	DQ379778.1	DQ993774.	-	AF402501.1	DQ379955.1	AF394972.1	-	DQ379841.1	DQ994139.1	-	-	-
175072-Primula halleri	DQ994143.1	DQ993963	DQ378346.1	EF218268.1	DQ994141.1	-	-	DQ379789.1	DQ994107.1	-	-	-
175077-Primula longiscapa	EF218528.1	AM920474.	-	EF218258.1	EF218347.1	-	-	EF218076.1	EF218437.1	-	-	-
175054-Primula darialica	EF218530.1	EF218165.	DQ378341.1	EF218256.1	EF218345.1	-	-	EF218074.1	EF218439.1	-	-	-
440715-Primula sachalinensis	EF218550.1	AM920472.	-	EF218278.1	EF218368.1	-	-	EF218097.1	EF218459.1	-	-	-
175058-Primula egaliksensis	EF218591.1	DQ993783	DQ378349.1	DQ378467.1	KT259604.1	KC483686.1	-	EF218138.1	DQ994121.1	-	-	KT259728.1
487793-Primula macrophylla	EU326085.1	-	-	JQ737174.1	-	-	-	-	-	-	-	-
487762-Primula schlagintweitiana	EU326086.1	-	-	-	-	-	-	-	-	-	-	-
170926-Primula sinensis	FJ794181.1	KM198430	FJ828584.2	-	FJ786550.1	JF943709.1	-	-	-	-	-	-
170921-Primula filchnerae	FJ794185.1	AF323702.	FJ828588.1	-	FJ786554.1	-	-	-	-	-	-	-
690507-Primula pseudodenticulata	FJ794187.1	KM198348	FJ828590.1	-	FJ786556.1	-	-	-	-	-	-	-
175068-Primula forrestii	FJ794188.1	MH117679	DQ378410.1	AF402549.1	FJ786557.1	MH116331.1	-	-	-	MH117237.1	-	-
690487-Primula caldaria	FJ794189.1	KM198350	FJ828592.1	-	FJ786558.1	-	-	-	-	-	-	-
690505-Primula partschiana	FJ794190.1	KM198352	FJ828593.1	-	FJ786559.1	JF943684.1	-	-	-	JN046558.1	-	-
175042-Primula algida	FJ794192.1	EU643659.	DQ378340.1	AF402468.1	FJ786561.1	-	DQ378745.1	-	-	-	-	-
55385-Cortusa matthioli	FJ794193.1	MH711270	DQ378420.1	AY528555.1	AY647597.1	Z83146.1	-	AY647874.1	-	-	AY647807.1	-
170923-Primula merrilliana	FJ794196.1	HQ199871.	FJ828589.2	-	FJ786565.1	-	-	-	-	-	KJ416073.1	-
170925-Primula rupestris	FJ794197.1	AF323697.	FJ828599.1	-	FJ786566.1	-	-	-	-	-	-	-
690483-Primula bella	FJ794198.1	KM198358	FJ828600.2	JQ737146.1	FJ786567.1	JF943598.1	-	-	-	-	-	JN046471.1
370656-Primula chionantha	FJ794199.1	KM198438	FJ828601.1	DQ378487.1	FJ786568.1	JF943625.1	-	-	-	JN046499.1	-	-
690513-Primula sertulum	FJ794203.1	KM198361	FJ828604.1	-	FJ786572.1	-	-	-	-	-	-	-
690504-Primula ovalifolia	HQ439126.1	KM198410	FJ828605.1	-	HQ439118.1	JF943683.1	-	HQ439149.1	-	JN046556.1	KJ416091.1	-
184991-Primula alpicola	FJ794205.1	GU444018	FJ828606.1	KT259540.1	KT259603.1	AF394987.1	-	-	-	-	-	KT259727.1
690489-Primula celsiiformis	FJ794232.1	KM198363	FJ828607.1	-	FJ786600.1	-	-	-	-	-	-	-
170922-Primula malacoides	FJ794210.1	KM198371	DQ378408.1	AF402541.1	FJ786579.1	AF394990.1	-	-	-	-	-	-
690509-Primula rubifolia	FJ794211.1	KM198372.	-	-	FJ786580.1	-	-	-	-	-	-	-
690508-Primula pycnoloba	FJ794212.1	KM198415	FJ828612.2	-	FJ786581.1	JF943698.1	-	-	-	JN046570.1	-	-
159014-Primula secundiflora	FJ794213.1	KP638597.	FJ828613.1	GQ885124.1	EF595540.1	HM018352.1	-	-	-	KP638717.1	-	-
690499-Primula moupinensis	FJ794214.1	KM198422	FJ828614.1	-	FJ786583.1	JF943669.1	-	-	-	JN046539.1	-	-
690493-Primula efarinosa	FJ794216.1	-	FJ828616.1	-	FJ786585.1	-	-	-	-	-	-	-
690512-Primula serratifolia	FJ794217.1	KP638598.	FJ828617.1	JQ737198.1	FJ786586.1	KC840117.1	-	-	-	KP638718.1	-	-
166117-Primula poissonii	FJ794219.1	KF934450.	FJ828619.1	GQ885123.1	FJ786588.1	AF394973.1	-	-	-	-	-	-
690486-Primula boreiocalliantha	FJ794220.1	KM198379	FJ828620.1	JQ737150.1	FJ786589.1	JF943611.1	-	-	-	JN046485.1	-	-
184996-Primula miyabeana	FJ794223.1	KP638588.	FJ828623.1	-	FJ786592.1	AF395003.1	-	-	-	-	-	-
690506-Primula polyneura	FJ794227.1	KM198435	FJ828627.1	JQ737192.1	FJ786596.1	JF943688.1	-	-	-	JN046559.1	-	-
690485-Primula blinii	FJ794229.1	KM198365	FJ828628.2	JQ737148.1	FJ786597.1	JF943606.1	-	-	-	-	-	JN046482.1
110763-Primula sikkimensis	FJ794231.1	KY624405.	FJ828642.1	KT259546.1	KT259609.1	AF213799.1	-	-	-	-	-	KT259733.1
690481-Primula aromatica	FJ794233.1	KM198388	FJ828630.2	-	FJ786628.1	JF943596.1	-	-	-	-	-	-
690494-Primula helodoxa	FJ794236.1	KP638583.	FJ828633.1	-	FJ786604.1	HM018328.1	-	-	-	KP638703.1	-	-
690514-Primula sinomollis	FJ794237.1	-	FJ828634.2	-	FJ786605.1	-	-	-	-	-	-	-
175070-Primula geraniifolia	FJ794242.1	KM198395	DQ378417.1	AF402546.1	FJ786610.1	-	DQ378822.1	-	-	-	-	-
690515-Primula smithiana	FJ794243.1	KP638600.	FJ828639.2	-	FJ786611.1	HM018318.1	-	-	-	KP638720.1	-	-
690510-Primula rugosa	FJ794248.1	KM198353	KU359372.1	-	KU359379.1	JF943700.1	-	-	-	-	-	-
690490-Primula chapaensis	FJ794249.1	KM198403	KU359371.1	-	FJ786617.1	JF943620.1	-	-	-	JN046494.1	-	-
690488-Primula calyptrata	FJ794250.1	KU359362.	FJ828646.1	-	FJ786618.1	-	-	-	-	-	-	-
690482-Primula barbicalyx	FJ794251.1	KM198405	FJ828647.2	-	FJ786619.1	-	-	-	-	-	-	-
690516-Primula wangii	FJ794252.1	KM198407	FJ828648.1	-	FJ786620.1	JF943726.1	-	-	-	JN046598.1	-	-
690484-Primula blattariformis	FJ794255.1	KM198411	FJ828654.1	-	FJ786627.1	JF943605.1	-	-	-	JN046478.1	-	-
690511-Primula saturata	FJ794256.1	KM198412	FJ828650.1	-	FJ786623.1	-	-	-	-	-	-	-
690498-Primula malvacea	FJ794257.1	KM198413	FJ828651.2	JQ737175.1	FJ786624.1	JF943660.1	-	-	-	JN046533.1	-	-
175096-Primula septemloba	FJ794263.1	MH117681	FJ828656.1	AF402545.1	FJ786629.1	JF943703.1	-	-	-	MH117240.1	-	-
272082-Primula frigida	GQ244845.1	MG217448	AY647471.1	AY528515.1	AY647545.1	MG221226.1	AY647685.1	AY647823.1	-	-	AY647755.1	-
669787-Primula pumila	GQ245346.1	-	-	JQ737194.1	-	-	-	-	-	-	-	-
1227644-Primula leucophylla	JX231096.1	JX231021.	-	JX231059.1	-	-	-	-	-	-	-	-
303286-Dionysia gaubae	KF907998.1	AY680740.	KF907871.1	KF907960.1	AY680783.1	-	-	-	-	-	-	-
303269-Dionysia haussknechtii	KF907999.1	AY680720.	KF907870.1	KF907961.1	AY680763.1	-	-	-	-	-	-	-
184182-Primula glaucescens	KF908003.1	AJ427774.	KF907864.1	AJ427893.1	-	HG417031.1	-	-	JQ755541.1	HG800561.1	-	-
175095-Primula scotica	KF908005.1	DQ993984.	KF907902.1	DQ379851.1	DQ379904.1	KF997463.1	-	DQ379791.1	DQ994110.1	-	-	-
184189-Primula villosa	KF908006.1	AJ427797.	KF907863.1	KF907974.1	-	-	-	-	JQ755531.1	-	-	-
1430407-Primula violacea	KF908007.1	-	KF907866.1	KF907975.1	-	-	KF908009.1	-	-	-	-	-
1430408-Primula walshii	KF908008.1	-	KF907877.1	KF907976.1	-	-	KF908010.1	-	-	-	-	-
175046-Primula bracteata	KM198461.1	KM198421	KM198451.1	AF402548.1	KM198456.1	-	-	-	-	-	-	-
1637976-Primula kwangtungensis	KM198463.1	KM198447	KM198452.1	-	KM198457.1	-	-	-	-	-	-	-
1637977-Primula kweichouensis	KM198464.1	KM198449	KM198454.1	-	KM198459.1	-	-	-	-	-	-	-
1703807-Primula conspersa	KT259797.1	-	KT259484.1	KT259547.1	KT259611.1	-	-	-	-	-	-	KT259734.1
1703808-Primula pamirica	KT259835.1	-	KT259522.1	KT259585.1	KT259648.1	-	-	-	-	-	-	KT259772.1
1703809-Primula tibetica	KT259845.1	-	KT259530.1	KT259598.1	KT259661.1	-	-	-	-	-	-	KT259780.1
1703810-Primula zambalensis	KT259851.1	-	KT259538.1	KT259601.1	KT259664.1	-	-	-	-	-	-	KT259788.1
1915070-Primula undulifolia	KU359387.1	KU359364.	KU359373.1	-	KU359380.1	-	-	-	-	-	-	-
1915069-Primula hunanensis	KU359390.1	KU359367.	KU359378.1	-	KU359383.1	-	-	-	-	-	-	-
931088-Primula ranunculoides	KY038342.1	HQ199862.	-	-	-	-	-	-	-	-	-	-
1648221-Primula chrysochlora	KY400253.1	KY400265.	KP638616.1	-	-	KP638656.1	-	-	-	KP638696.1	-	-
175073-Primula hidakana	LC199720.1	LC199822.	LC199521.1	AF402544.1	LC199573.1	LC198614.1	-	LC199777.1	LC199626.1	LC199677.1	-	-
184995-Primula jesoana	LC199729.1	LC199830.	LC199530.1	-	LC199580.1	AF394966.1	-	LC199780.1	LC199629.1	LC199680.1	-	-
262422-Primula kisoana	LC199734.1	LC199835.	DQ378414.1	DQ378507.1	LC199584.1	LC198615.1	AB161507.1	AB161505.1	LC199634.1	LC199685.1	-	-
1608504-Primula reinii	LC199749.1	LC199843.	LC199547.1	-	LC199599.1	LC198616.1	-	LC199798.1	LC199643.1	LC199697.1	-	-
59983-Primula sieboldii	LC199751.1	LC199850.	LC199550.1	-	LC199601.1	U96657.1	AB161491.1	AB161479.1	LC199650.1	AB381925.1	-	-
175100-Primula takedana	LC199758.1	LC199857.	LC199558.1	AF402543.1	LC199607.1	-	-	LC199807.1	LC199655.1	LC199707.1	-	-
370686-Primula tosaensis	LC199761.1	LC199862.	DQ378411.1	DQ378504.1	LC199610.1	LC198617.1	-	LC199810.1	LC199661.1	LC199709.1	-	-
1044911-Primula agleniana	-	JF977932.	JF955648.1	JQ737143.1	-	JF943586.1	-	-	-	JN046460.1	-	-
184171-Primula allionii	-	JQ755792.	-	AJ427887.1	-	-	-	-	JQ755565.1	-	-	-
184172-Primula apennina	-	AJ427754.	-	-	-	-	-	-	JQ755534.1	-	-	-
184173-Primula auricula	-	AM920498	-	-	-	-	-	-	JQ755533.1	-	-	-
166115-Primula beesiana	-	KP638571.	KP638611.1	JQ737145.1	-	HM018331.1	-	-	-	KP638691.1	-	-
184188-Primula cottia	-	AJ427796.	-	AJ427904.1	-	-	-	-	JQ755535.1	-	-	-
184181-Primula daonensis	-	AJ427772.	-	-	-	-	-	-	JQ755536.1	-	-	-
1044912-Primula diantha	-	JF977983.	JF955700.1	JQ737151.1	-	JF943637.1	-	-	-	JN046511.1	-	-
1271601-Primula handeliana	-	MH711131	-	JQ737202.1	-	-	-	-	-	-	-	-
152139-Primula latifolia	-	JQ755720.	-	AJ427897.1	-	-	-	-	JQ755561.1	-	-	-
547292-Primula longipes	-	EU643662.	HQ535973.1	JQ737170.1	-	-	-	-	-	-	-	-
1044917-Primula munroi	-	JF978016.	JF955736.1	JQ737179.1	-	JF943672.1	-	-	-	-	-	JN046545.1
184185-Primula pedemontana	-	AJ427791.	-	-	-	-	-	-	JQ755537.1	-	-	-
1044919-Primula prattii	-	JF978033.	JF955753.1	JQ737193.1	-	JF943690.1	-	-	-	-	-	JN046563.1
1271606-Primula purdomii	-	MH711136	-	JQ737195.1	-	-	-	-	-	-	-	-
159015-Primula spectabilis	-	AJ427794.	-	AJ427902.1	-	-	-	-	JQ755532.1	-	-	-
1044920-Primula spicata	-	JF978061.	JF955783.1	JQ737201.1	-	JF943718.1	-	-	-	-	-	JN046590.1
184187-Primula tyrolensis	-	AJ427795.	-	AJ427903.1	-	-	-	-	JQ755530.1	-	-	-
184190-Primula wulfeniana	-	AJ427799.	-	AJ427859.1	-	-	-	-	JQ755529.1	-	-	-
2037948-Primula jiugongshanensis	-	KX960953.	-	-	-	-	-	-	-	-	-	-
152138-Primula bulleyana	-	KF934445.	KP638613.1	AJ427860.1	-	AF394980.1	-	-	-	KP638693.1	-	-
1826189-Dionysia robusta	-	KU697386.	-	-	-	-	-	-	-	-	-	-

49651-Primula sorachiana	-	AB011628.	-	-	-	-	D85700.1	AB003573.1	-	-	-	-
184170-Primula albenensis	-	AJ427751.1	-	AJ427886.1	-	-	-	-	-	-	-	-
184180-Primula carniolica	-	AJ427768.1	-	AJ427890.1	-	-	-	-	-	-	-	-
184186-Primula recubariensis	-	AJ427793.1	-	AJ427901.1	-	-	-	-	-	-	-	-
272081-Primula latiloba	-	MG217443	-	-	-	MG221218.1	-	-	-	-	-	-
1044918-Primula oreodoxa	-	KM198414.	JF955741.1	-	-	JF943678.1	-	-	MF590644.1	JN046551.1	-	-
1049951-Primula grandis	-	HM629086	-	-	-	-	-	-	-	-	HM629004.1	-
1049952-Primula renifolia	-	HM629164	-	-	-	-	-	-	-	-	HM629013.1	-
1430312-Primula subpyrenaica	-	KF669876.1	-	-	-	-	-	-	-	-	-	-
1044913-Primula duclouxii	-	KM198444.	JF955701.1	-	-	JF943639.1	-	-	-	JN046512.1	-	-
1637978-Primula palmata	-	KM198427.	-	-	-	-	-	-	-	-	-	-
1044914-Primula epilosa	-	JF977985.1	JF955703.1	-	-	JF943640.1	-	-	-	JN046516.1	-	JN046514.1
1044915-Primula kialensis	-	JF977999.1	JF955718.1	-	-	JF943655.1	-	-	-	-	-	JN046529.1
1044916-Primula melanops	-	JF978005.1	JF955725.1	-	-	JF943661.1	-	-	-	JN046534.1	-	-
1044921-Primula szechuanica	-	JF978063.1	JF955785.1	-	-	JF943720.1	-	-	-	-	-	-
1044922-Primula tardiflora	-	JF978065.1	JF955787.1	-	-	JF943722.1	-	-	-	JN046595.1	-	-
1648219-Primula anisodora	-	KP638568.	KP638608.1	-	-	KP638648.1	-	-	-	-	-	-
1648220-Primula burmanica	-	KP638574.	KP638614.1	-	-	KP638654.1	-	-	-	KP638694.1	-	-
1648222-Primula mallophylla	-	KP638584.	KP638624.1	-	-	KP638664.1	-	-	-	KP638705.1	-	-
1648223-Primula melanodonta	-	KP638586.	KP638626.1	-	-	KP638666.1	-	-	-	KP638706.1	-	-
486436-Primula botschantzevii	-	AM920490.	-	-	-	-	-	-	-	-	-	-
486438-Primula fistulosa	-	AM920473.	-	-	-	-	-	-	-	-	-	-
486439-Primula kaufmanniana	-	AM920489.	-	-	-	-	-	-	-	-	-	-
486440-Primula kawasimae	-	AM920467.	-	-	-	-	-	-	-	-	-	-
486442-Primula mazurenkoae	-	AM920471.	-	-	-	-	-	-	-	-	-	-
486444-Primula patens	-	AM920485.	-	-	-	-	-	-	-	-	-	-
486449-Primula poloninensis	-	AM920483.	-	-	-	-	-	-	-	-	-	-
486445-Primula ruprechtii	-	AM920480.	-	-	-	-	-	-	-	-	-	-
486446-Primula saxatilis	-	AM920487.	-	-	-	-	-	-	-	-	-	-
486447-Primula turkestanica	-	AM920492.	-	-	-	-	-	-	-	-	-	-
486448-Primula xanthobasis	-	AM920494.	-	-	-	-	-	-	-	-	-	-
59684-Ternstroemia stahlii	-	-	HQ437951.1	-	-	HQ437968.1	-	-	-	-	-	-
1044923-Primula virginis	-	-	JF955789.1	-	-	JF943724.1	-	-	-	JN046596.1	-	-
175053-Primula concinna	-	-	-	AF402491.1	-	-	-	-	-	-	-	-
184177-Primula balbisii	-	-	-	AJ427889.1	-	-	-	-	-	-	-	-
370684-Primula tanneri	-	-	-	DQ378480.1	-	-	-	-	-	-	-	-
1271604-Primula melanantha	-	-	-	JQ737166.1	-	-	-	-	-	-	-	-
1271602-Primula laciniata	-	-	-	JQ737167.1	-	-	-	-	-	-	-	-
1271603-Primula limbata	-	-	-	JQ737169.1	-	-	-	-	-	-	-	-
1271605-Primula obtusifolia	-	-	-	JQ737185.1	-	-	-	-	-	-	-	-
1271608-Primula sinoplantaginea	-	-	-	JQ737199.1	-	-	-	-	-	-	-	-
1271607-Primula russeola	-	-	-	JQ737197.1	-	-	-	-	-	-	-	-
1271609-Primula tangutica	-	-	-	JQ737203.1	-	-	-	-	-	-	-	-
1271610-Primula woodwardii	-	-	-	JQ737208.1	-	-	-	-	-	-	-	-
110764-Primula veitchiana	-	-	-	-	-	AF213802.1	-	-	-	-	-	-
1384030-Primula grignensis	-	-	-	-	-	HG417032.1	-	-	-	HG800562.1	-	-
1198092-Primula boveana	-	-	-	-	-	KY656738.1	-	-	-	-	-	-
184992-Primula cusickiana	-	-	-	-	-	-	-	-	JQ755527.1	-	-	-
1050596-Primula inayatii	-	-	-	-	-	-	-	-	-	-	HM748214.1	-

TABLE S4: Accession matrix for Lupinus resulting from oneTwoTree. The left column shows the species name and the taxonomy ID according to the NCBI taxonomy database. The top row contains the cluster description assigned by oneTwoTree and the remaining cells contain the GenBank accession number if applicable.

Specie\Loci	26-ITS	1-Lupinus grayi LEGCYC1A793 cycloidea-like protein group 1A gene partial cds	2-Lupinus sarmentosus clone B15 glycerol-3-phosphate acyltransferase gene partial sequence	3-Lupinus odoratus strain CSD 0311A01 tRNA-Leu (trnL) gene partial sequence chloroplast	4-Lupinus mutabilis voucher FHO: Hughes 2009 clone B cycloidea-like protein group 1A (LEGCYC1A) gene partial cds	5-Lupinus weberbaueri isolate LUP1152 maturase K (matK) gene partial cds chloroplast	6-Lupinus argenteus strain CSD 026601 trnT-trnL intergenic spacer partial sequence chloroplast	7-Lupinus bicolor trnS-trnG intergenic spacer partial sequence chloroplast	8-Lupinus alopecuroides isolate Q3 external transcribed spacer and 18S ribosomal RNA gene partial sequence	9-Lupinus nanus LEGCYC1B gene complete cds	10-L.pilosus chloroplast rbcL gene	11-Lupinus paraguariensis isolate BZ1 symbiotic receptor-like kinase (SymRK) gene partial cds	12-Lupinus angustifolius isolate DIH106 ndhF-trnL intergenic spacer partial sequence and ribosomal protein L32 (rpl32) gene complete cds chloroplast	13-Lupinus lyallii voucher CCDB-23954-C08 ribulose-1,5-bisphosphate carboxylase/oxygenase large subunit (rbcL) gene partial cds chloroplast	14-Lupinus cosentinii voucher MAF167706 trnL-trnF intergenic spacer partial sequence chloroplast	15-Lupinus digitatus clone T4Ty1C5 retrotransposon Ty1/copia-like reverse transcriptase-like gene partial sequence	16-Lupinus longifolius isolate DIH161 petA-psbJ intergenic spacer partial sequence and PsbJ (psbJ) gene partial cds chloroplast	17-Lupinus mutabilis clone C1 glycerol-3-phosphate acyltransferase gene partial sequence	18-Lupinus gibertianus ycf1-rps15 intergenic spacer region complete sequence ribosomal protein S15 (rps15) gene complete cds rps15-ndhH intergenic spacer region complete sequence and NADH dehydrogenase subunit 7 (ndhH) gene partial cds chloroplast	19-Lupinus diffusus ribosomal protein S16 (rps16) gene exons 1 2 and partial cds chloroplast	20-Lupinus digitatus clone 2 hypothetical protein Ycf1 (ycf1) gene partial cds chloroplast	21-Lupinus cosentinii DNA fragment of chalcone isomerase gene 1	22-Lupinus diffusus rps16 accD intergenic spacer partial sequence and acetyl-CoA carboxylase beta subunit (accD) gene partial cds chloroplast	25-Lupinus pilosus tRNA-Phe (trnF-GAA) gene trnF-trnL intergenic spacer region tRNA-Leu (trnL-UAA) gene trnL-trnT intergenic spacer region and tRNA-Thr (trnT-UGU) gene complete sequence and trnT-rps4 intergenic spacer partial sequence chloroplast
49830-Lupinus albifrons	AH006090.2	JQ966690.1	-	DQ417091.1	-	KX162836.1	DQ416994.1	DQ416897.1	-	-	Z70053.1	-	GQ889950.1	-	-	-	GQ889907.1	-	-	-	-	-	-	-
3870-Lupinus albus	AY338946.1	AY338920.1	DQ852367.1	DQ417005.1	-	-	DQ416908.1	DQ416811.1	-	AY338871.1	Z70068.1	KC981658.1	-	-	AF538702.1	-	-	-	-	-	-	AB759124.1	-	-
3872-Lupinus arboreus	AY338944.1	AY338918.1	DQ852382.1	DQ417083.1	DQ529754.1	KX162838.1	DQ416986.1	DQ416889.1	GU574619.1	HM562700.1	Z70054.1	JF304510.1	GQ889960.1	-	-	-	GQ889889.1	DQ852548.1	-	-	-	-	-	-
53231-Lupinus microcarpus	DQ524253.1	DQ529935.1	DQ852405.1	DQ417030.1	DQ529936.1	KX162847.1	DQ416932.1	DQ416839.1	-	-	Z70063.1	JF304506.1	-	-	-	-	-	-	-	-	-	-	-	-
61120-Lupinus sparsiflorus	AF007482.1	-	-	DQ417049.1	-	JQ619990.1	DQ416952.1	DQ416855.1	-	-	-	-	-	-	-	-	-	-	-	-	-	-	-	-
28959-Lupinus texensis	AY338949.1	AY338923.1	DQ852411.1	DQ417018.1	-	JQ619989.1	DQ416920.1	DQ416823.1	GU574617.1	AY338874.1	-	JF304513.1	-	MH749103.1	AF538707.1	GU189888.1	-	-	KX147753.1	-	KX147738.1	AB759136.1	KX147697.1	KX147711.1
3871-Lupinus angustifolius	DQ524193.1	AH015549.2	DQ852368.1	DQ417006.1	DQ529758.1	KM487292.1	JQ041824.1	DQ416812.1	-	AH015550.2	Z70064.1	KC981675.1	-	-	AF538699.1	-	-	DQ852541.1	-	KX787910.1	-	-	-	-
53215-Lupinus arcticus	MG234821.1	-	-	GQ245089.1	-	KX677464.1	-	-	-	-	Z70055.1	-	-	-	-	-	-	-	-	-	-	-	-	-
53238-Lupinus bicolor	DQ524209.1	DQ529962.1	DQ852388.1	DQ417076.1	DQ529963.1	KX677529.1	DQ416979.1	DQ416883.1	-	-	-	-	GQ889968.1	KX678971.1	-	-	-	DQ852552.1	-	-	-	-	-	-
291860-Lupinus diffusus	AY609190.1	-	-	AY618505.1	-	MH551800.1	-	-	-	-	KJ773656.1	-	-	KY626985.1	-	-	-	-	KX147743.1	KX787896.1	KX147728.1	-	KX147688.1	KX147702.1
53225-Lupinus digitatus	AH006079.2	AY338922.1	-	DQ417011.1	-	-	DQ416914.1	DQ416817.1	GU574601.1	AY338873.1	Z70071.1	JF304525.1	-	-	-	GU189993.1	-	-	KX147744.1	KX787897.1	KX147729.1	AB759128.1	KX147689.1	KX147703.1
53226-Lupinus elegans	AH006094.2	-	-	DQ417059.1	-	-	DQ416962.1	DQ416865.1	GU574626.1	-	-	JF304509.1	-	-	-	-	-	-	-	KX787898.1	-	-	-	-
61109-Lupinus hirsutissimus	DQ524235.1	DQ529944.1	DQ852400.1	DQ417046.1	DQ529947.1	KX162819.1	DQ416949.1	DQ416852.1	-	-	-	-	-	-	-	-	-	DQ852553.1	-	KX787899.1	-	-	-	-
53229-Lupinus latifolius	DQ524243.1	DQ529942.1	DQ852402.1	DQ417094.1	DQ529943.1	KX677734.1	DQ416997.1	DQ416900.1	-	-	Z70059.1	-	GQ889974.1	-	-	-	GQ889903.1	-	-	-	-	-	-	-
61111-Lupinus littoralis	AH006089.2	-	-	-	-	KX676835.1	-	-	-	-	-	-	-	KX678170.1	-	-	-	-	-	-	-	-	-	-
61112-Lupinus luteolus	AF007490.1	-	-	DQ417035.1	-	KX162854.1	DQ416938.1	DQ416841.1	GU574605.1	-	-	JF304514.1	-	-	-	-	-	-	-	KX787900.1	-	-	-	-
3873-Lupinus luteus	DQ524249.1	DQ529782.1	DQ852371.1	DQ417012.1	-	HM851129.1	DQ416915.1	DQ416818.1	FJ839561.1	-	Z70066.1	JF304519.1	-	-	FJ839604.1	-	-	-	-	-	-	AB759130.1	-	-
857201-Lupinus mariae josephae	GU058033.1	GU045299.1	-	-	-	-	-	-	GU574608.1	-	GU045291.1	-	-	-	-	GU189829.1	-	-	-	KX787907.1	-	-	-	-
53230-Lupinus micranthus	Z72209.1	DQ529813.1	-	AY618495.1	-	-	-	-	GU574635.1	HM562704.1	Z70067.1	JF304529.1	-	-	AF538698.1	GU189945.1	-	-	-	KX787908.1	-	AB759131.1	-	-
53232-Lupinus mutabilis	DQ524270.1	DQ529778.1	DQ852429.1	KX147707.1	DQ529800.1	KX162839.1	DQ416967.1	DQ416868.1	GU574612.1	HM562696.1	Z70061.1	JF304535.1	-	-	-	GU189854.1	-	DQ852564.1	KX147748.1	KX787901.1	KX147733.1	-	KX147693.1	-
53233-Lupinus nanus	AH006084.2	-	-	DQ417079.1	-	KX162821.1	DQ416982.1	DQ416884.1	-	AY382155.1	Z70056.1	-	GQ889970.1	-	-	-	-	-	-	KX787902.1	-	-	-	-
3874-Lupinus polyphyllus	AY338930.1	AY338904.1	-	KX668014.1	-	KX677174.1	DQ416996.1	DQ416899.1	GU574615.1	AY338855.1	Z70052.1	JF304542.1	GQ889984.1	-	-	GU189981.1	GQ889913.1	-	KX147751.1	-	KX147736.1	-	KX147695.1	KX147710.1
61075-Lupinus sericeus	AH006082.2	AY338909.1	-	GQ984177.1	-	KX677480.1	-	-	-	AY338860.1	-	-	-	KX678918.1	-	-	-	-	-	-	-	-	-	-
213032-Lupinus villosus	DQ524322.1	DQ529749.1	DQ852375.1	DQ417015.1	DQ529750.1	KY607282.1	DQ416918.1	DQ416820.1	GU574602.1	-	-	JF304508.1	-	KX397853.1	AF538708.1	-	-	-	-	KX787909.1	-	-	-	-
49836-Retama monosperma	HE602407.1	DQ529755.1	DQ852364.1	AJ304871.1	-	KY046194.1	-	-	DQ289723.1	-	Z70117.1	-	-	-	AY264056.1	-	-	-	-	-	-	-	-	-
238488-Genista hirsuta	DQ524182.1	-	DQ852363.1	AJ890991.1	-	-	-	-	-	-	-	-	-	-	-	-	-	-	-	-	-	-	-	-
53214-Lupinus albescens	DQ524190.1	DQ529974.1	DQ852503.1	-	DQ529975.1	-	-	-	-	-	Z70074.1	-	-	-	-	-	-	-	-	-	-	-	-	-
53216-Lupinus argenteus	AH006092.2	AY338905.1	DQ852378.1	DQ417089.1	-	AY386956.1	DQ416992.1	DQ416894.1	GU574616.1	AY338854.1	-	-	GQ889985.1	MG248001.1	AF538706.1	-	GQ889914.1	-	-	-	-	-	-	-
61102-Lupinus arizonicus	DQ524198.1	DQ529968.1	DQ852385.1	DQ417051.1	DQ529969.1	KX162827.1	DQ416954.1	DQ416857.1	-	-	-	-	-	-	-	-	-	DQ852555.1	-	-	-	-	-	-
384393-Lupinus arvensis	DQ524199.1	DQ529877.1	DQ852490.1	-	DQ529878.1	-	-	-	-	-	-	-	-	-	-	-	-	-	-	-	-	-	-	-
384394-Lupinus ballianus	DQ524201.1	DQ529914.1	DQ852455.1	-	DQ529915.1	KX162825.1	-	-	-	-	-	-	-	-	-	-	-	-	-	-	-	-	-	-
377319-Lupinus bandelierae	DQ524202.1	DQ529820.1	DQ852500.1	DQ417021.1	DQ529821.1	KX162846.1	DQ416924.1	DQ416827.1	-	-	-	-	-	-	-	-	-	-	-	-	-	-	-	-
384395-Lupinus bangii	DQ524256.1	DQ529826.1	DQ852476.1	-	DQ529904.1	-	-	-	-	HM562693.1	-	-	-	-	-	-	-	-	-	-	-	-	-	-
61103-Lupinus bracteolaris	DQ524210.1	DQ529816.1	DQ852505.1	AY618506.1	DQ529817.1	-	-	-	GU574627.1	-	-	JF304504.1	-	-	-	GU189897.1	-	-	-	-	-	-	-	-
377321-Lupinus brevicaulis	DQ524213.1	-	-	DQ417022.1	-	EU025879.1	DQ416925.1	DQ416828.1	-	-	-	-	-	-	-	-	-	-	-	-	-	-	-	-
384396-Lupinus chachas	DQ524216.1	DQ529763.1	DQ852452.1	-	DQ529764.1	KX162851.1	-	-	-	HM562699.1	-	-	-	-	-	-	-	-	-	-	-	-	-	-
377323-Lupinus chamissonis	DQ524217.1	DQ529895.1	DQ852392.1	DQ417084.1	DQ529894.1	-	DQ416987.1	DQ416890.1	-	-	-	-	GQ889971.1	-	-	-	GQ889900.1	-	-	-	-	-	-	-
384397-Lupinus chrysanthus	DQ524220.1	DQ529793.1	DQ852464.1	-	DQ529902.1	-	-	-	-	HM562686.1	-	-	-	-	-	-	-	-	-	-	-	-	-	-
61074-Lupinus concinnus	DQ524214.1	DQ529960.1	DQ852389.1	DQ417047.1	DQ529959.1	-	DQ416950.1	DQ416853.1	GU574613.1	-	-	-	-	-	-	GU189863.1	-	-	-	-	-	-	-	-
53222-Lupinus cosentinii	AH006095.2	AY338921.1	DQ852372.1	DQ417008.1	-	AY386943.1	DQ416911.1	DQ416814.1	FJ839559.1	AY338872.1	Z70070.1	JF304539.1	-	-	FJ839603.1	GU189928.1	-	-	KX147742.1	-	KX147727.1	AB759127.1	KX147687.1	-
61105-Lupinus crotalarioides	DQ524223.1	DQ529855.1	DQ852510.1	-	DQ529864.1	-	-	-	-	-	-	-	-	-	-	-	-	-	-	-	-	-	-	-
377325-Lupinus cumulicola	DQ524226.1	DQ529745.1	DQ852374.1	DQ417016.1	DQ529746.1	-	DQ416919.1	DQ416822.1	-	-	-	-	-	-	-	-	-	-	-	-	-	-	-	-
384398-Lupinus ellsworthianus	DQ524215.1	DQ529885.1	DQ852484.1	-	DQ529886.1	-	-	-	-	-	-	-	-	-	-	-	-	-	-	-	-	-	-	-
384399-Lupinus gibertianus	DQ524229.1	DQ529851.1	DQ852512.1	KX147704.1	DQ529852.1	-	-	-	GU574582.1	-	-	JF304511.1	-	-	-	-	-	-	KX147745.1	-	KX147730.1	-	KX147690.1	-
384400-Lupinus guaraniticus	DQ524230.1	DQ529954.1	DQ852514.1	-	DQ529955.1	-	-	-	-	-	-	-	-	-	-	-	-	-	-	-	-	-	-	-
377327-Lupinus havardii	DQ524232.1	DQ529950.1	DQ852395.1	DQ417019.1	DQ529951.1	-	DQ416922.1	-	-	-	-	-	-	-	-	-	-	-	-	-	-	-	-	-
53228-Lupinus hispanicus	DQ524236.1	DQ529780.1	DQ852369.1	DQ417013.1	DQ529781.1	-	DQ416916.1	DQ416819.1	-	HM562701.1	Z70065.1	-	-	-	AF538701.1	-	-	DQ852542.1	-	-	-	AB759129.1	-	-
384401-Lupinus huaronensis	DQ524237.1	DQ529770.1	DQ852460.1	-	DQ529771.1	KX162855.1	-	-	-	HM562679.1	-	-	-	-	-	-	-	-	-	-	-	-	-	-
384402-Lupinus huigrensis	DQ524304.1	DQ529871.1	-	-	DQ529872.1	-	-	-	-	-	-	-	-	-	-	-	-	-	-	-	-	-	-	-
384390-Lupinus hybrid cultivar	DQ524185.1	-	-	-	-	-	-	-	-	-	-	-	-	-	-	-	-	-	-	-	-	-	-	-
384404-Lupinus lanatus	DQ524241.1	DQ529849.1	DQ852517.1	-	DQ529848.1	KX162822.1	-	-	-	-	-	-	-	-	-	-	-	-	-	-	-	-	-	-
61110-Lupinus lepidus	MG237260.1	DQ529940.1	DQ852401.1	DQ417087.1	DQ529941.1	KX162833.1	DQ416990.1	DQ416893.1	GU574598.1	-	-	-	GQ889981.1	MG249249.1	-	-	GQ889910.1	DQ852551.1	-	-	-	-	-	-
384405-Lupinus lindleyanus	DQ524247.1	DQ529889.1	DQ852480.1	-	DQ529890.1	KX162817.1	-	-	-	-	-	-	-	-	-	-	-	-	-	-	-	-	-	-
384406-Lupinus linearis	DQ524248.1	DQ529846.1	DQ852518.1	-	DQ529829.1	KX162864.1	-	-	-	-	-	-	-	-	-	-	-	-	-	-	-	-	-	-
384407-Lupinus magnistipulatus	DQ524250.1	DQ529937.1	DQ852520.1	-	DQ529831.1	-	-	-	GU574583.1	-	-	JF304531.1	-	-	-	-	-	-	-	-	-	-	-	-
384408-Lupinus mantaroensis	DQ524200.1	DQ529759.1	DQ852444.1	-	DQ529760.1	KX162845.1	-	-	-	HM562694.1	-	-	-	-	-	-	-	-	-	-	-	-	-	-
384409-Lupinus microphyllus	DQ524255.1	DQ529774.1	DQ852465.1	-	DQ529790.1	-	-	-	-	HM562677.1	-	-	-	-	-	-	-	-	-	-	-	-	-	-
384410-Lupinus misticola	DQ524257.1	DQ529887.1	DQ852482.1	-	DQ529888.1	KX162844.1	-	-	-	-	-	-	-	-	-	-	-	-	-	-	-	-	-	-
384411-Lupinus mollendoensis	DQ524258.1	DQ529933.1	DQ852496.1	-	DQ529934.1	-	-	-	-	-	-	-	-	-	-	-	-	-	-	-	-	-	-	-
384412-Lupinus montanus	DQ524259.1	DQ529809.1	DQ852427.1	-	DQ529810.1	-	-	-	-	HM562676.1	-	-	-	-	-	-	-	-	-	-	-	-	-	-
61116-Lupinus multiflorus	DQ524260.1	DQ529844.1	DQ852522.1	DQ417020.1	DQ529845.1	-	DQ416923.1	DQ416826.1	-	-	-	-	-	-	-	-	-	DQ852545.1	-	-	-	-	-	-
384413-Lupinus neomexicanus	DQ524274.1	DQ529931.1	DQ852406.1	-	DQ529932.1	-	-	-	-	-	-	-	-	-	-	-	-	-	-	-	-	-	-	-
384414-Lupinus nubigenus	DQ524275.1	DQ529875.1	DQ852492.1	-	DQ529876.1	KX162849.1	-	-	-	-	-	-	-	-	-	-	-	-	-	-	-	-	-	-
377329-Lupinus odoratus	DQ524276.1	DQ529930.1	DQ852403.1	DQ417024.1	-	EU025914.1	DQ416927.1	DQ416830.1	-	-	-	-	-	-	-	-	-	-	-	-	-	-	-	-
53235-Lupinus paraguariensis	DQ524277.1	DQ529926.1	DQ852525.1	AY618508.1	DQ529927.1	-	-	-	GU574586.1	-	Z70076.1	JF304512.1	-	-	AF538709.1	GU189784.1	-	-	KX147749.1	-	KX147734.1	-	KX147694.1	KX147708.1
384415-Lupinus paranensis	DQ524279.1	DQ529924.1	DQ852523.1	-	DQ529925.1	-	-	-	-	-	-	-	-	-	-	-	-	-	-	-	-	-	-	-
384416-Lupinus parvifolius	DQ524280.1	DQ529836.1	DQ852529.1	-	DQ529837.1	-	-	-	-	-	-	-	-	-	-	-	-	-	-	-	-	-	-	-
384417-Lupinus piurensis	DQ524284.1	DQ529814.1	DQ852434.1	-	DQ529815.1	-	-	-	-	HM562683.1	-	-	-	-	-	-	-	-	-	-	-	-	-	-
384418-Lupinus praestabilis	DQ524285.1	DQ529822.1	DQ852471.1	-	DQ529823.1	KX162840.1	-	-	-	-	-	-	-	-	-	-	-	DQ852561.1	-	-	-	-	-	-
384419-Lupinus prostratus	DQ524286.1	DQ529791.1	DQ852459.1	-	DQ529792.1	-	-	-	-	HM562685.1	-	-	-	-	-	-	-	-	-	-	-	-	-	-
53240-Lupinus pubescens	DQ524287.1	DQ529879.1	DQ852489.1	-	DQ529880.1	KX162850.1	-	-	-	-	-	-	-	-	-	-	-	-	-	-	-	-	-	-
384420-Lupinus pulvinaris	DQ524288.1	DQ529776.1	DQ852466.1	-	DQ529777.1	-	-	-	-	HM562688.1	-	-	-	-	-	-	-	-	-	-	-	-	-	-
384421-Lupinus purosericeus	DQ524238.1	DQ529772.1	DQ852461.1	-	DQ529773.1	KX162848.1	-	-	-	HM562692.1	-	-	-	-	-	-	-	-	-	-	-	-	-	-
384422-Lupinus ramosissimus	DQ524289.1	DQ529761.1	-	-	DQ529762.1	KX162860.1	-	-	-	HM562689.1	-	-	-	-	-	-	-	-	-	-	-	-	-	-
384423-Lupinus reitzii	DQ524290.1	DQ529832.1	DQ852530.1	-	DQ529833.1	-	-	-	-	-	-	-	-	-	-	-	-	-	-	-	-	-	-	-
384424-Lupinus rubriflorus	DQ524292.1	DQ529842.1	DQ852531.1	-	DQ529843.1	-	-	-	-	-	-	-	-	-	-	-	-	-	-	-	-	-	-	-
384425-Lupinus sarmentosus	DQ524187.1	DQ529805.1	DQ852487.1	-	DQ529882.1	-	-	-	-	HM562678.1	-	-	-	-	-	-	-	-	-	-	-	-	-	-
384426-Lupinus semperflorens	DQ524293.1	DQ529801.1	DQ852443.1	-	DQ529802.1	KX162843.1	-	-	-	HM562691.1	-	-	-	-	-	-	-	DQ852571.1	-	-	-	-	-	-
384427-Lupinus sierrae blancae	DQ524298.1	DQ529920.1	DQ852408.1	-	DQ529921.1	-	-	-	-	-	-	-	-	-	-	-	-	DQ852550.1	-	-	-	-	-	-
384428-Lupinus solanagrorum	DQ524294.1	DQ529803.1	-	-	DQ529804.1	-	-	-	-	HM562698.1	-	-	-	-	-	-	-	-	-	-	-	-	-	-
384429-Lupinus subacaulis	DQ524312.1	DQ529907.1	DQ852468.1	-	DQ529908.1	-	-	-	-	-	-	-	-	-	-	-	-	-	-	-	-	-	-	-
384430-Lupinus subsessilis	DQ524313.1	DQ529840.1	DQ852532.1	-	DQ529841.1	-	-	-	-	-	-	-	-	-	-	-	-	DQ852543.1	-	-	-	-	-	-
384431-Lupinus tarapacensis	DQ524314.1	DQ529899.1	DQ852498.1	-	DQ529900.1	-	-	-	-	-	-	-	-	-	-	-	-	-	-	-	-	-	-	-
384432-Lupinus tomentosus	DQ524317.1	DQ529905.1	DQ852470.1	-	DQ529906.1	-	-	-	-	-	-	-	-	-	-	-	-	-	-	-	-	-	-	-
384433-Lupinus tominensis	DQ524207.1	DQ529824.1	DQ852473.1	-	DQ529825.1	-	-	-	-	-	-	-	-	-	-	-	-	-	-	-	-	-	-	-
377344-Lupinus truncatus	DQ524318.1	DQ529916.1	DQ852414.1	DQ417048.1	DQ529917.1	KX162858.1	DQ416951.1	DQ416854.1	-	-	-	-	-	-	-	-	-	-	-	-	-	-	-	-
384434-Lupinus uleanus	DQ524319.1	DQ529838.1	DQ852533.1	-	DQ529839.1	-	-	-	-	-	-	-	-	-	-	-	-	-	-	-	-	-	-	-
384435-Lupinus velutinus	DQ524320.1	DQ529818.1	DQ852535.1	-	DQ529819.1	-	-	-	-	-	-	-	-	-	-	-	-	-	-	-	-	-	-	-
384436-Lupinus weberbaueri	DQ524324.1	DQ529811.1	DQ852457.1	-	DQ529812.1	KX162857.1	-	-	-	HM562681.1	-	-	-	-	-	-	-	-	-	-	-	-	-	-
61100-Lupinus affinis	AF007487.1	-	-	AY618503.1	-	-	-	-	GU574614.1	-	-	JF304515.1	-	-	AF538705.1	-	-	-	KX147739.1	-	KX147725.1	-	KX147685.1	KX147698.1
53218-Lupinus atlanticus	AH006080.2	-	-	DQ417007.1	-	-	DQ416910.1	DQ416813.1	GU574636.1	-	Z70069.1	JF304524.1	-	-	-	GU189912.1	-	-	-	-	-	AB759126.1	-	-
61117-Lupinus palaestinus	AF007479.1	-	-	DQ417010.1	-	-	DQ416913.1	DQ416816.1	GU574631.1	-	-	JF304520.1	-	-	-	GU189922.1	-	-	-	-	-	AB759133.1	-	-
53237-Lupinus pilosus	AH006081.2	-	-	DQ417009.1	-	-	DQ416912.1	DQ416815.1	GU574630.1	-	Z70073.1	JF304521.1	GQ890015.1	-	AF108089.1	GU190001.1	-	-	KX147750.1	-	KX147735.1	AB759134.1	-	KX147709.1
213031-Lupinus jaime hintonianus	AY609184.1	-	-	-	-	-	-	-	GU574599.1	-	-	-	-	-	AF538704.1	-	-	-	-	-	-	-	-	-
61076-Lupinus leucophyllus	AH006085.2	-	-	-	-	-	-	-	-	-	-	-	GQ889977.1	MG248960.1	-	-	GQ889906.1	-	-	-	-	-	-	-
61077-Lupinus mexicanus	AH006086.2	-	-	DQ417060.1	-	-	DQ416963.1	DQ416866.1	GU574618.1	-	-	JF304536.1	-	-	AF538703.1	-	-	-	KX147747.1	-	KX147732.1	-	KX147692.1	KX147706.1
61121-Lupinus sulphureus	AH006093.2	-	-	-	-	KX162818.1	-	-	-	-	-	-	-	MG246502.1	-	-	-	-	-	-	-	-	-	-
53220-Lupinus benthamii	Z72168.1	-	-	DQ417050.1	-	-	DQ416953.1	DQ416856.1	-	-	-	-	GQ889946.1	-	-	-	-	-	-	-	-	-	-	-
53227-Lupinus formosus	Z72172.1	-	-	DQ417092.1	-	KX162835.1	DQ416995.1	DQ416898.1	-	-	-	-	GQ889965.1	-	-	-	GQ889894.1	-	-	-	-	-	-	-
240338-Lupinus grayi	AY338939.1	AY338913.1	-	DQ417095.1	-	-	DQ416998.1	DQ416901.1	-	AY338864.1	-	-	-	-	-	-	-	-	-	-	-	-	-	-
53236-Lupinus perennis	MG235335.1	-	-	DQ417058.1	-	MK520282.1	DQ416961.1	DQ416863.1	-	-	Z70058.1	-	-	-	-	-	-	-	-	-	-	-	-	-
53242-Lupinus succulentus	AF007494.1	-	-	DQ417053.1	-	-	DQ416956.1	DQ416860.1	-	-	-	-	-	-	-	-	-	-	-	-	-	-	-	-
88767-Lupinus anatolicus	AF108085.1	-	-	AY618491.1	-	-	-	-	GU574600.1	-	-	JF304533.1	-	-	AF108087.1	GU189848.1	-	-	KX147740.1	-	-	-	-	KX147699.1
53234-Lupinus nootkatensis	MG234835.1	-	-	-	-	-	-	-	GU574621.1	-	Z70057.1	-	-	-	-	-	-	-	-	-	-	-	-	-
53239-Lupinus princei	Z72224.1	-	-	AY618492.1	-	-	-	-	GU574624.1	-	Z70072.1	JF304527.1	-	-	-	GU189933.1	-	-	-	-	-	-	-	-
175403-Genista tenera	AY338950.1	AY338924.1	-	JF338275.1	-	-	-	-	-	AY338875.1	Z70109.1	-	-	-	JF338611.1	-	-	-	-	-	-	-	-	-
240333-Lupinus andersonii	AY338934.1	AY338908.1	-	-	-	-	-	-	-	AY338859.1	-	-	GQ889964.1	-	-	-	-	-	-	-	-	-	-	-
53241-Lupinus rivularis	AY338937.1	AY338911.1	-	-	-	KX162853.1	-	-	-	AY338862.1	-	-	-	MG249387.1	-	-	-	-	-	-	-	-	-	-
61106-Lupinus duranii	AF007493.1	-	-	-	-	AY386910.1	-	-	-	-	-	-	-	-	-	-	-	-	-	-	-	-	-	-
61118-Lupinus pusillus	MG237001.1	-	-	-	-	KX162837.1	-	-	-	-	-	-	-	MG248905.1	-	-	-	-	-	-	-	-	-	-
2071485-Lupinus arbustus	MG236907.1	-	-	-	-	-	-	-	-	-	-	-	-	MG248801.1	-	-	-	-	-	-	-	-	-	-
2071486-Lupinus bingenensis	MG234942.1	-	-	-	-	-	-	-	-	-	-	-	-	MG247261.1	-	-	-	-	-	-	-	-	-	-
2071487-Lupinus kuschei	MG236415.1	-	-	-	-	-	-	-	-	-	-	-	-	MG249682.1	-	-	-	-	-	-	-	-	-	-
2071488-Lupinus lyallii	MG236720.1	-	-	-	-	-	-	-	-	-	-	-	-	MG249072.1	-	-	-	-	-	-	-	-	-	-
61115-Lupinus minimus	MG236113.1	-	-	-	-	-	-	-	-	-	-	-	-	MG247824.1	-	-	-	-	-	-	-	-	-	-
53221-Lupinus bogotensis	Z72192.1	-	-	-	-	-	-	-	-	-	Z70060.1	-	-	-	-	-	-	-	-	-	-	-	-	-
61107-Lupinus excubitus	AF007492.1	-	-	-	-	-	-	-	-	-	-	-	GQ889963.1	-	-	-	GQ889892.1	-	-	-	-	-	-	-
53219-Lupinus aureonitens	Z72210.1	-	-	-	-	-	-	-	-	-	Z70075.1	-	-	-	-	-	-	-	-	-	-	-	-	-
53217-Lupinus aschenbornii	Z72190.1	-	-	-	-	-	-	-	-	-	-	-	-	-	-	-	-	-	-	-	-	-	-	-
1136292-Lupinus oreganus	-	JN628016.1	-	-	-	-	-	-	-	-	-	-	-	-	-	-	-	-	-	-	-	-	-	-
377318-Lupinus albicaulis	-	JN628017.1	-	DQ417081.1	-	KX162832.1	DQ416983.1	DQ416887.1	GU574620.1	-	-	-	GQ889976.1	-	-	-	-	-	-	-	-	-	-	-
1136291-Lupinus biddlei	-	JN628018.1	-	-	-	-	-	-	-	-	-	-	-	-	-	-	-	-	-	-	-	-	-	-
1209938-Lupinus caudatus	-	JQ966695.1	-	-	-	-	-	-	-	-	-	-	-	-	-	-	-	-	-	-	-	-	-	-
377345-Lupinus uncialis	-	-	-	DQ417023.1	-	-	DQ416926.1	DQ416829.1	-	-	-	-	-	-	-	-	-	-	-	-	-	-	-	-
377331-Lupinus shockleyi	-	-	-	DQ417025.1	-	-	DQ416928.1	DQ416831.1	-	-	-	-	-	-	-	-	-	-	-	-	-	-	-	-

377324-Lupinus citrinus	-	-	-	DQ417045.1	-	-	DQ416948.1	DQ416851.1	-	-	-	-	-	-	-	-	-	-	-	-	-	-	-	-
377343-Lupinus stiversii	-	-	-	DQ417055.1	-	-	DQ416958.1	DQ416861.1	-	-	-	-	-	-	-	-	-	-	-	-	-	-	-	-
377326-Lupinus guadalupensis	-	-	-	DQ417056.1	-	-	DQ416959.1	DQ416862.1	-	-	-	-	-	-	-	-	-	-	-	-	-	-	-	-
377330-Lupinus pachylobus	-	-	-	DQ417075.1	-	KX162862.1	DQ416978.1	DQ416881.1	-	-	-	-	-	-	-	-	-	-	-	-	-	-	-	-
377322-Lupinus cervinus	-	-	-	DQ417082.1	-	-	DQ416985.1	DQ416888.1	-	-	-	-	-	-	-	-	-	-	-	-	-	-	-	-
247877-Lupinus tegeticulatus	-	-	-	DQ417085.1	-	-	DQ416988.1	DQ416891.1	-	-	-	-	-	-	-	-	-	-	-	-	-	-	-	-
377328-Lupinus nevadensis	-	-	-	DQ417090.1	-	KX162831.1	DQ416993.1	DQ416896.1	-	-	-	-	-	-	-	-	-	-	-	-	-	-	-	-
2528748-Lupinus oreophilus	-	-	-	MH115362.1	-	-	-	-	-	-	-	-	-	-	-	-	-	-	-	-	-	-	-	-
2528749-Lupinus subinflatus	-	-	-	MH115363.1	-	-	-	-	-	-	-	-	-	-	-	-	-	-	-	-	-	-	-	-
457905-Lupinus flavoculatus	-	-	-	-	-	EU025898.1	-	-	-	-	-	-	-	-	-	-	-	-	-	-	-	-	-	-
457906-Lupinus huachucanus	-	-	-	-	-	EU025906.1	-	-	-	-	-	-	-	-	-	-	-	-	-	-	-	-	-	-
1115965-Lupinus campestris	-	-	-	-	-	KX162828.1	-	-	KC914415.1	-	-	-	-	-	-	-	-	-	-	-	-	-	-	-
714519-Lupinus westianus	-	-	-	-	-	KY607283.1	-	-	-	-	-	-	-	KX397854.1	-	-	-	-	-	-	-	-	-	-
948800-Lupinus alopecuroides	-	-	-	-	-	-	-	-	GU574623.1	-	-	-	-	-	-	-	-	-	-	-	-	-	-	-
948801-Lupinus vavilovii	-	-	-	-	-	-	-	-	GU574649.1	-	-	JF304528.1	-	-	-	-	-	-	-	-	-	-	-	-
1381404-Lupinus splendens	-	-	-	-	-	-	-	-	KC914411.1	-	-	-	-	-	-	-	-	-	-	-	-	-	-	-
1381401-Lupinus hintonii	-	-	-	-	-	-	-	-	KC914416.1	-	-	-	-	-	-	-	-	-	-	-	-	-	-	-
749253-Lupinus variicolor	-	-	-	-	-	-	-	-	-	-	-	-	GQ889959.1	-	-	-	-	-	-	-	-	-	-	-
749251-Lupinus onustus	-	-	-	-	-	-	-	-	-	-	-	-	GQ889982.1	-	-	-	GQ889911.1	-	-	-	-	-	-	-
749240-Lupinus angustiflorus	-	-	-	-	-	-	-	-	-	-	-	-	GQ889983.1	-	-	-	GQ889912.1	-	-	-	-	-	-	-
749250-Lupinus ludovicianus	-	-	-	-	-	-	-	-	-	-	-	-	GQ889987.1	-	-	-	GQ889916.1	-	-	-	-	-	-	-
749252-Lupinus paynei	-	-	-	-	-	-	-	-	-	-	-	-	GQ889996.1	-	-	-	GQ889932.1	-	-	-	-	-	-	-
749249-Lupinus longifolius	-	-	-	-	-	-	-	-	-	-	-	-	GQ890012.1	-	-	-	GQ889939.1	-	-	-	-	-	-	-
1972999-Lupinus sellowianus	-	-	-	-	-	-	-	-	-	-	-	-	-	-	-	-	-	-	-	KX787903.1	-	-	-	-

TABLE S5: Accession matrix for Ranunculus resulting from oneTwoTree. The left column shows the species name and the taxonomy ID according to the NCBI taxonomy database. The top row contains the cluster description assigned by oneTwoTree and the remaining cells contain the GenBank accession number if applicable.

Specie\Loci	15-ITS	1-Ranunculus pensylvanicus voucher V. Zila 447002 trnK gene intron and maturase K (matK) gene complete cds chloroplast	2-Ranunculus sericeus voucher Emadzade 121 PsbJ (psbJ) gene partial cds and psbJ-petA intergenic spacer partial sequence chloroplast	3-Ranunculus alpestris ribulose-15-bisphosphate carboxylase/oxygenase large subunit gene partial cds chloroplast	4-Ranunculus seguieri isolate RS891 tRNA-Leu (trnL) gene complete sequence chloroplast	5-Ranunculus arcticus voucher WU:Schoenswetter & Tribsch 639 ribosomal protein L32 (rpl32) gene partial cds and rpl32-trnL intergenic spacer partial sequence chloroplast	6-Ranunculus rhomboideus voucher LE<RUS>:Hezns et al. s.n. psbE-petL intergenic spacer partial sequence chloroplast	7-Ranunculus pseudopygmaeus voucher WU:Hoerandl & Emadzade 9689 NADH dehydrogenase subunit 1 (ndhA) gene intron chloroplast	8-Ranunculus pygmaeus voucher WU:Larson & Granberg 9345 ndhC-trnV intergenic spacer partial sequence chloroplast	9-Batrachium bungei isolate 1-20 trnT-trnL intergenic spacer partial sequence chloroplast	10-Ranunculus godleyanus unknown gene chloroplast gene for chloroplast product	11-Ranunculus tripartitus isolate NMW4032 maturase K (matK) gene partial cds chloroplast	12-Ranunculus fluitans isolate 21Batr_fluit_Vilnia_2 trnH-psbA intergenic spacer partial sequence and photosystem II protein D1 (psbA) gene partial cds chloroplast	13-Ranunculus caucasicus chloroplast DNA tRNA-Leu (trnL) and trnL-trnF intergenic spacer partial sequence	14-Ranunculus omiophyllus isolate 372 trnL-rpl32 intergenic spacer partial sequence chloroplast
286847-Ranunculus aconitifolius	KU974069.1	AY954217.1	HQ338172.1	KF602169.1	EU792596.1	JX025321.1	-	-	-	-	-	-	-	-	-
286854-Ranunculus amplexicaulis	JQ801622.1	AY954223.1	HQ338262.1	-	-	JX025322.1	-	-	-	-	-	-	-	-	-
761494-Ranunculus cabrerensis	JQ801630.1	-	-	-	-	-	-	-	-	-	-	-	-	-	-
286874-Ranunculus cantoniensis	JQ439725.1	HM565150.1	HQ338177.1	FJ449861.1	DQ410736.1	-	-	-	-	-	-	-	-	-	-
376246-Ranunculus chinensis	JQ763144.1	HQ338349.1	HQ338184.1	-	DQ410739.1	JQ762698.1	-	-	-	-	-	-	-	-	-
376247-Ranunculus diffusus	JQ439817.1	HQ338351.1	HQ338197.1	-	DQ410734.1	-	-	-	-	-	-	-	-	-	-
235900-Ranunculus glacialis	JX105174.1	AY954219.1	GU258027.1	KF602157.1	GQ244636.1	JX118539.1	-	-	-	-	-	-	-	-	-
286907-Ranunculus gramineus	JX025232.1	AY954227.1	HQ338211.1	-	KY697505.1	JX025325.1	-	-	-	-	-	-	-	-	-
105186-Ranunculus lingua	KX167029.1	AY954206.1	HQ338236.1	JN892595.1	-	-	-	-	-	-	-	-	-	JX280910.1	-
286960-Ranunculus parnassiifolius	JQ801610.1	-	-	-	-	-	-	-	-	-	-	-	-	-	-
286985-Ranunculus pyrenaeus	JQ801618.1	AY954225.1	GU258041.1	-	-	JX025353.1	-	-	-	-	-	-	-	-	-
137665-Ranunculus repens	JQ439869.1	HM565166.1	HQ338287.1	KF602173.1	JQ041850.1	-	-	-	-	-	-	JN114770.1	-	-	-
376250-Ranunculus shuichengensis	JQ439580.1	-	-	-	DQ410741.1	-	-	-	-	-	-	-	-	-	-
376251-Ranunculus sieboldii	JQ439799.1	-	-	FJ449860.1	DQ410733.1	-	-	-	-	-	-	-	-	-	-
376255-Ranunculus trigonus	JQ763251.1	-	-	-	DQ410738.1	JQ762822.1	-	-	-	-	-	-	-	-	-
376256-Ranunculus vaginatus	JQ439765.1	-	-	-	DQ410732.1	-	-	-	-	-	-	-	-	-	-
37489-Anemone nemorosa	KX167066.1	KU213024.1	-	KM360632.1	KX667945.1	-	-	-	-	-	-	-	-	-	-
286838-Ceratocephala orthoceras	AY680190.1	AY954230.1	-	KU662947.1	KF312704.1	-	-	-	-	-	-	-	-	-	-
327927-Clematis ganpiniana	KU853296.1	FJ626495.1	-	AY954491.1	FJ626541.1	-	-	-	-	-	-	-	-	-	-
3447-Ranunculus acris	KX165735.1	AY954199.1	KY499657.1	AY395557.1	KX667979.1	-	-	-	-	-	-	-	HQ596809.1	-	-
633653-Ranunculus bungei	KP336399.1	FJ626491.1	-	FJ626579.1	FJ626538.1	-	KC117504.1	-	-	GU733853.1	-	-	-	-	KC117509.1
278071-Ranunculus flammula	KX166222.1	AY954204.1	GU258025.1	HM850295.1	KX668071.1	-	-	-	-	-	-	-	-	-	-
286919-Ranunculus japonicus	MH710907.1	AY954200.1	HQ338226.1	FJ449862.1	DQ410744.1	-	-	-	-	-	-	-	KC840105.1	-	-
286924-Ranunculus lanuginosus	AY680163.1	AY954194.1	HQ338231.1	-	KX668006.1	-	-	-	-	-	-	-	-	-	-
1899342-Ranunculus limosella	KX640978.1	-	-	-	-	-	-	-	-	-	-	-	-	-	-
286898-Ranunculus fluitans	AY680069.1	AY954129.1	FJ619880.1	JN891886.1	-	-	-	-	-	-	-	HQ894446.1	MF167629.1	AB296150.1	MG162724.1
286964-Ranunculus peltatus	KX166651.1	-	-	JN892102.1	-	-	-	-	-	-	-	JN894996.1	HQ894438.1	-	MG162763.1
286966-Ranunculus penicillatus	MG098966.1	-	-	JN892100.1	-	-	-	-	-	-	-	KF871230.1	MF167611.1	AB296157.1	MG162771.1
147635-Ranunculus sceleratus	KX277667.1	GU257993.1	GU258043.1	AB517148.1	DQ410746.1	-	KC842059.1	KC841989.1	KC842093.1	KC842024.1	-	-	HQ596811.1	-	KC842129.1
286837-Ceratocephala falcata	AY680191.1	AY954229.1	-	-	-	-	-	-	-	-	-	-	-	-	-
59993-Myosurus minimus	AJ347913.1	FJ626502.1	-	DQ099441.1	AJ413305.1	-	-	-	-	-	-	AJ414344.1	-	-	-
286857-Ranunculus arcticus	KT960247.1	AY954125.1	KP687312.1	KT960601.1	GQ245367.1	KC842098.1	KC842029.1	KC841958.1	KC842063.1	KC841993.1	-	-	-	-	-
286916-Ranunculus hyperboreus	KT960156.1	AY954135.1	HQ338224.1	KT960610.1	GQ245372.1	-	-	-	-	-	-	-	-	-	-
286950-Ranunculus nivalis	MG237558.1	AY954123.1	GU258032.1	KT960681.1	DQ860598.1	KC842118.1	KC842049.1	KC841978.1	KC842082.1	-	-	-	-	-	-
286984-Ranunculus pygmaeus	MG237006.1	AY954122.1	KP687335.1	KT960698.1	DQ860599.1	KC842126.1	KC842056.1	KC841986.1	KC842090.1	KC842021.1	-	-	-	-	-
395310-Ranunculus sulphureus	MG236227.1	FM242752.1	JF510003.1	KT960425.1	DQ860600.1	KC842130.1	KC842060.1	KC841990.1	KC842094.1	KC842025.1	-	-	-	-	-
74828-Ranunculus bulbosus	KX166669.1	-	-	HM850293.1	KY697496.1	-	-	-	-	-	-	HM851057.1	FJ493303.1	FJ490812.1	-
147621-Ranunculus buchananii	EF017689.1	-	-	-	-	-	-	-	-	-	AF323329.1	-	-	-	-
286879-Ranunculus carpaticola	KY672019.1	AY954111.1	FJ619869.1	-	-	KC842102.1	KC842033.1	KC841962.1	KC842067.1	KC841997.1	-	-	-	-	-
147626-Ranunculus grahamii	EF017680.1	-	-	-	-	-	-	-	-	-	AF323336.1	-	-	-	-
147628-Ranunculus haastii	EF017671.1	-	-	-	FJ744229.1	-	-	-	-	-	FJ711922.1	-	FJ744173.1	-	-
147689-Ranunculus piliferus	EF017695.1	-	-	-	-	-	-	-	-	-	AF323351.1	-	-	-	-
286926-Ranunculus lapponicus	MG234753.1	AY954134.1	-	MK525595.1	DQ860546.1	-	-	-	-	-	-	-	-	-	-
147630-Ranunculus lyallii	EF017670.1	AY954142.1	GU258029.1	EU053921.1	FJ744233.1	-	-	-	-	-	AF323324.1	-	FJ744178.1	-	-
231656-Clematis patens	AB120184.1	AB110503.1	-	-	-	-	-	-	-	-	-	-	-	-	-
945262-Ranunculus amblyolobus	AB617666.1	HM565148.1	HQ338250.1	-	-	-	-	-	-	-	-	-	-	AB617671.1	-
286858-Ranunculus arvensis	KX166591.1	AY954193.1	GU258017.1	JN892029.1	-	KC842099.1	KC842030.1	KC841959.1	KC842064.1	KC841994.1	-	-	-	AB617672.1	-
430041-Ranunculus ashibetsuensis	KR996518.1	AB296104.1	-	-	-	-	-	-	-	-	-	-	-	AB296107.1	KR996572.1
568535-Ranunculus brutius	AB617667.1	FM242795.1	HQ338171.1	-	-	-	-	-	-	-	-	-	-	AB617673.1	-
286883-Ranunculus caucasicus	AY680178.1	AY954192.1	GU258023.1	-	-	-	-	-	-	-	-	-	-	AB617674.1	-
147622-Ranunculus circinatus	KX165828.1	-	-	GU344677.1	-	-	-	-	-	-	-	HQ894448.1	HQ894442.1	AB296146.1	MG162710.1
945268-Ranunculus constantinopolitanus	AB617668.1	HQ338350.1	HQ338188.1	-	-	-	-	-	-	-	-	-	-	AB617675.1	-
945274-Ranunculus kotschyi	AB617669.1	HQ338356.1	HQ338227.1	-	-	-	-	-	-	-	-	-	-	AB617676.1	-
286974-Ranunculus polyanthemos	MN151385.1	AY954185.1	GU258040.1	-	HM590338.1	-	-	-	-	-	-	-	-	AB617679.1	-
945285-Ranunculus sericeus	HQ338340.1	HM565167.1	HQ338294.1	-	-	-	-	-	-	-	-	-	-	AB617677.1	-
168837-Ranunculus sileifolius	HQ338341.1	HQ338367.1	HQ338295.1	-	-	-	-	-	-	-	-	-	-	-	-
945286-Ranunculus sojakii	AB617670.1	HQ338368.1	HQ338151.1	-	-	-	-	-	-	-	-	-	-	AB617678.1	-
286996-Ranunculus sphaerospermus	AY680066.1	AY954132.1	GU258044.1	-	-	-	-	-	-	-	-	-	-	AB296161.1	-
22903-Ranunculus trichophyllus	DQ311658.1	AY954133.1	GU258046.1	L08766.1	-	-	-	-	-	-	-	HQ894447.1	HQ894441.1	AB296165.1	MG162780.1
376248-Ranunculus ficariifolius	DQ410729.1	HQ338375.1	HQ338203.1	-	DQ410745.1	-	-	-	-	-	-	-	-	-	-
286945-Ranunculus muricatus	DQ410718.1	AY954191.1	HQ338255.1	HM850296.1	DQ410740.1	-	-	-	-	-	-	-	-	-	-
376249-Ranunculus polii	DQ410717.1	-	-	-	DQ410743.1	-	-	-	-	-	-	-	-	-	-
54805-Ranunculus taisanensis	HQ338344.1	HQ338370.1	HQ338157.1	-	-	-	-	-	-	-	-	-	-	-	-
376254-Ranunculus ternatus	DQ410716.1	-	-	-	DQ410742.1	-	-	-	-	-	-	-	-	-	-
568533-Ranunculus auricomus	KX165825.1	FM242739.1	-	HE574635.1	-	-	-	-	-	-	-	-	-	-	-
286869-Ranunculus brotherusii	GU444012.1	AY954119.1	KP687317.1	-	-	KC842100.1	KC842031.1	KC841960.1	KC842065.1	-	-	-	-	-	-
568530-Ranunculus aquatilis	KX166597.1	-	KC620491.1	MG247653.1	-	-	-	-	-	-	-	JN893994.1	KC820498.1	-	MG162700.1
529701-Ranunculus asiaticus	GU257963.1	FM242781.1	GU258018.1	KX421114.1	-	-	-	-	-	-	-	-	-	-	-
568534-Ranunculus baudotii	KX165824.1	-	-	JN891012.1	-	-	-	-	-	-	-	KP036406.1	-	-	MG162709.1
1155352-Ranunculus hederaceus	KX166970.1	-	-	JN892536.1	-	-	-	-	-	-	-	JN895320.1	-	-	MG162752.1
1155353-Ranunculus omiophyllus	KX165461.1	-	-	JN893041.1	-	-	-	-	-	-	-	JN895679.1	-	-	MG162756.1
568561-Ranunculus polyanthemoides	FM242865.1	FM242801.1	-	-	KU974025.1	-	-	-	-	-	-	-	-	-	-
35930-Ranunculus sardous	KX166649.1	AY954186.1	HQ338290.1	MG249692.1	-	-	-	-	-	-	-	-	-	-	-
286999-Ranunculus tanguticus	KX181008.1	-	-	KT280148.1	-	-	-	-	-	-	-	KT280252.1	-	-	-
1155354-Ranunculus tripartitus	KX166809.1	-	-	JN892309.1	-	-	-	-	-	-	-	JN895146.1	-	-	MG162784.1
147619-Ranunculus acaulis	KY242759.1	KY247127.1	KY242770.1	-	-	-	-	-	-	-	-	-	-	-	-
2036007-Ranunculus amphitrichus	KY242760.1	KY247126.1	KY242768.1	-	-	-	-	-	-	-	-	-	-	-	-
286862-Ranunculus biternatus	KY242766.1	KY247128.1	KY242771.1	-	-	-	-	-	-	-	-	-	-	-	-
286891-Ranunculus crassipes	KY242767.1	KY247131.1	KY242774.1	-	-	-	-	-	-	-	-	-	-	-	-
286899-Ranunculus fuegianus	FJ605809.1	AY954136.1	KY242780.1	-	-	-	-	-	-	-	-	-	-	-	-
2036008-Ranunculus glabrifolius	KY242762.1	KY247133.1	KY242769.1	-	-	-	-	-	-	-	-	-	-	-	-
147629-Ranunculus insignis	FJ711803.1	AY954141.1	KY242781.1	-	FJ744231.1	-	-	-	-	-	AF323356.1	-	FJ744175.1	-	-
2036009-Ranunculus moseleyi	KY242763.1	KY247134.1	KY242778.1	-	-	-	-	-	-	-	-	-	-	-	-
147633-Ranunculus pinguis	AF323299.1	KY247135.1	KY242782.1	-	-	-	-	-	-	-	AF323349.1	-	-	-	-
286982-Ranunculus pseudotrullifolius	KY242765.1	AY954139.1	KY242777.1	-	-	-	-	-	-	-	-	-	-	-	-
286998-Ranunculus subscaposus	AY680132.1	KY247137.1	KY242784.1	-	-	-	-	-	-	-	-	-	-	-	-
147638-Ranunculus verticillatus	AF323303.1	KY247136.1	KY242783.1	-	-	-	-	-	-	-	AF323353.1	-	-	-	-
568559-Ranunculus pedatifidus	MG235509.1	FM242744.1	GU258036.1	MF158745.1	-	KC842122.1	KC842052.1	KC841982.1	KC842086.1	KC842017.1	-	-	-	-	-
286928-Ranunculus longicaulis	KY624411.1	AY954117.1	HQ338237.1	KT280147.1	-	KC842114.1	KC842045.1	KC841974.1	KC842078.1	KC842009.1	-	-	-	-	-
2291151-Ranunculus kamchaticus	MH711387.1	-	-	-	-	-	-	-	-	-	-	-	-	-	-
286903-Ranunculus gmelinii	MG235770.1	AY954128.1	-	MG247389.1	GQ245369.1	-	-	-	-	-	-	KC475661.1	-	-	-
286986-Ranunculus reptans	AY680186.1	AY954205.1	HQ338288.1	-	GQ245381.1	-	-	-	-	-	-	-	-	-	-
568571-Ranunculus sabinei	MG235740.1	FM242751.1	-	MG247350.1	GQ245382.1	-	-	-	-	-	-	-	-	-	-
568576-Ranunculus turneri	MG236256.1	FM242753.1	-	MG247998.1	GQ245388.1	-	-	-	-	-	-	-	-	-	-
857728-Ranunculus hystriculus	MF964078.1	GU257983.1	GU258008.1	MF963151.1	-	-	-	-	-	-	-	-	-	-	-
286845-Ranunculus abortivus	MG236677.1	AY954126.1	-	HQ590231.1	-	-	-	-	-	-	-	-	HQ596808.1	-	-
945261-Ranunculus alismifolius	MG237037.1	HM565147.1	HQ338228.1	MG248951.1	-	-	-	-	-	-	-	-	-	-	-
1301440-Ranunculus allenii	MG236594.1	-	-	KC483819.1	-	-	-	-	-	-	-	KC475649.1	-	-	-
286877-Ranunculus cardiophyllus	MG236741.1	AY954124.1	HQ338179.1	MG247310.1	-	KC842101.1	KC842032.1	KC841961.1	KC842066.1	KC841996.1	-	-	-	-	-
2071521-Ranunculus cooleyae	MG235977.1	-	-	MG248097.1	-	-	-	-	-	-	-	-	-	-	-
286895-Ranunculus eschscholtzii	MG236552.1	JF740080.1	HQ338200.1	MG248356.1	-	KC842104.1	KC842035.1	KC841964.1	KC842069.1	-	-	-	-	-	-
568547-Ranunculus fascicularis	MG236200.1	FM242786.1	HQ338201.1	MG249247.1	-	-	-	-	-	-	-	-	-	-	-
2071522-Ranunculus flabellaris	MG234993.1	-	-	MG246194.1	-	-	-	-	-	-	-	-	-	-	-
286902-Ranunculus gelidus	MG236625.1	AY954114.1	HQ338205.1	MG248441.1	-	KC842106.1	KC842037.1	KC841966.1	KC842071.1	KC842001.1	-	-	-	-	-
1017150-Ranunculus glaberrimus	MG237256.1	JF509974.1	JF509988.1	MG247649.1	-	KC842107.1	KC842038.1	KC841967.1	KC842072.1	KC842002.1	-	-	-	-	-
476038-Ranunculus hispidus	MG235879.1	HQ338355.1	HQ338221.1	EU053920.1	-	KC842109.1	KC842040.1	KC841969.1	KC842074.1	KC842004.1	-	-	KP643458.1	-	-
568552-Ranunculus inamoenus	MG237080.1	KP687301.1	KP687326.1	MG249011.1	-	KP702731.1	KP702732.1	KP702734.1	KP702733.1	-	-	-	-	-	-
2044358-Ranunculus kauffmanii	MG098948.1	-	-	-	-	-	-	-	-	-	-	-	-	-	MG162753.1
568556-Ranunculus macounii	MG237407.1	HM565159.1	HQ338238.1	MG249425.1	-	-	-	-	-	-	-	-	-	-	-
286952-Ranunculus occidentalis	MG236278.1	HM565164.1	HQ338263.1	MG248024.1	-	-	-	-	-	-	-	-	-	-	-
945283-Ranunculus orthorhynchus	MG236632.1	HQ338364.1	HQ338267.1	MG248448.1	-	-	-	-	-	-	-	-	-	-	-
286962-Ranunculus parviflorus	MG237667.1	AY954202.1	HQ338270.1	HM850297.1	-	-	-	-	-	-	-	-	-	-	-
46994-Ranunculus recurvatus	MG237519.1	AY954175.1	-	HQ590233.1	-	-	-	-	-	-	-	-	KP643336.1	-	-
568568-Ranunculus rhomboideus	MG236754.1	FM242790.1	JF510000.1	JX848518.1	-	KC842127.1	KC842057.1	KC841987.1	KC842091.1	KC842022.1	-	-	-	-	-
568570-Ranunculus rionii	MG098973.1	FM242791.1	-	-	-	-	-	-	-	-	-	-	-	-	MG162778.1
857732-Ranunculus uncinatus	MG235096.1	GU257994.1	GU258047.1	MG246548.1	-	-	-	-	-	-	-	-	-	-	-
286846-Ranunculus acetosellifolius	MG779953.1	AY954226.1	HQ338261.1	-	-	MG779975.1	-	-	-	-	-	-	-	-	-
945259-Ranunculus acriformis	HQ338296.1	HQ338378.1	HQ338181.1	-	-	-	-	-	-	-	-	-	-	-	-
286848-Ranunculus adoneus	KP687265.1	HM565145.1	HQ338195.1	-	-	KC842095.1	KC842026.1	KC841955.1	KC842061.1	-	-	-	-	-	-
286849-Ranunculus aduncus	AY680088.1	AY954143.1	HQ338206.1	-	-	-	-	-	-	-	-	-	-	-	-
945260-Ranunculus afghanicus	HQ338297.1	HM565146.1	HQ338217.1	-	-	-	-	-	-	-	-	-	-	-	-
286851-Ranunculus alpestris	AY680078.1	AY954221.1	HQ338239.1	KF602171.1	-	-	-	-	-	-	-	-	-	-	-
286856-Ranunculus apenninus	AY680091.1	AY954150.1	HQ338273.1	-	-	-	-	-	-	-	-	-	-	-	-
568532-Ranunculus argyreus	FM242844.1	FM242780.1	HQ338150.1	-	-	-	-	-	-	-	-	-	-	-	-
945263-Ranunculus aucheri	HQ338301.1	HQ338379.1	HQ338161.1	-	-	-	-	-	-	-	-	-	-	-	-
286859-Ranunculus baldshuanicus	AY680174.1	AY954195.1	HQ338168.1	-	-	-	-	-	-	-	-	-	-	-	-
286861-Ranunculus bilobus	AY680077.1	AY954220.1	HQ338169.1	-	-	-	-	-	-	-	-	-	-	-	-
945264-Ranunculus brachylobus	HQ338302.1	HQ338347.1	HQ338192.1	-	-	-	-	-	-	-	-	-	-	-	-
286871-Ranunculus bullatus	AY680114.1	AY954161.1	HQ338175.1	-	-	-	-	-	-	-	-	-	-	-	-
945265-Ranunculus cacuminis	HQ338305.1	HQ338373.1	HQ338176.1	-	-	-	-	-	-	-	-	-	-	-	-
286875-Ranunculus cappadocicus	AY680117.1	AY954173.1	HQ338178.1	-	-	-	-	-	-	-	-	-	-	-	-
286876-Ranunculus caprarum	AY680151.1	HM565151.1	HQ338193.1	-	-	-	-	-	-	-	-	-	-	-	-
286878-Ranunculus carinthiacus	AY680093.1	AY954145.1	HQ338180.1	-	-	-	-	-	-	-	-	-	-	-	-
286880-Ranunculus carpaticus	AY680096.1	AY954154.1	HQ338182.1	-	-	-	-	-	-	-	-	-	-	-	-
568538-Ranunculus cassius	FM242848.1	FM242784.1	HQ338183.1	-	-	-	-	-	-	-	-	-	-	-	-
286885-Ranunculus chius	AY680176.1	AY954201.1	HQ338185.1	-	-	-	-	-	-	-	-	-	-	-	-
286886-Ranunculus cicutarius	AY680103.1	AY954167.1	HQ338186.1	-	-	-	-	-	-	-	-	-	-	-	-
286887-Ranunculus collinus	AY680059.1	AY954137.1	HQ338187.1	-	-	-	-	-	-	-	-	-	-	-	-
286889-Ranunculus cornutus	AY680153.1	-	HQ338189.1	-	-	-	-	-	-	-	-	-	-	-	-
286890-Ranunculus cortusifolius	KF418317.1	AY954160.1	HQ338190.1	HM850294.1	-	-	-	-	-	-	-	-	-	-	-
286892-Ranunculus crenatus	AY680086.1	AY954228.1	HQ338191.1	-	-	-	-	-	-	-	-	-	-	-	-
945269-Ranunculus damascenus	HQ338309.1	HM565153.1	HQ338196.1	-	-	-	-	-	-	-	-	-	-	-	-
945270-Ranunculus elbrusensis	HQ338311.1	HQ338352.1	HQ338199.1	-	-	-	-	-	-	-	-	-	-	-	-
286897-Ranunculus flagelliformis	AY680182.1	AY954208.1	HQ338202.1	-	-	-	-	-	-	-	-	-	-	-	-
286900-Ranunculus garganicus	AY680107.1	AY954165.1	HQ338204.1	-	-	-	-	-	-	-	-	-	-	-	-
568548-Ranunculus glabriusculus	HQ338315.1	FM242748.1	HQ338207.1	-	-	-	-	-	-	-	-	-	-	-	-
286905-Ranunculus gouanii	AY680098.1	AY954151.1	HQ338209.1	-	-	-	-	-	-	-	-	-	-	-	-
286906-Ranunculus gracilis	AY680120.1	AY954171.1	HQ338210.1	-	-	-	-	-	-	-	-	-	-	-	-
286908-Ranunculus granatensis	AY680165.1	AY954197.1	HQ338212.1	-	-	-	-	-	-	-	-	-	-	-	-
286909-Ranunculus grandiflorus	AY680053.1	AY954203.1	HQ338213.1	-	-	-	-	-	-	-	-	-	-	-	-
286912-Ranunculus gregarius	AY680100.1	AY954159.1	HQ338214.1	-	-	-	-	-	-	-	-	-	-	-	-
945271-Ranunculus hawaiensis	HQ338316.1	HM565155.1	HQ338215.1	-	-	-	-	-	-	-	-	-	-	-	-
945272-Ranunculus heterorrhizus	HQ338317.1	HM565156.1	HQ338216.1	-	-	-	-	-	-	-	-	-	-	-	-
945273-Ranunculus hierosolymitanus	HQ338318.1	HQ338354.1	HQ338218.1	-	-	-	-	-	-	-	-	-	-	-	-
286913-Ranunculus hirtellus	AY680038.1	AY954120.1	HQ338220.1	-	-	KC842108.1	KC842039.1	KC841968.1	KC842073.1	KC842003.1	-	-	-	-	-
286914-Ranunculus hybridus	AY680189.1	AY954211.1	HQ338222.1	-	-	-	-	-	-	-	-	-	-	-	-
286915-Ranunculus hydrophilus	AY680181.1	HM565157.1	HQ338223.1	-	-	-	-	-	-	-	-	-	-	-	-
286917-Ranunculus illyricus	AY680119.1	AY954162.1	HQ338225.1	-	-	-	-	-	-	-	-	-	-	-	-
286923-Ranunculus laetus	AY680172.1	HQ338357.1	HQ338229.1	-	-	-	-	-	-	-	-	-	-	-	-
286927-Ranunculus lateriflorus	AY680179.1	AY954209.1	HQ338233.1	-	-	-	-	-	-	-	-	-	-	-	-
945275-Ranunculus leptorrhynchus	HQ338323.1	HQ338358.1	HQ338234.1	-	-	-	-	-	-	-	-	-	-	-	-
945276-Ranunculus linearilobus	HQ338324.1	HQ338359.1	HQ338235.1	-	-	-	-	-	-	-	-	-	-	-	-
945277-Ranunculus macropodoides	HQ338326.1	HQ338360.1	HQ338240.1	-	-	-	-	-	-	-	-	-	-	-	-
945278-Ranunculus macrorrhynchus	HQ338327.1	HM565160.1	HQ338241.1	-	-	-	-	-	-	-	-	-	-	-	-
945279-Ranunculus magellensis	HQ338328.1	HQ338376.1	HQ338242.1	-	-	-	-	-	-	-	-	-	-	-	-
945280-Ranunculus makaluensis	HQ338329.1	HM565161.1	HQ338243.1	-	-	-	-	-	-	-	-	-	-	-	-
286932-Ranunculus marginatus	AY680150.1	AY954177.1	HQ338244.1	-	-	-	-	-	-	-	-	-	-	-	-
286933-Ranunculus marschlinsii	AY680089.1	AY954147.1	HQ338245.1	-	-	-	-	-	-	-	-	-	-	-	-
945281-Ranunculus mauiensis	HQ338330.1	HM565162.1	HQ338246.1	-	-	-	-	-	-	-	-	-	-	-	-
286935-Ranunculus membranaceus	HQ338331.1	HQ338361.1	HQ338247.1	-	-	-	-	-	-	-	-	-	-	-	-
502446-Ranunculus meyeri	EU288400.1	EU288374.1	HQ338248.1	-	-	-	-	-	-	-	-	-	-	-	-
286936-Ranunculus micranthus	AY680042.1	AY954113.1	HQ338249.1	-	-	KC842116.1	KC842047.1	KC841976.1	KC842080.1	-	-	-	-	-	-
286938-Ranunculus millefoliatus	AY680108.1	AY954166.1	HQ338251.1	-	-	-	-	-	-	-	-	-	-	-	-
945282-Ranunculus millefolius	HQ338332.1	HQ338362.1	HQ338252.1	-	-	-	-	-	-	-	-	-	-	-	-
286941-Ranunculus montanus	AY680094.1	AY954149.1	HQ338253.1	KF602172.1	-	-	-	-	-	-	-	-	-	-	-
286943-Ranunculus multifidus	AY680162.1	AY954183.1	HQ338254.1	-	-	-	-	-	-	-	-	-	-	-	-
286948-Ranunculus neapolitanus	AY680123.1	AY954187.1	HQ338256.1	-	-	-	-	-	-	-	-	-	-	-	-
286929-Ranunculus nephelogenes	HQ338333.1	HM565163.1	HQ338258.1	-	-	KC842117.1	KC842048.1	KC841977.1	KC842081.1	KC842012.1	-	-	-	-	-
430044-Ranunculus nipponicus	FM242834.1	FM242770.1	HQ338259.1	-	-	-	-	-	-	-	-	-	-	-	-
286954-Ranunculus ollissiponensis	AY680109.1	AY954157.1	HQ338264.1	-	-	-	-	-	-	-	-	-	-	-	-
286955-Ranunculus ophioglossifolius	AY680180.1	AY954207.1	HQ338265.1	-	-	-	-	-	-	-	-	-	-	-	-
502447-Ranunculus oreophytus	EU288413.1	HQ338377.1	HQ338266.1	-	-	KC842120.1	KC842051.1	KC841980.1	KC842084.1	KC842015.1	-	-	-	-	-
286957-Ranunculus paludosus	AY680102.1	AY954155.1	HQ338268.1	-	-	-	-	-	-	-	-	-	-	-	-
286959-Ranunculus papulentus	AY680058.1	AY954138.1	HQ338269.1	-	-	-	-	-	-	-	-	-	-	-	-
568560-Ranunculus petiolaris	HQ338336.1	HQ338365.1	HQ338274.1	-	-	-	-	-	-	-	-	-	-	-	-
502448-Ranunculus pinnatus	EU288415.1	EU288388.1	HQ338275.1	-	-	-	-	-	-	-	-	-	-	-	-
286971-Ranunculus platanifolius	EU792846.1	AY954216.1	HQ338276.1	-	EU792600.1	-	-	-	-	-	-	-	-	-	-
286973-Ranunculus pollinensis	AY680097.1	AY954152.1	HQ338277.1	-	-	-	-	-	-	-	-	-	-	-	-
286978-Ranunculus pseudohirculus	AY680111.1	AY954118.1	HQ338278.1	-	-	-	-	-	-	-	-	-	-	-	-
286980-Ranunculus pseudomillefoliatus	AY680110.1	AY954156.1	HQ338279.1	-	-	-	-	-	-	-	-	-	-	-	-
286981-Ranunculus pseudomontanus	AY680090.1	AY954146.1	HQ338280.1	-	-	-	-	-	-	-	-	-	-	-	-
286983-Ranunculus psilostachys	AY680106.1	AY954170.1	HQ338281.1	-	-	-	-	-	-	-	-	-	-	-	-
568564-Ranunculus pulchellus	HQ338337.1	FM242792.1	HQ338282.1	-	-	KC842124.1	KC842054.1	KC841984.1	KC842088.1	KC842019.1	-	-	-	-	-
568565-Ranunculus punctatus	FM242818.1	FM242754.1	JF509999.1	-	-	KC842125.1	KC842055.1	KC841985.1	KC842089.1	KC842020.1	-	-	-	-	-
568566-Ranunculus radicans	FM242857.1	FM242793.1	HQ338260.1	-	-	-	-	-	-	-	-	-	-	-	-
502449-Ranunculus raeae	EU288416.1	EU288390.1	HQ338286.1	-	-	-	-	-	-	-	-	-	-	-	-
945284-Ranunculus regelianus	HQ338338.1	HQ338366.1	HQ338271.1	-	-	-	-	-	-	-	-	-	-	-	-
286988-Ranunculus rumelicus	AY680104.1	AY954168.1	HQ338289.1	-	-	-	-	-	-	-	-	-	-	-	-

286989-Ranunculus sartorianus	AY680095.1	AY954148.1	HQ338283.1	-	-	-	-	-	-	-	-	-	-	-	-
568572-Ranunculus septentrionalis	FM242832.1	FM242768.1	HQ338292.1	-	-	-	-	-	-	-	-	-	-	-	-
286994-Ranunculus serbicus	AY680166.1	AY954196.1	HQ338293.1	-	-	-	-	-	-	-	-	-	-	-	-
320425-Ranunculus spicatus	AY954244.1	AY954158.1	HQ338152.1	-	-	-	-	-	-	-	-	-	-	-	-
286997-Ranunculus sprunerianus	AY680105.1	AY954169.1	HQ338153.1	-	-	-	-	-	-	-	-	-	-	-	-
502451-Ranunculus stagnalis	EU288419.1	EU288392.1	HQ338154.1	-	-	-	-	-	-	-	-	-	-	-	-
945287-Ranunculus strigillosus	HQ338343.1	HQ338369.1	HQ338155.1	-	-	-	-	-	-	-	-	-	-	-	-
568575-Ranunculus submarginatus	FM242841.1	FM242777.1	HQ338156.1	-	-	-	-	-	-	-	-	-	-	-	-
502452-Ranunculus tembensis	EU288421.1	EU288393.1	HQ338158.1	-	-	-	-	-	-	-	-	-	-	-	-
945288-Ranunculus tenuirostris	HQ338345.1	HQ338371.1	HQ338159.1	-	-	-	-	-	-	-	-	-	-	-	-
945289-Ranunculus termei	HQ338346.1	HQ338372.1	HQ338160.1	-	-	-	-	-	-	-	-	-	-	-	-
320426-Ranunculus traunfellneri	AY954245.1	AY954222.1	HQ338162.1	-	-	-	-	-	-	-	-	-	-	-	-
287001-Ranunculus trilobus	AY680149.1	AY954176.1	HQ338163.1	-	-	-	-	-	-	-	-	HM851063.1	-	-	-
287004-Ranunculus velutinus	AY680173.1	AY954198.1	HQ338164.1	-	-	-	-	-	-	-	-	-	-	-	-
287005-Ranunculus venetus	AY680087.1	AY954144.1	HQ338165.1	-	-	-	-	-	-	-	-	-	-	-	-
287006-Ranunculus villarsii	AY680099.1	AY954153.1	HQ338166.1	-	-	-	-	-	-	-	-	-	-	-	-
502453-Ranunculus volkensii	EU288424.1	EU288395.1	HQ338167.1	-	-	-	-	-	-	-	-	-	-	-	-
286831-Ranunculus apiifolius	AY680092.1	AY954140.1	GU258016.1	-	-	-	-	-	-	-	-	-	-	-	-
286850-Ranunculus allemannii	AY680039.1	JF509972.1	JF509987.1	-	-	-	-	-	-	-	-	-	-	-	-
286852-Ranunculus altaicus	AY680112.1	AY954116.1	-	-	-	-	-	-	-	-	-	-	-	-	-
286853-Ranunculus amerophyllus	AY680146.1	-	-	-	-	-	-	-	-	-	-	-	-	-	-
286860-Ranunculus basilobatus	AY680131.1	-	-	-	-	-	-	-	-	-	-	-	-	-	-
286863-Ranunculus bonariensis	AY680183.1	GU257986.1	GU258019.1	-	-	-	-	-	-	-	-	-	-	-	-
286864-Ranunculus borealis	AY680168.1	FM242766.1	-	-	-	-	-	-	-	-	-	-	-	-	-
286865-Ranunculus brassii	AY680127.1	-	-	-	-	-	-	-	-	-	-	-	-	-	-
286868-Ranunculus breyninus	AY680115.1	AY954172.1	GU258021.1	-	-	-	-	-	-	-	-	-	-	-	-
286872-Ranunculus calandrinioides	AY680073.1	-	-	-	-	MG779993.1	-	-	-	-	-	-	-	-	-
286881-Ranunculus carpinetorum	AY680031.1	-	-	-	-	-	-	-	-	-	-	-	-	-	-
286882-Ranunculus cassubicifolius	KF672026.1	AY954112.1	FJ619867.1	-	-	KC842103.1	KC842034.1	KC841963.1	KC842068.1	KC841998.1	-	-	-	-	-
286884-Ranunculus chilensis	AY680157.1	AY954179.1	-	-	-	-	-	-	-	-	-	-	-	-	-
286888-Ranunculus colonorum	AY680139.1	-	-	-	-	-	-	-	-	-	-	-	-	-	-
320420-Ranunculus creticus	AY954239.1	AY954163.1	-	-	-	-	-	-	-	-	-	-	-	-	-
320421-Ranunculus cupreus	AY954240.1	AY954164.1	-	-	-	-	-	-	-	-	-	-	-	-	-
286893-Ranunculus dissectifolius	AY680144.1	-	-	-	-	-	-	-	-	-	-	-	-	-	-
286894-Ranunculus eichleranus	AY680138.1	-	-	-	-	-	-	-	-	-	-	-	-	-	-
286901-Ranunculus gayeri	AY680028.1	-	-	-	-	-	-	-	-	-	-	-	-	-	-
286910-Ranunculus grandifolius	AY680169.1	FM242772.1	-	-	-	-	-	-	-	-	-	-	-	-	-
286911-Ranunculus graniticola	AY680141.1	-	-	-	-	-	-	-	-	-	-	-	-	-	-
286920-Ranunculus kochii	AY680193.1	AY954231.1	-	-	-	-	-	-	-	-	-	-	-	-	-
286925-Ranunculus lappaceus	AY680140.1	-	-	-	-	-	-	-	-	-	-	-	-	-	-
286930-Ranunculus lowii	AY680128.1	-	-	-	-	-	-	-	-	-	-	-	-	-	-
286931-Ranunculus maclovianus	AY680158.1	AY954181.1	GU258030.1	-	-	-	-	-	-	-	-	-	-	-	-
286934-Ranunculus melzeri	AY680036.1	-	-	-	-	-	-	-	-	-	-	-	-	-	-
286937-Ranunculus millanii	AY680134.1	-	-	-	-	-	-	-	-	-	-	-	-	-	-
286939-Ranunculus minutiflorus	AY680156.1	-	-	-	-	-	-	-	-	-	-	-	-	-	-
286940-Ranunculus monophyllus	AY680043.1	-	-	-	-	-	-	-	-	-	-	-	-	-	-
286942-Ranunculus muelleri	AY680143.1	-	-	-	-	-	-	-	-	-	-	-	-	-	-
286944-Ranunculus multiscapus	AY680133.1	-	-	-	-	-	-	-	-	-	-	-	-	-	-
286946-Ranunculus nanus	AY680142.1	-	-	-	-	-	-	-	-	-	-	-	-	-	-
286947-Ranunculus natans	AY680113.1	AY954134.1	GU258031.1	-	-	-	-	-	-	-	-	-	-	-	-
286949-Ranunculus niphophilus	AY680145.1	-	-	-	-	-	-	-	-	-	-	-	-	-	-
286951-Ranunculus notabilis	AY680033.1	AY954115.1	FJ619873.1	-	-	KC842119.1	KC842050.1	KC841979.1	KC842083.1	KC842014.1	-	-	-	-	-
286958-Ranunculus pannonicus	AY680032.1	JF509979.1	JF509996.1	-	-	-	-	-	-	-	-	-	-	-	-
286963-Ranunculus peduncularis	AY680154.1	AY954180.1	-	-	-	-	-	-	-	-	-	-	-	-	-
286968-Ranunculus pensylvanicus	AY680147.1	AY954190.1	GU258038.1	KJ841512.1	-	-	-	-	-	-	-	-	-	-	-
286969-Ranunculus pilisiensis	AY680034.1	JF509981.1	JF509998.1	-	-	-	-	-	-	-	-	-	-	-	-
286970-Ranunculus pimpinellifolius	AY680136.1	-	-	-	-	-	-	-	-	-	-	-	-	-	-
286972-Ranunculus plebeius	AY680137.1	-	-	-	-	-	-	-	-	-	-	-	-	-	-
286975-Ranunculus praemorsus	AY680161.1	-	-	-	-	-	-	-	-	-	-	-	-	-	-
286976-Ranunculus prasinus	AY680057.1	-	-	-	-	-	-	-	-	-	-	-	-	-	-
286977-Ranunculus propinquus	AY680170.1	-	-	-	-	-	-	-	-	-	-	-	-	-	-
286979-Ranunculus pseudolowii	AY680130.1	-	-	-	-	-	-	-	-	-	-	-	-	-	-
286987-Ranunculus rufosepalus	AY680047.1	AY954121.1	GU258042.1	-	-	-	-	-	-	-	-	-	-	-	-
286990-Ranunculus saruwagedicus	AY680129.1	-	-	-	-	-	-	-	-	-	-	-	-	-	-
286991-Ranunculus scapiger	AY680135.1	-	-	-	-	-	-	-	-	-	-	-	-	-	-
286992-Ranunculus seguieri	EU792856.1	AY954215.1	-	-	EU792610.1	KF528845.1	-	-	-	-	-	-	-	-	-
286995-Ranunculus sericocephalus	AY680155.1	-	-	-	-	-	-	-	-	-	-	-	-	-	-
287000-Ranunculus thora	AY680188.1	AY954210.1	GU258045.1	-	-	-	-	-	-	-	-	-	-	-	-
287002-Ranunculus trullifolius	AY680159.1	-	-	-	-	-	-	-	-	-	-	-	-	-	-
287003-Ranunculus variabilis	KF672008.1	-	-	-	-	-	-	-	-	-	-	-	-	-	-
287007-Ranunculus vindobonensis	AY680035.1	JF509984.1	JF510004.1	-	-	-	-	-	-	-	-	-	-	-	-
320427-Ranunculus weyleri	AY954246.1	AY954189.1	-	-	-	-	-	-	-	-	-	-	-	-	-
1017148-Ranunculus adoxifolius	JF509959.1	JF509970.1	-	-	-	KC842096.1	KC842027.1	KC841956.1	-	-	-	-	-	-	-
1017149-Ranunculus allegheniensis	JF509960.1	JF509971.1	JF509986.1	-	-	KC842097.1	KC842028.1	KC841957.1	KC842062.1	KC841992.1	-	-	-	-	-
1301442-Ranunculus confervoides	KR996524.1	-	-	KC483835.1	-	-	-	-	-	-	-	KC475658.1	-	-	KR996581.1
857731-Ranunculus formosa montanus	GU257966.1	GU257988.1	GU258026.1	-	-	KC842105.1	KC842036.1	KC841965.1	KC842070.1	KC842000.1	-	-	-	-	-
1017151-Ranunculus jovis	KP687280.1	JF509975.1	KP687329.1	-	-	KC842110.1	KC842041.1	KC841970.1	KC842075.1	KC842005.1	-	-	-	-	-
1017152-Ranunculus junipericola	JF509964.1	JF509976.1	JF509991.1	-	-	KC842111.1	KC842042.1	KC841971.1	KC842076.1	KC842006.1	-	-	-	-	-
568554-Ranunculus krylovii	FM242826.1	FM242762.1	JF509992.1	-	-	KC842112.1	KC842043.1	KC841972.1	-	KC842007.1	-	-	-	-	-
568555-Ranunculus lasiocarpus	FM242827.1	FM242763.1	JF509993.1	-	-	KC842113.1	KC842044.1	KC841973.1	KC842077.1	KC842008.1	-	-	-	-	-
1017153-Ranunculus macauleyi	JF509965.1	JF509977.1	JF509994.1	-	-	KC842115.1	KC842046.1	KC841975.1	KC842079.1	-	-	-	-	-	-
1017154-Ranunculus palmatifidus	JF509966.1	JF509978.1	JF509995.1	-	-	KC842121.1	-	KC841981.1	KC842085.1	-	-	-	-	-	-
568569-Ranunculus rigescens	FM242809.1	FM242745.1	JF510001.1	-	-	KC842128.1	KC842058.1	KC841988.1	KC842092.1	KC842023.1	-	-	-	-	-
568526-Ranunculus affinis	FM242811.1	FM242747.1	JF509985.1	JX848517.1	-	-	-	-	-	-	-	-	-	-	-
1385424-Ranunculus montenegrinus	KF528832.1	-	-	-	-	KF528841.1	-	-	-	-	-	-	-	-	-
1497447-Ranunculus potaninii	KF233845.1	-	-	-	KF233865.1	-	-	-	-	-	-	-	-	-	-
1385425-Ranunculus wettsteinii	KF528837.1	-	-	-	-	KF528849.1	-	-	-	-	-	-	-	-	-
1747521-Ranunculus mongolicus	KR996527.1	-	-	-	-	-	-	-	-	-	-	-	-	-	KR996585.1
1017155-Ranunculus pegaeus	JF509967.1	JF509980.1	JF509997.1	-	-	KP723464.1	KP723463.1	KP723461.1	KP723462.1	-	-	-	-	-	-
1747522-Ranunculus schmalhausenii	KR996539.1	-	-	-	-	-	-	-	-	-	-	-	-	-	KR996600.1
857730-Ranunculus cheirophyllus	GU257965.1	GU257987.1	GU258024.1	-	-	-	-	-	-	-	-	-	-	-	-
568558-Ranunculus oxyspermus	GU257967.1	FM242799.1	GU258033.1	-	-	-	-	-	-	-	-	-	-	-	-
857741-Ranunculus papyrocarpus	GU257968.1	GU257990.1	GU258034.1	-	-	-	-	-	-	-	-	-	-	-	-
857742-Ranunculus pinardi	GU257970.1	GU257992.1	GU258039.1	-	-	-	-	-	-	-	-	-	-	-	-
568527-Ranunculus ampelophyllus	FM242842.1	FM242778.1	-	-	-	-	-	-	-	-	-	-	-	-	-
568528-Ranunculus amurensis	FM242820.1	FM242756.1	-	-	-	-	-	-	-	-	-	-	-	-	-
568529-Ranunculus anadyriensis	FM242802.1	FM242738.1	-	-	-	-	-	-	-	-	-	-	-	-	-
568536-Ranunculus californicus	FM242846.1	FM242782.1	-	-	-	-	-	-	-	-	-	-	-	-	-
568537-Ranunculus canus	FM242847.1	FM242783.1	-	-	-	-	-	-	-	-	-	-	-	-	-
568543-Ranunculus dahuricus	FM242823.1	FM242759.1	-	-	-	-	-	-	-	-	-	-	-	-	-
568736-Ranunculus fallax	FM242824.1	FM242760.1	-	-	-	-	-	-	-	-	-	-	-	-	-
568557-Ranunculus novus	FM242833.1	FM242769.1	-	-	-	-	-	-	-	-	-	-	-	-	-
568562-Ranunculus polyphyllus	FM242838.1	FM242774.1	-	-	-	-	-	-	-	-	-	-	-	-	-
568563-Ranunculus polyrhizos	FM242839.1	FM242775.1	-	-	-	-	-	-	-	-	-	-	-	-	-
568567-Ranunculus reptabundus	FM242819.1	FM242755.1	-	-	-	-	-	-	-	-	-	-	-	-	-
568573-Ranunculus steveni	FM242864.1	FM242800.1	-	-	-	-	-	-	-	-	-	-	-	-	-
568574-Ranunculus subcorymbosus	FM242810.1	FM242746.1	-	-	-	-	-	-	-	-	-	-	-	-	-
286921-Ranunculus kuepferi	EU792758.1	-	-	-	EU792561.1	-	-	-	-	-	-	-	-	-	-
1017156-Ranunculus rubrocalyx	JF509968.1	JF509982.1	JF510002.1	-	-	-	-	-	-	-	-	-	-	-	-
502444-Ranunculus bequaertii	EU288399.1	EU288372.1	-	-	-	-	-	-	-	-	-	-	-	-	-
502450-Ranunculus simensis	EU288418.1	EU288391.1	-	-	-	-	-	-	-	-	-	-	-	-	-
147623-Ranunculus crithmifolius	FJ711784.1	-	-	-	FJ744225.1	-	-	-	-	-	FJ711904.1	-	FJ744170.1	-	-
38867-Ranunculus enysii	FJ711796.1	-	-	-	FJ744227.1	-	-	-	-	-	AF323368.1	-	FJ744171.1	-	-
667039-Ranunculus hungaricus	FJ619894.1	FJ625803.1	FJ619875.1	-	-	-	-	-	-	-	-	-	-	-	-
147637-Ranunculus sericophyllus	FJ711875.1	-	-	-	FJ744236.1	-	-	-	-	-	AF323338.1	-	FJ744181.1	-	-
2590995-Ranunculus olgae	MN151381.1	-	-	-	-	-	-	-	-	-	-	-	-	-	-
2590996-Ranunculus paucidentatus	MN151379.1	-	-	-	-	-	-	-	-	-	-	-	-	-	-
2590997-Ranunculus songoricus	MN151377.1	-	-	-	-	-	-	-	-	-	-	-	-	-	-
2592877-Ranunculus talassicus	MN151383.1	-	-	-	-	-	-	-	-	-	-	-	-	-	-
147620-Ranunculus anemoneus	AF323273.1	-	-	-	-	-	-	-	-	-	AF323323.1	-	-	-	-
147687-Ranunculus paucifolius	AF323312.1	-	-	-	-	-	-	-	-	-	AF323362.1	-	-	-	-
147624-Ranunculus godleyanus	AF323309.1	-	-	-	-	-	-	-	-	-	AF323360.1	-	-	-	-
147625-Ranunculus gracilipes	AF323314.1	-	-	-	-	-	-	-	-	-	AF323365.1	-	-	-	-
147627-Ranunculus gunnianus	AF323298.1	-	-	-	-	-	-	-	-	-	AF323348.1	-	-	-	-
147631-Ranunculus nivicola	AF323308.1	-	-	-	-	-	-	-	-	-	AF323358.1	-	-	-	-
147632-Ranunculus pachyrrhizus	AF323295.1	-	-	-	-	-	-	-	-	-	AF323346.1	-	-	-	-
147634-Ranunculus recens	AF323320.1	-	-	-	-	-	-	-	-	-	-	-	-	-	-
147636-Ranunculus scrithalis	AF323305.1	-	-	-	-	-	-	-	-	-	AF323355.1	-	-	-	-
147639-Ranunculus viridis	AF323297.1	-	-	-	-	-	-	-	-	-	AF323347.1	-	-	-	-
430042-Ranunculus yezoensis	-	AB296108.1	-	-	-	-	-	-	-	-	-	-	-	AB296111.1	-
430043-Ranunculus kadzusensis	-	AB296112.1	-	-	-	-	-	-	-	-	-	-	-	AB296116.1	-
323237-Ranunculus lomatocarpus	-	AY954178.1	-	-	-	-	-	-	-	-	-	-	-	-	-
334596-Ranunculus macranthus	-	DQ069586.1	-	DQ069502.1	-	-	-	-	-	-	-	-	-	-	-
502443-Ranunculus aberdaricus	-	EU288371.1	-	-	-	-	-	-	-	-	-	-	-	-	-
502445-Ranunculus cryptanthus	-	EU288373.1	-	-	-	-	-	-	-	-	-	-	-	-	-
568541-Ranunculus buhsei	-	-	HQ338173.1	-	-	-	-	-	-	-	-	-	-	-	-
1301443-Ranunculus subrigidus	-	-	-	KC483866.1	-	-	-	-	-	-	-	KC475675.1	-	-	-
1000426-Ranunculus tuberosus	-	-	-	KF602158.1	-	-	-	-	-	-	-	-	-	-	-
1793844-Ranunculus ranceorum	-	-	-	KT626770.1	-	-	-	-	-	-	-	-	-	-	-
669637-Ranunculus eradicatus	-	-	-	-	GQ244634.1	-	-	-	-	-	-	-	-	-	-
669798-Ranunculus grayi	-	-	-	-	GQ245370.1	-	-	-	-	-	-	-	-	-	-
669799-Ranunculus subborealis	-	-	-	-	GQ245385.1	-	-	-	-	-	-	-	-	-	-
568539-Ranunculus cassubicus	-	-	-	-	KX668008.1	-	-	-	-	-	-	-	-	-	-
945266-Ranunculus pseudopygmaeus	-	-	-	-	-	KC842123.1	KC842053.1	KC841983.1	KC842087.1	KC842018.1	-	-	-	-	-
671259-Ranunculus peruvianus	-	-	-	-	-	-	-	-	-	-	-	GQ429081.1	GQ429142.1	-	-

TABLE S6: Model comparison under 100 randomly resolved polytomies. Best performing models from nine different models of three genera and three abundance distribution thresholds (niche parameters), every number represents the frequency with which the model performed best. The model abbreviations are Brownian motion (BM), Ornstein-Uhlenbeck (OU), early burst (EB), jump normal (JN), variance Gamma (VG), normal inverse Gaussian (NIG) and combinations of Brownian motion and jump processes (BM+JN, BM+NIG, BM+VG). Grey marked are the models that over all 100 phylogenies performed best. represents one comparison where the model performed best. The model abbreviations are Brownian motion (BM), Ornstein-Uhlenbeck (OU), early burst (EB), jump normal (JN), variance Gamma (VG), normal inverse Gaussian (NIG) and combinations of Brownian motion and jump processes (BM+JN, BM+NIG, BM+VG).

Genus	niche parameter	BM	OU	EB	JN	VG	NIG	BM+JN	BM+VG	BM+NIG
					Lévy Processes					
Primula	lower end	0.99	0.01	0	0	0	0	0	0	0
	niche center	0	0	0	0.15	0.23	0.62	0	0	0
	upper end	0.63	0.33	0	0	0.03	0.01	0	0	0
Lupinus	lower end	0.10	0.18	0	0.62	0.08	0.02	0	0	0
	niche center	0	0	0	0.91	0.05	0.03	0.01	0	0
	upper end	1.00	0	0	0	0	0	0	0	0
Ranunculus	lower end	0.26	0.74	0	0	0	0	0	0	0
	niche center	0.07	0.87	0	0.06	0	0	0	0	0
	upper end	0.14	0.86	0	0	0	0	0	0	0

TABLE S7: GenBank accession numbers of genome assemblies, transcriptome shotgun assemblies and sequence read archives used for the bait design. Including Trimmomatic settings (if applicable).

Name	Accession	Type	Surce database	Content	Trimmomatic settings
Primula veris	PRJNA238546	WGS	BioProject	8'756 unplaced-scaffolds; coverage: 116x	
Primula maximowiczii	SRR6830996	SRA	Sequence Read Archive	Bases: 5G ; Spots: 27'727'537	
Primula vulgaris	GBRY00000000.1	TSA	GenBank	1'329 contigs	
Primula ovalifolia	SRR5377219	SRA	Sequence Read Archive	Bases: 12.4G ; Spots: 49'094'910	
Primula sikkimensis	SRR7346504	SRA	Sequence Read Archive	Bases: 141.8M ; Spots: 1'625'293	SE -phred33 ILLUMINACLIP:TruSeq3-SE.fa:2:30:10 LEADING:3 TRAILING:3 SLIDINGWINDOW:4:15 MINLEN:36
Primula forbesii	SRR3355026	SRA	Sequence Read Archive	Bases: 61.5G; Spots: 203,618,671; L-morph	PE ILLUMINACLIP:TruSeq3-PE.fa:2:30:10:2:keepBothReads LEADING:3 TRAILING:3
Primula veris	SRR3355043	SRA	Sequence Read Archive	Bases: 6.7G; Spots: 33'538'227; S-morph	
Primula obconica	SRR866502	SRA	Sequence Read Archive	Bases: 52.3G; Spots: 261'588'296	PE ILLUMINACLIP:TruSeq3-PE.fa:2:30:10:2:keepBothReads LEADING:3 TRAILING:3
Primula sinensis	SRR3307913	SRA	Sequence Read Archive	Bases: 7.1G; Spots: 23'448'286	PE ILLUMINACLIP:TruSeq3-PE.fa:2:30:10:2:keepBothReads LEADING:3 TRAILING:3
Primula chrysochlora	SRR2039591	SRA	Sequence Read Archive	Bases: 290.8M; Spots: 428'716	SE -phred33 ILLUMINACLIP:TruSeq3-SE.fa:2:30:10 LEADING:3 TRAILING:3 SLIDINGWINDOW:4:15 MINLEN:36
Primula wilsonii	SRR640158	SRA	Sequence Read Archive	Bases: 2.5G; Spots: 13'867'141	
Primula poissonii	SRR629689	SRA	Sequence Read Archive	Bases: 2.5G; Spots: 13'764'249	
Lupinus luteus	SRR2075858	SRA	Sequence Read Archive	Bases: 5.7G; Spots: 28'392'144	PE ILLUMINACLIP:TruSeq3-PE.fa:2:30:10:2:keepBothReads LEADING:3 TRAILING:3
Lupinus albus	PRJNA592024	WGS	BioProject	25 chromosomes	
Lupinus angustifolius	PRJNA299755	WGS	BioProject	20 chromosomes	
Ranunculus sceleratus	SRR3291759	SRA	Sequence Read Archive	Bases: 8.4G; Spots: 46,672,970	
Ranunculus trichophyllus	SRR3212981	SRA	Sequence Read Archive	Bases: 10.7G; Spots: 52,867,748	PE ILLUMINACLIP:TruSeq3-PE.fa:2:30:10:2:keepBothReads LEADING:3 TRAILING:3
Ranunculus bungei	SRR1822529	SRA	Sequence Read Archive	Bases: 9.6G; Spots: 53,128,403	
Ranunculus brotherusii	SRR1822558	SRA	Sequence Read Archive	Bases: 9.6G; Spots: 53,290,081	
Ranunculus cantoniensis	SRR1737526	SRA	Sequence Read Archive	Bases: 9.3G; Spots: 51,411,991	
Ranunculus carpaticola	SRR958847	SRA	Sequence Read Archive	Bases: 13.8G; Spots: 69,095,358	PE ILLUMINACLIP:TruSeq3-PE.fa:2:30:10:2:keepBothReads LEADING:3 TRAILING:3 SLIDINGWINDOW:5:10 MINLEN:36
Primula vulgaris	PRJEB7311	WGS	BioProject	229 unplaced-scaffolds; coverage: NA	
Primula septemloba	SRR11445727	SRA	Sequence Read Archive	Bases: 16.3G; Spots: 54,967,782	
Primula littledalei	SRR9110566	SRA	Sequence Read Archive	Bases: 6.9G; Spots: 24,074,505	
Primula pumilio	SRR9110567	SRA	Sequence Read Archive	Bases: 7G; Spots: 24,333,856	

TABLE S8: GenBank accession numbers of 11 additional transcriptomes.

Species	Sample accession	Number of raw reads
Lupinus ramosissimus	SAMN04869603	43148608
Lupinus mantaroensis	SAMN04869566	22195166
Lupinus ellsworthianus	SAMN04869578	146825614
Lupinus texensis	SAMN04869576	91194120
Lupinus linearis	SAMN04869558	29929366
Lupinus montanus	SAMN04869559	32228856
Lupinus campestris	SAMN04869552	26859430
Lupinus nanus	SAMN04869593	39323636
Lupinus luteolus	SAMN04869584	38869710
Lupinus latifolius	SAMN04869583	38419894
Lupinus concinnus	SAMN04869582	20066512

References

Bankevich, A., S. Nurk, D. Antipov, A. A. Gurevich, M. Dvorkin, A. S. Kulikov, V. M. Lesin, S. I. Nikolenko, S. Pham, A. D. Prjibelski, A. V. Pyshkin, A. V. Sirotkin, N. Vyahhi, G. Tesler, M. A. Alekseyev, and P. A. Pevzner. 2012. SPAdes: A New Genome Assembly Algorithm and Its Applications to Single-Cell Sequencing. J. Comput. Biol. 19:455–477.

Bolger, A. M., M. Lohse, and B. Usadel. 2014. Trimmomatic: a flexible trimmer for Illumina sequence data. Bioinformatics 30:2114–2120.

Danecek, P., and S. A. McCarthy. 2017. BCFtools/csq: haplotype-aware variant consequences. Bioinformatics 33:btx100.

Drummond, C. S., R. J. Eastwood, S. T. S. Miotto, and C. E. Hughes. 2012. Multiple Continental Radiations and Correlates of Diversification in Lupinus (Leguminosae): Testing for Key Innovation with Incomplete Taxon Sampling. Syst. Biol. 61:443–460.

Emadzade, K., and E. Hörandl. 2011. Northern Hemisphere origin, transoceanic dispersal, and diversification of Ranunculeae DC. (Ranunculaceae) in the Cenozoic. J Biogeogr 38:517–530.

Gurevich, A., V. Saveliev, N. Vyahhi, and G. Tesler. 2013. QUAST: quality assessment tool for genome assemblies. Bioinformatics 29:1072–1075.

Li, H., and R. Durbin. 2009. Fast and accurate short read alignment with Burrows–Wheeler transform. Bioinformatics 25:1754–1760.

Li, H., B. Handsaker, A. Wysoker, T. Fennell, J. Ruan, N. Homer, G. Marth, G. Abecasis, R. Durbin, and 1000 Genome Project Data Processing Subgroup. 2009. The Sequence Alignment/Map format and SAMtools. Bioinformatics 25:2078–2079.

Nevado, B., G. W. Atchison, C. E. Hughes, and D. A. Filatov. 2016. Widespread adaptive evolution during repeated evolutionary radiations in New World lupins. Nat. Commun. 7:12384.

Potente, G., É. Léveillé-Bourret, N. Yousefi, R. R. Choudhury, B. Keller, S. I. Diop, D. Duijsings, W. Pirovano, M. Lenhard, P. Szövényi, and E. Conti. 2022. Comparative genomics elucidates the origin of a supergene controlling floral heteromorphism. Mol. Biol. Evol. 39:msac035-.

Quinlan, A. R., and I. M. Hall. 2010. BEDTools: a flexible suite of utilities for comparing genomic features. Bioinformatics 26:841–842.

Vos, J. M. de, C. E. Hughes, G. M. Schneeweiss, B. R. Moore, and E. Conti. 2014. Heterostyly accelerates diversification via reduced extinction in primroses. Proc Royal Soc B Biological Sci 281:20140075.

Chapter III: Environment and Life History Drive Episodes of Jump-Like Trait Evolution In Western American Lupinus (Fabaceae)

Livio Bätscher, Colin E. Hughes, Jurriaan M. de Vos

Manuscript in preparation for submission to *New Phytologist*.

SUMMARY

The longstanding idea that morphological characters evolve under rates that vary over time, or even evolve jump-like, has rarely been phylogenetically demonstrated. Phylogenetic Lévy processes provide a powerful modeling approach to test whether trait evolution involves episodes of exceptionally rapid evolutionary change but remains rarely used, especially in plants.

Here we test and explore why pulsed evolution happens by leveraging the Western American radiation of *Lupinus*, a remarkably diverse, fast-radiating clade of Legumes. Hereto, we reconstruct species climatic niches, measure a diverse set of morphological traits, compare support for different evolutionary models (including Lévy processes), reconstruct ancestral trait values, and describe trait differentiation and environmental association with a phylomorphospace approach.

We show that some but not all traits have multiple tempi of evolution. Life forms show clear environmental associations and episodes of rapid trait change only occur in perennial Andean plants in aseasonal environments.

We conclude that episodes of rapid change are driven by a propensity to evolve life forms in particular environmental conditions – here the absence of temperature seasonality – leads in the observed *Lupinus* clades to pulsed evolution and/or an increased trait space coverage. We argue that this pattern resembles Simpson's famous quantum evolution.

INTRODUCTION

A very significant contribution to the Modern Synthesis of Darwin's evolution theory was made by Theodosius Dobzhansky's 1937 published book "Genetics and the Origin of Species", Ernst Mayr's (1942) "Systematics and the Origin of Species", and George G. Simpsons (1944) "Tempo and Mode in Evolution". The latter coined the terms: "tempo" as summarizing the acceleration or deceleration of evolutionary rates leading from very slow up to very fast evolution, and "mode" as the pattern or manner of evolution, here tempo is a factor, it also includes changes over time of the abundance distribution in adaptive zones/subzones. Underpinned with examples of fossil records, three different evolutionary rate distributions (tempi) are presented: (1) phyla with "standard rate" distributions are described as "horotelic", (2) low-rate phyla are considered "bradytelic" and (3) "tachytelic" phyla show exceptionally high rates of evolution. Simpson's final aim was to describe three different modes in evolution: (1) "speciation", where populations move into different subzones and become more locally adapted; (2) "phyletic" evolution, describing the overall shifts of characters within populations, explaining approximately 90% of paleontological data; and (3) "quantum" evolution, describes the relatively rapid shift in a population away from the ancestral character (Simpson, 1944). Yet, in the early 20th century, statistical methods to estimate species relatedness from DNA sequences or reconstruct non-constant trait changes through time on a phylogeny did not exist, and it was not possible to test if living individuals followed rate changes or quantum evolution.

Decades later Felsenstein's (1985) work solved the problem that trait data from closely related species violate statistical independence, giving rise to a broad array of phylogenetic comparative methods (Cornwell & Nakagawa, 2017). Nonetheless, it took another quarter of a century for model development, to introduce the first model without a constant evolutionary rate: the early-burst process (EB; Harmon et al., 2010) allows for a rapid rate of evolution, followed by evolutionary stasis as the lineage becomes older. However, if e.g., Simpson's quantum evolution occurs mid-lineage (creating a pattern of low/normal rate of evolution, followed by high rate, and again low/normal rate) such a scenario cannot be accurately modeled by EB. Nonetheless, a stochastic process allowing for sudden and independent increments/declines is the Lévy process which consists of Brownian motion (BM), a pure-jump process (drawing jumps from a Lévy measure), and an optional trend (Ken-Iti, 1999). These processes were recently integrated into phylogenetic comparative methods (e.g., Landis et al., 2013; Duchen et al., 2017; Landis & Schraiber, 2017; Bastide & Didier, 2023). However, the frequently cited Lévy processes are barely used, about 15 from approximately 280 citations (Google Scholar; December 2023) apply the algorithms, and only two on plants, see Ogburn & Edwards (2015) and

Bätscher *et al.* (in prep.). Nonetheless, do these technical achievements allow us to address when, where, and why changes in rates (i.e., pulses) in trait evolution happened?

Potential determinants for pules in rates of morphological characters are the life form and the environment. It is intuitively, that different longevity e.g., being annual, biennial, long-lived, or having different growth forms e.g., herb, subshrub, shrub, tree drastically shape the morphology of plants. Thus, these easily accessible characteristics are still used in modern Floras and descriptive keys (e.g., Aeschimann et al., 2004; Konrad et al., 2018). Further, there is evidence that life forms affect morphology e.g., is trait variability between life forms larger than within (Costa *et al.*, 2018). On the other hand, it is well known from adaptive radiations, that species can adapt their morphology to new phenotypes (e.g., Schluter, 2000). Here, one of the most impressive textbook examples is how the leaflet length in the Hawaiian silversword alliance changes under different environments. However, it remains unknown if the evolution of life forms or the distribution across continents (respectively different continental climates) drives pulsed/jump-like trait evolution.

A particularly suitable study clade to address this question is the genus *Lupinus* L. (Fabaceae). This monophyletic clade is species-rich, known for its large-scale distribution, presence in different biomes, a large variety of life forms, and morphological traits (e.g., Hughes & Eastwood, 2006; Drummond, 2008; Drummond et al., 2012; Nürk et al., 2019). Furthermore, western New World *Lupinus* clades form multiple rapid radiations, where clear shifts of net diversification happened, associated with the key innovation of changing longevity from annual to perennial (Drummond *et al.*, 2012), and it was also shown that this key innovation enables *Lupinus* to move into mountain systems (i.e., sky-islands), where the evolutionary rate of plant height tends to be higher (Nürk *et al.*, 2019). However, it remains unclear if multiple morphological traits show evidence for different tempi of evolution, where in the phylogeny acceleration/deceleration happens, and whether it might be possible to make conclusions about different modes of evolution under consideration of species occurrences and adaptation.

In this study, we tested how plant traits from the western New World *Lupinus* clades evolved. We focus on examining if morphological measurements are better represented with one single rate (constant tempo) or multiple rates of evolution (different tempi), and if applicable, where, and why accelerations/decelerations in rates occurred. First, we used the latest dated *Lupinus* phylogeny (Bätscher et. al, in prep.) to test the hypothesis if phylogenetic comparative models of incremental or non-incremental better describe observed trait data and considered two possible outcomes: (1) higher model support for one single constant rate i.e., Brownian motion or Ornstein-Uhlenbeck, (2) higher explanatory power for an explosive (early burst) or pulsed model (Lévy process). We reveal that three out of eight traits show strong evidence for pulsed trait evolution, which leads to the follow-up questions: where in the phylogeny and under what ecological circumstances does "jumpy" evolution occur? Therefore, we performed ancestral state reconstructions (of traits best explained by a Cauchy process). Additionally, we classified the measured species by life forms, plus extracted from occurrence records bioclimatic variables to analyze the occupied trait and climatic space with phylomorphospace plots. We tested if pulsed evolution and therefore, changes in trait space correlate with (1) the life form or (2) specific environment-phenotype interactions. This study reveals that both hypotheses cannot be rejected: increased evolutionary rates and larger coverage of trait space can only be found in certain life forms: perennial herbs and shrubs/trees, additionally, a suitable environment is required allowing for the new phenotype, here the absence of a temperature seasonality in South America.

MATERIAL AND METHODS

Clade selection and phylogeny

We selected the species-rich western North and South American *Lupinus* L. clades (ca. 171 ssp. in both clades; Drummond et al., 2012) because they cover a broad morphological range (Nürk *et al.*, 2019), occupy climatically diverse niches, and shifted into mountain systems (Drummond *et al.*, 2012), which strongly affected the species connectivity and the geneflow (Nevado *et al.*, 2018). Here the latest, most complete, time-calibrated *Lupinus* phylogeny from Bätscher *et al.* (in prep) is used to model trait evolution in a Bayesian framework to account for phylogenetic uncertainty.

Trait data

For the morphological data, we selected measurements representing the growth and reproduction investment i.e., leaflet length and leaf width, length of the petiole, peduncle, pedicel, inflorescence, petal length of the banner, and number of flowers per inflorescence. To obtain measurements for correctly identified *Lupinus* specimens of the western South American clade we examined 212 expert-identified herbarium vouchers (many of them are loans), in the herbarium of Zürich (Z+ZT). Additionally, we measured 58 high-resolution images of vouchers from the Oregon State University herbarium, including specimens from Oregon State University (OSC) and Willamette University

(WILLU). Furthermore, we downloaded from the iDigBio portal (https://www.idigbio.org/portal, accessed July 2022) high-resolution images of 113 georeferenced vouchers, to cover the whole elevational gradient we selected one lowland, one high elevation, and three specimens with intermediate elevation. Whenever possible five replicates per species are measured (using only one individual per specimen), high-resolution images were examined with ImageJ (Wayne Rasband, National Institute of Mental Health, Bethesa, Maryland, USA), and we computed the median trait-wise and per species. A total of 72 species were examined representing approximately 42% ssp. of the selected clades (list of measured species, voucher ID, and raw trait data in the supplementary; Table S1).

Climate data and biogeography

For accessing climate data to describe niches, occurrence data was collected, cleaned, and linked to multiple global high-resolution climatic products. First, we downloaded all *Lupinus* occurrence records from GBIF (https://doi.org/10.15468/dl.xkw2rg, accessed Mai 2023), cleaned them with the R package "CoordinateCleaner" (Zizka *et al.*, 2019) excluding spatial points close to zoos, botanical gardens, capitals, national or regional centroids, and the GBIF headquarters. Further, coordinates that are identical, have uncertainties >100km, do not match the origin country, or are within the sea were removed, plus we identified and excluded rasterized data sets. After correcting species names based on expert opinion, a maximum of 200 occurrences were selected: first preferring records with an elevation, then points with a high coordinate accuracy and last selecting random observations. If not applicable (<200 occurrences), records from the herbarium vouchers were added (measured and additional vouchers from iDigBio). Due to frequent species misidentifications in the Andes, we used only hand-cleaned expert occurrence data instead.

For all occurrence records, abiotic variables were extracted from the CHELSA v2.1 (Karger *et al.*, 2017) i.e., mean annual air temperature, precipitation amount, temperature seasonality, precipitation seasonality, growing season length, and growing season temperature. In case of a missing elevation, it was inferred from the digital elevation model GTOPO30 (Miliaresis & Argialas, 1999). To compute distances to the local treeline for every coordinate, we used the R package ElevDistr (Bätscher and de Vos, accepted), with default settings, and the recommended input raster layers (i.e., GTOPO30, growing season length, and temperature from CHELSA). Finally, all relevant abiotic variables were summarized by computing the species median. Additionally, we assigned a discrete class to all species consisting of main distribution (North or South America) and life form (annual/perennial and herb/shrub or tree; see Table S2). The biogeographic information comes from Plants of the World Online (https://powo.science.kew.org/, POWO), the life form was assigned based on the herbarium vouchers including label information and assigned classes have been expert validated.

Testing different modes of trait evolution

To find out how morphological diversity in *Lupinus* evolved, we tested different evolutionary models, comparing two fundamentally different types: models with constant tempo (e.g., Brownian motion [BM] or Ornstein-Uhlenbeck [OU]) and models with different tempi (e.g., early burst [EB] or Lévy processes [LP]). Because a limited number of tools exist, that allow modeling explosive and pulsed evolution, we decided to use “pulseR” (Landis & Schraiber, 2017) and “cauphy” (Bastide & Didier, 2023) to test a variety of different Lévy processes.

First, we tested every morphological measurement against BM, OU, EB, and the best-fitting LP out of six slightly different processes (jump normal [JN], variance Gamma [VG], normal inverse Gaussian [NIG] with and without a BM component). Model fitting (in “pulseR”) was repeated across 100 posterior phylogenies, results were plotted as abundance distributions (for any model trade-wise), mean and median AICc weights were computed. We define, a model as significantly better if the mean AICc weight is twice as large as the second-best model. The mean was chosen because it preserves the mathematical idea behind the weights, that they sum up to one, which is not necessarily the case for the median. However, the median can be used to describe how different posterior phylogenies react to the model and how strong the consensus across the phylogenies is.

For every trait that showed significant evidence for pulsed trait evolution (i.e., mean AICc weight of the LP was twice as large as any of the other models), the model fitting procedure was repeated using “cauphy”. Currently, this is the only tool that allows computing and visualizing anagenetic and cladogenetic change under a Lévy process. However, because the Cauphy process (CP) is a different Lévy process than “pulseR” can test for, we tested again for the best-performing model: comparing BM, OU, EB, and CP across the 100 posterior phylogenies. Again, the AICc weight abundance was plotted trait-wise, and the mean plus median was computed. In case CP was the significantly best model, we inferred the ancestral range reconstruction, which allows identifying phylogenetic branches where strong “jump-like” changes happened.

Descriptive analysis of trait and niche space

Often changes in morphology are associated with adaptations to a new environment (e.g., in adaptive radiations; Schluter & Dolph, 2000). To further investigate how abiotic changes might have affected the plant morphology we plotted the mean annual temperature, mean annual precipitation, and median distance to the treeline, category-wise (see discrete classes above) into a Box-Whisker-Plot.

Additionally, we plotted two-dimensional trait combinations and a projection of the phylogeny (phylomorphospace) for all morphological traits where pulsed evolution was favored (under "pulseR") using "phytools" (Revell, 2012). Further, we computed a "phyloclimatespace" (phylomorphospace with abiotic instead of trait values) for precipitation against temperature seasonality. It is important to note, that the phylomorphospace function (Sidlauskas, 2008) uses a squared-change parsimony reconstruction of the ancestral states (Maddison, 1991) that is based on a Brownian motion, which does not properly reflect a trait best explained with a Lévy process. Therefore, we have to assume that branches having a lot of incremental change i.e., a pulse, would be represented by a too short branch in the phylomorphospace plot. However, phylomorphospaces are still useful for illustrating changes along branches and we assume that for most branches morphometric change was inferred correctly.

To better visualize the effect of the distribution across continents and life forms in the phylomorphospaces, the nodes were color-coded based on the assigned categories, plus a convex hull for each category was computed and plotted. For a numerical comparison, we computed the polygon areas using Gauss's area formula, using instead of absolute coordinates the trait value divided by its maximum and multiplied it by ten. This transition was performed for two reasons: first because large absolute values (e.g. peduncle length) would contribute much more to the area than small values (e.g. leaflet length) and second scaling traits/abiotic variables to ten leas to a maximum area of 100, allowing to present the trait/climate space in a percent manner and facilitating comparisons between different phylomorphospaces.

RESULTS

Identifying "jump-like" trait evolution

Here we tested for all traits if Brownian motion (BM), Ornstein-Uhlenbeck (OU), early burst (EB), or the optimal Lévy process (LP) explains trait evolution best, a model is significant if the mean AICc weight is twice as large as any other model (Landis & Schraiber, 2017). For six out of eight traits a significant model was identified: BM for the petiole (mean AICc weight: 0.43), and petal length (0.46); OU for the pedicel length (0.50); LP for leaflet (0.79), peduncle length (1.0), and the number of flowers per inflorescence (0.51; Fig. 1 and S1; Table S3). The LP describing leaflet length and number of flowers per inflorescence best, is a jump normal (JN) process, and for the peduncle length, it is a combination of Brownian motion plus variance Gamma (BMVG; Fig. 1 and Table S3). Overall, mean, and median AICc weights are congruent, except for the number of flowers per inflorescence with a mean of 0.51 and a median of 0.17 (Table S3), reflecting the bimodal pattern in the density distribution of the AICc weights (Fig. 1). This distribution shows, in ~50% of posterior phylogenies JN outperforms BM, wherein the other half BM is the better model, what is likely driven by differences in the time estimation. However, beyond all phylogenetic uncertainty, the mean AICc weight of the JN process is still clearly larger than the remaining models and therefore LP is significantly

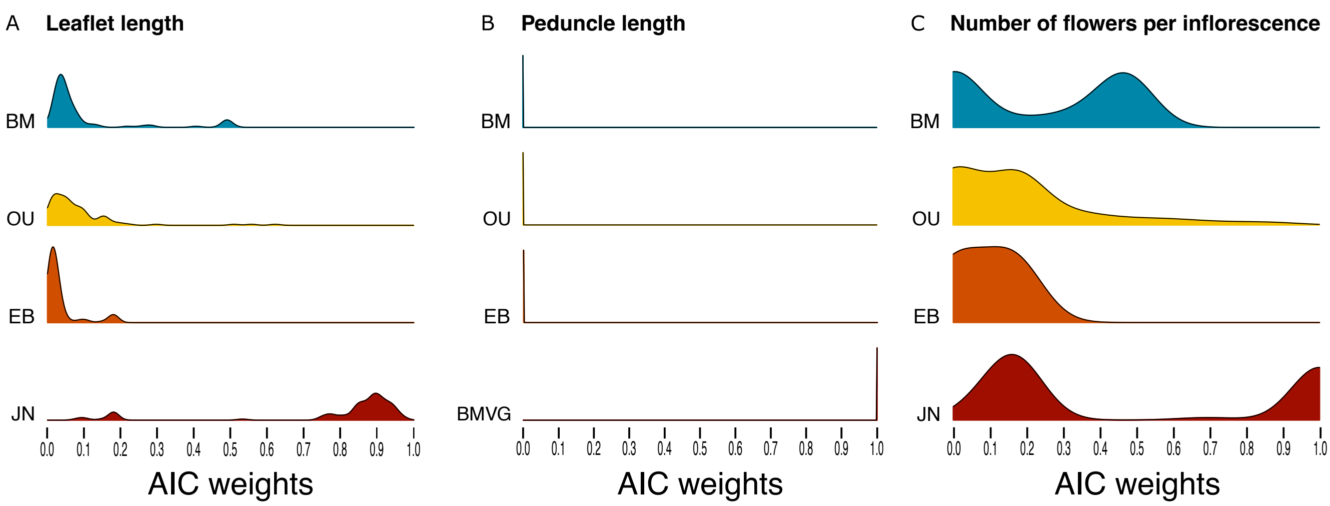

FIGURE 1: Density distribution of Akaike weights (across 100 posterior phylogenies), of the different significant traits: A) leaflet length, B) peduncle length, and C) number of flowers per inflorescence. The different rows represent the different models: Brownian motion (BM), Ornstein-Uhlenbeck (OU), early burst (EB), and the best fitting Lévy processes i.e., jump normal (JN) or BM plus variance Gamma (BMVG).

better (Table S3). For the inflorescence length, it was not possible to find a significant model: BM (mean AICc weight: 0.30) and a JN Lévy process (0.48) are the two best-performing models with a slight tendency towards preferring an LP (Fig. S1; Table S3). Even less clear is the leaf width, where all four models BM (0.38), OU (0.22), EB (0.14), and LP (0.26), performed equally with a slight tendency towards a BM.

For the traits where LP was the significantly better model (leaflet and peduncle length plus number of flowers per inflorescence), we tested if a Cauchy process (CP) would outperform the other models (BM, OU, and EB). If the CP is the significantly best model, it is possible and meaningful to perform an ancestral state reconstruction (only available for CP). A Cauchy process is a pure-jump Lévy process, forming a special case of an α-stable process, where α=1 (Bastide & Didier, 2023). Here, for the peduncle length a CP is the significantly best model (mean AICc weight: 1.000), for leaflet length the best model is an OU (0.976), and for the number of flowers per inflorescence it is either OU (0.585), or CP (0.412) with no clear significance (Table 1, Fig. S2). Therefore, we used an ancestral trait reconstruction only for the peduncle length. This ancestral state reconstruction reveals five very strong branch increments (anagenetic change) on four terminal branches (of *Lupinus jelskianus*, *L. sufferrugineus*, *L. praestabilis*, and *L. semperflorens*), one non-terminal branch (ancestor of *L. luisanae* and *L. interruptus*), and internal node changes (cladogenetic changes) are barely visible. Remarkably, none of the pulses (here strong branch increments) appear in annual nor North American species; all appear in perennial Andean lineages (Fig. 2).

TABLE 1: Model support of 100 posterior phylogenies for three selected plant traits. Each clade was fitted to four models: Brownian motion (BM), Ornstein-Uhlenbeck (OU), early burst (EB), and Cauchy process (CP). As model selection criterion mean and median AICc weight for leaflet and peduncle length, plus the number of flowers per inflorescence, were computed and significant mean values are highlighted in gray.

Trait	**Statistical location**	**BM**	**OU**	**EB**	**CP**
Leaflet length	mean	0.018	0.976	0.006	$4.356*10^{-5}$
	median	0.004	0.994	0.002	$1.115*10^{-5}$
Peduncle length	mean	$7.489*10^{-24}$	$6.793*10^{-20}$	$2.755*10^{-24}$	1.000
	median	$2.795*10^{-25}$	$3.252*10^{-20}$	$1.028*10^{-25}$	1.000
Number of flowers per inflorescence	mean	0.003	0.585	$9.788*10^{-4}$	0.412
	median	$8.481*10^{-4}$	0.639	$3.120*10^{-4}$	0.361

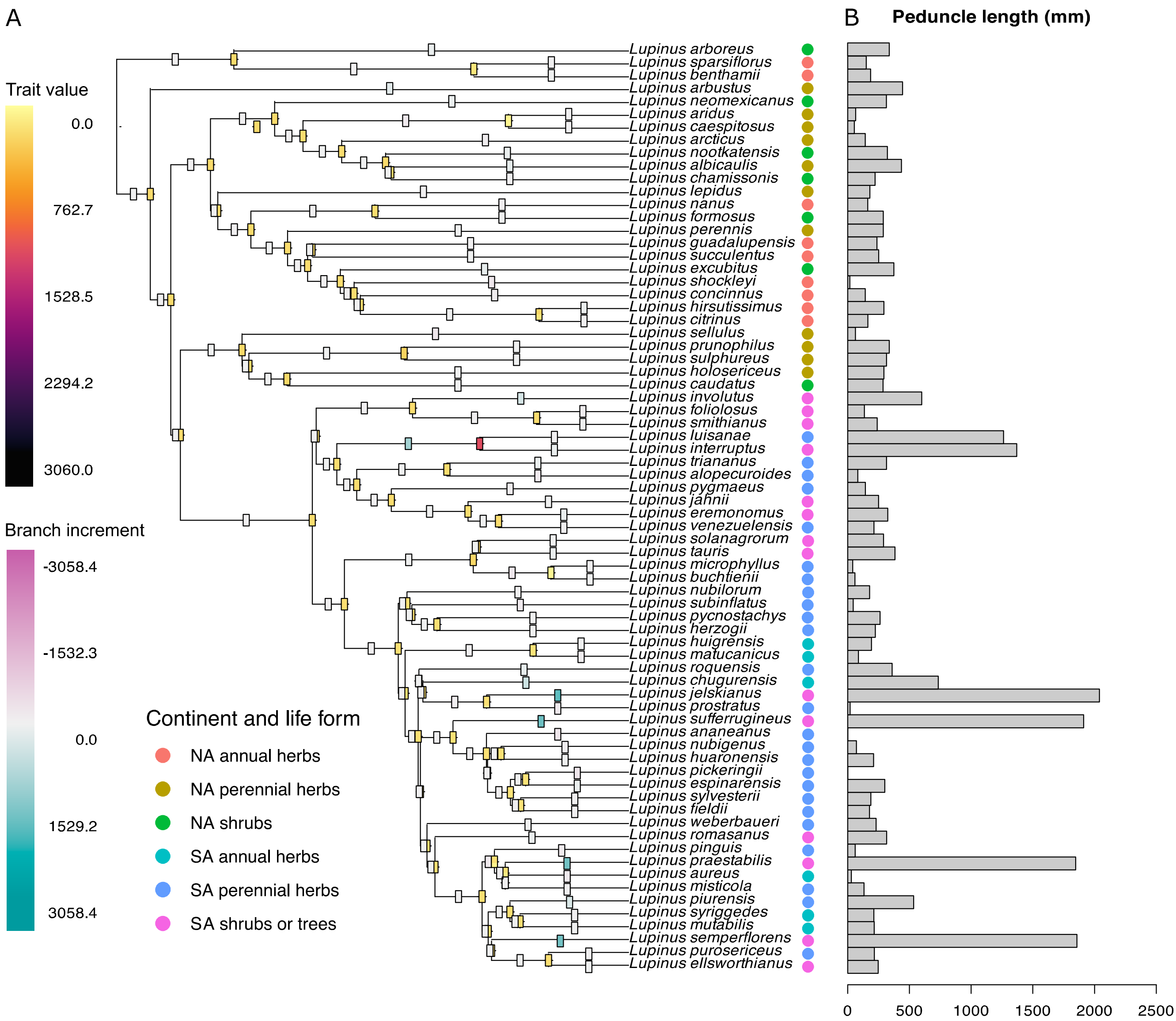

FIGURE 2: Ancestral trait reconstruction for peduncle length of the *Lupinus* radiation. A) Time-calibrated phylogeny of the eastern North and South American clade. The absolute reconstructed trait value is plotted on the internal nodes, reaching from small (light yellow) to large peduncle length (dark purple). The box in the middle of each branch describes the trait increment, which can be absent (grey), positive (cyan), or negative (pink). The colored circles represent the continent a species grows on and its life form. B) Median peduncle length of each species.

Descriptive analysis of abiotic factors

To describe similarities and differences between niches of different life forms, we used cleaned occurrence data to extract species medians for climatic data (i.e., annual precipitation amount, mean annual temperature) and computed the median distance to the treeline. The results show that North American perennial species occur at lower mean annual precipitation sum, than western South American perennials. Here, NA perennial herbs have a median of 638 mm (minimum: 409 mm; maximum: 1,429 mm), and shrubs 494 mm (429 mm; 1,238 mm), whereas SA perennial herbs have a median sum of 1,688 mm (390 mm; 2,786 mm), respectively 1,429 mm (749 mm; 2,395 mm) for shrubs/trees. Additionally, annual species occur under the overall driest continental conditions, NA annuals have the lowest precipitation amount of 409 mm (168 mm; 1,277 mm), and SA annuals 1,018 mm (49 mm; 1,459 mm; Fig 3A).

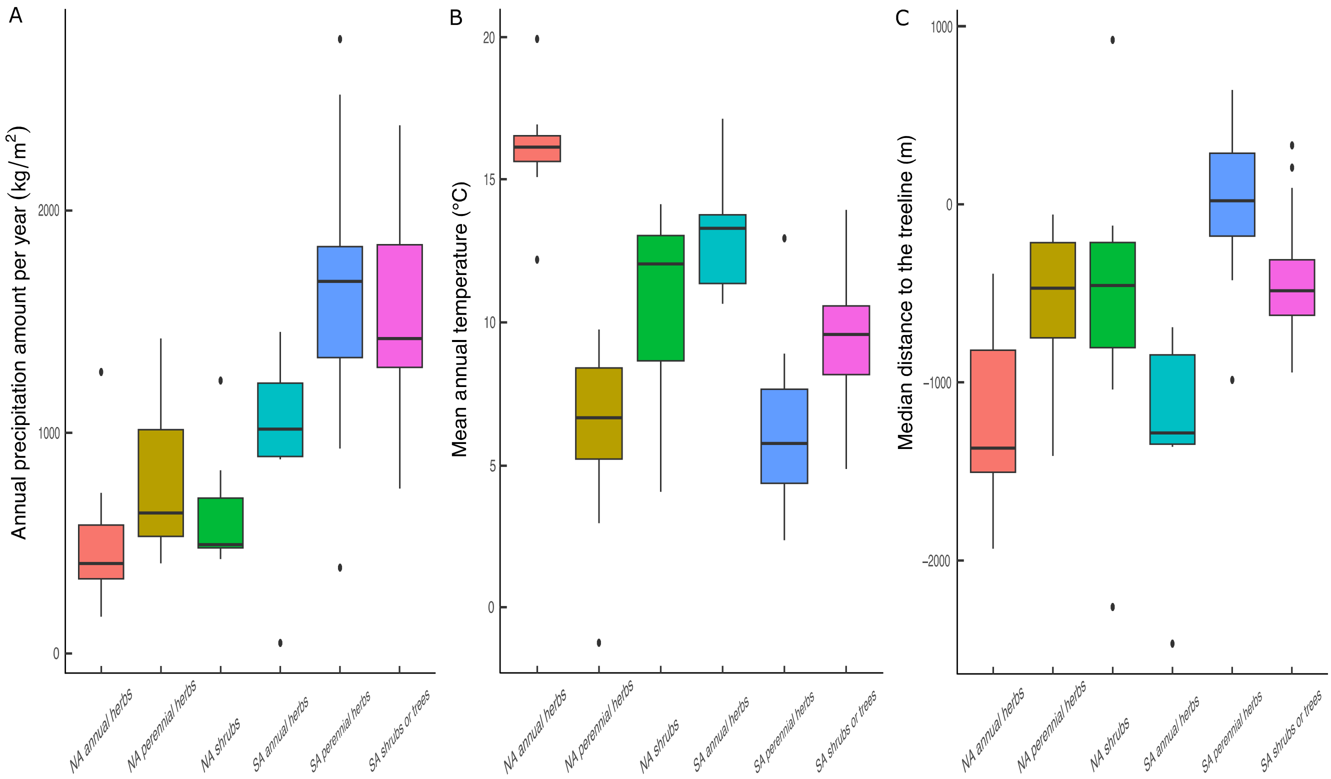

Figure 3. Summary statistics of three environmental variables, separated by groups representing the continent plus the life form. A) Annual precipitation sums per year, B) mean annual temperature and C) median distance to the treeline (negative values are below and positive above the treeline).

Differences in mean annual temperature between continents are much lower; North and South American annuals occur at the highest temperatures with a median of 16.15 °C (minimum: 12.2 °C; maximum 19.95 °C), respectively 13.3 °C (10.65 °C; 17.15 °C). Perennial herbs are present at the lowest temperatures, for North America: 6.65 °C (-1.25 °C; 9.75 °C), respectively 5.75 °C (2.35 °C; 12.95 °C), and shrubs/trees occur at intermediate temperatures around medians of 12.05 °C (4.05 °C; 14.15 °C) for North, respectively 9.58 °C (4.85 °C; 13.95 °C) for South America (Fig. 3B).

The distance to the local treeline is the horizontal distance relative to the center of the species abundance, here positive values represent a niche center above, and negative values below the treeline. This analysis reveals that annuals show the lowest distribution with an overall median at -1,370 m (minimum: -1,935 m; maximum: -391 m) for North, and at-1,285 m (-2,468 m; -691 m) for South America. All remaining life forms show a similar distance: NA shrubs at -457 m (-2,262 m; 922 m), SA shrubs/trees -487 m (-945 m; 330 m), and NA perennial herbs -472 m (-1,414 m; -59 m). However, SA perennial herbs are the exception, with a median niche center just above the treeline at 19 m (-987 m; 642 m; Fig. 3C).

Phylospace of traits and seasonality

We plotted all traits that show different tempi of evolution against each other plus precipitation and temperature seasonality to compute relative coverage of the trait/climate space in percent for each lifeform and continent. The phylomorphospace plots (Fig. 4A-C) plus the occupied trait spaces reveal, that South American perennial plants cover a much larger trait space. For leaflet against peduncle length, the trait space is covered as follows: NA annual herbs 1.36%, NA perennial herbs 2.87%, NA shrubs 0.71%, SA annuals 3.63%, SA perennial herbs 24.20% and SA shrubs/trees 33.50% (Fig. 4A). A similar pattern can be seen in leaflet length against the number of flowers per inflorescence, in North America annuals cover 3.59%, perennial herbs 4.95%, and shrubs 0.39%, respectively for South America 3.23%, 36.36%, and 7.59% (Fig. 4B). When comparing peduncle length and the number of flowers per inflorescence, it is in NA for annuals 1.46%, for perennial herbs 3.01%, and for shrubs 0.19%, respectively 0.85%, 30.69%, and 14.99% for SA (Fig. 4C). Here, North and South American annuals cover a similar trait space, while South American perennial herbs and shrubs/trees take eight to eighty times the trait space than the western North American Lupins.

Opposing, for precipitation and temperature seasonality, where North American species cover an abiotic space larger than the one of the South American species: annuals cover 3.77%, perennial herbs 9.09%, and shrubs 15.78%, respectively for South America 0.76%, 5.30%, and 2.42% (Fig. 4D). Furthermore, NA and SA species cover almost the identical range in precipitation seasonality, but temperature seasonality differs drastically. Even allowing to fully separate NA and SA species from each other, based on whether their temperature seasonality is smaller or larger than 2 °C, and (already shown in Fig. 2) the transition from NA to SA only happened once. Finally, South American life

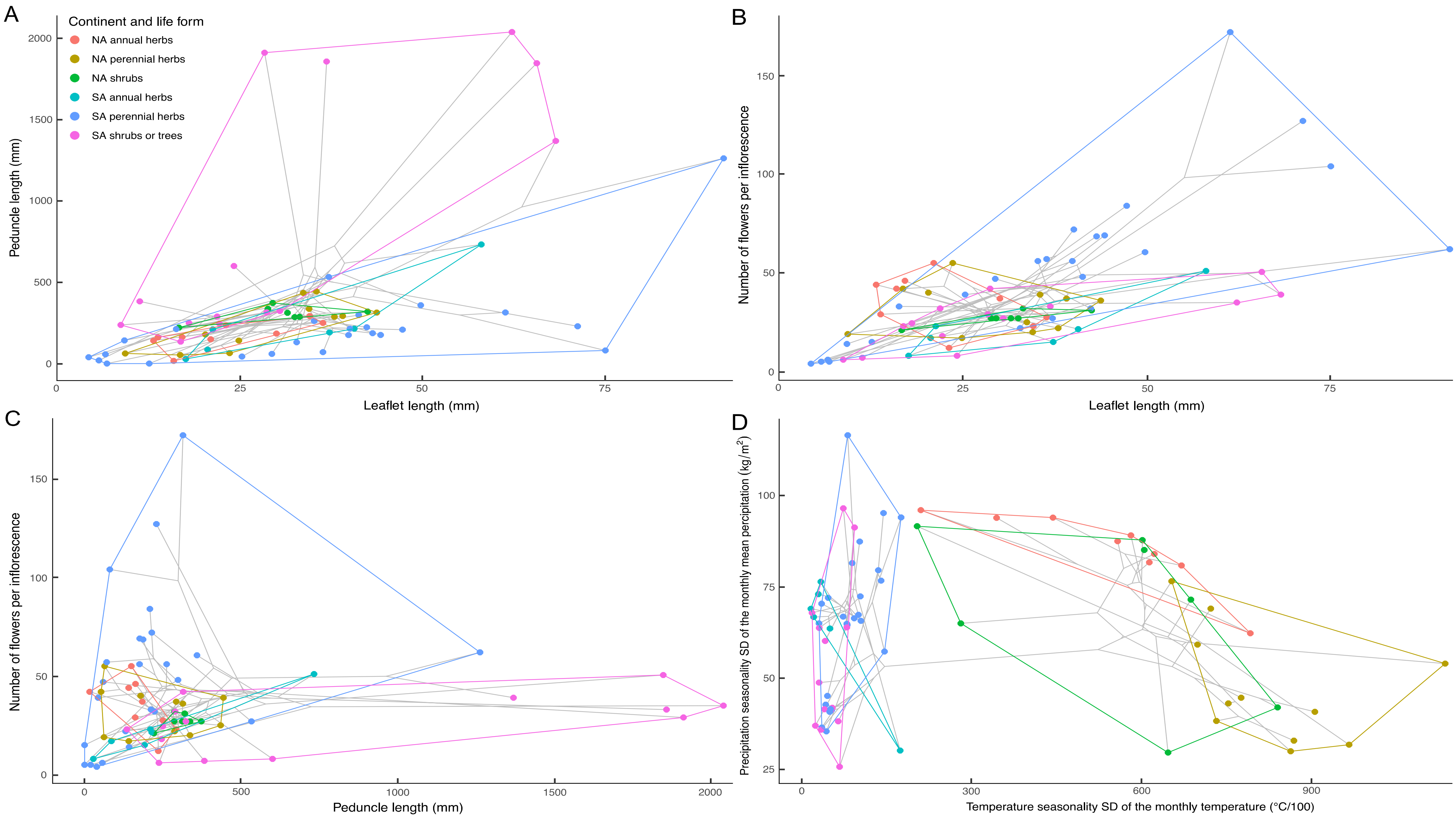

FIGURE 4: Phylomorphospace of selected traits or climatic variables. The colored circles represent the continent a species grows on plus its life form, and the gray line represents the phylogenetic relationships of the points. A) leaflet against peduncle length, B) number of flowers per inflorescence against leaflet length, C) number of flowers per inflorescence vs. peduncle length, and D) temperature against precipitation seasonality

forms show a strong overlap of the climatic space, whereas North American classes have an overall smaller overlap.

DISCUSSION

Here we investigated if one single rate of evolution is sufficient to explain trait evolution in the western New World *Lupinus*, or if multiple rates are superior. Therefore, we tested if the measured traits are better explained by incremental (BM or OU) or non-incremental models (EB or LP). The findings demonstrate that three out of eight traits are best explained with a Lévy process (Fig. 1, S1, and S2; Table 1 and S3). Because incremental models have sometimes low explanatory power, we reject the hypothesis that one tempo is sufficient to explain trait evolution and conclude that different characters are best explained with a variety of evolutionary models. Since different traits favor different models, their data must contain a different structure, leading to the conclusion that evolutionary rates can differ within and between traits. This indicates that different traits might follow different forms of evolution.

To test whether changes in rates and the covered trait space are caused by (1) life forms or (2) species-environment interactions, we first wanted to exclude correlations between life forms and climatic variables. However, the following macroevolutionary patterns were identified (Fig. 3): annuals are dominant in the Xeric lowlands (dry: 408.6 [median NA] and 1018.0 kg/m3 [median SA], hot: 16.2 and 13.3 °C, and below the treeline: -1370.0 and -1284.5 m), shrubs/trees dominate the "intermediate" climatic space (intermediate precipitation: 494.0 and 1428.6 kg/m3, intermediate temp: 12.1 and 9.5 °C, and in the montane belt: -457.0 and -486.5 m), and perennial herbs prefer cooler more moist habitats (moist: 637.9 and 1688.0 kg/m3, cool: 6.7 and 5.8 °C, and in the montane up to the alpine belt: -472 and 18.5 m). This leads to the conclusion, that life form and climate are dependent and that both could be responsible for changes.

Next, an ancestral range reconstruction for one trait was performed and trait coverage percentages were computed from a phylomorphospace. The detected pulses in peduncle length (Fig. 2) and increased trait spaces (Fig. 4) were only found in perennial Andean Lupins, but not in annuals, nor in North America. Therefore, we argue that life form liability alone is not sufficient to trigger an evolutionary rate change, but in combination with a suitable environment, this can happen. Here it is very likely, that the lack of temperature seasonality in South America caused the rate shift after early North American Lupins evolved life form lability.

"Explosive" evolution in some, but not all traits

This study reveals in three out of eight cases clear evidence for pulsed trait evolution in *Lupinus*: leaflet length, peduncle length, and number of flowers per inflorescence are best explained by a Lévy process. This is demonstrated with the mean AICc weights (Table S3) and the posterior density distribution of the AICc weights (Fig. 1). For the number of flowers per inflorescence the mean AICc weight favors in 24% of all cases BM and 51% JN (Table S3) therefore, a bimodal distribution for the Lévy process is visible (Fig. 1C). However, simulations (published with the used R package) showed that under an error-free posterior tree with 105 taxa, 20-40% of the simulated JN traits are miss-identified as a BM (Landis & Schraiber, 2017), therefore analysis with about 100 species are likely to have binominal distributions. Consequently, we conclude that the number of flowers per inflorescence does not show a weak signal for pulsed evolution, but leaflet and peduncle length show an extraordinarily strong signal.

An explanation of why different traits have different rates might be the trait lability/evolvability, specifically the number of mutations needed for a trait change. Some examples, therefore, are the petal-to-septal homeotic mutant in an *Aquilegia* population caused by single mutations (Cabin *et al.*, 2022), the evolutionary liability of life history in Montiaceae which facilitates evolutionary transitions (Ogburn & Edwards, 2015) or siRNA which is a "master regulator" of floral pigmentation in *Mimulus* (Liang *et al.*, 2023). Another explanation could be varying selective pressures on traits, is selection negative, neutral/very weak, or very strong e.g., in adaptive radiations. Highly-cited examples of the latt,er are Galápagos finches (e.g., Grant & Grant, 1989), west Indian *Anolis* lizards (e.g., Lister, 1976), Hawaiian silversword alliance (e.g., Robichaux et al., 1990), or columbines *Aquilegia* (e.g., Stebbins, 1970). Despite all potential explanations, rate variabilities between traits are (to our knowledge) rarely documented, but a simulation study in paleontology showed that it is unlikely, that one rate of evolution fits all traits and time scales (Hunt, 2012) and our findings lie in line a basic theorem of evolutionary rates: "The rates of evolution of two or more characters within a single phylum may change independently." (p. 12; Simpson, 1944).

Additionally, it is important to evaluate technical expertise which leads to the identification of rate variation between traits. First, Lévy processes are suitable to identify evolutionary rate changes with pure-jumps (symbolizing very short period of very high evolutionary rates), especially because they provide a variety of models with different Lévy measures (Landis *et al.*, 2013; Duchen *et al.*, 2017; Landis & Schraiber, 2017; Bastide & Didier, 2023). Our results highlight the importance of applying different models to identify potential rate changes because best-fitting models differ between traits (Fig. 1, Table S3). Furthermore, leaflet length and number of flowers per inflorescence are best explained by JN and peduncle length by BMVG however, only the latter could in a second analysis outperform BM, OU, and EB in favor of a CP (Table 1, Fig. S2). The reason, why leaflet length and number of flowers per inflorescence cannot be explained by a CP is likely caused by the differences in the Lévy measure: JN infers a rate of jumps, where CP and VG are infinitely active processes jumping all the time. Therefore, we conclude that JN and CP capture different patterns of trait data: JN is meant to capture periods of stasis followed by jumps to new evolutionary zones, whereas CP represents a more frequent quick response to environmental changes (Landis & Schraiber, 2017). Because different Lévy processes capture different patterns of rate changes it is relevant to have multiple models, highlighting the importance of developing new comparative methods. Second, it is important to understand that the heavy-tailed pattern in trait data (identified by Lévy processes), is sensitive against log transformations. These transformations can eliminate accelerations/decelerations in evolutionary rates and potentially worse, create a pattern of pulsed evolution if normally distributed traits are log-transformed.

Abiotic trends of different life forms

Previous studies described life form liability of Western New World *Lupins*, interpreted changes as a relevant key innovation, and identified annual herbs as ancestral character (Drummond *et al.*, 2012; Nürk *et al.*, 2019). This study confirms frequent changes of life forms (Fig. 2A) and further investigates, why this ubiquitous pattern appears, and if it is caused by adaptation to different environments.

The descriptive analysis of climatic data (Fig. 3) gives interesting insights into the adaptive potential, revealing correlations between life forms and climatic data on a macroevolutionary scale. As suggested by Drummond et al. (2012), we found proof, that annual herbs accrue in the Xeric lowland: occupying on both continents the lowest annual precipitation (Fig. 3A), highest mean annual temperature (Fig. 3B), and largest negative distance to the treeline (i.e., occurring below the alpine habitat in the lowland; Fig. 3C). Annual species are well adapted to xeric habitats, because of their short life cycle, allowing to avoid the extreme seasonal drought and heat, by potentially outliving the most stress-full period of the year as seeds; a well-known strategy (e.g., Mooney et al., 1976; Heschel & Riginos, 2005; Boyko et al., 2023). However, species with a short life span cannot grow as tall as their perennial relatives, and are therefore not as competitive, leading to a trait-off between having a short life span and being competitive. Our results suggest that annual *Lupins*, are not capable of occurring outside of dry and hot environments. Therefore, we conclude that *Lupinus* annuals are not capable of surviving in cooler and more moist environments with strong competition, this lies in line with numerous other studies (e.g., Smith & Beaulieu, 2009; Drummond et al., 2012; Boyko et al., 2023).

A similar adaptation can be found in mountain systems where a fundamental principle is, that alpine species have a preferentially long lifespan (Arx *et al.*, 2006; Šťastná *et al.*, 2012). In consequence, are perennial plants more suitable to environmental conditions in mountains, visible in the relative distance to the treeline (Fig. 3C) and supported by the fact that annual species contribute about 2% to the alpine flora i.e., on average only 2-3 species can be found in alpine habitat (Körner, 2021). Here, only Andean perennial herbaceous species manage to jump above the treeline (a positive distance to the treeline represents a niche center in the alpine biome), aligning with the well-known concept, that small herbaceous species benefit from the alpine microclimate by decoupling from the air temperature (Körner, 2023). Physiological large shrubs and trees are not capable of decoupling from the air temperature, but dwarf-shrubs/subshrubs (like *L. arboreus*, and sometimes *L. involutus*, *L. smithianus*, *L. solanagrorum*, *L. tauris*) are (Körner, 2012, 2021). However, the absence of alpine herbaceous species in the North American clade, is a reminder that having a suitable plant height alone is not enough to shift into the alpine biome.

Additionally, this study shows, the occurrence of perennial herbs in habitats with the lowest mean annual temperature, (Fig. 3B), a plausible explanation is again plat size. Being closer to the ground protects small perennial herbs from frost, especially in case of a snow cover, which allows them to use the isolative aspects of the snow (Körner, 2021, 2023) to endure the cold winter air temperatures (e.g., in Alaska). Benefits trees and shrubs do not have (except for dwarf shrubs) and therefore, these life forms inhabit environments with higher mean annual temperatures.

In conclusion, different life forms in the New World *Lupinus* clades occur in different climatic conditions: annual herbs are most adapted to the Xeric lowland, perennial herbs to rather cool environments, and shrubs/trees to an environment “in-between” the extremes (temperature and precipitation). Therefore, we conclude, that not all *Lupinus* life forms are equally suitable for all environments. Moreover, especially extreme climatic conditions select against unsuitable traits and life forms (forming “environmental restrictions”), and vice versa having different life forms empowers adaptation to different environments (loosening “environmental restrictions”). Thus, we speculate that life form liability is an important evolutionary change, allowing easier adaptation and quicker movement. Furthermore, it is potentially also beneficial for *Lupinus* to move into the mountain to increase species connectivity during warm interglacial periods (Flantua *et al.*, 2019) and to inhabit a more similar environment, because species prefer to shift into biomes that are climatically similar to their ancestral biome (Cardillo *et al.*, 2017).

Conditions for comprehensive trait change

Furthermore, this study reveals, that severe morphological changes only occur in perennial Andean Lupins. Indeed, this is supported by two different analyses, (1) the ancestral range reconstruction of peduncle length (Fig. 2A) identified large branch increments only in SA perennials, and (2) the largest trait spaces (of the phylomorphospace; Fig. 4A-C) are covered by perennial herbs and shrubs/trees occurring in the Andes. To disentangle these findings, we first discuss the role of life forms, and then move on to the geographical component.

Annual species occupy a relatively small trait space (covered phylomorphospaces from 0.85% to 3.63%), matching a study that compared New World *Lupinus* clades, indicating lower phenotypic rates of plant height in annuals (Nürk *et al.*, 2019). Further, strong branch increments from the ancestral trait reconstruction are never associated with annuals (Fig. 2A). Both findings can be explained by the fact that annual species invest most resources into seed production, whereas perennials invest more into vegetative structure (Kumari *et al.*, 2020). In combination with the extended longevity, perennials develop larger vegetative structures leading to larger trait space coverage. Therefore, these findings unequivocally establish that life form lability is beneficial to change trait evolvability.

Because large changes in rates of peduncle length evolution (Fig 2A) and in trait space occupation (Fig. 4A-C) occur only in the Andes, life form liability alone is not enough to alter the tempo of evolution. We find the largest trait spaces always in perennial herbs and shrubs/trees from SA (covered phylomorphospaces from 7.59% to 36.36%), unveiling the question: why drastic trait space enlargements in NA remain absent (Fig. 4A-C). This absence is an indicator that SA species might have adapted to new habitats (simply not present in NA), respectively climatic conditions in NA prevent altering phenological characters drastically. A very promising climatic pattern is revealed with the "phyloclimatespace" (Fig. 4D): while North and South American Lupins seem to share a similar precipitation seasonality (minimum: 29.65 to maximum 96 respectively 25.75-116.5 kg/m^3), the temperature seasonality (204.5-1,134.65 and 17.3-174.6 °C/100) does not overlap at all. Therefore, we suggest that temperature seasonality in NA environments selects actively against extreme phenotypes, forming an "environmental restriction". Moreover, the Andes itself could also contribute to this effect, since *Lupinus* species occur here in small and isolated populations where gene flow was observed, suggesting an isolation-driven divergence, probably driven by habitat changes e.g., Pleistocene glaciation (Nevado *et al.*, 2018).

Here, we discovered and examined the following evolutionary pattern: (1) gaining life form liability; (2) species with a non-ancestral life form (perennial) moved out of the Xeric environment; (3) eventually under suitable climatic conditions drastic morphological changes become possible. This creates in *Lupinus* a large trait variability caused by radical changes in a relatively short time, consequently leading to high rates of evolution. Our conjecture is, that these characteristics have a lot in common with Simpson's concept of quantum evolution. Here in an adaptive phase, the equilibrium of the ancestors is lost, next in the "preadaptive phase" a group moves towards a new equilibrium, to finally establish a new equilibrium. Therefore, a preadaptation is necessary (here: life form liability), and it leads to radical morphological change (Fig. 2B and 4A-C) causing high rates of evolution (Fig. 1; Table S3) for a sharp shift from one position to another (Fig. 2A). If this hypothesis is correct, this evolutionary sequence should be convergent with other taxa showing life form liability. In addition to the lower physiological rate of annual *Lupinus* (Nürk *et al.*, 2019), dos Santos et al. (2022) showed in the *Aeonium* radiation on the Canary Islands, that trait-environment adaptations are driven by the life forms, providing another example of how traits are dependent from the environment and the life form. Another study leading to many congruent results is Ogburn and Edwards (2015) study on Montiaceae, a family found in the western American mountain systems (except for three genera and a few species). This study reveals that annuals are favored in hot deserts with seasonal rainfall, whereas in short and cool growing seasons perennials are favored, and they argue that evolutionary lability facilitates shifts between habitats. Finally, they present a clear link between climate niche variation and growth form; the only missing component is the evaluation of continuous characters.

CONCLUSION

In summary, this study reveals pulsed evolution in some but not all morphological traits and that different traits seem to evolve at different rates because a variety of different models is needed for an adequate fit. Furthermore, we argue that evolutionary liability of growth forms and life cycle are likely to help *Lupinus* move into new habitats or biomes. Most interesting is that life form liability leads only in combination with a suitable environment to evolutionary rate changes, allowing morphological characters to change comprehensively and alter the tempo of evolution in peduncle length. Finally, we point out potential similarities between western New World *Lupins* evolution and Simpson's quantum evolution, asking ourselves if the described interactions are likely to be found in other plant clades.

ACKNOWLEDGEMENT

We thank Serafin Streiff, Bianca Modespacher, and Jankó Weibel for helping with the morphological measurement collection, and our colleagues from the Physiological Plant Ecology Group in Basel for discussing the content of this paper and for providing useful advice and comments. This work was supported by the Swiss National Science Foundation (grant 310030_185251 to JMdV).

REFERENCES

Aeschimann D, Lauber K, Moser DM, Theurillat J-P. **2004**. *Flora alpina: atlas des 4500 plantes vasculaires des Alpes*. Haupt Publisher.

Arx G von, Edwards PJ, Dietz H. **2006**. EVIDENCE FOR LIFE HISTORY CHANGES IN HIGH-ALTITUDE POPULATIONS OF THREE PERENNIAL FORBS. *Ecology* **87**: 665–674.

Bastide P, Didier G. **2023**. The Cauchy Process on Phylogenies: a Tractable Model for Pulsed Evolution. *Systematic Biology*.

Boyko JD, Hagen ER, Beaulieu JM, Vasconcelos T. **2023**. The evolutionary responses of life-history strategies to climatic variability in flowering plants. *New Phytologist* **240**: 1587–1600.

Cabin Z, Derieg NJ, Garton A, Ngo T, Quezada A, Gasseholm C, Simon M, Hodges SA. **2022**. Non-pollinator selection for a floral homeotic mutant conferring loss of nectar reward in Aquilegia coerulea. *Current Biology* **32**: 1332-1341.e5.

Cardillo M, Weston PH, Reynolds ZKM, Olde PM, Mast AR, Lemmon EM, Lemmon AR, Bromham L. **2017**. The phylogeny and biogeography of Hakea (Proteaceae) reveals the role of biome shifts in a continental plant radiation. *Evolution* **71**: 1928–1943.

Cornwell W, Nakagawa S. **2017**. Phylogenetic comparative methods. *Current Biology* **27**: R333–R336.

Costa DS, Zotz G, Hemp A, Kleyer M. **2018**. Trait patterns of epiphytes compared to other plant life-forms along a tropical elevation gradient. *Functional Ecology* **32**: 2073–2084.

Drummond CS. **2008**. Diversification of Lupinus (Leguminosae) in the western New World: Derived evolution of perennial life history and colonization of montane habitats. *Molecular Phylogenetics and Evolution* **48**: 408–421.

Drummond CS, Eastwood RJ, Miotto STS, Hughes CE. **2012**. Multiple Continental Radiations and Correlates of Diversification in Lupinus (Leguminosae): Testing for Key Innovation with Incomplete Taxon Sampling. *Systematic Biology* **61**: 443–460.

Duchen P, Leuenberger C, Szilágyi SM, Harmon L, Eastman J, Schweizer M, Wegmann D. **2017**. Inference of Evolutionary Jumps in Large Phylogenies using Lévy Processes. *Systematic Biology* **66**: syx028.

Felsenstein J. **1985**. Phylogenies and the Comparative Method. *The American Naturalist* **125**: 1–15.

Flantua SGA, O'Dea A, Onstein RE, Giraldo C, Hooghiemstra H. **2019**. The flickering connectivity system of the north Andean páramos. *Journal of Biogeography* **46**: 1808–1825.

Grant BR, Grant PR. **1989**. Natural Selection in a Population of Darwin's Finches. *The American Naturalist* **133**: 377–393.

Harmon LJ, Losos JB, Davies TJ, Gillespie RG, Gittleman JL, Jennings WB, Kozak KH, McPeek MA, Moreno-Roark F, Near TJ, *et al.* 2010. Early bursts of body size and shape evolution are rare in comparative data. *Evolution* **64**: 2385–2396.

Heschel MS, Riginos C. **2005**. Mechanisms of selection for drought stress tolerance and avoidance in Impatiens capensis (Balsaminaceae). *American Journal of Botany* **92**: 37–44.

Hughes C, Eastwood R. **2006**. Island radiation on a continental scale: Exceptional rates of plant diversification after uplift of the Andes. *Proceedings of the National Academy of Sciences* **103**: 10334–10339.

Hunt G. **2012**. Measuring rates of phenotypic evolution and the inseparability of tempo and mode. *Paleobiology* **38**: 351–373.

Karger DN, Conrad O, Böhner J, Kawohl T, Kreft H, Soria-Auza RW, Zimmermann NE, Linder HP, Kessler M. **2017**. Climatologies at high resolution for the earth's land surface areas. *Scientific Data* **4**: 170122.

Ken-Iti S. **1999**. *Lévy processes and infinitely divisible distributions*. Cambridge university press.

Konrad L, Gerhard W, Andreas G. **2018**. *Flora helvetica*. Bern, Switzerland: Haupt.

Körner C. **2012**. *Alpine Treelines, Functional Ecology of the Global High Elevation Tree Limits*.

Körner C. **2021**. *Alpine Plant Life, Functional Plant Ecology of High Mountain Ecosystems*.

Körner C. **2023**. Concepts in Alpine Plant Ecology. *Plants* **12**: 2666.

Kumari R, Hamal U, Sharma N. **2020**. Reproductive Ecology of Flowering Plants: Patterns and Processes. : 157–171.

Landis MJ, Schraiber JG. **2017**. Pulsed evolution shaped modern vertebrate body sizes. *Proceedings of the National Academy of Sciences* **114**: 13224–13229.

Landis MJ, Schraiber JG, Liang M. **2013**. Phylogenetic Analysis Using Lévy Processes: Finding Jumps in the Evolution of Continuous Traits. *Systematic Biology* **62**: 193–204.

Liang M, Chen W, LaFountain AM, Liu Y, Peng F, Xia R, Bradshaw HD, Yuan Y-W. **2023**. Taxon-specific, phased siRNAs underlie a speciation locus in monkeyflowers. *Science* **379**: 576–582.

Lister BC. **1976**. The nature of niche expansion in West Indian Anolis lizards II: evolutionary components. *Evolution* **30**: 677–692.

Maddison WP. **1991**. Squared-Change Parsimony Reconstructions of Ancestral States for Continuous-Valued Characters on a Phylogenetic Tree. *Systematic Biology* **40**: 304–314.

Miliaresis GC, Argialas DP. **1999**. Segmentation of physiographic features from the global digital elevation model/GTOPO30. *Computers & Geosciences* **25**: 715–728.

Mooney HA, Ehleringer J, Berry JA. **1976**. High Photosynthetic Capacity of a Winter Annual in Death Valley. *Science* **194**: 322–324.

Nevado B, Contreras-Ortiz N, Hughes C, Filatov DA. **2018**. Pleistocene glacial cycles drive isolation, gene flow and speciation in the high-elevation Andes. *New Phytologist* **219**: 779–793.

Nürk NM, Atchison GW, Hughes CE. **2019**. Island woodiness underpins accelerated disparification in plant radiations. *New Phytologist* **224**: 518–531.

Ogburn RM, Edwards EJ. **2015**. Life history lability underlies rapid climate niche evolution in the angiosperm clade Montiaceae. *Molecular Phylogenetics and Evolution* **92**: 181–192.

Revell LJ. **2012**. phytools: an R package for phylogenetic comparative biology (and other things). *Methods in Ecology and Evolution* **3**: 217–223.

Robichaux RH, Carr GD, Liebman M, Pearcy RW. **1990**. Adaptive Radiation of the Hawaiian Silversword Alliance (Compositae- Madiinae): Ecological, Morphological, and Physiological Diversity. *Annals of the Missouri Botanical Garden* **77**: 64.

Santos P dos, Brilhante MÂ, Messerschmid TFE, Serrano HC, Kadereit G, Branquinho C, Vos JM de. **2022**. Plant growth forms dictate adaptations to the local climate. *Frontiers in Plant Science* **13**: 1023595.

Schluter D. **2000**. *The ecology of adaptive radiation*. OUP Oxford.

Sidlauskas B. **2008**. Continuous and arrested morphological diversification in sister clades of characiform fishes: a phylomorphospace approach. *Evolution* **62**: 3135–3156.

Simpson GG. **1944**. *Tempo and Mode in Evolution*. Columbia University Press.

Smith SA, Beaulieu JM. **2009**. Life history influences rates of climatic niche evolution in flowering plants. *Proceedings of the Royal Society B: Biological Sciences* **276**: 4345–4352.

Šťastná P, Klimešová J, Doležal J. **2012**. Altitudinal changes in the growth and allometry of Rumex alpinus. *Alpine Botany* **122**: 35–44.

Stebbins GL. **1970**. Adaptive Radiation of Reproductive Characteristics in Angiosperms, I: Pollination Mechanisms. *Annual Review of Ecology and Systematics* **1**: 307–326.

Zizka A, Silvestro D, Andermann T, Azevedo J, Ritter CD, Edler D, Farooq H, Herdean A, Ariza M, Scharn R, *et al.* **2019**. CoordinateCleaner: Standardized cleaning of occurrence records from biological collection databases. *Methods in Ecology and Evolution* **10**: 744–751.

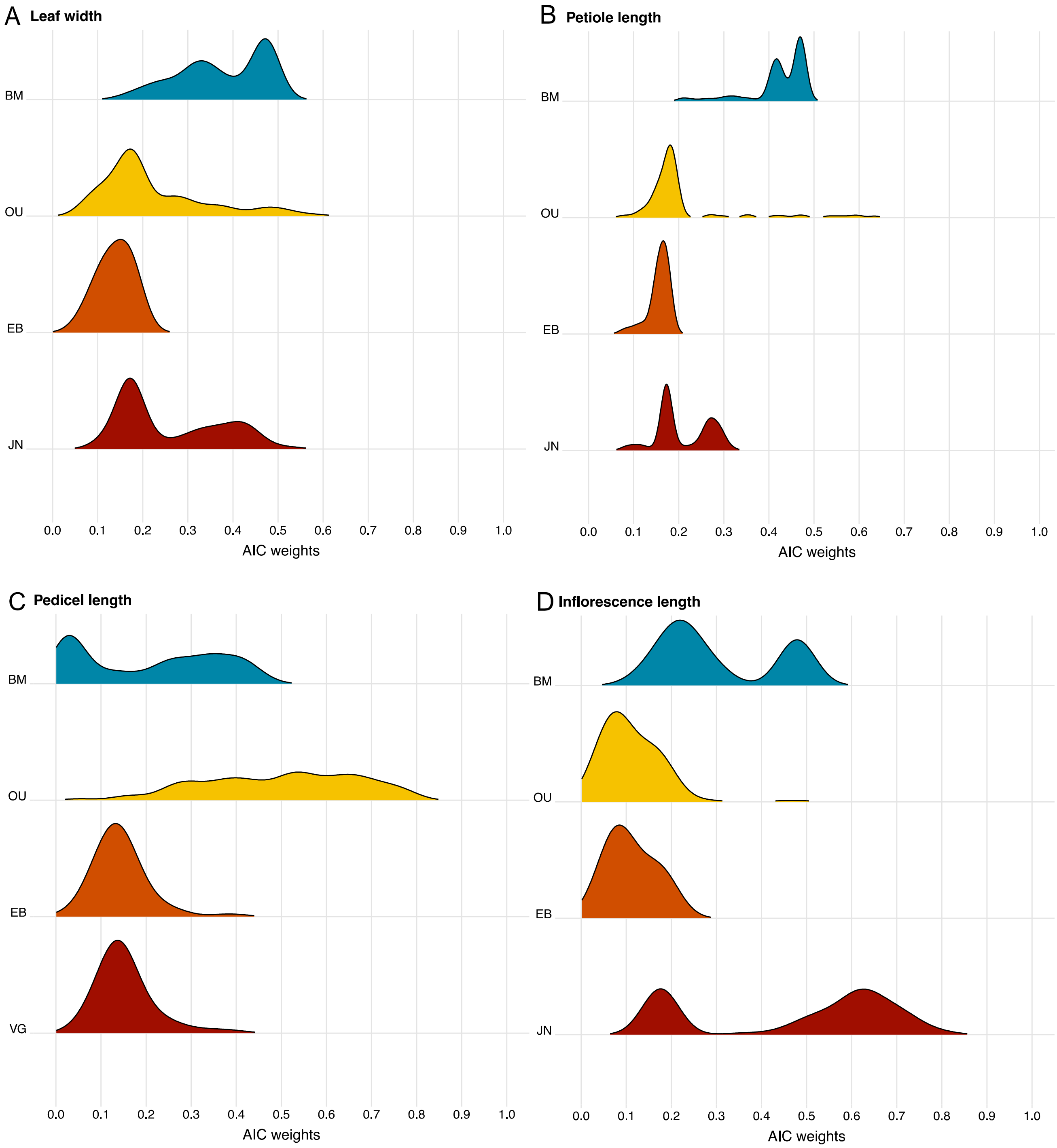
A Leaf width
BM
OU
EB
JN
0.0 0.1 0.2 0.3 0.4 0.5 0.6 0.7 0.8 0.9 1.0
AIC weights
B Petiole length
BM
OU
EB
JN
0.0 0.1 0.2 0.3 0.4 0.5 0.6 0.7 0.8 0.9 1.0
AIC weights
C Pedicel length
BM
OU
EB
VG
0.0 0.1 0.2 0.3 0.4 0.5 0.6 0.7 0.8 0.9 1.0
AIC weights
D Inflorescence length
BM
OU
EB
JN
0.0 0.1 0.2 0.3 0.4 0.5 0.6 0.7 0.8 0.9 1.0
AIC weights

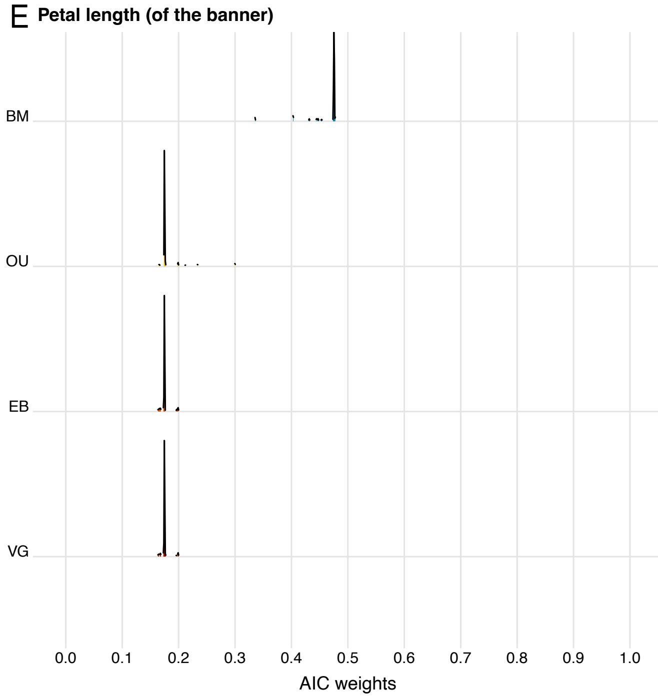

FIGURE S1: Density distribution of Akaike weights (under 100 posterior phylogenies), of the different non-significant traits: A) leaf width, B) petiole length, C) pedicel length, D) inflorescence length, and E) petal length of the banner. The different rows represent the different models: Brownian motion (BM), Ornstein-Uhlenbeck (OU), early burst (EB), and the best fitting Lévy processes i.e., jump normal (JN) or variance Gamma (VG).

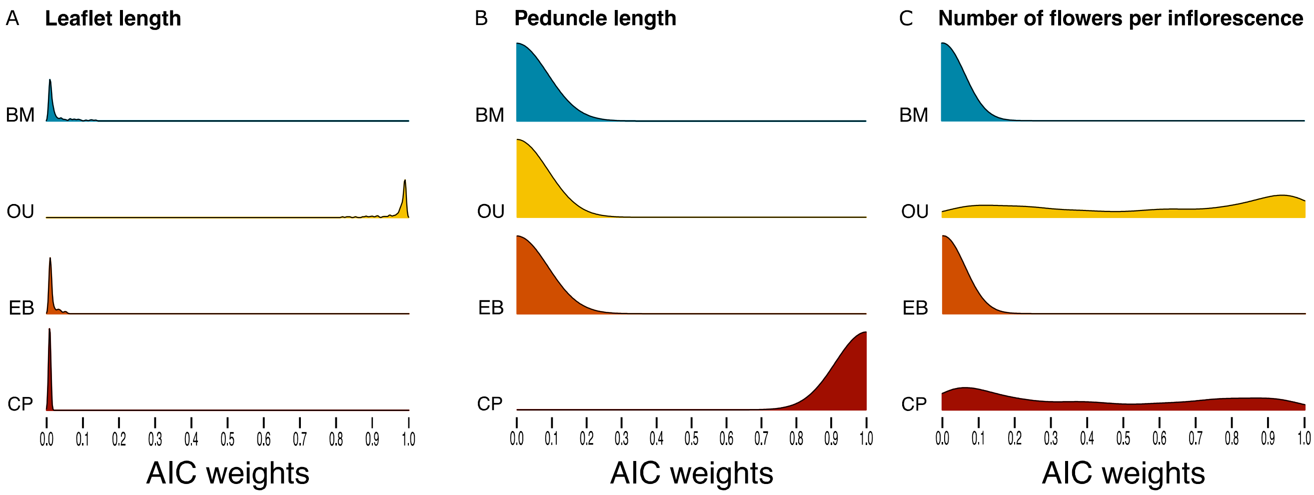

FIGURE S2: Density distribution of Akaike weights (under 100 posterior phylogenies), of the different significant traits: A) leaflet length, B) peduncle length, and C) number of flowers per inflorescene. The different rows represent the different models: Brownian motion (BM), Ornstein-Uhlenbeck (OU), early burst (EB), and the Cauchy processes (CP).

TABLE S1: A detailed list with all the raw data (units if applicable are in brackets), species name, and Barcode.

Species	Barcode	Leaflet length (mm)	Leaf width (mm)	Petiole length (mm)	Peduncle leangth (mm)	Pedicel length (mm)	Inflorescence length (mm)	Petal length of the banner (mm)	Number of flower per inflorescence
Lupinus holosericeus	OSC-V-024943	39.009	64.495	71.2	112.378	2.205	7.396	32	42.807
Lupinus holosericeus	OSC-V-024947	29.237	55.468	42.464	176.454	2.018	7.338	37	71.313
Lupinus holosericeus	OSC-V-024948	42.077	77.407	88.915	292.433	3.842	10.889	84	176.828
Lupinus aridus	OSC-V-024976	23.046	42.586	71.279	27.926	2.519	10.911	28	61.998
Lupinus aridus	OSC-V-024982	45.634	69.142	200.532	64.09	1.868	10.102	55	118.543
Lupinus aridus	OSC-V-025013	31.996	55.254	84.005	232.582	4.075	9.547	102	176.499
Lupinus aridus	OSC-V-025021	23.514	42.682	140.065	183.636	2.18	8.721	65	103.889
Lupinus aridus	OSC-V-025027	19.227	29.382	52.573	50.354	2.326	6.303	47	65.96
Lupinus lepidus	OSC-V-026206	16.59	26.16	82.613	242.495	2.115	7.731	74	110.46
Lupinus lepidus	OSC-V-026208	30.333	50.683	120.777	168.226	1.834	9.203	68	176.704
Lupinus lepidus	OSC-V-026209	19.664	39.654	118.896	240.823	3.045	10.156	40	119.829
Lupinus lepidus	OSC-V-026211	20.197	36.456	82.602	142.91	2.166	8.959	31	92.644
Lupinus lepidus	OSC-V-026217	26.854	42.324	37.314	178.845	3.281	10.173	28	99.803
Lupinus sellulus	OSC-V-026287	6.923	13.8	21.933	42.311	1.968	7.365	15	18.83
Lupinus sellulus	OSC-V-026372	7.674	14.684	25.783	35.941	2.857	9.943	25	20.25
Lupinus holosericeus	WILLU-00193	31.081	46.759	79.305	406.963	3.939	9.871	36	65.793
Lupinus holosericeus	WILLU-00194	51.895	105.358	84.358	466.676	4.258	8.703	37	70.281
Lupinus sellulus	WILLU-00377	9.451	16.574	32.325	77.446	0.769	7.237	23	24.433
Lupinus sellulus	WILLU-00378	10.423	17.444	55.854	61.891	2.31	6.368	19	32.095
Lupinus sellulus	WILLU-00380	9.209	12.429	40.186	72.704	2.459	9.843	17	30.71
Lupinus albicaulis	OSC-V-024800	36.5386	58.0932	29.3856	344.8202	5.1855	12.4205	5	26.3473
Lupinus albicaulis	OSC-V-024802	26.9734	45.1039	29.957	371.1936	4.5208	13.6131	35	86.7155
Lupinus albicaulis	WILLU-00018	25.7648	47.7767	20.7146	236.1503	3.7024	11.71	26	82.6417
Lupinus albicaulis	WILLU-00032	20.8915	34.7281	18.9177	571.4336	5.3535	20.1059	54	233.68
Lupinus albicaulis	WILLU-00035	41.6929	54.5638	24.9843	474.1151	4.1164	12.2317	41	75.5588
Lupinus albicaulis	WILLU-00036	49.033	87.646	50.991	475.204	5.172	11.336	48	161.292
Lupinus albicaulis	WILLU-00041	25.067	44.574	22.249	275.58	2.741	14.412	24	81.042
Lupinus albicaulis	WILLU-00055	33.475	46.402	30.375	576.623	5.9	10.199	20	82.884
Lupinus albicaulis	OSC-V-024731	38.686	49.841	22.312	394.177	7.849	11.499	10	105.71
Lupinus albicaulis	WILLU-00058	33.732	58.71	54.339	649.808	3.857	13.338	15	78.432
Lupinus arbustus	WILLU-00099	40.605	74.319	48.82	302.808	3.77	9.503	40	125.284
Lupinus arbustus	WILLU-00110	25.711	43.705	23.855	267.35	2.667	8.509	18	38.571
Lupinus arbustus	WILLU-00113	40.441	80.172	33.739	491.339	6.863	15.137	58	140.518
Lupinus arbustus	WILLU-00115	32.316	72.411	42.572	430.752	5.729	9.88	63	147.864
Lupinus arbustus	WILLU-00117	21.734	42.909	37.726	177.169	5.525	8.575	35	89.955
Lupinus arbustus	WILLU-00120	35.003	86.95	55.11	456.173	4.426	9.937	43	130.406
Lupinus arbustus	WILLU-00124	28.133	38.709	35.546	348.099	5.044	10.568	18	73.959
Lupinus arbustus	WILLU-00125	21.566	46.74	74.464	274.76	3.965	8.203	65	105.399
Lupinus arbustus	WILLU-00134	48.283	76.081	181.664	528.35	3.208	9.397	30	90.213
Lupinus arbustus	OSC-V-025416	33.197	69.39	24.926	618.546	5.171	10.662	46	123.707
Lupinus arbustus	WILLU-00138	66.212	127.052	64.964	473.432	6.603	8.702	18	76.47
Lupinus caudatus	OSC-V-024842	38.337	75.991	48.833	394.858	3.888	9.799	21	64.701
Lupinus caudatus	OSC-V-024852	33.728	53.234	22.747	241.616	4.73	10.281	21	62.381
Lupinus caudatus	OSC-V-024853	32.433	55.426	43.952	248.633	4.247	10.752	39	92.331
Lupinus caudatus	OSC-V-024875	24.726	38.496	30.051	388.465	4.294	10.295	16	48.902
Lupinus caudatus	OSC-V-024917	25.13	50.535	123.834	285.73	3.216	8.153	31	70.587
Lupinus caudatus	OSC-V-024924	23.783	57.865	20.679	292.362	3.447	11.265	32	58.752
Lupinus caudatus	WILLU-00175	36.881	53.725	31.44	279.195	3.312	8.101	27	171.613
Lupinus sulphureus	OSC-V-027211	43.669	111.161	74.834	371.949	5.401	8.896	55	96.746
Lupinus sulphureus	OSC-V-027213	55.598	84.765	108.314	313.655	8.424	10.992	31	108.2461
Lupinus sulphureus	OSC-V-027218	43.415	69.91	110.905	387.38	8.894	11.63	36	141.361
Lupinus sulphureus	OSC-V-027219	49.507	94.881	74.937	196.296	7.512	10.88	53	206.884
Lupinus sulphureus	OSC V 027220	33.359	57.27	84.24	289.879	5.337	13.451	34	124.436
Lupinus caespitosus	OSC-V-026495	16.737	32.587	58.025	79.389	4.519	9.432	42	22.828
Lupinus caespitosus	OSC-V-026497	12.654	22.411	55.631	61.426	4.23	6.761	39	21.003
Lupinus caespitosus	OSC-V-026498	17.889	34.817	82.936	45.034	2.77	11.838	40	12.08
Lupinus caespitosus	OSC-V-026500	17.47	29.433	47.63	39.098	0.803	9.777	62	28.079
Lupinus caespitosus	WILLU-00415	15.519	33.685	140.111	52.609	0.931	8.788	86	52.056
Lupinus arboreus	CSLA001823	37.482	70.651	30.08	239.46	8.227	16.727	21	127.453
Lupinus arboreus	CSLA002056	23.664	40.576	39.433	386.707	6.983	14.233	23	156.17
Lupinus arboreus	OBI117911	38.734	69.251	44.605	335.524	7.515	13.854	31	93.156
Lupinus arboreus	OBI117951	18.591	39.825	12.551	213.499	5.408	21.007	11	20.926
Lupinus arboreus	RSA0070145	26.257	51.093	24.511	384.343	8.08	15.969	32	97.043
Lupinus arboreus	SD00024544	31.247	58.948	29.806	337.354	6.601	12.991	46	45.027
Lupinus arbustus	BLMMD03118	42.268	74.09	37.048	455.739	7.285	10.468	38	128.879
Lupinus arbustus	CIC041701	39.257	90.096	98.345	480.41	8.772	9.964	51	136.141
Lupinus arbustus	CIC048045	35.809	67.142	43.707	324.591	2.795	7.781	32	62.062
Lupinus arbustus	ID064291	47.522	86.271	115.077	481.478	6.43	9.012	24	180.108
Lupinus arbustus	ID172337	32.196	60.619	57.418	315.868	4.107	10.268	105	38.212
Lupinus arcticus	H1238329	24.77	55.37	47.683	114.474	6.286	12.775	13	47.854
Lupinus arcticus	H1238331	19.792	46.627	48.821	128.253	6.706	14.972	13	30.564
Lupinus arcticus	H1238347	27.807	51.094	63.379	213.797	4.29	9.645	17	38.927
Lupinus arcticus	ID064332	14.282	29.737	38.201	141.143	2.133	9.441	17	23.938
Lupinus arcticus	UAAH 005281	67.306	120.537	176.193	293.954	3.9	13.075	18	51.662
Lupinus benthamii	ASU0295943	53.757	84.576	97.622	357.427	5.159	9.2	37	139.893
Lupinus benthamii	2284499	37.427	61.243	57.593	160.012	4.862	9.669	24	75.865
Lupinus benthamii	2284509	27.236	49.36	43.693	167.219	6.177	9.456	84	149.229
Lupinus benthamii	2284519	29.931	49.262	72.931	184.338	8.678	12.874	21	92.144
Lupinus benthamii	2284521	19.218	32.924	77.162	393.973	5.112	6.42	38	179.788
Lupinus chamissonis	CSLA001902	18.332	36.757	24.878	481.953	5.758	20.849	21	67.633
Lupinus chamissonis	RSA0060562	16.563	33.561	16.135	221.041	6.774	14.055	15	38.726
Lupinus chamissonis	SDSU04665	13.809	23.657	23.955	247.852	4.691	10.126	39	124.847
Lupinus chamissonis	SFV106566	20.546	39.613	32.914	191.795	5.54	12.586	29	112.851
Lupinus chamissonis	UCSC100001536	13.978	35.584	17.634	134.958	6.092	12.713	13	68.93
Lupinus citrinus	AHUC105090	22.536	30.868	32.915	162.563	3.694	8.956	50	67.371
Lupinus citrinus	COLO01611136	12.868	25.605	20.517	176.812	2.907	5.901	23	23.243
Lupinus citrinus	NMNH-02284970	16.774	33.012	23.692	192.629	4.069	10.894	34	31.054
Lupinus citrinus	OBI112884	22.433	38.84	33.254	107.521	4.823	8.474	46	56.356
Lupinus citrinus	RMBL0001850	17.004	29.786	29.151	83.301	4.383	8.191	109	98.55
Lupinus concinnus	OBI108110	9.519	17.297	31.662	45.701	1.588	6.253	7	17.368
Lupinus concinnus	SBBG204615	19.07	32.507	20.294	275.79	3.829	9.727	178	161.36
Lupinus concinnus	SBBG208801	7.039	14.412	13.342	140.75	2.11	6.624	138	22.378
Lupinus concinnus	SJNM-V-0034747	13.086	19.378	27.728	51.546	1.847	8.426	21	49.399
Lupinus concinnus	UTEPF6064	23.262	40.343	63.029	150.455	3.825	5.908	44	92.231
Lupinus excubitus	CSLA001958	18.834	37.075	53.17	372.635	4.845	11.044	21	68.96
Lupinus excubitus	DAV336494	36.476	65.578	100.646	375.895	4.622	9.744	42	202.14
Lupinus excubitus	RSA0036453	29.424	58.338	75.362	421.487	5.079	12.802	20	101.113
Lupinus excubitus	SBBG208628	18.755	32.512	81.919	190.952	4.597	9.558	27	204.594
Lupinus excubitus	UCSC100001542	30.957	64.873	79.424	252.39	6.714	15.14	56	126.787
Lupinus formosus	SBBG208570	24.676	45.038	29.48	287.447	3.748	13.724	42	59.317
Lupinus formosus	SBBG208571	33.249	56.998	35.18	329.689	3.75	11.664	32	110.791
Lupinus formosus	SBBG209210	17.067	37.612	81.917	226.384	5.537	12.156	15	86.301
Lupinus formosus	SDSU04975	40.89	65.568	66.375	310.059	3.763	10.64	5	103.729
Lupinus formosus	SFV106602	33.092	64.134	57.968	274.206	7.687	11.883	113	186.031
Lupinus guadalupensis	SBBG181747	22.789	35.864	33.968	235.341	5.717	11.662	6	46.452
Lupinus guadalupensis	SD00017168	21.442	25.311	28.79	223.559	6.365	13.503	7	23.139
Lupinus guadalupensis	SD00032910	27.871	47.467	42.42	292.617	7.837	13.917	19	91.358
Lupinus guadalupensis	SD00032911	28.742	57.793	51.472	227.796	5.097	10.592	12	25.201
Lupinus guadalupensis	SD00032915	23.003	48.976	38.307	237.972	7.446	12.187	14	36.217
Lupinus hirsutissimus	SBBG209167	34.479	64.525	85.833	285.909	4.45	12.654	31	214.337
Lupinus hirsutissimus	SD00015976	38.071	69.069	86.097	149.873	4.44	14.226	23	233.776
Lupinus hirsutissimus	SDSU14277	41.496	67.658	124.804	292.136	4.553	13.649	14	57.993
Lupinus hirsutissimus	SDSU19990	24.764	37.998	60.889	398.37	3.49	12.876	22	107.762
Lupinus hirsutissimus	SFV106608	28.051	43.194	65.591	313.029	3.994	14.226	24	179.79
Lupinus mutabilis	IND0052004	34.706	60.119	46.366	174.58	7.322	16.106	32	104.822
Lupinus mutabilis	IND0052011	23.955	48.323	19.918	105.874	13.345	17.062	12	102.839
Lupinus mutabilis	NMNH-02289254	44.666	76.522	70.604	167.247	10.85	16.108	19	111.992
Lupinus mutabilis	USF113141	12.812	28.281	10.965	295.571	4.943	15.38	2	29.862
Lupinus mutabilis	USF197203	37.784	62.232	43.341	254.133	12.406	15.59	5	46.003
Lupinus nanus	DAV336945	19.127	32.567	45.244	295.632	3.276	9.937	29	97.979
Lupinus nanus	RSA0072108	13.692	23.646	36.184	155.134	6.225	10.87	12	46.416

Lupinus nanus	SBBG219337	10.879	19.14	28.384	137.683	4.869	10.302	28	101.098
Lupinus nanus	SDSU05021	12.94	20.654	32.1	344.553	5.389	9.411	107	86.125
Lupinus nanus	UTC00284091	15.142	31.958	34.443	161.614	4.35	10.896	45	45.975
Lupinus neomexicanus	UNM0045168	28.317	48.023	48.624	167.888	5.466	11.902	13	93.048
Lupinus neomexicanus	UNM0045178	42.965	59.291	49.225	359.76	7.381	11.017	15	214.283
Lupinus neomexicanus	UTEPD9067	32.769	53.226	110.153	341.266	4.211	8.56	39	147.578
Lupinus neomexicanus	UTEPD9068	30.116	54.889	51.767	282.636	5.666	10.2	48	175.373
Lupinus nootkatensis	ALA-H1238489	41.339	66.775	41.987	226.206	10.37	15.148	37	142.444
Lupinus nootkatensis	OBI108381	43.513	62.71	32.311	413.118	9.794	12.747	25	110.015
Lupinus perennis	ACM0192	43.713	76.33	85.632	236.779	7.265	13.81	20	228.657
Lupinus perennis	CM265591	44.937	83.927	61.329	363.477	5.675	12.115	15	52.627
Lupinus perennis	NMNH-02286705	30.115	54.235	97.669	317.139	4.357	11.581	22	84.272
Lupinus perennis	PH00199903	37.873	68.504	86.15	183.703	6.534	12.767	27	195.157
Lupinus perennis	PH00199919	30.49	58.315	75.043	287.349	5.536	11.768	27	119.575
Lupinus prunophilus	DES00033743 lg	29.239	60.807	76.906	180.935	7.344	11.417	20	96.149
Lupinus prunophilus	FLD0006026	50.493	87.694	119.432	597.355	9.202	13.054	24	124.123
Lupinus prunophilus	MESA05839	28.18	55.678	101.82	592.201	8.16	7.809	36	205.43
Lupinus prunophilus	RSA0003497	65.479	123.332	92.524	336.412	9.174	10.813	19	244.34
Lupinus prunophilus	SJNM-V-0034874	34.402	61.298	44.38	157.644	5.244	10.085	14	56.614
Lupinus shockleyi	RSA0047881	7.71	11.978	21.866	13.675	0.784	2.457	6	6.507
Lupinus shockleyi	RSA0061123	13.913	24.198	25.692	9.905	0.002	0.005	5	9.217
Lupinus shockleyi	RSA0103044	17.856	32.547	72.966	63.215	4.063	4.498	93	26.863
Lupinus shockleyi	RSA0167800	19.843	40.898	76.812	16.213	2.551	5.173	70	30.18
Lupinus shockleyi	SD00023739	15.851	31.86	66.692	54.632	5.568	0.006	42	66.126
Lupinus sparsiflorus	ASU0299597 lg	15.722	29.926	45.079	85.071	4.322	9.133	22	68.281
Lupinus sparsiflorus	CSLA001812	27.067	45.151	70.672	287.551	5.002	8.395	50	275.553
Lupinus sparsiflorus	DES00029700 lg	13.452	21.621	32.637	127.895	4.559	8.635	55	97.195
Lupinus sparsiflorus	DES00084646 lg	23.956	40.83	50.671	237.063	2.661	0.008	100	59.747
Lupinus sparsiflorus	LOB105665	20.922	37.597	43.321	149.259	3.402	8.412	57	37.929
Lupinus succulentus	DAV340494	33.182	64.828	49.443	253.269	3.514	16.033	20	67.268
Lupinus succulentus	DES00039444 lg	21.685	36.329	63.603	246.538	4.123	8.854	28	35.598
Lupinus succulentus	IRVC113292	51.039	90.023	83.213	463.883	4.635	12.831	35	103.482
Lupinus succulentus	RSA0088387	42.896	71.287	118.352	206.463	7.802	12.32	27	277.39
Lupinus succulentus	SD00033358	27.427	52.904	56.105	407.832	3.379	11.777	20	58.027
Lupinus succulentus	sfv106718	39.418	70.643	127.176	213.157	4.974	14.887	40	123.873
Lupinus syriggedes	2481	21.2	31.3	43.1	213	2.2	8.2	23	164
Lupinus syriggedes	11625	15.1	24.8	22.5	99	4.4	9	21	45.5
Lupinus syriggedes	3202	12.2	29.9	34	210.2	1.3	8.8	23	73.5
Lupinus syriggedes	88	52.8	55.1	31.5	193.5	6.2	12.2	43	214.5
Lupinus syriggedes	2000	58.6	59.5	50	393.4	5.5	9.9	30	145.5
Lupinus huigrensis	147	49.4	34.7	39.8	260.3	5.9	11.5	16	65.3
Lupinus huigrensis	3307	22.1	37.1	38.5	112.8	5.1	7.7	14	53.6
Lupinus huigrensis	2208	31.7	49.8	47.2	220.8	5.4	11.2	15	63.8
Lupinus huigrensis	815	47.5	51.2	36.3	111.2	5.5	11.1	14	71
Lupinus huigrensis	2668	37.2	35	47.2	191.5	7.4	13.1	19	90.2
Lupinus matucanicus	237	28.3	36.3	46.1	210.5	3.1	8.5	9	38.9
Lupinus matucanicus	141	20.5	32.7	51.2	54.5	4.5	9.1	20	55.4
Lupinus matucanicus	11454	16.8	19.7	18.3	57.3	2.9	6.8	7	11.8
Lupinus matucanicus	3087	16.1	29.8	31.1	85.5	4.9	9.6	18	58.3
Lupinus matucanicus	3020	22.2	34.6	33	162.1	4.4	9.9	17	87.4
Lupinus aureus	188	24.9	57.9	50.4	147.3	5.8	11.8	13	89.5
Lupinus aureus	15763	15.4	21.9	28.5	11.5	3.1	8.6	4	6.2
Lupinus aureus	301	17	21.6	36.9	15.7	4.6	8.9	4	15.9
Lupinus aureus	2571	17.5	23.7	34.4	28	3.8	8.8	8	31.1
Lupinus aureus	97/703	31.9	34.1	39.5	247.6	5.6	11.1	13	43.1
Lupinus chugurensis	3079	79	87.3	98.5	1668.2	6.7	17.2	51	331.8
Lupinus chugurensis	1822	47.3	84.4	61.5	NA	6.1	13.6	27	181
Lupinus chugurensis	235	40.4	46.5	58.6	15	1253	13.1	47	247
Lupinus chugurensis	2002	120.3	124.8	100	980	5.6	18.9	53	220
Lupinus chugurensis	102	58	96.2	66.4	484.8	5.5	13.3	77	315.2
Lupinus espinarensis	657	29.2	50.5	86.2	298.2	3.7	8.1	43	101.8
Lupinus espinarensis	11023	49.8	50.7	93.3	630.1	4	8.4	48	69.9
Lupinus espinarensis	2392	51.1	57.7	80.3	191.1	3.9	7.9	99	158.9
Lupinus espinarensis	12040	32.3	34.6	63.6	NA	4.6	9.8	52	94.9
Lupinus espinarensis	7080	41.2	43.7	42.8	NA	9.8	9.3	39	93.8
Lupinus roquensis	2005	80.9	95.1	85.2	358.7	5.8	12.1	31	91.3
Lupinus roquensis	6491	36.2	43.3	58.8	NA	8	11.5	107	342.9
Lupinus roquensis	3080	29.3	44.4	51.2	670.8	7.9	11.6	30	129.2
Lupinus roquensis	2199	63.2	51.3	132.5	303.6	6.1	11.9	90	296.4
Lupinus fieldii	7566	21.8	30.9	79.7	175.4	3.8	10.5	73	128.6
Lupinus fieldii	163	41.5	80.8	96.3	65.8	4.7	10.4	84	175.7
Lupinus fieldii	1556	25.6	30.4	109.8	107.8	6.3	10.7	52	135.3
Lupinus fieldii	157	48.8	76.3	164.5	217.2	3.9	9.4	56	84.7
Lupinus fieldii	994	39.8	57.2	84.4	266.1	5.1	12.8	53	183.1
Lupinus misticola	2301	24.9	35.4	55.4	65.3	6.8	9.2	12	33.7
Lupinus misticola	2391	45.5	37.7	140.4	130.8	5.6	8.4	67	122.6
Lupinus misticola	2355	34.1	41.9	130.2	177.5	6.3	10.1	36	115.5
Lupinus misticola	2365	29.2	29.7	102.4	7.3	178.2	10.8	22	61.4
Lupinus misticola	2350	32.7	48.8	131.2	202.3	7.1	12.6	14	94.6
Lupinus pickeringii	11200	6.7	6.9	12.9	0	2.2	5.8	5	0
Lupinus pickeringii	13760	6.7	11.7	21.1	0	2.9	8.5	3	0
Lupinus pickeringii	2333	3.6	5.3	17.7	0	1.5	5.4	3	0
Lupinus pickeringii	51	12	14.6	30.6	0	2.7	6.9	8	0
Lupinus pickeringii	2267	13.3	13.5	16.5	0	3.7	7.3	23	0
Lupinus ananeanus	6	12.5	21.2	33.1	0	3.1	6	12	28.4
Lupinus ananeanus	6298	8.9	17.9	35.5	0	3	6.5	16	31.8
Lupinus ananeanus	1732	11.1	15.9	55.4	0	2.8	4.8	15	25.4
Lupinus ananeanus	2266	19.7	26.1	84.7	31.2	7.7	7.6	16	42.6
Lupinus ananeanus	2438	17.6	35.4	71.2	0	3.1	6.8	9	42.5
Lupinus nubigenus	10789	36.3	60.2	140.4	70.3	4.8	9.3	99	110
Lupinus nubigenus	7404	25.4	41.3	93.6	80.5	4.4	11.2	42	69
Lupinus nubigenus	704	35.8	47.6	121	42.2	9.3	NA	32	101.7
Lupinus nubigenus	200	43.4	74.6	141.5	80.4	4.2	10.7	57	102.8
Lupinus nubigenus	2239	38.6	67.8	125.4	50.2	3.3	11.1	74	125.4
Lupinus pycnostachys	2374	67.8	58.9	75.6	NA	3.6	5.4	48	106
Lupinus pycnostachys	2370	16.8	25.9	74.6	466.9	4.2	8.3	82	133.1
Lupinus pycnostachys	2443	34.4	36.8	73.3	134.3	3	8.2	27	31.3
Lupinus pycnostachys	2445	38	53.1	55.6	389.6	2.7	8.7	58	110.4
Lupinus pycnostachys	2367	35.1	40	32.6	123.9	3.1	7.2	56	100.2
Lupinus pinguis	5458	24.6	32.4	137.4	59.3	5.9	9.1	47	64.8
Lupinus pinguis	7581	48.5	69.5	186.3	49.8	6.7	13.6	70	89.2
Lupinus pinguis	7581	34	45.1	170.1	62.4	4.1	9.2	74	96.5
Lupinus pinguis	160	19.2	32.3	6.4	57.6	5.2	12.8	14	23.3
Lupinus pinguis	160	NA	37.7	23.5	84.9	32.2	10.9	38	82.1
Lupinus subinflatus	2319	23.7	46.2	73.5	21.4	4	4.6	39	78.9
Lupinus subinflatus	8619	26.1	33.4	89	43.3	2.1	7.8	40	83.2
Lupinus subinflatus	3621	27.6	34.9	14.2	72.2	2.9	5.1	41	58.3
Lupinus subinflatus	213	25.2	26.9	63.5	43.1	2.2	5.6	17	25.3
Lupinus subinflatus	2000/24	20.6	44.2	82.5	7.8	1.1	4.4	28	29.7
Lupinus weberbaueri	4314	74.5	111.2	125.3	153.4	6.8	10.5	121	337.1
Lupinus weberbaueri	12597	68.2	91.6	156.2	1360.9	5.1	15.1	113	239.1
Lupinus weberbaueri	909	71.2	87.5	150.5	NA	NA	NA	127	190.3
Lupinus weberbaueri	2233	59.4	56	122.3	192.3	6.6	14.4	224	495.6
Lupinus weberbaueri	52	134.5	149.5	201.3	266.2	5.1	14.2	271	903.8
Lupinus huaronensis	2241	47.2	62.1	114.6	137.3	3	8.1	179	320.5
Lupinus huaronensis	2048	55.9	80	90.4	254.6	2.3	9.4	96	195.5
Lupinus huaronensis	91	26.6	38.9	43.5	36.9	2.3	10.8	72	127.7
Lupinus huaronensis	4229	94.2	94.1	104.3	208.5	3.2	13.4	84	212.8
Lupinus huaronensis	155	37.5	72.1	112.2	262.6	1.9	10.1	81	159.9
Lupinus purosericeus	2209	37.2	40.9	97.6	309.3	5.2	10.9	79	123.5
Lupinus purosericeus	2248	40	65.4	140.1	205.4	4.8	9.9	72	200.3
Lupinus purosericeus	1850	53.4	77.2	322.2	444.9	5.1	11.9	70	140.5
Lupinus purosericeus	5258	21.9	47	119.6	214.3	3.2	9.6	79	135.2

Lupinus purosericeus	1295	42.5	66	123.4	214.5	4.9	11.5	55	85.7
Lupinus sylvesterii	514	50.1	66.4	117.5	NA	NA	NA	NA	NA
Lupinus sylvesterii	1341	43.1	56.7	68.2	164.7	4.1	11.6	72	155.5
Lupinus sylvesterii	1153	51.2	65.8	92.8	21.6	3.9	10.2	77	216.9
Lupinus sylvesterii	1353	24.3	23.5	47.1	208.5	4.4	12.8	65	136.8
Lupinus sylvesterii	1363	30.7	61.6	94.1	248.4	4.3	13.5	48	188.8
Lupinus herzogii	2252	25.4	47.1	57.2	225.2	4.1	6.2	27	74.8
Lupinus herzogii	2332	12.9	29	34.5	221.4	3.7	7.4	32	78.6
Lupinus herzogii	2296	48	29.7	115.3	NA	2.1	9.5	12	28.2
Lupinus herzogii	2297	42.3	71.1	79.6	NA	2.6	12.2	55	149.2
Lupinus herzogii	37273	67.1	96.8	99.9	NA	4.6	9.3	101	237.4
Lupinus nubilorum	2421	56.3	85.4	107.2	311.9	3.7	10.1	69	188.1
Lupinus nubilorum	27796	24.6	37.3	54.6	169.8	2.3	9.2	23	50.5
Lupinus nubilorum	2439	41.4	69.1	175.5	333.4	3.6	9.2	161	366.6
Lupinus nubilorum	2437	44.2	81.3	59.8	175.9	3.9	9.6	68	174.1
Lupinus nubilorum	7838	46.7	87.9	72.2	111.6	2.1	8.4	192	341.2
Lupinus alopecuroides	9926	93.5	87.8	131.2	94.3	2.7	10.5	77	214.9
Lupinus alopecuroides	E-455	47.4	69.2	68.1	85.5	3.6	9.9	104	248.1
Lupinus alopecuroides	10564	44.9	41.8	62.3	75.5	3.1	6.8	149	280.8
Lupinus alopecuroides	6783	75	49.4	178.3	NA	7.4	8.4	118	284.9
Lupinus alopecuroides	378	81.9	93.2	137.3	40.7	2.9	11.9	90	183.4
Lupinus triananus	25770	37.9	24.3	34.1	136.8	4.1	8.2	104	229.1
Lupinus triananus	41	48	61.6	89.3	NA	4.8	5.4	217	405.3
Lupinus triananus	55	122.2	101	158.9	NA	6.6	16.5	172	618.3
Lupinus triananus	27016	61.3	94.8	121.4	NA	9.1	10.7	254	365.4
Lupinus triananus	26002	75.1	107.8	74.9	491.5	6.4	10.4	57	152.9
Lupinus luisanae	51	91.2	42	207.8	1262.2	11.1	10.2	62	237.8
Lupinus luisanae	49	70.1	39.2	130.8	NA	6.4	NA	NA	NA
Lupinus luisanae	50	295.1	269.3	162.6	NA	5.3	11.2	NA	NA
Lupinus jelskianus	17870	69.8	66.9	39.5	5.8	1159.3	11.6	56	340.7
Lupinus jelskianus	2202	62.2	68	37.2	1689.7	8.9	13.1	33	110.3
Lupinus jelskianus	7104	23.7	42.3	15.4	NA	4.5	13.5	28	160.6
Lupinus jelskianus	105	36.3	62.1	43.9	2388.8	6.8	12.2	35	111.2
Lupinus jelskianus	2004	83.7	89.1	73.6	2467.08	6.9	13.6	47	32.92
Lupinus semperflorens	3629	36.8	58.6	38.2	1857.6	7.6	13.2	32	142.4
Lupinus semperflorens	219	700.8	56.9	61.2	1363.5	7.2	13.1	33	136.5
Lupinus semperflorens	2012	29.4	49.6	37.3	NA	8.2	13.5	41	163.2
Lupinus semperflorens	2032	74.9	80.1	56.3	NA	8.9	16.5	50	221.4
Lupinus semperflorens	109	36.6	46.8	20.4	4872.1	9.9	19.1	30	127.9
Lupinus mutabilis	2280	46	67.2	45.1	8.2	1624.4	15.8	24	175.6
Lupinus mutabilis	2326	43.4	60.6	40.4	NA	6.2	12.9	25	130.6
Lupinus mutabilis	2253	48.9	52	55.6	1288.9	11.8	19.2	28	211.1
Lupinus mutabilis	2279	37.2	57.5	45.7	1605.2	11.3	17.9	24	194.8
Lupinus mutabilis	62458	43.9	84.9	55.5	NA	7.8	17.1	7	38.1
Lupinus piurensis	214	33.4	33.4	43.4	918.9	6.2	104.8	15	81.1
Lupinus piurensis	134	47.1	56.1	107.2	6.8	357.9	15.4	28	242.1
Lupinus piurensis	2663	50.8	68.1	53.1	438.3	6.9	11.9	17	122.5
Lupinus piurensis	122	37.1	54.9	38.5	532.6	6.8	13.8	27	67.4
Lupinus piurensis	2196	36.8	52.7	506	600	7	11.8	40	174.7
Lupinus ellsworthianus	2246	37.2	39	24.5	654.2	6.1	10.5	44	145.8
Lupinus ellsworthianus	25223	24	38.9	31.2	225.5	8.3	8.8	12	57.6
Lupinus ellsworthianus	881716	21.9	29.3	32.4	245.9	4.9	7.5	15	54.1
Lupinus ellsworthianus	15924	20.4	29.4	27.5	268.4	4.9	10.6	33	122.5
Lupinus ellsworthianus	805	22.1	22.9	9.8	158.2	4.1	9.3	18	41.8
Lupinus praestabilis	30409	69.9	73.8	122.1	NA	8.6	14.8	51	271.2
Lupinus praestabilis	142	65.6	85.4	57.2	1972.8	5.6	12.8	37	27.2
Lupinus praestabilis	2000/581	65.2	63.6	31.5	NA	15.8	46	NA	172.3
Lupinus praestabilis	143	135.6	139.9	52.6	1721.6	8.1	14.1	62	278.4
Lupinus praestabilis	2353	52.6	55	83.1	NA	9	15.2	50	215.4
Lupinus romasanus	2229	21.5	29.9	34.1	300	2.9	10.1	42	145.4
Lupinus romasanus	33	52.9	51.6	40.4	253.8	4.6	7.8	42	146.2
Lupinus romasanus	41	27.2	17.9	17.2	314.8	6.9	11	26	85.2
Lupinus romasanus	65	28.6	55.9	25.5	1385	5.6	10.1	42	115
Lupinus romasanus	2017	64.9	66.1	35.4	878.4	7.1	11.7	42	121.6
Lupinus tauris	42	15.1	19.9	7.2	521.8	5.6	NA	7	28.2
Lupinus tauris	5938	9	8.1	3.5	382.4	4.2	9.1	5	17.6
Lupinus tauris	10220	12	17	3.9	679.6	4.2	9.2	7	20.4
Lupinus tauris	172	7.8	15.1	4.5	277.9	3.2	10.4	9	22.1
Lupinus tauris	171	11.2	17.2	21.7	195.2	3.7	8.1	7	22.1
Lupinus smithianus	11002	8.1	11.1	3.1	186.4	4.1	9.1	4	13.6
Lupinus smithianus	368	8.6	9.9	4.6	NA	2.9	9.1	8	16.2
Lupinus smithianus	10786	14.5	20.8	7	292.7	2.3	5.9	6	7.3
Lupinus smithianus	10768	3.4	6.1	4.9	142.4	2.6	8.8	8	7.2
Lupinus smithianus	10775	11.3	12.5	9.2	288.4	2.6	9.1	4	11.6
Lupinus solanagrorum	2007	30.1	25.9	10.8	317.8	4	11.4	NA	82.2
Lupinus solanagrorum	2014	25.9	32.2	7.6	189.6	8	12.7	27	110.4
Lupinus solanagrorum	129	8.1	19.7	12.9	197.6	4.8	13.2	44	102.4
Lupinus solanagrorum	106	21.8	18.9	13.6	289.2	6.4	12	37	110.8
Lupinus solanagrorum	2660	18.9	21.8	13.2	452.9	4.8	12.5	20	71.4
Lupinus involutus	10727	24.1	25.2	15.7	358.6	9.3	11.9	11	41.4
Lupinus involutus	10726	25.5	31	14.4	242.3	6.9	12.6	8	57.7
Lupinus involutus	11254	23.2	45.3	25.1	1478.4	10.1	11.4	8	21.6
Lupinus involutus	11901	24.6	39.1	25.9	944.7	8.1	14.4	6	55.3
Lupinus involutus	194	18.1	15.1	12.8	600	11.9	13.2	16	29.8
Lupinus foliolosus	184	25.4	23.8	15.4	550.9	5.1	8.9	23	49.1
Lupinus foliolosus	21976	15	25.1	12.1	134.8	4.3	10.6	16	35.6
Lupinus foliolosus	595	16.8	29	16	2.4	417.1	9.1	34	82.9
Lupinus foliolosus	165	19.6	26.4	14.6	453.2	4	10.3	26	46.8
Lupinus foliolosus	8481	12.8	17.1	13.1	123.1	8.4	NA	12	43.8
Lupinus microphyllus	81	3.1	4.4	3.3	45.6	0.4	4.9	4	4.4
Lupinus microphyllus	64	2.6	3.1	3	2.7	61.4	6.2	6	7.8
Lupinus microphyllus	9824	4.2	4.3	4.1	38.8	0.1	4.6	5	3.1
Lupinus microphyllus	23147	6.1	6.4	3.2	46.2	2.8	7.9	2	2.5
Lupinus microphyllus	1764	5.1	6.1	2.1	21.4	0.1	5.6	3	2.1
Lupinus prostratus	2049	8.6	11.1	8.2	139.4	0	8.9	5	9.7
Lupinus prostratus	162	4.7	6.2	7.4	18.1	0	8	3	1.8
Lupinus prostratus	2042	5.6	7.2	11.1	19.4	0	6.1	6	5.5
Lupinus prostratus	2240	6.3	6.6	5.1	53.1	0	5.1	6	15.2
Lupinus prostratus	2236	3.6	4.3	3.9	10.5	0	5.5	4	4.1
Lupinus sufferrugineus	2322	25.4	36.8	25.1	1908.9	6.5	12.5	29	91.1
Lupinus sufferrugineus	2325	28.3	51.5	30.9	1924.4	6.9	10.5	27	75.6
Lupinus sufferrugineus	2330	26.9	50	37.1	1914.7	7	9.6	26	85.3
Lupinus sufferrugineus	2368	51.9	53.1	71.8	1351.4	4.2	9.4	34	148.6
Lupinus sufferrugineus	2372	41.3	41.9	100.8	NA	3.9	9	42	59
Lupinus buchtienii	2328	9.4	10.4	5.9	57.4	1.6	6.4	8	15.7
Lupinus buchtienii	2371	5.9	5.2	7.8	56.7	1.5	6.2	6	10.4
Lupinus buchtienii	2265	6.9	4.9	6.8	94.6	0.5	5.8	8	18.3
Lupinus buchtienii	985	5.5	6	7.3	28.3	1.4	5.1	6	5.4
Lupinus buchtienii	957	6.5	7.2	11.2	19.1	1	5.9	5	8.5
Lupinus interruptus	59	55.8	61	36.2	810	4.9	12.1	56	190
Lupinus interruptus	40	93.1	90.9	66	1369.1	5.1	13.3	32	130.9
Lupinus interruptus	45	38.4	44	51.1	1366.5	6	11.2	41	133.5
Lupinus interruptus	5903	133.9	147.4	74.5	1842.5	5.4	13.8	39	157.5
Lupinus interruptus	53	68.2	55.6	27.3	1463.7	2.9	9.9	18	36.3
Lupinus jahnii	42	13.2	18.3	13.1	225.6	7.9	11	29	74.4
Lupinus jahnii	44	20.4	23.1	15.5	118.1	7.5	11.1	39	81.9
Lupinus jahnii	39	10	11.4	8.1	267.2	6.2	13.9	48	170.7
Lupinus jahnii	41	21.2	21.1	13.6	329	4.2	11.5	38	71
Lupinus jahnii	43	13.2	14.5	4.6	231.5	3.9	11.4	7	15
Lupinus eremonomus	207	37.9	41.2	46.5	688.8	4.9	9.8	35	11.2
Lupinus eremonomus	30	43.2	42	43	323.4	5.1	11.5	35	87.3
Lupinus eremonomus	88	30.4	39	21.1	497.9	5.8	14.2	20	102.1
Lupinus eremonomus	197	12.5	17.2	15.5	244.1	4.8	10.3	22	49.7

Lupinus eremonomus	199	24.2	34.3	20.6	264.1	4.8	10.3	27	69.8
Lupinus venezuelensis	138	22.5	17.2	63.6	274.2	7.2	11.2	41	25.8
Lupinus venezuelensis	137	15.9	22	39.7	212.1	4.8	9.2	45	266.2
Lupinus venezuelensis	140	11.1	12.9	53.3	179.4	8.5	10.5	30	114.2
Lupinus venezuelensis	36	16.2	19.9	34.4	151.2	4	10.1	33	154.3
Lupinus venezuelensis	35	17	28.2	50.6	293.3	6.6	11.6	25	89.4
Lupinus jahnii	159	15.7	26.1	11.2	269.5	5.5	9.8	38	130.5
Lupinus jahnii	153	14	17.9	4.2	25.8	4.3	9.8	5	16.2
Lupinus jahnii	151	29.2	43.8	19.7	553.8	4.1	9.3	20	46.2
Lupinus jahnii	180	24.9	29.5	23.8	152.1	4.1	11.9	19	93.2
Lupinus jahnii	150	20.2	37.6	17.1	541.4	4.5	10.2	18	58.6
Lupinus pygmaeus	17	13	13.2	21.7	145.1	2.9	7.8	14	35.2
Lupinus pygmaeus	20	9.1	15.1	19.1	111.2	1.3	7.6	8	15.3
Lupinus pygmaeus	119	5.8	8.1	20.2	82.3	3.2	10.1	9	25.1
Lupinus pygmaeus	118	5.1	11.1	21.3	142.2	6.1	9.6	19	98.9
Lupinus pygmaeus	141	10.5	10.2	12.4	148.6	4.8	9.1	22	88.5

TABLE S2: Expert-validated discrete variables describing the global distribution and the life forms of the different species.

Species	Distribution	Longevity	Life form
Lupinus albicaulis	western North America	Perennial	Herbacouse flowering plant
Lupinus alopecuroides	western South America	Perennial	Herbacouse flowering plant
Lupinus ananeanus	western South America	Perennial	Herbacouse flowering plant
Lupinus arboreus	western North America	Perennial	Shrub, or dwarf-shrub
Lupinus arbustus	western North America	Perennial	Herbacouse flowering plant
Lupinus arcticus	western North America	Perennial	Herbacouse flowering plant
Lupinus aridus	western North America	Perennial	Herbacouse flowering plant
Lupinus aureus	western South America	Annual	Herbacouse flowering plant
Lupinus benthamii	western North America	Annual	Herbacouse flowering plant
Lupinus buchtienii	western South America	Perennial	Herbacouse flowering plant
Lupinus caespitosus	western North America	Perennial	Herbacouse flowering plant
Lupinus caudatus	western North America	Perennial	Shrub, or dwarf-shrub
Lupinus chamissonis	western North America	Perennial	Shrub, or dwarf-shrub
Lupinus chugurensis	western South America	Annual	Herbacouse flowering plant
Lupinus citrinus	western North America	Annual	Herbacouse flowering plant
Lupinus concinnus	western North America	Annual	Herbacouse flowering plant
Lupinus ellsworthianus	western South America	Perennial	Shrup, or tree
Lupinus eremonomus	western South America	Perennial	Shrup, or tree
Lupinus espinarensis	western South America	Perennial	Herbacouse flowering plant
Lupinus excubitus	western North America	Perennial	Shrub, or dwarf-shrub
Lupinus fieldii	western South America	Perennial	Herbacouse flowering plant
Lupinus foliolosus	western South America	Perennial	Shrup, or tree
Lupinus formosus	western North America	Perennial	Shrub, or dwarf-shrub
Lupinus guadalupensis	western North America	Annual	Herbacouse flowering plant
Lupinus herzogii	western South America	Perennial	Herbacouse flowering plant
Lupinus hirsutissimus	western North America	Annual	Herbacouse flowering plant
Lupinus holosericeus	western North America	Perennial	Herbacouse flowering plant
Lupinus huaronensis	western South America	Perennial	Herbacouse flowering plant
Lupinus huigrensis	western South America	Annual	Herbacouse flowering plant
Lupinus interruptus	western South America	Perennial	Shrup, or tree
Lupinus involutus	western South America	Perennial	Shrup, or tree
Lupinus jahnii	western South America	Perennial	Shrup, or tree
Lupinus jelskianus	western South America	Perennial	Shrup, or tree
Lupinus lepidus	western North America	Perennial	Herbacouse flowering plant
Lupinus luisanae	western South America	Perennial	Herbacouse flowering plant
Lupinus matucanicus	western South America	Annual	Herbacouse flowering plant
Lupinus microphyllus	western South America	Perennial	Herbacouse flowering plant
Lupinus misticola	western South America	Perennial	Herbacouse flowering plant
Lupinus mutabilis	western North America	Annual	Herbacouse flowering plant
Lupinus nanus	western North America	Annual	Herbacouse flowering plant
Lupinus neomexicanus	western North America	Perennial	Shrub, or dwarf-shrub
Lupinus nootkatensis	western North America	Perennial	Shrub, or dwarf-shrub
Lupinus nubigenus	western South America	Perennial	Herbacouse flowering plant
Lupinus nubilorum	western South America	Perennial	Herbacouse flowering plant
Lupinus perennis	western North America	Perennial	Herbacouse flowering plant

Lupinus pickeringii	western South America	Perennial	Herbacouse flowering plant
Lupinus pinguis	western South America	Perennial	Herbacouse flowering plant
Lupinus piurensis	western South America	Perennial	Herbacouse flowering plant
Lupinus praestabilis	western South America	Perennial	Shrup, or tree
Lupinus prostratus	western South America	Perennial	Herbacouse flowering plant
Lupinus prunophilus	western North America	Perennial	Herbacouse flowering plant
Lupinus purosericeus	western South America	Perennial	Herbacouse flowering plant
Lupinus pycnostachys	western South America	Perennial	Herbacouse flowering plant
Lupinus pygmaeus	western South America	Perennial	Herbacouse flowering plant
Lupinus romasanus	western South America	Perennial	Shrup, or tree
Lupinus roquensis	western South America	Perennial	Herbacouse flowering plant
Lupinus sellulus	western North America	Perennial	Herbacouse flowering plant
Lupinus semperflorens	western South America	Perennial	Shrup, or tree
Lupinus shockleyi	western North America	Annual	Herbacouse flowering plant
Lupinus smithianus	western South America	Perennial	Shrup, or tree
Lupinus solanagrorum	western South America	Perennial	Shrup, or tree
Lupinus sparsiflorus	western North America	Annual	Herbacouse flowering plant
Lupinus subinflatus	western South America	Perennial	Herbacouse flowering plant
Lupinus succulentus	western North America	Annual	Herbacouse flowering plant
Lupinus sufferrugineus	western South America	Perennial	Shrup, or tree
Lupinus sulphureus	western North America	Perennial	Herbacouse flowering plant
Lupinus sylvesterii	western South America	Perennial	Herbacouse flowering plant
Lupinus syriggedes	western South America	Annual	Herbacouse flowering plant
Lupinus tauris	western South America	Perennial	Shrup, or tree
Lupinus triananus	western South America	Perennial	Herbacouse flowering plant
Lupinus venezuelensis	western South America	Perennial	Herbacouse flowering plant
Lupinus weberbaueri	western South America	Perennial	Herbacouse flowering plant

TABLE S3: Model support of 100 posterior phylogenies for 8 plant traits. Each clade was fitted to nine models: Brownian motion (BM), Ornstein-Uhlenbeck (OU), early burst (EB), and Lévy process (LP). The model's name of the Lévy process is in brackets, the abbreviations represent jump normal (JN), variance Gamma (VG), and normal inverse Gaussian (NIG) with and without a Brownian motion (BM+). As model selection criterion mean and median AICc weight for leaflet length, leaf width, petiole, peduncle, pedicel, inflorescence, petal length (of the banner), and number of flowers per inflorescence, were computed and significant mean values are highlighted in gray.

Trait	Statistical location	BM	OU	EB	LP
Leaflet length	Mean	0.09	0.08	0.03	0.79 (JN)
	Median	0.04	0.05	0.02	0.88 (JN)
Leaf width	Mean	0.38	0.22	0.14	0.26 (JN)
	Median	0.38	0.17	0.14	0.17 (JN)
Petiole length	Mean	0.43	0.21	0.16	0.21 (JN)
	Median	0.44	0.18	0.16	0.17 (JN)
Peduncle length	Mean	0.00	0.00	0.00	1.00 (BM+VG)
	Median	0.00	0.00	0.00	1.00 (BM+VG)
Pedicel length	Mean	0.21	0.50	0.14	0.15 (VG)
	Median	0.23	0.52	0.14	0.14 (VG)
Inflorescence length	Mean	0.30	0.11	0.11	0.48 (JN)
	Median	0.24	0.08	0.09	0.58 (JN)
Petal length (of the banner)	Mean	0.46	0.19	0.17	0.17 (VG)
	Median	0.48	0.17	0.17	0.17 (VG)
Number of flowers per inflorescence	Mean	0.24	0.17	0.09	0.51 (JN)
	Median	0.26	0.17	0.09	0.17 (JN)

General Discussion

This thesis aimed to identify potential variations in evolutionary rates within and between alpine plant clades. I decided to set the focus on exploring two different kinds of rates: dispersal (covered in **Chapters I** and **II**) and trait evolution (**Chapter III**). Here, I will synthesize my findings and highlight the novel contributions my thesis makes to the field. The discussion is structured into three subchapters covering (1) challenges and optimization proposals while reconstructing biome shifts, (2) technical pitfalls when detecting evolutionary pulses, and (3) ubiquitous changes in evolutionary rates.

ALPINE BIOME SHIFTS

The initial idea of this thesis was to identify where in space and when in time biome transitions in and out of the alpine zone happened. I discovered multiple challenges and pitfalls when reconstructing alpine biome shifts on a global scale which are addressed in this subchapter. Further, I discuss reasons why the ElevDistr development was necessary (**Chapter I**) and why the focus was readjusted from biome shifts towards niche proxy shifts (**Chapter II**).

A study by Kong et al. (2021) explores the diversification of *Oreocharis* within the Hengduan Mountains, they argue that diversification dynamics in mountain ecosystems over time are rarely studied and that even fewer studies (e.g., Ding et al., 2020; Xing & Ree, 2017) work with multiple lineages. The benefit of studying multiple lineages lies in its ability to enable lineage comparison. This principle guided the study design of **Chapter II**, which includes the genera: *Primula*, *Lupinus*, and *Ranunculus*. However, working with multiple large plant clades also comes with daunting challenges and I assume, these challenges are the reasons why few multi-lineage studies are conducted. Fortunately, the scientific community has overcome technical and computational limitations to infer large phylogenies, because nowadays, there are many examples of phylogenetic trees with a thousand or more tips (e.g., Ding et al., 2020; Figueroa et al., 2022; Kerkhoff et al., 2014; Ringelberg et al., 2023; Zanne et al., 2014). Nonetheless, a particularly demanding challenge I experienced was obtaining sufficient high-quality data. For example, **Chapter III** was planned with a multiple-clade comparison but, it had to be narrowed down to *Lupinus* due to missing trait data. To prevent a similar issue for occurrence data, we used data from the Global Biodiversity Information Facility (GBIF) in all chapters.

However, when accessing millions of data points from GBIF, low- and high-quality data needs to be separated to avoid problems in the downstream analysis (Beck et al., 2014; Qian et al., 2018).

Despite having methods for automated data cleaning (e.g., Chamberlain et al., 2022; Zizka et al., 2019) the main finding of **Chapter I** revealed, that classifying cleaned GIBIF occurrence records as alpine and non-alpine is a critical task and if neglected causes bias in the downstream analysis. We identified increased error rates when classifying species with large grid cells e.g., the global thermal belt layers (resolution 2’ 30”; Körner et al., 2011), and unfortunately, such approaches are still used (e.g., Figueroa et al., 2022). Further, we demonstrated that large geographical uncertainties in the occurrence data, combined with the high environmental heterogeneity of mountains, lead to many miss classifications. Therefore, it was important to develop a new algorithm (ElevDistr) that provides solid classifications and avoids exponentially biased dispersal or extirpation rates.

Nevertheless, this does not explain the reasons behind selecting a continuous niche proxy over a biome shift reconstruction (in **Chapter II**). Here, the major difficulty is the lack of a definition for alpine species (Körner, 2021), even though it was suggested that only species with a niche center above the treeline should be considered alpine species (Gjaerevoll, 1990), this idea has never established itself. Further, dispersal-extirpation-cladogenesis (DEC) models (e.g., Höhna et al., 2016; Landis et al., 2018; Ree et al., 2008), which are frequently used to determine biome shifts (e.g., Cardillo et al., 2017; Ebersbach et al., 2017; Favre et al., 2016; Landis et al., 2021) are not capable of processing abundance distributions. DEC models belong to the category of multiple-area range models and exclusively allow absences or presences of a predefined area (per lineage) as input (Hackel & Sanmartín, 2021). Assuming two areas: above the treeline “alpine” and below “non-alpine”; this restriction causes two major problems: (1) a species that occurs 1m above sea level has the same category as species occurring 1m below the tree line. (2) In the European Alpine Arch only 20 species (0.6%) are classified as “exclusively” alpine (see **Chapter I** extracted the Flora Alpina; Aeschimann et al., 2004), this means a DEC model would barely infer any losses of the “non-alpine” potentially leading to a too low extirpation rate. Finally, the computational complexity of DEC models increases quadratically when areas are added, leading to a complexity maximum of about ten areas (Landis, Schraiber, et al., 2013). This limitation makes tasks e.g., comparing mountain systems on a global scale, much more demanding. Thus, I argue that DEC models are still helpful in the context of island biogeography (Landis, Schraiber, et al., 2013), but obsolete for biome shifts; especially if abundance distributions relative to the biome border are available.

Another advantage of abundance distributions is their continuous nature, which (instead of discrete DEC model areas) allows the use of different phylogenetic comparative methods. This allows e.g., to test if data is best explained by continuous or non-continuous evolution. DEC model on the other hand can just estimate dispersal and extirpation rates (Hackel & Sanmartín, 2021). Finally, these facts highlight the importance of ElevDistr (**Chapter** I) which provides continuous distributions relative to the biome border. Moreover, without this new algorithm, it would not have been possible to detect pulsed niche shift evolution in *Primula* and *Lupinus* (**Chapter II**).

However, it remains unclear whether this concept can be extended to describe other biome borders characterized by continuous abundance distributions along an environmental gradient. If so, it would be interesting to test whether pulsed niche shifts are unique to mountain ecosystems or if they occur everywhere and at what rates. Furthermore, I realized while working with continuous distributions, that to my knowledge phylogenetic comparative methods are unable to process whole distributions. Instead, phylogeneticists are forced to use mean or medians for the tips, which is an unsatisfactory solution, because it ignores the information from the standard deviation. Therefore, new methods are needed to disentangle changes in the niche center from changes in niche breadth.

DETECTING PULSED EVOLUTION

A crucial point discussed in **Chapter III** is that log transformations can significantly impact the overall model evaluation. To illustrate the potential magnitude of this effect, another aspect of the data is presented here: trait data from **Chapter III** were log-transformed and fitted to four different processes. Identically to the untransformed traits (**Chapter III**), I fitted Brownian Motion (BM; Felsenstein, 1985), Ohrnstein-Uhlenbeck (OU; Martins, 1994), Early Burst (EB; Harmon et al., 2010), and the best Lévy process (here variance gamma: VG; Landis & Schraiber, 2017) to every transformed trait. These models were fitted to 100 posterior trees from phylogenetic dating, the AICc weights were computed, and the weight distribution was plotted trait- and species-wise. Figure 1 shows the comparison of non-transformed (left side) and log-transformed traits (right side), I selected two particularly extreme examples. First, this reveals that untransformed peduncle length favors a Lévy process (Fig. 1A), however when log-transformed a Brownian motion outperforms the remaining models (Fig. 1B). This indicates that a transformation can eliminate the excess kurtosis which is used to identify Lévy processes (Landis, Matzke, et al., 2013). Further, the inversed is also true, the petal length of the banner favors a Brownian motion process (Fig. 1C), and log-transformed a Lévy process

(Fig. 1D). I argue that the untransformed banner length is normally distributed and therefore a Brownian motion represents the best model. However, a transformation leads to a tailed distribution ("tailedness" is often described by the kurtosis), which is best described with a Lévy process. However, further studies are needed to evaluate if this new hypothesis is true. Nonetheless, hypothesis testing should be straightforward because the R package used in **Chapter III** "pulseR" (Landis & Schraiber, 2017) already includes methods for simulating data.

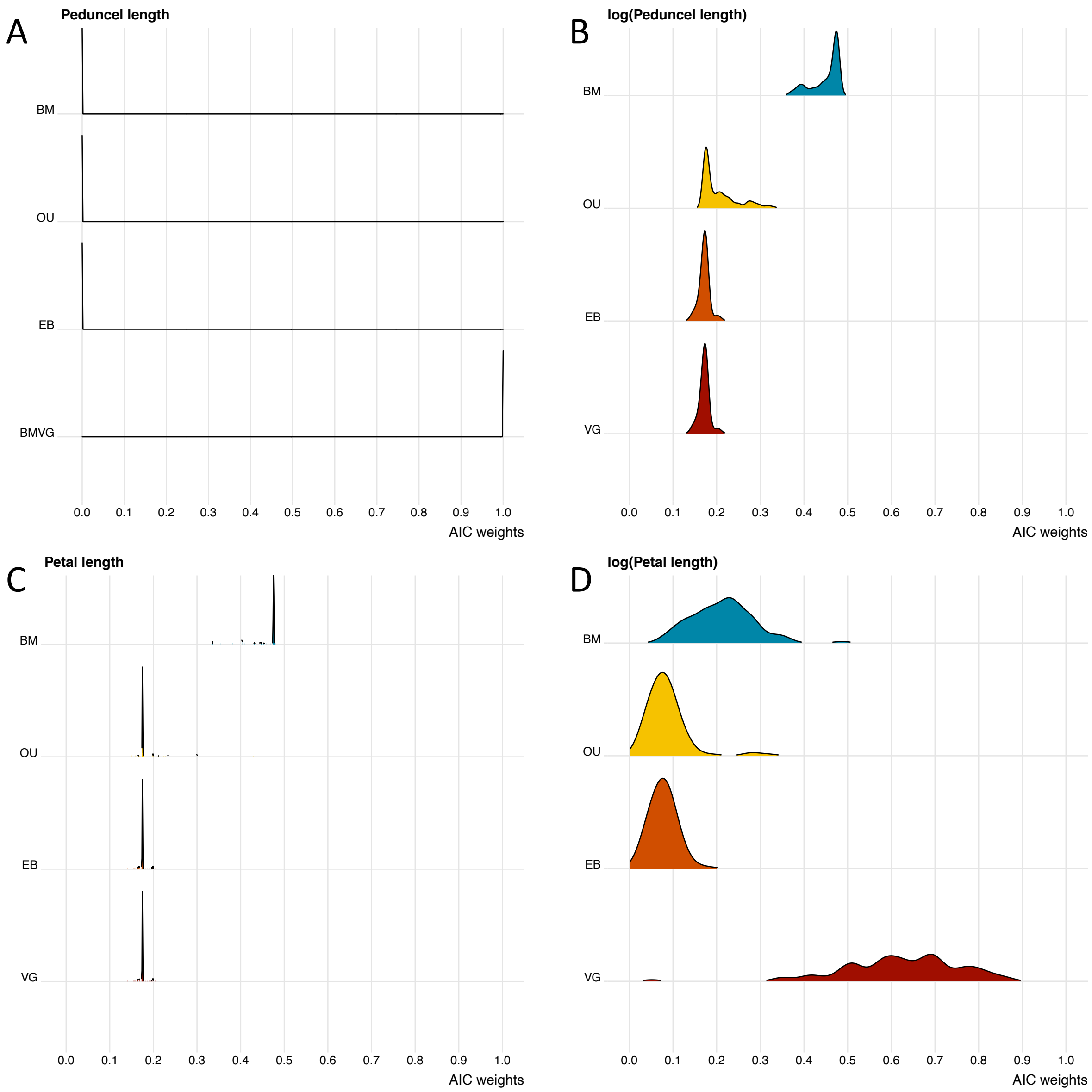

FIGURE 1: Density distribution of AICc weights of the best-supported Lévy process across the posterior of phylogenies versus the three models of gradual evolution against four traits: A) peduncle length, B) log-transformed peduncle length, C) petal length of the banner and D) log-transformed petal length.

Further, I was not able to find in the literature an answer to the question: “Why are log transformations of trait data often used?”. Nevertheless, Simpson (1944) concluded that traits can evolve at different rates, explained by the comparison of horse skull (X) and face length (Y). Further, he describes the data relative to each other with the formula: $Y = 0.25*X^{1.23}$, and the data points are plotted on a graph that has log log-transformed axis. Despite, the exponent in this function, it is mathematically far away from exponential, plus the log-transformed axes are just a design decision. When considering skull lengths from 10 to 80, a linear regression (e.g., $Y = 0.73X-4.99$) has a very similar explanatory power.

Another important aspect covered in the discussion of **Chapter II** concerns the absence of pulses on long phylogenetic branches. We pointed out that excess kurtosis decreases over time, which makes the detection of pulsed evolution on long branches difficult (Landis & Schraiber, 2017). Thus, the absence of a pulse on a long branch should considered with caution. Therefore, interpreting pulses as being exclusively detected on short branches is risky, as they may be easier to detect (M. Landis, personal communication, June 6, 2023).

In conclusion, this thesis demonstrates that data transformation and phylogenetic branch length can significantly influence the detection of pulsed evolution. Nonetheless, **Chapters II** and **III** present clear evidence for pulsed evolution, and therefore, I argue discussed issues do not affect the detection of pulses in untransformed niche and trait data.

RATE VARIABILITY IN EVOLUTION

Besides the mountain ecosystems, the second overarching topic of this thesis is the variability of evolutionary rates. The theoretical concept is that evolutionary changes are not necessarily continuous; they can oscillate between periods of slower, more stable evolution and relatively rapid and intense evolutionary changes. This idea goes back to Simpson’s (1944) book “Tempo and Mode in Evolution”. While the concept is older and often cited, only a few examples of evolutionary pulses are known, and before this thesis, none in plants had been identified in plants. In this final paragraph, I synthesize the knowledge gained from investigating rates of evolution in different clades of dispersal (**Chapters I** and **II**) and trait evolution (**Chapter III**).

The results from **Chapter I** show that in six focal clades *Campanula*, *Carex*, *Festuca*, *Ranunculus*, *Saxifraga,* and *Viola* from the Alpine Arc, dispersal and extirpation rates of the clades are contrasting. The extirpation rate varied less from 0.39 (*Carex*) to 0.87 (*Viola*) shifts per lineage per million years, than the dispersal rate from 0.0079 (*Viola*) to 9.2 (*Saxifraga*) shifts. However, these rates should be compared with care because the sampled species are all from the Alps (i.e., species within the Flora Alpina; Aeschimann et al., 2004). Because this sampling criterion does not lead to a monophyletic clade, this can cause biased rates. Nonetheless, these results are supported by Smyčka et al. (2022), who also found clade-specific rates in the European Alps. Assuming that rates are not heavily biased and can be compared, it is reasonable to conclude that clades have distinct evolutionary histories and consequently, different rates. I argue that different genera might be better adapted to life in an alpine environment, this can explain why biome shifts are highly clustered in plant phylogenies (Donoghue & Edwards, 2014).

Notably, **Chapter II** also provides support for clade-specific niche Evolution. In this chapter, I inferred phylogenies of three large plant genera *Primula*, *Lupinus*, and *Ranunculus*. Further, I computed with ElevDistr (from **Chapter I**) the niche proxies relative to the local upper climatic treeline selecting a niche center plus the upper and lower niche limit. Finally, I tested if niche proxies evolve continuously or pulsed, and compared different clades, and different niche proxies. The results reveal strong evidence for pulsed niche center shift in *Primula* and *Lupinus*, but not *Ranunculus,* and the niche limits evolve differently from the niche centers. I argue that different biogeographical history and trait evolvability might cause this pattern. Here, *Lupinus* shows an evolutionary jump all ~7.0 Myr equivalent to ~3.6 Myr of Brownian motion and compared to *Primula*, has fewer but relatively large jumps. Further, *Lupinus* is also known for its large morphological variety and occupying various habitats (Drummond et al., 2012; Hughes & Eastwood, 2006; Nürk et al., 2019). Adittionaly, *Ranunculus* with its rather homogenous growth forms (Aeschimann et al., 2004), and its niche evolution is best explained by continuous drift (OU process), which is known to support the common evolutionary pattern of stasis (Hunt, 2007). Unfortunately, the geographical ancestry of *Ranunculus* remains unknown (Emadzade & Hörandl, 2011). I speculate that ancestors might have been present in the tundra, potentially leading to an early pre-adaptation to climatic conditions similar to the alpine environments. Therefore, *Ranunculus* ancestors diversified into various forms, followed by evolutionary stasis - a different mode of evolution distinct from that of modern *Lupinus*.

Results from **Chapter III** show indeed support for the idea that *Lupinus* is in a non-stationary mode of evolution. In this chapter, I use the phylogeny inferred in **Chapter II** to examine whether trait evolution also follows a pulsed pattern, and if so, determine whether variation in life form or habitat climate serves as a primary driving factor. This study reveals that multiple pulses can be found in some but not all traits. Further, different life forms are not equally adapted to different climatic conditions, and pulsed changes in the rates of trait evolution are only observed in Andean perennials. Here, I conclude that like the evolution of clades, traits can also have different evolutionary histories, this might be driven by how simple or complex genetical change for a trait is (e.g., how many specific or unspecific mutations are needed for a change morphology) or if these traits are under selective pressure. Because only the combination of a suitable life form and a favorable environment leads to pulses, I argue that this reminds of Simpson's (1944) quantum evolution. The observed pattern: (1) sudden life form changes, (2) non-ancestral species moving out of the Xeric environment, (3) leading (in a suitable environment) to radical morphological changes; has many parallels to the "inadaptive", "preadaptive" and "adaptive phase" of quantum evolution (Simpson, 1944). However, to thoroughly test this new hypothesis, additional traits, and fine-scaled environment data are required.

Finally, I demonstrate in my thesis that there is plenty of evidence for rate change in mountain clades. I found clade-specific rates of biome shift and niche shift, niche borders evolve differently than niche centers, and morphological characters follow a variety of different tempi. Therefore, this thesis delivers multiple shreds of evidence, supporting Simpson's idea that different tempi of evolution are true. Further, this means that the assumption of continuous evolution might be wrong in many cases and scientists must pay attention when selecting models. What remains unanswered, and where additional studies are needed is to determine whether the phenomena of pulsed evolution can only be associated with mountain ecosystems or if this happens also in other biomes. Further, it remains unknown if different clades have different traits that show increased evolutionary rates or if the pattern described in **Chapter III** is ubiquitous (to the plant world). I am also wondering if there are pulses in niche shift that align with pulses in trait evolution, this might be likely and the ultimate proof of different tempi and modes of evolution.

CONCLUSION

In conclusion, this thesis indicates that in certain cases continuous niche proxy shifts are more valuable for reconstructing species movement in an alpine context than biome shifts. Further, I demonstrated the complexity of inferring niche and biome shifts meaningfully in the alpine environments (**Chapters I** and **II**). As a highlight, this thesis identified multiple examples of pulsed niche shift (**Chapter II**) and trait evolution (**Chapter III**). This strongly suggests that always assuming gradual evolution is incorrect. I argue that pulses in evolution are valuable indicators for rapid adaptations and strong selection and that phylogenies contain the statistical signal to detect them. Therefore, models of pulsed evolution might become a tool powerful to better understand evolution. All under the assumption that the phylogenetic research community is willing to use models with the Lévy process more frequently and let go of unwarranted log transformations, which might eliminate the relevant evolutionary signal in the trait data.

REFERENCES

Aeschimann, D., Lauber, K., Moser, D. M., & Theurillat, J.-P. (2004). *Flora alpina: atlas des 4500 plantes vasculaires des Alpes*. Haupt Publisher. https://doi.org/10.2307/25065454

Beck, J., Böller, M., Erhardt, A., & Schwanghart, W. (2014). Spatial bias in the GBIF database and its effect on modeling species' geographic distributions. *Ecological Informatics*, *19*, 10–15. https://doi.org/10.1016/j.ecoinf.2013.11.002

Cardillo, M., Weston, P. H., Reynolds, Z. K. M., Olde, P. M., Mast, A. R., Lemmon, E. M., Lemmon, A. R., & Bromham, L. (2017). The phylogeny and biogeography of Hakea (Proteaceae) reveals the role of biome shifts in a continental plant radiation. *Evolution*, *71*(8), 1928–1943. https://doi.org/10.1111/evo.13276

Chamberlain, S., Oldoni, D., & Waller, J. (2022). *rgbif: Interface to the Global Biodiversity Information Facility API.*

Ding, W.-N., Ree, R. H., Spicer, R. A., & Xing, Y.-W. (2020). Ancient orogenic and monsoon-driven assembly of the world's richest temperate alpine flora. *Science*, *369*(6503), 578–581. https://doi.org/10.1126/science.abb4484

Donoghue, M. J., & Edwards, E. J. (2014). Biome Shifts and Niche Evolution in Plants. *Annual Review of Ecology, Evolution, and Systematics*, *45*(1), 1–26. https://doi.org/10.1146/annurev-ecolsys-120213-091905

Drummond, C. S., Eastwood, R. J., Miotto, S. T. S., & Hughes, C. E. (2012). Multiple Continental Radiations and Correlates of Diversification in Lupinus (Leguminosae): Testing for Key Innovation with Incomplete Taxon Sampling. *Systematic Biology*, *61*(3), 443–460. https://doi.org/10.1093/sysbio/syr126

Ebersbach, J., Muellner-Riehl, A. N., Michalak, I., Tkach, N., Hoffmann, M. H., Röser, M., Sun, H., & Favre, A. (2017). In and out of the Qinghai-Tibet Plateau: divergence time estimation and historical biogeography of the large arctic-alpine genus Saxifraga L. *Journal of Biogeography*, *44*(4), 900–910. https://doi.org/10.1111/jbi.12899

Emadzade, K., & Hörandl, E. (2011). Northern Hemisphere origin, transoceanic dispersal, and diversification of Ranunculeae DC. (Ranunculaceae) in the Cenozoic. *Journal of Biogeography*, *38*(3), 517–530. https://doi.org/10.1111/j.1365-2699.2010.02404.x

Favre, A., Michalak, I., Chen, C., Wang, J., Pringle, J. S., Matuszak, S., Sun, H., Yuan, Y., Struwe, L., & Muellner-Riehl, A. N. (2016). Out-of-Tibet: the spatio-temporal evolution of Gentiana (Gentianaceae). *Journal of Biogeography*, *43*(10), 1967–1978. https://doi.org/10.1111/jbi.12840

Felsenstein, J. (1985). Phylogenies and the Comparative Method. *The American Naturalist*, *125*(1), 1–15. https://doi.org/10.1086/284325

Figueroa, H. F., Marx, H. E., Cortez, M. B. de S., Grady, C. J., Engle-Wrye, N. J., Beach, J., Stewart, A., Folk, R. A., Soltis, D. E., Soltis, P. S., & Smith, S. A. (2022). Contrasting patterns of phylogenetic diversity and alpine specialization across the alpine flora of the American mountain range system. *Alpine Botany*, *132*(1), 107–122. https://doi.org/10.1007/s00035-021-00261-y

Gjaerevoll, O. (1990). *Alpine plants*. The Royal Norwegian Society of Sciences and Tapir Publishers, Trondheim.

Hackel, J., & Sanmartín, I. (2021). Modelling the tempo and mode of lineage dispersal. *Trends in Ecology & Evolution*, *36*(12), 1102–1112. https://doi.org/10.1016/j.tree.2021.07.007

Harmon, L. J., Losos, J. B., Davies, T. J., Gillespie, R. G., Gittleman, J. L., Jennings, W. B., Kozak, K. H., McPeek, M. A., Moreno-Roark, F., Near, T. J., Purvis, A., Ricklefs, R. E., Schluter, D., II, J. A. S., Seehausen, O., Sidlauskas, B. L., Torres-Carvajal, O., Weir, J. T., & Mooers, A. Ø. (2010). Early bursts of body size and shape evolution are rare in comparative data. *Evolution*, *64*(8), 2385–2396. https://doi.org/10.1111/j.1558-5646.2010.01025.x

Höhna, S., Landis, M. J., Heath, T. A., Boussau, B., Lartillot, N., Moore, B. R., Huelsenbeck, J. P., & Ronquist, F. (2016). RevBayes: Bayesian Phylogenetic Inference Using Graphical Models and an Interactive Model-Specification Language. *Systematic Biology*, *65*(4), 726–736. https://doi.org/10.1093/sysbio/syw021

Hughes, C., & Eastwood, R. (2006). Island radiation on a continental scale: Exceptional rates of plant diversification after uplift of the Andes. *Proceedings of the National Academy of Sciences*, *103*(27), 10334–10339. https://doi.org/10.1073/pnas.0601928103

Hunt, G. (2007). The relative importance of directional change, random walks, and stasis in the evolution of fossil lineages. *Proceedings of the National Academy of Sciences*, *104*(47), 18404–18408. https://doi.org/10.1073/pnas.0704088104

Kerkhoff, A. J., Moriarty, P. E., & Weiser, M. D. (2014). The latitudinal species richness gradient in New World woody angiosperms is consistent with the tropical conservatism hypothesis. *Proceedings of the National Academy of Sciences*, *111*(22), 8125–8130. https://doi.org/10.1073/pnas.1308932111

Kong, H., Condamine, F. L., Yang, L., Harris, A. J., Feng, C., Wen, F., & Kang, M. (2021). Phylogenomic and Macroevolutionary Evidence for an Explosive Radiation of a Plant Genus in the Miocene. *Systematic Biology*, *71*(3), syab068. https://doi.org/10.1093/sysbio/syab068

Körner, C. (2021). *Alpine Plant Life, Functional Plant Ecology of High Mountain Ecosystems*. https://doi.org/10.1007/978-3-030-59538-8

Körner, C., Paulsen, J., & Spehn, E. M. (2011). A definition of mountains and their bioclimatic belts for global comparisons of biodiversity data. *Alpine Botany*, *121*(2), 73. https://doi.org/10.1007/s00035-011-0094-4

Landis, M. J., Edwards, E. J., & Donoghue, M. J. (2021). Modeling Phylogenetic Biome Shifts on a Planet with a Past. *Systematic Biology*, *70*(1), 86–107. https://doi.org/10.1093/sysbio/syaa045

Landis, M. J., Freyman, W. A., & Baldwin, B. G. (2018). Retracing the Hawaiian silversword radiation despite phylogenetic, biogeographic, and paleogeographic uncertainty. *Evolution*, *72*(11), 2343–2359. https://doi.org/10.1111/evo.13594

Landis, M. J., Matzke, N. J., Moore, B. R., & Huelsenbeck, J. P. (2013). Bayesian Analysis of Biogeography when the Number of Areas is Large. *Systematic Biology*, *62*(6), 789–804. https://doi.org/10.1093/sysbio/syt040

Landis, M. J., & Schraiber, J. G. (2017). Pulsed evolution shaped modern vertebrate body sizes. *Proceedings of the National Academy of Sciences*, *114*(50), 13224–13229. https://doi.org/10.1073/pnas.1710920114

Landis, M. J., Schraiber, J. G., & Liang, M. (2013). Phylogenetic Analysis Using Lévy Processes: Finding Jumps in the Evolution of Continuous Traits. *Systematic Biology*, *62*(2), 193–204. https://doi.org/10.1093/sysbio/sys086

Martins, E. P. (1994). Estimating the Rate of Phenotypic Evolution from Comparative Data. *The American Naturalist*, *144*(2), 193–209. https://doi.org/10.1086/285670

Nürk, N. M., Atchison, G. W., & Hughes, C. E. (2019). Island woodiness underpins accelerated disparification in plant radiations. *New Phytologist*, *224*(1), 518–531. https://doi.org/10.1111/nph.15797

Qian, H., Deng, T., Beck, J., Sun, H., Xiao, C., Jin, Y., & Ma, K. (2018). Incomplete species lists derived from global and regional specimen-record databases affect macroecological analyses: A case study on the vascular plants of China. *Journal of Biogeography*, *45*(12), 2718–2729. https://doi.org/10.1111/jbi.13462

Ree, R. H., Smith, S. A., & Baker, A. (2008). Maximum Likelihood Inference of Geographic Range Evolution by Dispersal, Local Extinction, and Cladogenesis. *Systematic Biology*, *57*(1), 4–14. https://doi.org/10.1080/10635150701883881

Ringelberg, J. J., Koenen, E. J. M., Sauter, B., Aebli, A., Rando, J. G., Iganci, J. R., Queiroz, L. P. de, Murphy, D. J., Gaudeul, M., Bruneau, A., Luckow, M., Lewis, G. P., Miller, J. T., Simon, M. F., Jordão, L. S. B., Morales, M., Bailey, C. D., Nageswara-Rao, M., Nicholls, J. A., … Hughes, C. E. (2023). Precipitation is the main axis of tropical plant phylogenetic turnover across space and time. *Science Advances*, *9*(7), eade4954. https://doi.org/10.1126/sciadv.ade4954

Simpson, G. G. (1944). *Tempo and Mode in Evolution*. Columbia University Press. https://doi.org/10.7312/simp93040

Smyčka, J., Roquet, C., Boleda, M., Alberti, A., Boyer, F., Douzet, R., Perrier, C., Rome, M., Valay, J.-G., Denoeud, F., Šemberová, K., Zimmermann, N. E., Thuiller, W., Wincker, P., Alsos, I. G., Coissac, E., Roquet, C., Boleda, M., Alberti, A., … Lavergne, S. (2022). Tempo and drivers of plant diversification in the European mountain system. *Nature Communications*, *13*(1), 2750. https://doi.org/10.1038/s41467-022-30394-5

Xing, Y., & Ree, R. H. (2017). Uplift-driven diversification in the Hengduan Mountains, a temperate biodiversity hotspot. *Proceedings of the National Academy of Sciences*, *114*(17), E3444–E3451. https://doi.org/10.1073/pnas.1616063114

Zanne, A. E., Tank, D. C., Cornwell, W. K., Eastman, J. M., Smith, S. A., FitzJohn, R. G., McGlinn, D. J., O'Meara, B. C., Moles, A. T., Reich, P. B., Royer, D. L., Soltis, D. E., Stevens, P. F., Westoby, M., Wright, I. J., Aarssen, L., Bertin, R. I., Calaminus, A., Govaerts, R., …

Beaulieu, J. M. (2014). Three keys to the radiation of angiosperms into freezing environments. *Nature*, *506*(7486), 89–92. https://doi.org/10.1038/nature12872

Zizka, A., Silvestro, D., Andermann, T., Azevedo, J., Ritter, C. D., Edler, D., Farooq, H., Herdean, A., Ariza, M., Scharn, R., Svantesson, S., Wengström, N., Zizka, V., & Antonelli, A. (2019). CoordinateCleaner: Standardized cleaning of occurrence records from biological collection databases. *Methods in Ecology and Evolution*, *10*(5), 744–751. https://doi.org/10.1111/2041-210x.13152

Acknowledgments

I want to start this acknowledgment by citing George Simpson's first sentence in his 1944 book *Tempo and Mode in Evolution*: "The basic problems of evolution are so broad that they cannot hopefully be attacked from the point of view of a single scientific discipline." To me, the essence of this sentence is that outstanding science can only be achieved if scientists work together as a unit (regardless of their core interests). It is of greater importance to me that readers are aware that this scientific contribution also owes its characteristics to many people in the background, which I would like to thank in the following paragraphs.

First and foremost, I am grateful to Jurriaan de Vos for supervising this thesis! His passion for research, creativity, and knowledge fascinates me and helps me to stay motivated. I will miss our long and countless discussions about science, society, and life. Juri belongs with his personality to the (unfortunately rare) kind of supervisor who is more interested in the personal development of his students than in the output. This creates the absolute best environment for learning, working, and exploring. I am also grateful to Seraina Rodewald, Patrícia dos Santos, and Serafin Streiff for their invaluable assistance in enhancing my comprehension of evolution. I am happy that they never stopped answering my annoying questions and requests. Special thanks to Ursina Studer for accompanying me during my fieldwork. Without her, these trips would have been less lively and less productive. I also thank the remaining members of Juri's group who helped with suggestions and ideas, Rafael Pülfer, Michelangelo Moerland, and Maya Bosshard.

Further, I am very thankful that I had the privilege of being a *Physiological Plant Ecology* (PPE) group member. I want to thank Ansgar Kamen for creating the possibility to work in this extraordinary environment and being part of my committee. Further, I would also like to thank Walter Salzburger for being the second supervisor of this thesis, contributing valuable comments, and being present at my defense. I thank Aelys Humphreys for writing a report and joining my defense as an external expert. Additionally, I would like to express my gratitude to Erika Hiltbrunner, Patrick Möhl, Maria Vorkauf, and Christian Körner for assisting me in gaining a deeper insight into alpine ecosystems and avoiding common pitfalls. Next, I would love to thank Marie-Louise Schärer and Cedric Zahnd for their countless encouragements, coffees, and beers we drank together, for being my partners in crime and friends. I am grateful for meeting Richard Peters, who showed me the joy of bouldering, provided guidance on writing introductions, and consistently engaged in enriching discussions without tiring. Also, thanks to my current and past officemates Tobias Zhorzel, Anupa Mathew, Yating Li, David

Steger, Jochem Baan, and Florian Cueni for discussions and for tolerating the many noises I produced while searching for bugs. Also, I would like to thank Günter Hoch and Georg Armbruster for sharing their wisdom with me and welcoming me into their non-competitive “Jass” evenings. And thanks to all the remaining PPE and Plant Ecology and Evolution group members, who made working in the botanical institute enjoyable with their countless and friendly interactions.

Finally, I would like to thank all my friends outside of academia for their support and for listening to my ideas and problems. I am grateful to my mother Susanne Bätscher, my brother Fabrizio Bätscher, and my late father Remo Bätscher, for supporting me, helping restructure phrases, and eliminating countless typos. I am also thankful to my partner, Selina Jakober, for supporting me to encounter myself during the final phase of my thesis with a lot of mindfulness and self-love.